Systems biology analysis of global mRNA translational regulation in *Saccharomyces cerevisiae*

A thesis submitted to the University of Manchester for the degree of

Doctor of Philosophy

in the Faculty of Engineering and Physical Sciences

2010

Shichina Kannambath

School of Chemical Engineering and Analytical Science

Table of contents

Total word count - 42893

List of Figures

List of Tables

List of Abbreviations

DNA	DeoxyriboNucleic Acid
RNA	RiboNucleic Acid
mRNA	Messenger RNA
tRNA	transfer RNA
Met-tRNA$_i$	methionyl initiator transfer RNA
rRNA	ribosomal RNA
eIF	Eukaryotic Initiation Factor
Pab1p	poly (A) binding protein
MFC	MultiFactoral Complex
UTR	UnTranslated Region
RRM	RNA Recognition Motifs
GEF	Guanidine nucleotide Exchange Factor
eEF	Eukaryotic Elongation Factor
eRF	Eukaryotic Release Factor
RRF	Ribosome Release Factor
m^{7}G	7-methylGuanosine cap
IRES	Internal Ribosome Entry Site
miRNA	micro-RNA
GDP	Guanosine DiPhosphate
GTP	Guanosine TriPhosphate
GFP	Green Fluorescent Protein
TCM	Tetra Cysteine Motif
FlAsH	Fluorescein Arsenical Helix binder
EDT	1,2-EthaneDiThiol
LB	Luria-Bertani
IPTG	IsoPropyl β-D-1-ThioGalactopyranoside
YPD	Yeast extract-Peptone-glucose

YNB	Yeast Nitrogen Base
G418	Geneticin
Amp	Ampicillin
Doxy	Doxycycline
rpm	Revolutions per minute
Min	Minute
Sec	Seconds
h	Hours
µl	microliter
ml	milliliter
l	Liter
µg	Microgram
mg	Milligram
g	gram
kg	Kilogram
$CaCl_2$	Calcium chloride
M	Molar
OD	Optical Density
TE	Tris(hydroxymethyl)aminomethane
LiOAc	Lithium acetate
EDTA	EthyleneDiamineTetraAcetic acid
PCR	Polymerase Chain Reaction
PEG	PolyEthylene Glycol
HCl	Hydrochloric acid
SDS	Dodium Dodecyl Sulfate
KOAc	Potassium acetate
NaAc	Sodium acetate
SDS-PAGE	Sodium Dodecyl Sulfate PolyAcrylamide Gel Electrophoresis
HEPES	4-(2-HydroxyEthyl)-1-PiperazineEthaneSulfonic acid
NaCl	Sodium chloride
KCl	Potassium chloride

Na_2HPO_4	Disodium hydrogen phosphate
KH_2PO_4	Potassium dihydrogen phosphate
PBS	Phosphate buffered saline
DAPI	4',6-DiAmidino-2-PhenylIndole
NaOH	Sodium hydroxide
TBS	Tris Buffered Saline
FITC	Fluorescein IsoThioCyanate
$MgCl_2$	Magnesium chloride
NH_4Cl	Ammonium chloride
UV	Ultra Violet
mCi	milliCurie
TCA	1,1,1-TriChloroethane
PLB	Passive Lysis Buffer
COPASI	Complex PAthway Simulator
URA	Uracil
R^J	Response coefficient
R^{Sp}	System specificity ratio

Abstract

mRNA translation is one of the fundamental and well controlled cellular process requiring the combined function of a large number of molecular components. The three main stages of translation, initiation, elongation and termination are facilitated by more than 20 proteins known as translation factors. Translation is the final step in the flow of genetic information, and regulation at this level allows for an immediate and rapid response to changes in physiological conditions. The control exerted at the systems level of translation has not precisely been characterized. Three different techniques have been employed to quantitative the control exerted by the respective translation factors.

In the first approach, employing the microscopic techniques, i*n vivo* intra-cellular distribution of translation elongation and release factors were analysed with TCM and GFP tags. The result indicates that the factors are cytoplasmically distributed which cannot influence the overall translational control. In the second approach, the protein expression levels of the elongation and release factors were titrated progressively to explore their control effects on global translation regulation. The endogenous promoter of each translation factor was substituted by the *tetO7* synthetic promoter to regulate the expression level in response to varying concentrations of doxycycline. Measurement of protein synthesis rate and the growth rate at different levels of the elongation and release factors provide insight to system-level control. The results indicate that the elongation factors eEF1A and eEF2 and the release factor eRF1 exert an unexpectedly high degree of control over translation rate. Moreover, these factors, along with elongation factor eEF3 were found to be functionally dedicated to translation, in contrast to eEF1B and eRF3, which is evidently multifunctional. In the third approach, a mathematical model has been developed to represent the control landscape of the translational machinery. This translation model is a powerful tool that will be used in the quantitative analysis of translation when two factors are made limiting at a time. The extensive study carried out on the translational regulation of *Saccharomyces cerevisiae* reveals an interesting observation of the involvement of each translation factors. For the first time, the quantitative measurement of the translational regulation reveals the translational regulation exerted by individual translation factors.

Declaration

This thesis is a presentation of my original research work and where other sources of information have been used, they have been acknowledged.

No portion of the work referred to in the thesis has been submitted in support of an application for another degree or qualification of this or any other university or other institute of learning.

Signature: …….

Date: …….

Copyright Statement

Acknowledgements

First and foremost I offer my sincerest gratitude to my supervisor Professor John E.G. McCarthy for providing me this excellent opportunity to work in his laboratory and his supervision throughout my Ph.D work. I am thankful to Professor Hans Westerhoff, Professor David Broomhead, Dr. Pedro Mendes and Dr. Gerold Baier for their guidance and suggestions during my Ph. D.

I owe my deepest gratitude to Dr. Sheona Drummond for her valuable guidance, suggestions and supports and moreover, critically reading the whole thesis. I would like to thank Dr. Helena Firczuk (Maja) who made available her support in a number of ways. She made my after-hours working an enjoyable experience. I am indebted to Dr. Juergen Pahle, who supported me every stages of mathematical modeling and shown a light at the end of the tunnel. I would like to thank Mrs. Helen Bryant and Dr. John Hughes for proof reading my thesis and valuable suggestions. I thoroughly enjoyed all discussions with Helen about topics varying from history to current affairs.

It is a pleasure to thank all the members of McCarthy lab for providing such a wonderful environment of work. I would like to thank the Doctoral Training Centre, Manchester and all the organisers including Dr. Maria Nardelli and Ms. Lynne Davies for their whole hearted support and help at each stages of this thesis. In addition, I am thankful to the entire fellow DTC student and all my friends who made my stay in UK a wonderful experience.

I am also grateful to the Dorothy Hodgkin Postgraduate Awards (DHPA) and The School of Chemical Engineering and Analytical Science (CEAS) for generosity and supporting this project.

Finally, I am highly grateful to my parents and family for their immense support, understanding and encouragements.

I dedicate this Ph.D thesis to my parents,
Mrs. V.O. Sushama and **Mr. V. P. Ramachandran**,
without whom this work never would have been a reality.

Chapter 1

Introduction

1.1. Translation : A fundamental process for life

Translation is one of the fundamental processes that occur throughout all the kingdoms of life. It is a very complex and very well controlled process involving many proteins and RNA molecules. Protein synthesis is one of the most energy-consuming cellular processes, and is carried out by highly complex molecular machinery. During translation, messenger RNA (mRNA) is decoded and synthesized into specific proteins. Due to the enormous molecular investment and underlying complexity, each stage of translation is precisely monitored to avoid errors. Translation consists of four stages, initiation, elongation, termination and recycling (reviewed in Kapp and Lorsch, 2004a). During initiation, ribosome, other initiation factors and methionyl initiator transfer RNA (Met-tRNA$_i$) assemble at the initiation codon of mRNA to start translation. During the elongation stage, mRNA is decoded with appropriate transfer RNA (tRNA) and the polypeptide is synthesized. Elongation continues until the stop codon on the mRNA is recognized that leads to termination. During termination, the newly synthesized polypeptide is released from the ribosome. The last stage is recycling where ribosomal subunits, initiation and elongation factors dissociate from the mRNA and become free to function in subsequent translation reactions.

1.2. Essential components of translation machinery

1.2.1. Ribosomes

The ribosome is a large ribonucleoprotein particle that consists of a number of ribosomal RNAs (rRNA) and a collection RNA binding proteins. The architecture of the ribosome is highly conserved from one kingdom to other. Between species the core structure of the ribosome is conserved however there are differences in the protein components as resultantly the overall mass and dimensions of the ribosomes. The yeast ribosome, 80S has two subunits, the large subunit (60S) and the small subunit (40S). The 60S subunit is composed of three rRNA molecules: 28S rRNA of 3392 nucleotides, 5.8S rRNA of 158 nucleotides and 5S RNA of 21 nucleotides whereas the 40S subunit contains one rRNA; the 18S of 1798 nucleotides. There are 42 proteins in the large subunit with a mass ratio of 61% RNA to 39% protein and in small subunit there are 32 proteins giving a mass ratio of 54% RNA to 46% protein (Verschoor et al., 1998). The ribosomal subunits 40S and 60S associate during translation to form 80S. The prokaryotic ribosome consists of large (50S) and small (30S) subunit which forms a 70S ribosome. The 50S subunit contains two rRNAs: 23S RNA of ~2900 nucleotides and 5S RNA of ~120 nucleotides and the 30S subunit consists of 16S RNA of ~1500 nucleotides. The large sub-unit has about 30 proteins whereas small subunit has about 20 proteins (Schmeing and Ramakrishnan, 2009). The crystal structure of the 70S ribosome from bacteria has broadened the understanding of the ribosome and its involvement in each stage of translation (Schmeing and Ramakrishnan, 2009). Mammalian ribosomes differ from yeast ribosomes in size. Mammalian rRNAs are 10% larger in the 40S subunit and nearly 33% larger in the 60S subunit. Not all ribosomal proteins are essential for the survival, though, they are important for the optimal assembly, stability, function of the ribosome and accuracy of translation (Baronas-Lowell and Warner, 1990, Alksne et al., 1993). The majority of the yeast ribosomal proteins have homologous in mammals apart from Ribosomal Protein Large sub-unit 28 (rpL28) which has only been identified in mammals and plants (Verschoor et al., 1998). However, it is believed that the internal features such as the mRNA tunnel,

polypeptide exit tunnel, peptidyl synthesis region, A, P and E site are strikingly similar in all species.

Multiple ribosomes bind to the mRNA during translation. The number of ribosomes translating a single mRNA depends upon the length of the mRNA and the requirement of the resultant peptide (Mathews et al. 2000). In eukaryotes, each ribosome bound to an mRNA occupies 10-15 codons (Mathews et al. 2000). The mRNA binds the 40S subunit where its codon interacts with the complimentary anticodon of the tRNA. In the ribosome, there are three binding sites for tRNA, the A, P and E sites. The A site binds to the incoming aminoacyl-tRNA, the P site holds the peptidyl-tRNA attached to the nascent polypeptide chain, and the E site where the deacylated P-site tRNA moves after peptide-bond formation before its removal from the ribosome (Schmeing and Ramakrishnan, 2009).

1.2.2. mRNA

The cellular-level of mRNA is determined by transcription rates, active transport of the mRNA to the cytoplasm and mRNA degradation rates. Maturation of mRNA varies from prokaryotes to eukaryotes. In eukaryotes, mRNA undergoes a series of molecular processes such as 5' cap-structure formation, 3' poly (A) tail formation and mRNA splicing prior to translation. The translation factors recognise these structures therefore they serve to ensure that the mRNA is not degraded before translation. These structures are necessary for the initiation factors to recognize the non-degraded mRNA and for the mRNA transport to the cytoplasm. Eukaryotic pre-mRNA can contain introns, the non-coding regions which are removed before translation and exons, the coding regions. The removal of introns from pre-mRNA messages is through a process called splicing which can occur in several different ways, allowing a single gene to encode multiple proteins (Geoghegan et al. 1979).

Many studies have demonstrated that the mRNA localizes to distinct regions within the cell (St Johnston. 1995). This is believed to be an efficient way to localize the proteins. Specific localisation of a few mRNA molecules is presumably more energy efficient than transporting many protein molecules (Johnston and Lasko, 2001). The number of times

each mRNA is translated is based on the requirement of the protein that it encodes. Recent studies have indicated that mRNAs are also stored in bodies called as P-bodies for future use or prior to degradation (Parker and Sheth, 2007). mRNAs can exhibit a range of life-spans in bacteria varying from seconds to hours, in yeast cells varying from less than 1 min to more than 60 min and in mammalian cells varying from minutes to days.

1.2.3. tRNA

tRNA plays one of the most important roles in mRNA translation: amino acid delivery. tRNA is a small RNA molecule with 73-93 nucleotides in length (Hou, 1997). In yeast there are approximately 275 genes that code for tRNA. There is a unique tRNA for each codon. tRNA has an acceptor stem which is the base pairing of the 5'-terminal nucleotide with the 3'-terminal nucleotide. The terminal 3' nucleotide contains a CCA sequence that recognises the amino acid and a covalent bond is formed between the amino acid and the tRNA during aminoacylation. The aminoacylation is catalyzed by 20 molecules of aminoacyl tRNA synthetase (Hou, 1997). The anticodon stem of the tRNA recognises the mRNA codon during translation.

There are two classes of tRNA present in all organisms; Initiator tRNA and elongation tRNA. Initiator tRNA binds to the P site of the ribosome and the elongation tRNA binds to the A site. Moreover, the initiator tRNAs are not capable of binding to the A site of the ribosome to be part of elongation (Varshney et al., 1993). Initiator tRNAs possesses some unique sequence/structures, 1) A mismatch between the nucleotides 1 and 72 (Cl-A72) at the end of the acceptor stem, 2) the presence of a sequence of three guanines and three cytosines at the bottom of the anticodon stem forming three consecutive G-C base pairs, and 3) the presence of a purine-11-pyrimidine-24 base pair in contrast to a pyrimidine-11-purine-24 base pair in other tRNAs (Varshney et al., 1993).The important feature for targeting the tRNA to the P site on the ribosome is believed to be the three consecutive G-C base pairs in the anticodon stem (Varshney et al., 1993). Studies have shown that an elongation tRNA can be changed into an initiator tRNA by introducing a Cl-A72 mismatch

and with an anticodon sequence change to which allows the elongation tRNA to function in initiation (Varshney et al., 1993).

1.3. Translation in prokaryotes and eukaryotes

The process of translation is conserved in all kingdoms of life. Even though the underlying molecular mechanism remains the same, there are specific differences in the four stages of translation from species to species. The translation pathway is more complex in eukaryotes than in prokaryotes (McCarthy, 1998). In bacteria, translation is coupled with the transcription process and believed to be faster than in eukaryotes (reviewed in Kapp and Lorsch, 2004a). In contrast, in eukaryotes, the fully transcribed mRNA has to be exported from the nucleus, to the cytoplasm, where it is translated.

1.3.1. Initiation

One of the most important differences between prokaryotic and eukaryotic translation initiation is the number of initiation factors involved in the process. The 3 initiation factors in the prokaryote are replaced by at least 12 initiation factors in eukaryotes (Figure 1.1) (Kapp and Lorsch, 2004a). Translation initiation in bacteria is facilitated by factor 1 (eIF1), 2 (eIF2) and 3 (eIF3). All the initiation factors involved in eukaryotic initiation are listed in Table 1.1.

Translation initiation consists of four major events, 1) formation of the ternary complex and association of initiation factors with mRNA, 2) association of the small subunit (40S) with mRNA, 3) identification of the initiation codon and 4) binding of the 40S and 60S ribosomal subunits.

Table 1.1 : List of all yeast translation initiation factors with respective subunits.

Protein Name	Subunit	Gene name	Mass (kDa)	Function	Reference
eIF1	NA*	SUI1	12.3	Component of a complex involved in recognition of the initiator codon; modulates translation accuracy at the initiation phase	Cui et al., 1998
eIF1A	NA*	TIF11	17.4	Forms complex with eIF1 and 40S and scans for the start codon. C-terminus associates with eIF5B and N terminus interacts with eIF2 and eIF3	Maag et al., 2005
eIF2	α	SUI2	34.7	Involved in identification of the start codon; phosphorylation of Ser51 is required for regulation of translation by inhibiting the exchange of GDP for GTP	Laurino et al., 1999
	β	SUI3	31.6	Involved in the identification of the start codon; proposed to be involved in mRNA binding	Donahue et al., 1988
	γ	GCD11	57.9	Involved in identification of the start codon; binds GTP when forming the ternary complex with GTP and tRNAi-Met	Laurino et al., 1999
eIF2B	α	GCN3	34.0	The guanine-nucleotide exchange factor for eIF2; activity regulated by phosphorylation of eIF2.	Pavitt et al., 1998
	β	GCD7	42.6		
	γ	GCD1	65.7		
	δ	GCD2	70.9		
	ε	GCD6	81.2		

eIF3	α	RPG1 /TIF32	110.3	Form subcomplex that stimulates binding of mRNA and tRNA(i)Met to ribosomes	Phan et al., 2001
	β	PRT1	88.1		
	γ	NIP1	93.2	Involved in the assembly of preinitiation complex and start codon selection	Valasek et al., 2003
	δ	TIF35	30.5	Subunits of eIF3 which are essential for translation	Phan et al., 1998
	ε	TIF34	38.8		
	ζ	HCR1	29.6	A substoichiometric component of eIF3 required for processing of 20S pre-rRNA; binds to eIF3 subunits Rpg1p and Prt1p and 18S rRNA	Phan et al., 2001
eIF4AI/ II	NA*	TIF1/ TIF2	45.1	DEAD-box RNA helicase that couples ATPase activity to RNA binding and unwinding, interacts with eIF4G	Caruthers et al., 2000
eIF4B	NA*	TIF3	48.5	Has RNA annealing activity; contains an RNA recognition motif and binds to single-stranded RNA	Altmann et al., 1995
eIF4E	NA*	CDC33	24.3	The eIF4E-cap complex is responsible for mediating cap-dependent mRNA translation via interactions with translation initiation factor eIF4G	Fortes et al., 2000
eIF4GI/ II	NA*	TIF4631/ TIF4632	107.1	Interacts with Pab1p and eIF4A and also has a role in biogenesis of the large ribosomal subunit	Neff and Sachs, 1999

eIF5	NA*	TIF5	45.2	N-terminal domain functions as a GTPase-activating protein to mediate hydrolysis of ribosome-bound GTP; C-terminal domain is the core of ribosomal preinitiation complex formation	Das et al., 2001
eIF5B	NA*	FUN12	112.3	GTPase, required for general translation initiation by promoting Met-tRNAiMet binding to ribosomes and ribosomal subunit joining; homolog of bacterial IF2	Lee et al., 2002
Pab1p	NA*	PAB1	64.3	Part of the 3'-end RNA-processing complex, mediates interactions between the 5' cap structure and the 3' mRNA poly(A) tail, involved in control of poly(A) tail length, interacts with translation factor eIF-4G	Kessler and Sachs, 1998
Ded1p	NA*	DED1	65.5	Required for translation initiation of all yeast mRNAs	Iost et al., 1999

NA* - Not applicable

1.3.1.1. Ternary complex formation and interaction of initiation factors with mRNA

The first step of eukaryotic translation initiation is ternary complex formation by the assembly of eukaryotic initiation factor 2 (eIF2) and Met-tRNA$_i$ (Figure 1.1). Prior to this assembly, eIF2-GDP is converted to eIF2-GTP by eukaryotic initiation factor 2B (eIF2B). eIF2 has ~100-fold higher affinity for GDP than for GTP (Panniers et al., 1988), hence eIF2B is essential for recycling of eIF2-GTP. eIF2 is a heteromultimer, with three subunits

of a total molecular mass of ~125 kDa (Laurino et al., 1999). The γ subunit of eIF2 interacts with both GTP and Met-tRNAi (Erickson and Hannig, 1996, Naranda et al., 1995). The γ subunit of eIF2 is homologous to the eukaryotic elongation factor 1A (eEF1A) and prokaryotic elongation factor Tu (EF-Tu) (Kyrpides and Woese, 1998).

Concurrent to the ternary complex formation, the eukaryotic initiation factor 4F (eIF4F) complex, consisting of eukaryotic initiation factor 4A (eIF4A), 4B (eIF4B), 4E (eIF4E) and 4G (eIF4G) binds to the mRNA cap (7-methylguanosine). Binding of this complex is thought to unwind secondary structures found in the 5'-untranslated region (5' UTR) of mRNA (reviewed in Kapp and Lorsch, 2004a). eIF4E binds directly to the 5'-cap structure of the mRNA. The highly conserved electron-rich tryptophans in eIF4E have high specificity for the positively charged 7-methylguanosine of the eukaryotic mRNA 5'-cap (Marcotrigiano et al., 1997). Secondary structure found near the 5'-cap of the mRNA can inhibit interaction with 40S. eIF4A is a RNA-dependent ATPase and has been proposed to function as a RNA helicase that unwinds the secondary and tertiary structure in the 5'-ends of mRNAs (Linder, 1992). eIF4B, an RNA-binding protein is believed to assist eIF4A in unwinding structures in mRNAs (Altmann et al., 1993). Another RNA-dependent ATPase of the DEAD box family, Ded1p is also believed to be involved in unwinding the 5'-UTR secondary structure (Iost et al., 1999, Berthelot et al, 2004).

Addition to 5'-cap binding proteins, one initiation factor, poly (A) binding protein (PAB), binds to the 3'-poly (A) tail of eukaryotic mRNA. PAB contains four RNA recognition motifs (RRMs) which recognise the poly (A) tail of the mRNA. More than one PAB protein can simultaneously bind to the poly (A) tail with approximately one PAB molecule bound per 27 nucleotides of the mRNA poly (A). The average length of a yeast mRNA poly (A) tail is 70 nucleotides and possibly 2 to 10 PAB molecules can bind to the poly (A) tail of an mRNA (Baer and Kornberg, 1980, Baer and Kornberg, 1983). The RRM of the Pab1p contain the binding site for eIF4G and the poly (A) tail of an mRNA with Pab1p form a multivalent attachment site for eIF4G (Gray et al., 2000). The interaction between Pab1p and eIF4G can potentially form a circular structure to the mRNA. Moreover, it has been suggested that PAB may interact with the 60S subunit directly indicating that in

addition to facilitating mRNA binding to the 43S-ternary complex, the poly(A) tail and PAB may influence ribosomal subunit joining as well (Sachs and Davis, 1989, Proweller and Butler, 1996). It has been proposed that circularization of the mRNA is a quality control mechanism in eukaryotes to verify that none of the truncated mRNA is translated. In contrast, this quality control step is seems to be absent in prokaryotes where proteins synthesized from aberrant/truncated mRNAs are degraded (reviewed in Kapp and Lorsch, 2004a).

1.3.1.2. Association of mRNA with 40S

In bacteria, loading of the 30S ribosomal subunit onto mRNA is accomplished through complementary base pairing between the 3' end of the 16S rRNA (the anti-Shine-Dalgarno) and the purine-rich Shine-Dalgarno sequence located upstream of the initiation codon in mRNA. The Shine-Dalgarno sequence is usually ~10 bases upstream of the initiation codon, therefore the peptidyl site (P site) of the small ribosomal subunit is placed near the initiation codon the 30S binds to the mRNA (reviewed in McCarthy, 1998). Thus, in bacteria, association of 30S subunits with mRNA and the recognition of the start codon occur as a single process.

In eukaryotes, the processes of association of 40S with mRNA and identification of the initiation codon occur separately and require additional initiation factors. Before association of the mRNA with 40S, the ternary complex (eIF2-GTP-Met-tRNA$_i$) binds with the 40S ribosomal subunit. This interaction is facilitated by several initiation factors, namely eukaryotic factors 1 (eIF1), 1A (eIF1A) and 3 (eIF3), collectively known as the multifactor complex (MFC) (Asano et al., 2000). The resulting 43S complex (40S- eIF2-GTP-Met-tRNA$_i$-eEF1-eEF1A-eIF3) is loaded onto the mRNA with the help of eIF4G and Pab1p which are bound to the 3'-poly (A) tail of mRNA (Asano et al., 2000).

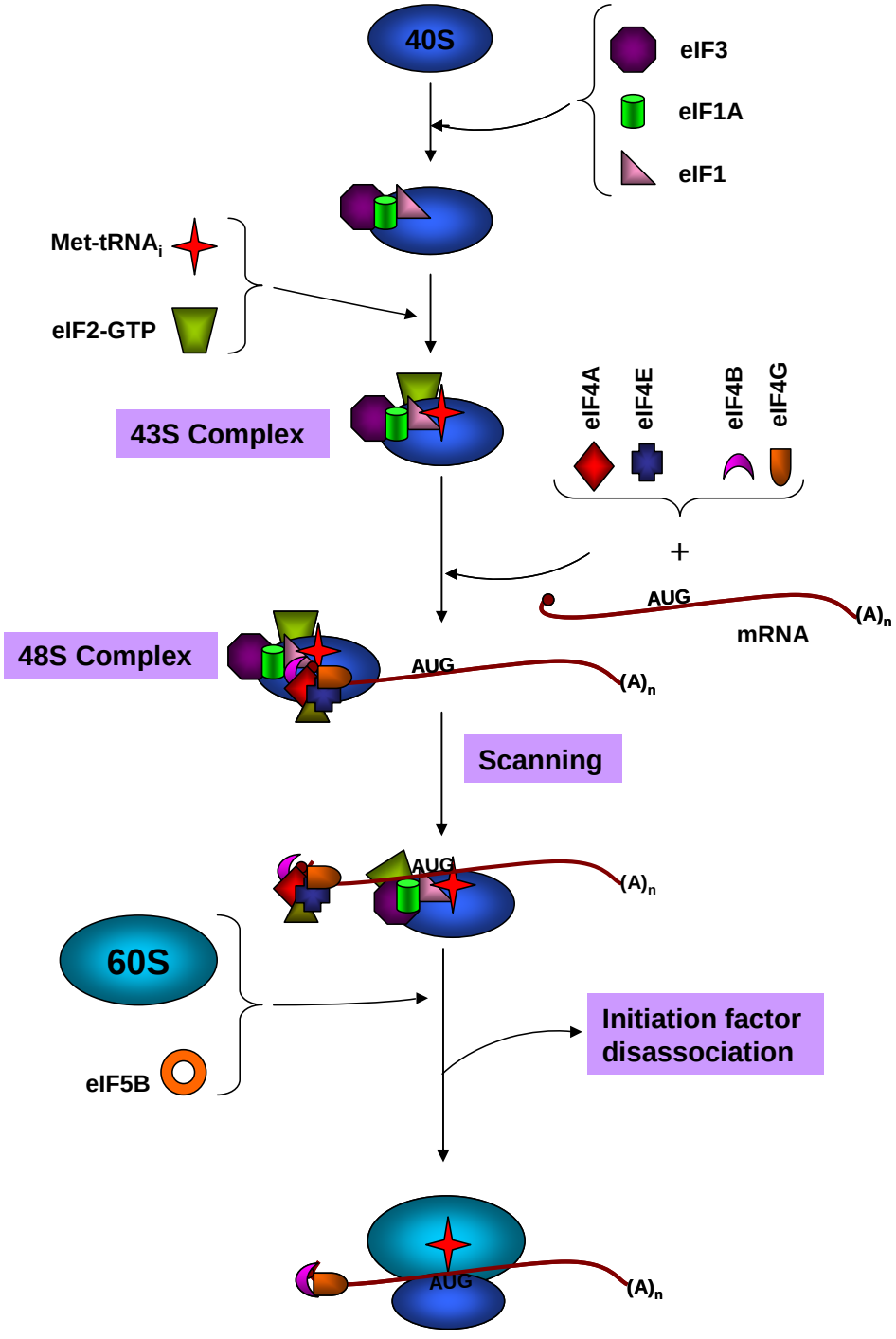

Figure 1.1 : Schematic representation of eukaryotic translation initiation. Eukaryotic initiation is facilitated by 13 initiation factors. The met-tRNA$_i$ and the initiation factors bind to the 40S ribosomal sub-unit to form a 43S complex. Subsequently, 43S is loaded on to the mRNA facilitated by the cap-binding factors to form 48S. 43S scans the mRNA from 5' to 3' to identify the initiation codon AUG. Once the initiation codon is identified, 60S associates with the 40S and starts poly-peptide synthesis.

The eIF3 protein complex facilitates the binding of both the ternary complex and the mRNA to the 40S subunit and plays an important role in the assembly of the translation initiation complex (Valasek et al., 2002). eIF3 is a heteromultimeric complex comprised of five core subunits in yeast (Phan et al., 1998) with a combined molecular mass of 360 kDa. This complex allows access to the ternary complex by altering the conformation of the 40S subunit, and may also allow the mRNA to access the 40S sub-unit to 40S. It has been suggested that the small factors such as eIF1 and eIF1A might alter the local conformation of the eIF2 binding site in the 40S subunit whereas the larger factor such as eIF3 might distort the conformation of the entire 40S subunit to facilitate easy access of the ternary complex. This theory explains the requirement for a large initiation factor such as eIF3 in the 43S complex (Kapp and Lorsch, 2004a).

1.3.1.3. Identification of the initiation codon in a cap-dependent translation

The 43S complex binds to mRNA and initiates scanning of the mRNA in a 5' to 3' direction to identify the translation initiation codon, AUG. The scanning process is not clearly understood however, eIF1 and eIF1A are thought to be involved in the process (Cui et al., 1998, Maag et al., 2005). It has been suggested that the scanning movement is via diffusion which is facilitated by the unwinding of mRNA structure by eIF4A and Ded1 allowing the ribosomal subunit movement (Kapp and Lorsch, 2004a). eIF4A and Ded1 are thought to hydrolyse ATP to drive the unwinding of mRNA secondary structure (Kozak, 1980). As the ribosomes move from 5' to 3', the mRNA secondary structure reforms behind it, preventing retrograde movement of the translating ribosome (Kapp and Lorsch, 2004a). Even though the bacterial 16S rRNA is very similar to eukaryotic 18S rRNA, 18S lacks the Shine-Dalgarno sequence that allows easy identification of the initiation codon. Instead, the 43S is loaded on the mRNA via the mRNA cap and then scans to locate the start codon.

1.3.1.4. Association of 40S and 60S ribosomal subunits

Subunit joining is the final step of the translation initiation. Once the initiation codon is identified, codon-anticodon base pairing takes place between the Met-tRNA$_i$ and the initiation codon. In contrast to elongation, where the codon-anticodon base pairing is confirmed in the Aminoacyl site (A site) of the ribosome, in the initiation stage codon-anticodon pairing happens at the P site and requires eIF1 to perform the inspection (Cui et al., 1998). Energy required for this base pairing is provided by the GTP hydrolysis of eIF2. After confirming the codon-anticodon base pairing, eIF1 induces eIF2 to initiate GTP hydrolysis. The main function of eIF2 is to provide the energy required for the release of Met-tRNA$_i$ from the ternary complex (Huang et al., 1997). eIF2-GDP, eIF1, eIF1A, eIF3 and eIF5, disassociate from the ribosomal subunit after the codon-anticodon base pairing. This facilitates binding of the ribosomal large subunit (60S) to the 40S-mRNA-Met-tRNA$_i$ complex. This event is triggered by the GTP hydrolysis of eukaryotic initiation factor 5B (eIF5B). It has been reported that the binding of eIF5B to the 60S ribosomal subunit may bring a structural change on the subunit facilitating the docking of the small subunit (Passmore et al., 2007, Marintchev et al., 2009). The interaction between the eIF5B and the C-terminus of eIF1A stimulates ribosomal subunit joining and eIF5B-GTP hydrolysis. This triggers eIF5B-GDP to be released from the initiation complex (Acker et al., 2006). eIF5B promotes the release of eIF1A from the 80S to empty the A site for first aminoacyl-tRNA (Fringer et al., 2007). eIF5B-GDP disassociates from the 60S ribosome after the formation of 80S. This completes the initiation stage and leads to the next stage of translation; elongation.

1.3.1.5. Additional translation initiation factors

In addition to the core initiation factors, a number of proteins are believed to be involved in translation initiation directly, for example eukaryotic initiation factor 5A (eIF5A) (Kang and Hershey, 1994). This factor was previously known to be an initiation factors, however, recently shown to be part of the elongation cycle (Gregio et al., 2009). Although it is an

essential protein in yeast, the functions of this factor is not clear. However it has been shown that the mutations of this factor have an affect on the elongation cycle and thereby translation.

.

1.3.2. Elongation

Unlike the initiation and termination stages of translation, the mechanism of translation elongation has been highly conserved across the three kingdoms of life. Elongation begins when the peptidyl tRNA is at the P site and the A site of the ribosome is vacant (Figure 1.2). In eukaryotes the translation elongation cycle is known to be facilitated by at least three elongation factors and in yeast four elongation factors known to be involved (Table 1.2). The first step of elongation involves the delivery of aa-tRNA to the ribosomal A site and this event is carried out by eukaryotic elongation factor 1A (eEF1A). eEF1A is a guanidine binding proteins (G-protein) and is normally found as a complex with GDP. However this is the inactive form of eEF1A and the transition between active and inactive is based on whether GTP or GDP, respectively, is bound (Bourne *et al*. 1990). Recycling of inactive eEF1A-GDP to active eEF1A-GTP is performed by eukaryotic elongation factor 1B (eEF1B), a guanidine nucleotide exchange factor (GEF).

There is more than 30% sequence similarity between the eEF1A across the species, with higher identity in the GTP binding domain (Merrick and Nyborg 2000). eEF1A has three functional and structural domains, of which domain 1 binds the nucleotides and this GTP binding domain is highly conserved (Merrick and Nyborg 2000). Domains 1 and 2 bind to eEF1B, and domain 3 is responsible for actin binding (Munshi et al. 2001). In yeast eEF1B contains two subunits, eEF1Bα and eEF1Bγ (Saha and Chakraburtty, 1986). eEF1Bα has catalytic activity whereas the function of eEF1Bγ is unknown.

eEF1A-GTP binds to aminoacyl tRNA to form the ternary complex (aa-tRNA-eEF1A-GTP). The ternary complex enters the A site of the ribosome where the codon-anticodon base-pairing is examined. After the codon-anticodon base pairing is confirmed, eEF1A undergo hydrolysis resulting tRNA-mRNA duplex. eEF1A-GDP releases the aminoacyl

tRNA into the A site and detaches from the ribosome. The ribosomal peptidyl transferase centre catalyzes the formation of a peptide bond between the incoming amino acid at A site and the peptidyl tRNA at the P site (Moore and Steitz, 2003). The result is a deacylated tRNA in a P/E hybrid state with its acceptor end in the exit (E) site of the large ribosomal subunit and its anticodon end in the P site of the small subunit (Green and Noller, 1997). The peptidyl-tRNA is in a similar hybrid state (A/P) with its acceptor end in the P site of the large subunit and its anticodon end in the A site of the small subunit.

The hybrid state of the tRNA is resolved in the second main event in the elongation cycle, translocation. In this process the deacylated-tRNA moves from P/E hybrid site to E site and the peptidyl-tRNA from A/P hybrid state to the P site. The translocation event is facilitated by eukaryotic elongation factor 2 (eEF2), in a GTP dependent manner (Jorgensen et al., 2006). eEF2 is another highly conserved factor and shares 36 % sequence identity across species. eEF2 is a monomer with six structural domain. These domains are organized in such a way that it divides the protein into two structural blocks. The N-terminal region contains the domains I ,II and G' and the C terminal region contains the domain III, IV and V (Jørgensen et al., 2003). A major structural conformational change occurs when this protein binds to the ribosome. The N-terminal region contains the GTP binding site which can be phosphorylated to render the protein inactive (Nairn and Palfrey 1987). The translocation of peptidyl-tRNA indirectly causes the repositioning of the ribosome to the next codon of mRNA. The movement of the ribosome to the next codon must be efficient and accurate in order to maintain the protein synthesis in-frame. After translocation, eEF2 leaves the ribosome, allowing the next aa-tRNA-eEF1A–GTP to enter the A site.

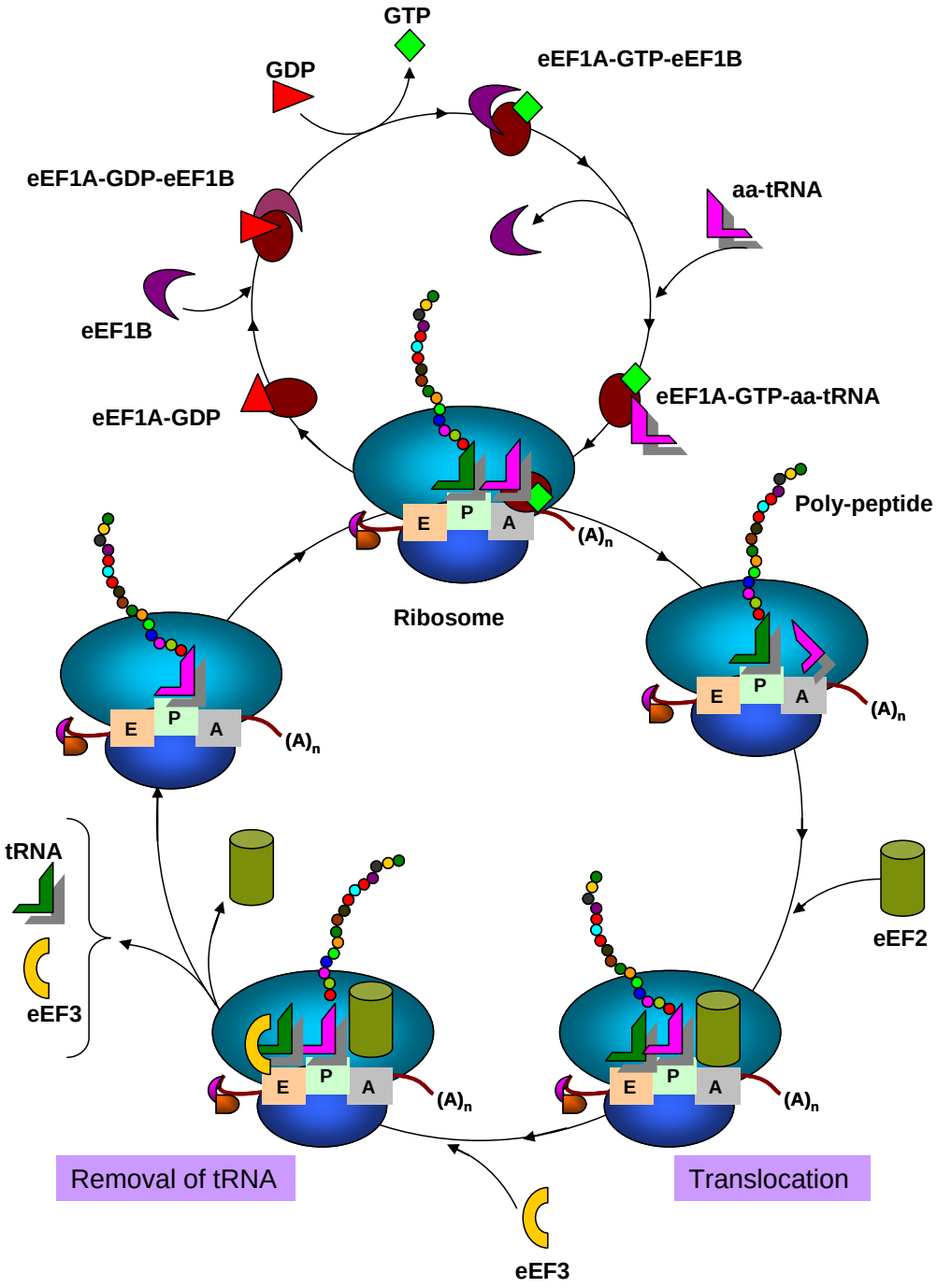

Figure 1.2: Schematic representation of the eukaryotic translation elongation cycle. The ribosome reads mRNA from 5' to 3' and decodes the mRNA sequence to synthesise the appropriate poly-peptide. eEF1A brings the amino acylated tRNA to the A site of the ribosome and the peptide bonds are formed at the P site. Translocation of the ribosome to the next codon of the mRNA is facilitated by eEF2. The tRNA in the E site of the ribosome is removed by eEF3. All the elongation steps are continued until the stop codon is recognised by the release factors.

The major difference between the elongation stage of yeast and that of other organisms is the presence of an exclusive translation elongation factor for fungi that facilitates the removal of tRNA from the E site of the ribosome. In yeast, the deacylated-tRNA from the E site is removed by eukaryotic elongation factor 3 (eEF3). eEF3 has been shown to be essential for the viability of yeast (Qin et al., 1990). eEF3 exhibits ribosome-dependent ATPase and GTPase activities (Dasmahapatra and Chakraburtty, 1981) and possesses a nucleotide binding motif typically found in membrane-associated ATP Binding Cassette (ABC) proteins (Qin et al., 1990). eEF3 is mainly found in the polysome fractions and is required for each round of peptide bond formation (Anand et al., 2003, Kapp and Lorsch, 2004a). eEF3 is hypothesised to facilitate the release of deacylated-tRNA from the E site that enables the efficient binding of the aa-tRNA-eEF1A-GTP ternary complex to the A site (Triana-Alonso et al., 1995). In some higher eukaryotes, some of the ribosomal proteins are suggested to have similar functions to eEF3. There have been reports of ATPase activity in the ribosome to remove the E site deacyl-tRNA (Rodnina et al., 1994). However, there is no evidence of an eEF3 homologous ribosomal protein in higher eukaryotes (El'skaya et al., 1997). eEF3 binds near the ribosomal E-site where it is capable of influencing the binding capacity of the head of 40S subunit and the L1 stalk, both of which contribute to the affinity of tRNA for the E-site. The ribosome undergoes a conformational change at this stage allowing the E site to open up and release the tRNA (Andersen et al 2006). Interaction of eEF3 with eEF1A has been proved and eEF3 believed to be competing with actin to bind to eEF1A (Anand et al., 2006).

1.3.3. Termination

Termination occurs in response to the identification of the stop codon in mRNA at the A site of the ribosome (Figure 1.3). This results in hydrolysis of the ester bond between the polypeptide and tRNA in the P site and the release of the completed polypeptide from the ribosome. In yeast, the stop codon is recognized by the eukaryotic releasing factor 1 (eRF1) which is stimulated by the GTPase activity of eukaryotic releasing factor 3 (eRF3) (Table 1.2). The peptidyl transferase centre of the ribosome is believed to catalyse the ester bond hydrolysis reaction (Kisselev and Buckingham, 2000).

Table 1.2 : List of yeast elongation and release factors and their respective subunits.

Protein Name	Subunit	Gene name	Mass (kDa)	Function	Reference
eEF1A	NA*	TEF1/ TEF2	50.0	Functions in the binding reaction of aminoacyl-tRNA (AA-tRNA) to ribosomes; may also have a role in tRNA re-export from the nucleus	Schirmaier and Philippsen, 1984
eEF1B	α	TEF5	22.6	Stimulates nucleotide exchange to regenerate eEF1A-GTP for the next elongation cycle; part of the EF-1 complex, which facilitates binding of aminoacyl-tRNA to the ribosomal A site	Kinzy and Woolford, 1995
	γ	TEF4	46.5	Stimulates the binding of aa-tRNA to ribosomes by releasing eEF1A from the ribosomal complex	Jeppesen et al., 2003
eEF2	NA*	EFT1/ EFT2	93.3	Catalyzes ribosomal translocation during protein synthesis; contains diphthamide, the unique post translationally modified histidine residue specifically ADP-ribosylated by diphtheria toxin	Justice et al., 1998
eEF3	NA*	*YEF3*	115.9	Stimulates the binding of aminoacyl-tRNA (aa-tRNA) to ribosomes by releasing eEF1A (Tef1p/Tef2p) from the ribosomal complex; contains two ABC cassettes; binds and hydrolyzes ATP	Anand et al., 2003

eRF1	NA*	SUP45	49.0	Involved in the termination of translation and Polypeptide release factor	Stansfield et al., 1995
eRF3	NA*	SUP35	76.6	Catalyse the nucleotide exchange of eRF1, altered protein conformation creates the [PSI(+)] prion, a dominant cytoplasmically inherited protein aggregate that alters translational fidelity and creates a nonsense suppressor phenotype	Salnikova et al., 2005

NA* - Not applicable

There are three stop codons in mRNA: UAA, UAG and UGA**.** In bacteria, the different stop codons are recognized by two release factors, RF1 and RF2; RF1 recognises UAA and UAG where as RF2 recognises UAA and UGA (Scolnick et al., 1968). In yeast eRF1 recognises all the three stop codons. The GGQ motif, which is required for the activation of the polypeptide-tRNA hydrolysis, is a universally conserved motif in all the class 1 release factors across all organisms (Seit-Nebi et al., 2001). The eRF1 has three functional domains: the first two are required for the identification of the stop codon, binding with the ribosome and triggering the hydrolysis of polypeptide-tRNA, and domain 3 is required for binding with eRF3 (Frolova et al., 2000).

eRF3 is an essential GTPase protein and its interaction with eRF1 is required for the optimum efficiency of translation termination (Zhouravleva et al., 1995). In bacteria, it has been reported that the counter part of the eRF3 protein, RF3, is required for the release of the RF1/RF2 complex from the ribosome after polypeptide release (Grentzmann et al., 1994). There is no sequence homology between eRF3 and RF3 apart from the GTP binding domain (Zhouravleva et al., 1995). eRF3 binds to GTP independently of eRF1. Yeast eRF3 has three domains and the carboxyl domain is very similar to that of eEF1A. This domain is essential for cellular viability and the GTP-dependent activity whereas the function of domains 1 and 2 remains unclear (Paushkin et al. 1997). Both eRF1 and eRF3 interact via

their C terminal regions. eRF3 has been shown to bind other proteins including cytoskeletal assembly protein Sla1 and the translation elongation factor eEF2 (Bailleul et al. 1999). eRF3 is also important for the dissociation of eRF1 from the A site of the ribosome (Freistroffer et al. 1997).

1.3.4. Recycling

Recycling is the fourth and last stage of translation where all the translation factors and ribosomal subunits are disassociated to be used in another round of translation (Figure 1.3). Recycling is much more clearly understood in bacteria than in yeast. After the termination stage, ribosomes remain bound to mRNA and the peptidyl-tRNA at the P/E site of the ribosome. In bacteria, the elongation factor EF-G and the ribosome releasing factor (RRF) are required for the recycling (Pisarev et al., 2007). RRF recognizes the complex structure of the ribosome and binds near the A site. As a result, the ribosomal subunit and associated translation factors are released. Along with EF-G, RRF disassociates ribosomal subunits from mRNA and tRNA. GTP-hydrolysis seems to be required to promote the separation of subunits and the GTP is believed to be contributed by EF-G. The GTP hydrolysis by EF-G could be used to trigger the release of the factors at the appropriate time (Kapp and Lorsch, 2004a).

In eukaryotes, no factor has yet been identified which is dedicated to the disassociation of the ribosome. There is no RRF homologue in eukaryotes; however, recent studies have demonstrated that eIF3, eIF1, eIF1A and eIF3j can promote eukaryotic recycling (Pisarev et al., 2007). eIF3 is believed to be the main factor involved in the disassociation of the ribosomal subunits and releasing of mRNA and tRNA from the ribosome and eIF1 and eIF1A facilitate this activity (Pisarev et al., 2007). Although eIF1 and eIF3 enhance dissociation of the subunits, their specific roles in tRNA and mRNA release are not yet clearly understood.

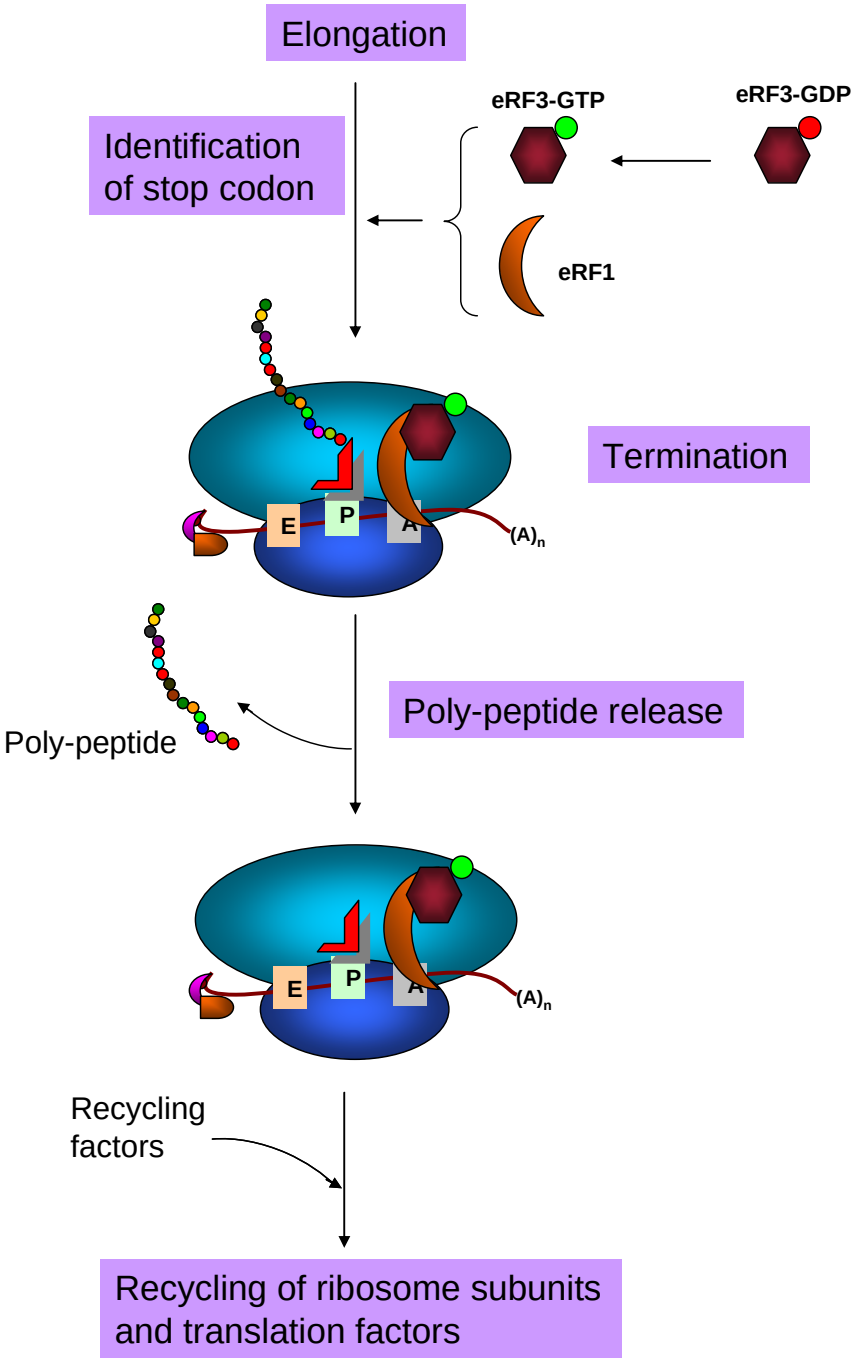

Figure 1.3: Schematic representation of the eukaryotic translation termination and recycling. The stop codon is recognised by the release factors and the poly-peptide is released from the ribosome. Ribosomal subunits along with translation factors and mRNA are recycled for another round of translation.

1.4. Global mRNA translation regulation

Translation is regulated to fine-tune the protein levels in the cell. It is the final step in the flow of the genetic information, and regulation at this level allows for an immediate and rapid response to changes in environmental conditions. Translational control was first hypothesized in early 1960 and highlighted as the essential part of cell survival (reviewed in Mathews et al. 2000**).** However, the mechanisms by which translation is controlled remain unclear. In a multistep pathway like translation, regulation may be exerted at different levels (McCarthy 1998). There are essentially two types of translational control: global translational control where translation of most of the mRNAs is controlled and mRNA-specific control, where specific mRNAs are controlled (Gebauer and Hentze, 2004). Global translational regulation normally occurs by controlling the translation factors whereas mRNA specific controls are modulated by specific protein complexes or micro-RNA (miRNA), which binds to the 5` and/or 3` UTRs of the specific mRNA. Global translational regulation is exerted on the cell, for example during amino acid starvation whereas the mRNA specific translation control is to regulate specific cellular functions. Previous studies have shown that there are localized translation controls in some eukaryotic cells (Johnstone and Lasko 2001). This may imply that translation in all organisms is at maximal levels (Verschoor et al., 1998). The intra-cellular concentrations of mRNAs are believed to be controlling translation rate to some extent (Mathews et al. 2000**)**. Similarly, when the quantity of ribosomes and the amino acids becomes limiting, global translation is rapidly repressed (Clemens et al. 1987).

1.4.1. Regulation of translation at the initiation stage

Initiation is the first stage of translation and is thought to be where translation is most strongly regulated. Translation regulation as a response to nutrient starvation is conserved throughout the eukaryotes (Hinnebusch et al., 2004). During amino acid starvation of yeast, uncharged tRNA binds to Gcn2p, a protein kinase that phosphorylates eIF2. Phosphorylation of the eIF2 α subunit blocks the GTP exchange reaction facilitated by eIF2B. As a consequence, global translation is down-regulated (Rowlands, 1988**)**.

However, the phosphorylation of the eIF2 α subunit activates the translation of the transcriptional activator GCN4 mRNA. GCN4 activates the transcription of more than 500 genes of diverse functions, the majority of which are involved in amino acid metabolism and rescue the cells from amino acid starvation. It has been reported that the GCN4 is translated in a cap-independent manner (Hinnebusch et al., 2004).

Availability of the mRNA cap-binding protein eIF4E also regulates the global translation rate. eIF4E interacts with eIF4G, which is required for the cap-dependent recruitment of the 43S subunit to the mRNA. A family of proteins, 4E-Binding proteins (4E-BPs), shares the binding site of eIF4E with eIF4G. These 4E-BPs inhibit the cap-dependent translation by binding to eIF4E inhibiting the interaction of eIF4G with eIF4E thereby inhibiting the recognition of the mRNA-cap for subsequent cap-dependent translation (Sonenberg and Hinnebusch, 2009). It has been shown that the formation of the MFC and the interaction of eIF5 with rest of the translation machinery are important for optimal translation rate (Hinnebusch et al., 2004). The binding of the 40S ribosomal subunits to mRNA is considered to be a highly rate-limiting step in translation (Sachs et al. 1997).

1.4.2. Regulation of translation during elongation and termination stages

Even though most translation regulation is exerted during the initiation stage, there is still signification regulation that can be exerted during the elongation and releasing stages. This occurs when the initiation rate is very fast compared to the elongation rate. As mentioned previously the ribosome that binds the start codon (AUG) also occupies 4-5 codons upstream therefore the next. The next ribosome can only bind to the mRNA if the previous ribosome has moved approximately 7 codons downstream of the start codon (McCarthy, 1998, Mathews et al. 2000). When the time required to leave the initiation codon exceeds or becomes the same as that of initiation, elongation becomes rate controlling. It has been shown that elongation rate is the same for all mRNAs; 3-8 amino acid per second per ribosome in eukaryotes and faster in prokaryotes (Lodish and Jacobsen 1972). The rate of elongation can vary as some pausing occurs due to the presence of rate amino acid codons or secondary structure in the mRNA. If the pausing interrupts initiation it becomes the rate

limiting step of translation (Wolin and Walter 1988). Translation elongation rate is affected by the phosphorylation/non-phosphorylation of elongation factors. The main factor, which is affected by non-phosphorylation is eEF2 and this happens in response to growth-promoting stimuli, calcium ion fluxes, and other agents (Mathews et al. 2000). Studies have shown that the action of eEF1B on eEF1A-GTP regeneration is the rate-limiting step in translation elongation. This is important because the spontaneous rate of GDP dissociation from eEF1A is very slow (Janssen et al., 1988), and the protein has no inherent preference for the type of nucleotide which it binds (Saha and Chakraburtty 1986).

1.4.3. Translation regulation by non-translating factors

Apart from translation factors, there are other factors in the cell that regulate mRNA translation. The concentration or the availability of ribosomes can regulate the rate of translation. It has been suggested that the translation speed is different for each mRNA based on its codons (Hou, 1997). Eventhough there are sufficient mRNA in the cytoplasm, studies have shown that availability of mRNA could regulate the rate of translation (Geoghegan et al. 1979). Both the primary and secondary structure of mRNA controls the translation rate. The primary structure of the 5’ cap region and upstream of the AUG sequences play a very important role in determining translation rate (Mathews et al. 2000).

Due to the variation in the concentrations of specific tRNAs, the rate of translation elongation can be different for each mRNA (Zhang et al., 2009). It was believed that the tRNAs which are highly abundant in the cell are incorporated faster compared to tRNAs which are rare (Zhang et al., 2010). However, studies have demonstrated that the concentration of the tRNA is not proportional to the rate of incorporation into the mRNA (Kanaya et al., 1999). Moreover it has been demonstrated that some of the codons that code for rare amino acids are translated with higher rates when compared to those of the most abundant amino acids (Bonekamp et al., 1989).

In mammalian systems, micro-RNAs (miRNA) are known to function in gene expression regulation. It has been demonstrated that the miRNAs regulate translation either by directly

inhibiting translation or by destabilizing the mRNA (Sonenberg and Hinnebusch, 2009). It has also been reported that in some cases miRNAs stimulate translation (Vasudevan et al., 2007). Recent studies have also shown that P-bodies have a role in miRNA-mediated translation regulation (Parker and Sheth, 2007). Stress granules, which are observed during the cell stress or translation repression, are also believed to be involved in translational regulation (Anderson and Kedersha, 2008).

1.5. Translation regulation due to the spatial distribution of translation factors

A cell is a heterogeneous environment packed with macromolecules. In the cytoplasm the spatial distribution of the translation factors can be a crucial aspect of translation regulation. Each of the translation factors should be readily available to ensure that the spatial distribution of the translation factors is not regulating translational rate. Many of the translation factors have been visualized to elucidate their distribution within the living cell (Huh et al., 2003). This study reported that all the translation factors are homogenously distributed in the cell. However, a recent study reported that a number of initiation factors are observed to have a specific localistation within the cell (Campbell et al., 2005). The initiation factors eIF2 (α and γ subunits) and eIF2B (γ and ε subunits) are shown to localise in the cytoplasm and continually shuttle between specific foci within the cytoplasm and a cytoplamic pool for GDP to GTP exchange (Campbell et al., 2005). Most of the other initiation factors were shown to be distributed in the cytoplasm without any specific localisation. However, much information about the distribution of the elongation and release factors is not completely available.

Visualising and tracking molecules within a live cell using different fluorescent tagging methods has revolutionised the field of molecular biology. There are a number of fluorescent probes and protein-tags that have been developed to improve the visualisation of cells and molecules. Some of the main techniques to visualise the target protein in the live cells are based on tagging the protein of interest with fluorescent proteins or pairing it with peptides which can bind to fluorescent dyes resulting in fluorescence or

immunostaining with antibodies conjugated to fluorescent dyes. The combination of advanced microscopic techniques and the wide range of fluorescent probes that are now available have complemented and furthered the study of gene expression and protein-protein interactions, and have added to the spatio-temporal understanding of molecular behavior *in vivo*.

The green fluorescent protein (GFP) is one of the most common fluorescent proteins identified, which revolutionised the visualisation of molecules within the cell. GFP emits green fluorescent light upon appropriate excitation (Shimomura et al., 1962). Many different mutants of GFP have been engineered such as red (RFP), yellow (YFP) and cyan (CFP) fluorescent proteins to cover a range of visualisation spectra. GFP can be fused with proteins of interest for visualisation. The molecular size of the GFP has been an issue of concern as it can affect the functional and localisation properties of the tagged protein. Numerous smaller fluorescent molecules have been developed in an attempt to overcome this issue.

Tetra cysteine motif (TCM) tagging is a relatively new technique for generating fluorescently tagged proteins that avoids a number of problems inherent in using the GFP or its derivatives (Griffin et al, 1998). In this method, a stable complex is formed between biarsenical compounds such as green fluorescent FlAsH or red fluorescent ReAsH to an amino acid sequence containing the tetra cysteine motif Cys–Cys–Pro–Gly–Cys–Cys. This short (approximately 10 a.a.) sequence can be introduced at the 5’ or 3’ end of the protein of interest (Griffin et al, 1998). Upon binding with the peptides, these dyes emit fluorescence which can be explored using fluorescent microscopes (Griffin et al, 1998). The rigid spacing of the two arsenics in FlAsH/ReAsH enables them to bind with high affinity and specificity to the tetracysteine motifs. Binding to endogenous cysteine pairs or lipoamide cofactors, which would cause toxicity and nonspecific labeling, is minimized by addition of a low concentration of antidotes (quenching agent) such as 1,2-ethanedithiol (EDT), which outcompetes endogenous pairs of thiols for FlAsH binding. As the tetracysteine motif length is from 6-12 amino acids, it has relatively negligible effect on the structural and functional properties of the protein of interest. Recently this technique has

been further refined by including some extra flanking regions to the motif which increases the specificity of binding (Martin et al, 2005).

1.6. The significance of understanding translation control

Translational regulation is crucial to protein synthesis and irregularities in translational regulation can cause a range of human disease including cancer and metabolic abnormalities (Silvera et al., 2010). It has been also demonstrated that the over-expression of eIF4E causes cancerous cell growth (Silvera et al., 2010). Moreover, over expression of 4E-BP was predicted to be a survival outcome for ovarian and breast cancers and childhood rhabdomyosarcoma (Armengol et al., 2007).

In all living organism, there is a balance between cap-dependent and cap-independent translation. Recent studies have shown that the inhibition of cap-dependent translation causes an increase in cap-independent translation which results in tumorigenesis. The tumor suppressor 14-3-3σ binds to several initiation factors causing the inhibition of cap-dependent translation (Wilker et al., 2007). In contrast, studies of Myc oncogenes have reported that they inhibit cap-independent translation and increase cap-dependent translation. This results in the reduction of Cdk11 levels, causing tumorigenesis. Theses results demonstrate the need of balance in cap-dependent and cap-independent translation in a normal cell (Sonenberg and Hinnebusch, 2009).

1.7. The quantitative analysis of translation

The information processing capability of a living organism with minimal errors has been investigated not only by experimental methods but also with a variety of mathematical and statistical methods. Mathematical modeling has evolved to be an interesting tool to elucidate complex behavior in biological systems. It can be used to identify the underlying mechanism and quantify the controlling parameters. A good mathematical model can be used to validate different hypotheses and understand the underlying mechanism. Biological

processes such as DNA replication, cell division, and mRNA translation have been explored using theoretical methods since the early 1970s (reviewed in May et al., 2004). Several mathematical models of translation initiation, elongation and the whole translation pathway have been developed to investigate translational regulation. However, these models have been generally poorly parameterized and thus unable to provide much insight into the functioning of the translation machinery.

1.7.1. Mathematical modelling of translation initiation

A number of mathematical models have been developed to explain the most complex stage of translation, initiation. In one of the models, translational initiation has been explained using the coding theory (May et al., 2004). The model investigates the error identification mechanisms in translation. In this model translation has been compared to the decoder in a communication system and uses the same theories of the decoder in translation to unfold errors attached with the decoding. In translation, mRNA sequence of size 'n' is decoded into protein of size 'k' and is similar to a decoder in a communication system, which decodes the messages of size 'n' to 'k', where k is always less that 'n'. The model was able to predict and distinguish the coding and non-coding regions of a bacterial genome. Moreover, it could identify the initiation site for each of the mRNAs (May et al., 2004). Another mathematical model of bacterial initiation has been developed to study the translational rate to produce a specific quantity of proteins. The model employs the mRNA folding dynamics, ribosome binding dynamics and the mRNA sequence information to measure the translation rate (Zhang et al., 2010). Another deterministic model of yeast translation initiation investigates the control of each initiation factor upon translation using flux control coefficients (Dimelow and Wilkinson, 2009). A recent deterministic model based on ordinary differential equations has been developed on the aminoacylation and initiation of yeast translation (You et al., 2010). The model investigates the kinetic behaviour of translation initiation factors in response to the amino acid limitation. The model also examines the changes in the translation initiation rate at varying concentrations of initiation factors and external perturbations (You et al., 2010).

1.7.2. Mathematical model of elongation

Recently, a translation elongation model of the amino acid incorporation rate in a ribosome based on bacterial translation elongation has been developed with both deterministic and stochastic approaches (Zhang et al., 2010). This model investigated the affect of the concentration of aa-tRNA-EF-GTP on the elongation rate of a single codon. The model has predicted that limitation of the aa-tRNA-EF-GTP complex has profound differences in the elongation rate at a single codon. This model claims to predict the probability of the translation outcome, either ribosome frame shifting or premature termination, based on the aa-tRNA-EF-GTP concentration (Zhang et al., 2010).

1.7.3. Mathematical model of translation including initiation, elongation and termination

Translation is a very complex biological process for mathematical modeling and owing to its complexity and lack of sufficient experimental data to fit the model, there are very few models which deal with all three stages of translation (Bergmann and Lodish, 1979). A kinetic rate-control deterministic model for the whole of translation has been developed which investigates the dependence of the translation rate on different parameters, such as the initiation, elongation, and termination rate constants, ribosome and initiation factor reduction. This model predicts that tRNA limitation can reduce the elongation rate; however the length of mRNA has been predicted to have no affect on the translation rate (Bergmann and Lodish, 1979). Some conclusions from this model were: 1) for small physiological values of initiation rate constants, initiation can be the rate-limiting step; 2) if termination is not rate-limiting, the overall translation rate is proportional to the rate of initiation; 3) Even if the initiation rate is so fast as to make elongation limiting, it does not cause ribosomal queuing on mRNA; and 4) when the termination rate is limited, ribosomes queue on mRNA (Bergmann and Lodish, 1979).

Another deterministic kinetic model based on bacterial translation has been developed which investigates the sensitivity of translation rate on kinetic parameters and on the

concentration of the translation factors (Zouridis and Hatzimanikatis, 2007). This model provides a detailed study of elongation by considering the ribosomal blocking of the mRNA codon during elongation. In contrast to previous translation models, this model predicts that the translation rate is limited by initiation, elongation and termination rates. It was predicted that elements such as ribosomal occupancy, ribosomal distribution with respect to the codon position along with mRNA length can also have a role in determining translation rate. The important model predictions were: 1) As the number of ribosomes translating mRNA increases, the translation rate increases, but after reaching an optimal level it becomes rate limiting; 2) termination rate becomes translation rate limiting when number of actively translating ribosomes were large 3) Ef-Tu:GDP removal was one of the rate limiting step in the elongation (Zouridis and Hatzimanikatis, 2007). However, all the above models have incorporated a large number of assumptions whilst containing very limited quantitative experimental data.

1.8. Yeast as a model organism to investigate eukaryotic translation

Saccharomyces cerevisiae is a eukaryotic organism the genome of which can be easily manipulated. *S. cerevisiae* was the first eukaryote of which the genome was completely sequenced (Sherman, 2002). Commonly known as bakers' yeast, *S. cerevisiae* shares a significant degree of sequence similarity with higher organisms and processes in yeast can be easily correlated with processes within other organisms. Moreover, the rapid growth, well defined genome, easy genetic manipulation, dispersed cells and easy DNA transformation system make it a favourite model organism for study. Yeast is a non-pathogenic organism and therefore is safe to handle. *S. cerevisiae* can exist in a haploid and a diploid state; most mutations are viable and recessive mutations are easily constructed in haploid strains (Sherman, 2002). A comprehensive data base of yeast has been developed with all the published information about its genes, the proteins encoded and phenotypes related to the gene mutations (http://yeastgenome.org/).

Genetic engineering of yeast chromosomes can be accomplished through relatively simple techniques. Integrative recombination of transforming DNA in yeast is readily achieved

through homologous recombination (Sherman, 2002). Extra copies of genes can be introduced into yeast strains using plasmids. Genes can be disrupted, replaced and deleted from the yeast genome very efficiently and inexpensively. Such easy and efficient molecular techniques have been extensively used in the analysis of gene regulation, structure-function relationships of proteins, chromosome structure, and other general questions in cell biology (Sherman, 2002). Yeast has been a very popular model organism to study mechanisms and regulations of translational (Hinnebusch et al., 2004). The high degrees of the evolutionary conservation of the translational machinery mean that findings in yeast are easily interpreted to other organisms.

1.9. Aim of this study

Growing evidence indicates that irregularities in translation regulation are related to various disease states. The control of translation plays a key role in determining growth and responses to appropriate variations in environmental conditions. However, translational control has not been a subjected to detailed quantitative analysis, particularly at the systems level. In this study, for the first time, translational control is explored at the systems level employing three different approaches: microscopic techniques, molecular biology techniques and mathematical modeling. The project employs a systems biology approach to generate the first ever comprehensive characteristics of translational control. Rather than focusing on role of individual factors at a time, the whole translation pathway is considered and studied together. With the systems level approach the data from individual experimental methods are integrated into an overview of control in the whole system. As part of a wider project exploring all parts of the translation pathway, this work concentrates on translational control exerted by elongation and release factors. The project quantitatively measures the translational control exerted by elongation and release factors and data are combined and analysed using mathematical modeling. Using microscopic techniques, the possibility that translational control might be at least partially attributable to sub-cellular localization of the elongation and release factors is investigated. A variety of molecular biology techniques are employed to explore the effect on translation control when the elongation and release factors are made limiting. Also, the translational control contributions of the individual elongation and release factors are quantitatively characterised. A mathematical model of the whole translational pathway is developed to provide a formal framework for defining translational control at a systems level. All together, this multiple approaches provides a novel and detailed analysis of the factors and processes involved in mRNA translation and contributes significantly to a greater understanding of translational control.

Chapter 2

Materials and methods

2.1. Strains, plasmids and primers

All the strains, plasmids and primers used in this study are listed below.

2.1.1. Yeast and bacterial strains

Table 2.1 : *Saccharomyces cerevisiae* strains

Strain Name	Strain collection number	Genotype	Source
PTC 41	PTC 41	MATα *ade2*-1 *ura3*-1 *leu2*-3, 112 *his3*-11,15 *can1*-100	M. Tuite, University of Kent
PTC 41_ΔTEF2	PTC354	MATα *ade2*-1 *ura3*-1 *leu2*-3, 112 *his3*-11,15 *can1*-100, *TEF2*-Δ	This study
PTC 41_ΔEFT2	PTC355	MATα *ade2*-1 *ura3*-1 *leu2*-3, 112 *his3*-11,15 *can1*-100, *EFT2*-Δ	This study

PTC 41_ΔTEF2-TEF1-TCM	PTC356	MATα *ade2*-1 *ura3*-1 *leu2*-3, 112 *his3*-11,15 *can1*-100, *TEF2*-Δ, *TEF1*-tcm:KanMX	This study
PTC 41-eEF1B-TCM	PTC357	MATα *ade2*-1 *ura3*-1 *leu2*-3, 112 *his3*-11,15 *can1*-100, *TEF5*-tcm:KanMX	This study
PTC 41_ΔEFT2-EFT1-TCM	PTC358	MATα *ade2*-1 *ura3*-1 *leu2*-3,1 12 *his3*-11,15 *can1*-100, *EFT2*-Δ, *EFT1*-tcm:KanMX	This study
PTC 41-eEF3-TCM	PTC359	MATα *ade2*-1 *ura3*-1 *leu2*-3, 112 *his3*-11,15 *can1*-100, *TEF3*-tcm:KanMX	This study
PTC 41-eRF1-TCM	PTC360	MATα *ade2*-1 *ura3*-1 *leu2*-3, 112 *his3*-11,15 *can1*-100, *SUP45*-tcm:KanMX	This study
PTC 41-eRF3-TCM	PTC361	MATα *ade2*-1 *ura3*-1 *leu2*-3, 112 *his3*-11,15 *can1*-100, *SUP35*-tcm:KanMX	This study
PTC 49	PTC 49	MATa/MATα *ade2*–1/*ade2*–1 *can1*–100/*can1*–100 *his3*–11,15/*his3*–11,15 *leu2*–3/*leu2*–3 trp1–1/trp1–1 *ura3*–1/*ura3*–1	Thomas and Rothstein , 1989

PTC 5	PTC 5	MATa *his3*Δ1 *leu2*Δ0 *met*15Δ0 *ura3*Δ0	EuroSCA RF
eEF1A-GFP	PTC296	MATa *his3*Δ1 *leu2*Δ0 *met*15Δ0 *ura3*Δ0, *TEF1-GFP*	Invitrogen
eEF1B-GFP	NA*	MATa *his3*Δ1 *leu2*Δ0 *met*15Δ0 *ura3*Δ0, *TEF5-GFP*	Invitrogen
eEF2-GFP	PTC308	MATa *his3*Δ1 *leu2*Δ0 *met15*Δ0 *ura3*Δ0, *EFT1-GFP*	Invitrogen
eEF3-GFP	PTC309	MATa *his3*Δ1 *leu2*Δ0 *met15*Δ0 *ura3*Δ0, *TEF3-GFP*	Invitrogen
eRF1-GFP	PTC295	MATa *his3*Δ1 *leu2*Δ0 *met15*Δ0 *ura3*Δ0, *SUP45-GFP*	Invitrogen
eRF3-GFP	PTC310	MATa *his3*Δ1 *leu2*Δ0 *met15*Δ0 *ura3*Δ0, *SUP35-GFP*	Invitrogen
tetO7-TEF1-ΔTEF2	PTC362	MATα *ade2*-1 *ura3*-1 *leu2*-3, 112 *his3*-11,15 *can1*-100, *TEF2*-Δ, *TEF1*-P*tetO7*:KanMX	This study
tetO7-TEF5	PTC363	MATα *ade2*-1 *ura3*-1 *leu2*-3, 112 *his3*-11,15 *can1*-100, *TEF5*-P*tetO7*:KanMX	This study

tetO7-EFT1-ΔEFT2	PTC364	MATα *ade2*-1 *ura3*-1 *leu2*-3, 112 *his3*-11,15 *can1*-100, *EFT2*-Δ, *EFT1*-P*tetO7*:KanMX	This study
tetO7-TEF3	PTC365	MATα *ade2*-1 *ura3*-1 *leu2*-3, 112 *his3*-11,15 *can1*-100, *TEF*3-P*tetO7*:KanMX	This study
tetO7-SUP45	PTC366	MATα *ade2*-1 *ura3*-1 *leu2*-3, 112 *his3*-11,15 *can1*-100, *SUP45*-P*tetO7*:KanMX	This study
tetO7-SUP35	PTC367	MATα *ade2*-1 *ura3*-1 *leu2*-3, 112 *his3*-11,15 *can1*-100, *SUP35*-P*tetO7*:KanMX	This study
PTC 41-pTefEx	PTC368	MATα *ade2*-1 *ura3*-1 *leu2*-3, 112 *his3*-11,15 *can1*-100 [pTefEx:*URA3*]	This study
PTC 41_ΔTEF2	PTC369	MATα *ade2*-1 *ura3*-1 *leu2*-3, 112 *his3*-11,15 *can1*-100, *TEF2*-Δ [pTefEx:*URA3*]	This study
tetO7-TEF1-ΔTEF2 - pTefEx	PTC370	MATα *ade2*-1 *ura3*-1 *leu2*-3, 112 *his3*-11,15 *can1*-100, *TEF2*-Δ, *TEF1*-P*tetO7*:KanMX, [pTefEx:*URA3*]	This study

tetO7-TEF5-pTefEx	PTC371	MATα *ade2*-1 *ura3*-1 *leu2*-3, 112 *his3*-11,15 *can1*-100, *TEF5*-P*tetO7*:KanMX, [pTefEx:*URA3*]	This study
tetO7-EFT1-ΔEFT2-pTefEx	PTC372	MATα *ade2*-1 *ura3*-1 *leu2*-3, 112 *his3*-11,15 *can1*-100, *EFT2*-Δ, *EFT1*-P*tetO7*:KanMX, [pTefEx:*URA3*]	This study
tetO7-TEF3-pTefEx	PTC373	MATα *ade2*-1 *ura3*-1 *leu2*-3, 112 *his3*-11,15 *can1*-100, *TEF3*-P*tetO7*:KanMX, [pTefEx:*URA3*]	This study
tetO7-SUP45-pTefEx	NA*	MATα *ade2*-1 *ura3*-1 *leu2*-3, 112 *his3*-11,15 *can1*-100, *SUP45*-P*tetO7*:KanMX, [pTefEx:*URA3*]	This study
tetO7-SUP35-pTefEx	PTC374	MATα *ade2*-1 *ura3*-1 *leu2*-3,112 *his3*-11,15 *can1*-100, *SUP35*-P*tetO7*:KanMX, [pTefEx:*URA3*]	This study
tetO7-TEF1-ΔTEF2-pTefEx-TEF1	PTC375	MATα *ade2*-1 *ura3*-1 *leu2*-3, 112 *his3*-11,15 *can1*-100, *TEF2*-Δ, *TEF1*-P*tetO7*:KanMX, [pTefEx-*TEF1*: *URA3*]	This study

tetO7-TEF5-pTefEx-TEF5	PTC376	MATα *ade2*-1 *ura3*-1 *leu2*-3, 112 *his3*-11,15 *can1*-100, *TEF5*-P*tetO7*:KanMX, [pTefEx-*TEF5*: *URA3*]	This study
tetO7-TEF3-pTefEx-TEF3	PTC377	MATα *ade2*-1 *ura3*-1 *leu2*-3, 112 *his3*-11,15 *can1*-100, *TEF3*-P*tetO7*:KanMX, [pTefEx- *TEF3*: *URA3*]	This study
tetO7-SUP35-pTefEx-SUP35	PTC378	MATα *ade2*-1 *ura3*-1 *leu2*-3, 112 *his3*-11,15 *can1*-100, *SUP35*-P*tetO7*:KanMX, [pTefEx- *SUP35*: *URA3*]	This study
tetO7-GCD	PTC273	MATα *ade2*-1 *ura3*-1 *leu2*-3, 112 *his3*-11,15 *can1*-100, *GCD112*-P*tetO7*:KanMX	This study
tetO7-TIF3	NA*	MATα *ade2*-1 *ura3*-1 *leu2*-3, 112 *his3*-11,15 *can1*-100, *TIF3*-P*tetO7*:KanMX	This study
PTC 41-pTefEx-pDLV-L2/L0	NA*	MATα *ade2*-1 *ura3*-1 *leu2*-3, 112 *his3*-11,15 *can1*-100 [pTefEx: *URA3*] [pDLV-L2/L0:*HIS*]	This study
tetO7-TEF1- ΔTEF2-pTefEx-TEF1- pDLV-L2/L0	NA*	MATα *ade2*-1 *ura3*-1 *leu2*-3,112 *his3*-11,15 *can1*-100, *TEF2*-Δ, *TEF1*-P*tetO7*:KanMX, [pTefEx-*TEF1*:*URA3*][pDLV-L2/L0:*HIS*]	This study

tetO7-TEF5-pTefEx-TEF5-pDLV-L2/L0	NA*	MATα *ade2*-1 *ura3*-1 *leu2*-3, 112 *his3*-11,15 *can1*-100, *TEF5*-P*tetO7*:KanMX, [pTefEx-tef5: *URA3*] [pDLV-L2/L0: *HIS*]	This study
tetO7-EFT1- ΔEFT2-pTefEx- pDLV-L2/L0	NA*	MATα *ade2*-1 *ura3*-1 *leu2*-3, 112 *his3*-11,15 *can1*-100, EFT2-Δ, EFT1-P*tetO7*:KanMX, [pTefEx: *URA3*] [pDLV-L2/L0: *HIS*]	This study
tetO7-TEF3-pTefEx-TEF3- pDLV-L2/L0	NA*	MATα *ade2*-1 *ura3*-1 *leu2*-3, 112 *his3*-11,15 *can1*-100, tef3-P*tetO7*:KanMX, [pTefEx-tef3: *URA3*] [pDLV-L2/L0: *HIS*]	This study
PTC 41-*tetO7*-SUP45-pTefEx- pDLV-L2/L0	NA*	MATα *ade2*-1 *ura3*-1 *leu2*-3, 112 *his3*-11,15 *can1*-100, sup45-P*tetO7*:KanMX, [pTefEx: *URA3*] [pDLV-L2/L0: *HIS*]	This study
PTC 41-*tetO7*-SUP35-pTefEx-SUP35-pDLV-L2/L0	NA*	MATα *ade2*-1 *ura3*-1 *leu2*-3, 112 *his3*-11,15 *can1*-100, sup35-P*tetO7*:KanMX, [pTefEx-sup35: *URA3*] [pDLV-L2/L0: *HIS*]	This study

NA* - Not applicable

Table 2.2 : Bacterial strains

Strains Name	Genotype	Remarks
DH5α	F^- endA1 glnV44 thi-1 recA1 relA1 gyrA96 deoR nupG Φ80d*lacZ*ΔM15 Δ(*lacZYA-argF*)U169, hsdR17(r_K^- m_K^+), λ–	Used for storage/cloning of plasmids
BL21 (DE3)	$F^–$ ompT gal dcm lon $hsdS_B(r_B^-$ $m_B^-)$ λ(DE3 [lacI lacUV5-T7 gene 1 ind1 sam7 nin5])	An *E. coli* strain with DE3, a λ prophage carrying the T7 RNA polymerase gene and $lacI^q$. Transformed plasmids containing T7 promoter driven expression are repressed until IPTG induction of T7 RNA polymerase from a lac promoter.
Top 10F’	F'[$lacI^q$ Tn10(tet^R)] mcrA Δ(mrr-hsdRMS-mcrBC) φ80lacZΔM15 ΔlacX74 deoR nupG recA1 araD139 Δ(ara-leu)7697 galU galK rpsL(Str^R) endA1 $λ^-$	Used for storage/cloning of plasmids

2.1.2. Plasmids

Table 2.3 : List of plasmids

Plasmid name	Remarks	Source
pNEWTC	Contains TCM tag and *KanMX4* selective marker. Used as PCR template for TCM addition.	This study
pUG6	Contains loxp-kanMX-loxp cassette for gene deletion. Used as PCR template to generate yeast selective marker.	Güldener et al 1996
pSH47	Contains the *cre* recombinase gene under control of a GAL promoter and *URA3* selective marker. Used for excision of the loxp-kanMX-loxp cassette	Güldener et al 1996
pCM225	Contains kanMX-tTA-*tetO*. Used as PCR template to prepare doxycycline regulatable promoter strains.	Bellı` et al 1998
pTefEx	Contains *TEF1* promoter and *URA3* selective marker. Used for preparing the gene complementation plasmid.	This study
pTrpEx	Contains *TRP1* promoter and *URA3* selective marker. Used for preparing the gene complementation plasmid.	This study

pTefEx-eEF1A	Contains *TEF1* promoter, *TEF1* gene and *URA3* selective marker. Used for preparing the gene complementation plasmid.	This study
pTefEx-eEF1B	Contains *TEF1* promoter, *TEF5* gene and *URA3* selective marker. Used for preparing the gene complementation plasmid.	This study
pTefEx-eEF3	Contains *TEF1* promoter, *TEF3* gene and *URA3* selective marker. Used for preparing the gene complementation plasmid.	This study
pTefEx-eRF3	Contains *TEF1* promoter, *SUP35* gene and *URA3* selective marker. Used for preparing the gene complementation plasmid.	This study
pDLV-L2/L0	Plasmid used for the double luciferase assay. The plasmid contains both the firefly and renilla gene with *TRP1* and *DCD1* promoters respectively. Plasmid contains *HIS* marker.	This study

2.1.3. Primer sets

Table 2.4 : List of oligonucleotides used for the removal and confirmation of the *EFT2* gene.

Name	Sequence (5' – 3')
EFT2-Del-F	TTTTGGTGTTTAGCATTCAGACTCAAAGACCACAAACACAAACTATA ACATAATTGCAAGCAGCTGAAGCTTCGTACGC
EFT2-Del-R	GCCCAATACATTACGACAAAAACTGAAAAAGTTAAATAATTAAAAA TTGTTTAACCATTCGCATAGGCCACTAGTGGAT
EFT2-Del-Check-F	CTTAAAAGTTTTTTTTCATTTTGTGAGCTTATTCTTCTTTTCTATATAT TCTTGATATCT
EFT2-Del-Check-R	ATGAAATAACACTATAGATGGTAAGTATACGTGAGAATAAACTACA AAAAAGTCAAAAGG

Table 2.5 : List of oligonucleotides used for construction and verification of the TCM tagged strains

Name	Sequence (5' – 3')
TEF1-TC-F	AGACATGAGACAAACTGTCGCTGTCGGTGTTATCAAGTCTGTTG ACAAGACTGAAAAGGCCGCTAAGGTTACCAAGGCTGCTCAAAA GGCTGCTAAGAAACACCGTTGGTGTTGTCCTGGT
TEF1-TC-R	TAAATCAACATTTGGACTGTCGCCTGTTAAGATATAACTGAAAA AAGAGGGGAATTTTTAGATACTGAAATGATATTTTATAACTATA GGGAGACCGGCAGAT
TEF1-TC-CHECK-F	GCTGTCGGTGTTATCAAGTCTG
TEF1-TC-CHECK-R	TTGGACTGTCGCCTGTTAAG
eEF1B-TC-F	CCTTGGATGACTTGCAACAAAGCATTGAAGAAGACGAAGACCA CGTCCAATCTACCGATATTGCTGCTATGCAAAAATTACACCGTTG GTGTTGTCCTGGT
eEF1B-TC-R	AATAAACACGATTCCTTATATAGTGGTTACACAAATTAGTAATA ATGTTTCGTGTGCAGTCGAAAAGTTTATCGTTCAAATAACTATAG GGAGACCGGCAG
eEF1B-TC-Check-F	TTTCGGTATCAAGAAGTTGCAAATTAACTGTGTTGTCGAAGATG ACAAGG

eEF1B-TC-Check-R	GAATATGAAAAGAGATATACATAACTTGAATATTCCCGGAATAAATTCAA
eEF2-TC-F	GTGAAATTGTTCTTGCTGCTCGTAAGAGACACGGTATGAAGGAAGAAGTTCCAGGCTGGCAAGAATATTACGACAAATTGCACCGTTGGTGTTGTCCTGGT
eEF2-TC-R	GTTCGATTGTAAACATTCGGAATATAACTATATGACAAAAATGTGTAAGAAAATAATATATAAGTCTATTACCATACTATTAACTATAGGGAGACCGGCAGAT
eEF2-TC-Check-F	CGACCATTGGTCCACTTTAGGTTCTGACCCATTGGACCCAACCTCTAAGG
eEF2-TC-Check-R	CCTCCCCCTCTACAAAGGGGGCGGTAATACGAAAAGGTCCATTTTTATGA
eEF3-TC-F	AATTGAGAAAGAAGAAGAAGGAAAGAATGAAGAAGAAGAAGGAATTGGGTGATGCTTACGTTTCTTCTGACGAAGAATTCCACCGTTGGTGTTGTCCTGGT
eEF3-TC-R	AGATGTCTGACTAATGGAACGCTTTTTCTTTTAAATAATGCCTTTCTTTATAATAAGGAAGTTGCGTCTATATTTTACCATAACTATAGGGAGACCGGCAGAT
eEF3-TC-Check-F	TATGGGTAACAAGATTGCCGGTGGTAAGAAGAAGAAGAAGTTGTCTTCTG
eEF3-TC-Check-R	AAAGGGTATGAGGCAATGCTCAATTTGCCTGAGCTTAAGAATGTATGAAA
SUP45-TC-F	AAGTTAATTTTGAACAACTAGTTGATGAATCTGAGGATGAATATTATGACGAAGATGAAGGATCCGACTATGATTTCATTCACCGTTGGTGTTGTCCTGGT
SUP45-TC-R	TATACACGGTCCTCTAAACCCACTATGTACTTTCAACAAAGGAATTAGCTCAATATAGAGCAAAAGGTTTACCAAGTATATAACTATAGGGAGACCGGCAGAT
SUP45-TC-CHECK-F	AAACTTCGGTGCTACCTTGG
SUP45-TC-CHECK-R	ATTTGACAGGTGGGCTAGTG
eRF3-TC-F	ATTACCCTCAATTAGGTAGATTCACTTTGAGAGATCAAGGTACCACAATAGCAATTGGTAAAATTGTTAAAATTGCCGAGCACCGTTGGTGTTGTCCTGGT
eRF3-TC-R	TATTTTTATGAAATTCTAGATATATTGAGAGGTGAAGTTTACCTTGTTTATGGTATATGGTACAAAAAGAACTAAACTAATAACTATAGGGAGACCGGCAGAT
eRF3-TC-Check-F	GGTCATCGCTGTTTTAGAAACTGAAGCTCCAGTTTGTGTGGAAACTTACC

eRF3-TC-Check-R	CCGGGGAAGGGTTATGATGAAAACGTGATTGAAGGAGTTGAAA CCTTGCT
Kan-Check-F	CTGGCTGACGGAATTTATGC
Kan-Check-R	ACTGAATCCGGTGAGAATGG
Kan-End-F	GAATGCTGGTCGCTATACTG

Table 2.6: List of oligonucleotides used for construction and verification of the *tetO7* promoter strains

Name	Sequence (5' – 3')
eEF1A-Doxy-F	AATAAACGGTCTTCAATTTCTCAAGTTTCAGTTTCATTTTTCTTGTT CTATTACAACTTTCAGCTGAAGCTTCGTACGC
eEF1A-Doxy-R	CGATAACGACAACGTTAATGTGAGACTTCTCTTTACCCATTTTGTA ATTAAAACTTAGATGCATAGGCCACTAGTGGAT
eEF1A-Doxy-Check-F	CCGAGTTGGAGGACATCA
eEF1A-Doxy-Check-R	CCAAAACCCAAGCGTACT
eEF1B-Doxy-F	AAGAAGCGCTTTAGAAATCAAAGCACAACGTAACAATTTGTCGAC AACCGAGCCTTTGAACAGCTGAAGCTTCGTACGC
eEF1B-Doxy-R	AGCCAAAGAAGCGTTTAATTGTTTCAAAGTTTCAATCTTGGAGAA ATCGGTGGATGCCATGCATAGGCCACTAGTGGAT
eEF1B-Doxy-Check-F	TCTTAGGGCTCAGAACCTGCAGGTG
eEF1B-Doxy-Check-R	CATACCCTTCAATGTATGACTTGTC
eEF2-Doxy-F	GAACAAGGTGATCTTTTTCCTTTAGTTGATATTAATCCCGGGTAAA CTTCCGTGTTGCACCAGCTGAAGCTTCGTACGC
eEF2-Doxy-R	ACGCACATTGGTAACTTTGTCCATTAAAGAACGCATTTGGTCAAC AGTGAAAGCAACCATGCATAGGCCACTAGTGGAT
EFT1_Doxy_F100	ATACCGAATTTGATGATGAACTATTCACTGAAGACGATGGGTACA ACTCTCAGCTGAAGCTTCGTACGC
EFT1_Doxy_R20	AGTAAAAAAACCAGTGAAGCGTTTAATACAACAGTAGTATGCAAT TGAGAGCATAGGCCACTAGTGGAT
eEF2-Doxy-Check-F	TATAAAGTAGAAAATTCATACCTTT
eEF2-Doxy-Check-R	CGACGTGAGCAATAACGGACATGTT

eEF3-Doxy-F	AAATTTTTTCGCTTCCTCGAGTATAATTATCTCATCTCATCTTTCAT ATAAGATAAGAAGCAGCTGAAGCTTCGTACGC
eEF3-Doxy-R	AACAGATAACTTCTGGAATAGTTCTTCTAGAACCTTAATGGATTGC TGGGAATCAGACATGCATAGGCCACTAGTGGAT
eEF3-Doxy-Check-F	TCTTTTTCTTTTTTTGCGTTGGTGA
eEF3-Doxy-Check-R	TTTCGTGTCTGTTGTCAGCAGTGGC
SUP45doxF	TCACTGTATTTTTAACTGATATACTGTTGGTGTGGCCTTAACGACA CCTTTATTTCTTAACAGCTGAAGCTTCGTACGC
SUP45doxR	AGATTGGACCAACTTCTTGACCTTCCAGATCTCAATATTTTTTTCA ACCTCGTTATCCATGCATAGGCCACTAGTGGAT
doxSUP45up	CCGGATTATTCCGTTGAC
doxSUP45down	CGAGGCAGTACCATATTC
eRF3-Doxy-F	ATGTACATTACAACCGGGTATTATATCTTACATCATCGTATAATAT GATCTTTCTTTATGCAGCTGAAGCTTCGTACGC
eRF3-Doxy-R	ACCGTTCTGGCTGTATTGCTGGTAGTTTTGCTGATTGTTGCCTTGGT TTGAATCCGACATGCATAGGCCACTAGTGGAT
eRF3-Doxy-Check-F	TTGTCACTTCTTACCTTGCTCTTAA
eRF3-Doxy-Check-R	ATCTGTTGTTACCTTGTTGTTGGTT

2.2. Growth and storage of bacterial and yeast cell strains

2.2.1. Bacterial culture

Bacterial cells were grown at 37 ^{0}C in Luria-Bertani (LB) broth (Ready mix 25 g/l ForMedium) or on LB agar medium with bacto-agar, 1.5 % (w/v) added to the LB broth. Media was supplemented with 100 μg/ml ampicillin (Sigma) for plasmid selection as appropriate. The bacterial colonies for blue-white screening were grown in LB-agar plate with 100 mM Isopropyl β-D-1-thiogalactopyranoside (IPTG) and 40 mg/ml X-Gal.

2.2.2. Yeast culture

Yeast cells were routinely grown in yeast extract-peptone-glucose medium (YPD) (1 % yeast extract (w/v), 2 % peptone (w/v) and 2 % glucose (w/v) or ready mixed medium (ForMedium). Agar plates were prepared by adding 2 % agar (w/v) to the appropriate medium. Yeast selective medium was prepared by mixing 6.9 g/l Yeast Nitrogen Base (YNB, readymade media mix, ForMedium) with appropriate amino acids. Yeast strains expressing the kanamycin resistance gene (*kanMX*) were selected in medium with 150 µg/ml Geneticin (G418, Sigma). The PTC 41 strain used in this study lacks the *ADE2* gene, this results in the accumulation of the adenine biosynthesis intermediate phosphoribosylaminoimidazole in the cell causing background fluorescence (Stotz and Linder, 1990). Therefore extra adenine (100 µg/ml) was added to avoid auto-fluorescence during microscopic experiments. Doxycycline sensitivity of the yeast *tetO7* promoter strains was determined by adding appropriate concentrations of doxycycline (1 ng/ml – 200 ng/ml) to the growth media. All the strains were grown at 30 ^{0}C unless otherwise specified.

2.2.3. Short and long-term storage of yeast and bacterial strains

For short-term storage, bacterial and yeast strains were grown overnight on the appropriate plates at 37 ^{0}C and 30 ^{0}C, respectively and stored at 4 ^{0}C. For long-term storage, glycerol stocks were prepared by adding sterile glycerol to overnight cultures to a final concentration of 20 % (v/v). The cultures were mixed thoroughly, snap frozen on dry ice and then stored at -80 ^{0}C.

2.2.4. Antibiotics

Table 2.7 : List of antibiotics used in this study

Antibiotics	Abbreviation	Working concentration	Source
Ampicillin	Amp	100 µg/ml	Sigma
Geneticin	G418	150 µg/ml	Sigma
Doxycycline	Doxy	200 µg/ml	Sigma

2.3. Cell methods

2.3.1. Generation of transformation competent bacterial cells

1-2 ml of the an overnight culture of appropriate bacterial strain was diluted into 100 ml LB broth and grown at 37 ^{0}C with constant agitation (200 rpm) until the culture reached OD_{600} of 0.5-0.6. The culture was kept on ice for 10 min and then harvested by centrifugation at 4000 rpm at 4 ^{0}C for 10 min. The cell pellets were resuspended very carefully in 50 ml ice cold 0.1 M $CaCl_2$ and kept on ice for another 30 min before centrifugation at 4000 rpm at 4 ^{0}C for 10 min. The pellet was resuspended in 4 ml of ice cold 0.1 M $CaCl_2$ and stored on ice for a minimum of 2 h. A final concentration of 20 % glycerol was added and 200 µl aliquots were snap frozen on dry ice or liquid nitrogen and stored at -80 ^{0}C.

2.3.2. *E.coli* transformation

An aliquot of glycerol stock of the competent cells was thawed on ice for 30 min. 2 µl of the desired plasmid DNA was added to 200 µl of the bacterial cell suspension and was incubated on ice for 30 min. Cells were then heat-shocked at 42 ^{0}C for 40 sec and immediately transferred to ice for a minimum of 5 min. 250 µl of LB media was added very carefully and incubated for 1 h at 37 ^{0}C with constant shaking (200 rpm). Cells were then spread on LB agar plates with 100 µg/ml ampicillin and incubated overnight at 37 ^{0}C.

2.3.3. *Saccharomyces cerevisiae* transformation

The yeast transformation procedure was adapted and modified from Güldener et al., 1996**.** Yeast strains were incubated overnight in YPD media at 30 ^{0}C with constant agitation (200 rpm). Cells were resuspended in 50 ml of YPD to a starting OD_{600} of 0.2 and grown to an OD_{600} of 0.7-1.0. The cells were then harvested by centrifugation at 4000 rpm at 4 ^{0}C for 5 min. The cell pellet was resuspended in 1 ml of sterile water and transferred to a 1.5 ml eppendorf tube and centrifuged at 5000 rpm for 1 min. The cell pellet was washed twice in 1 ml of sterile water and resuspended in freshly prepared sterile TE/LiOAc (10 mM Tris–

HCl pH 7.5, 1 mM EDTA, 0.1 M LiOAc pH 7.5 adjusted with dilute acetic acid). The cells were harvested and resuspended in 200 µl TE/LiOAc. For chromosomal integration ~5 mg/ml (12 µl) of the tranforming DNA (generated by PCR) was mixed with 5 µl of freshly denatured salmon sperm DNA (10 mg/ml, denatured at 92 ^{0}C for 1 min, then chilled on ice). 50 µl of cells in TE/LiOAc were added to the DNA and mixed carefully. 300 µl of freshly prepared sterile 40 % PEG/LiOAc (50 % PEG, 10 mM Tris–HCl pH 7.5, 1 mM EDTA, 0.1 M LiOAc pH 7.5 adjusted with dilute acetic acid) was added to the mixture immediately and carefully mixed. Yeast cells with the DNA fragment were incubated for 30 min at 30 ^{0}C with constant agitation (200 rpm) and heat shocked for 15 min at 42 ^{0}C. To recover the transformed cells, 800 µl sterile water was added, mixed carefully and the pellet was collected by centrifugation at 13000 rpm for 10 sec. The cell pellet was resuspended in 1 ml of YPD and incubated for 2–3 h at 30 ^{0}C. After 2-3 h of growth, cells were collected by centrifugation at 13000 rpm for 10 sec, resuspended in 200 µl of YPD and spread onto appropriate agar plates. Plates were incubated at 30 ^{0}C until colonies were visible. After 24-48 h these plates were replica-plated onto a new appropriate agar plates to eliminate any false positive colonies.

2.4. DNA purification and recombination method

2.4.1. Isolation of plasmid DNA from bacteria

1-2 ml of an overnight culture of appropriate bacterial strains was harvested by centrifugation at 4000 rpm for 5 min. Plasmid DNA was purified using a QIAprep Spin Miniprep kit (QIAGEN) according to the manufacturer's instructions. The collected plasmid was resuspended in 50 µl of sterile water and stored at 4 ^{0}C.

2.4.2. *Saccharomyces cerevisiae* genomic DNA preparation

5 ml of appropriate medium was inoculated with the yeast and incubated overnight at 30 ^{0}C (shaking at 200 rpm). Cells were harvested by centrifugation at 4000 rpm for 5 min. The cell pellet was washed twice in 1 ml of sterile water and centrifuged at 4000 rpm for 1 min.

The cell pellet was resuspended in 1 ml of buffer A (1 M Sorbitol, 50mM Tris-HCl pH 7.5, 10 mM EDTA and 1 % 2-mercaptoethanol). 5 µl of 10 mg/ml Lyticase (Sigma) and 5 µl of 10 mg/ml RNase A (Promega) were added and incubated at 37 ^{0}C for 1 h. The suspension was centrifuged at 13000 rpm for 1 min and the supernatant was discarded carefully. The pellet was resuspended gently in 1 ml of buffer B (10 mM Tris-HCl pH 7.5, 10 mM EDTA and 0.5 % SDS (w/v)) and incubated at 65 ^{0}C for 10 min. 150 µl of 8 M KOAc was added and mixed by inverting the tube and incubated on ice for 5 min. The suspension was centrifuged at 13000 rpm for 1 min and the supernatant was collected and transferred into a fresh 2 ml micro-tube. To precipitate the genomic DNA, 2 vol of isopropanol were added to the supernatant and mixed by inverting. The DNA pellet was collected by centrifugation at 13000 rpm for 1 min. The supernatant was discarded and the pellet was washed in 70 % ethanol. The DNA pellet was air dried and resuspended in 50 µl of sterile water.

2.4.3. Polymerase chain reaction (PCR)

DNA products were amplified from plasmid or genomic DNA using the PCR method. The reactions were carried out either in a MJ-Mini (Bio-Rad) or a DNA Engine (MJ-Research now Bio-Rad) instrument in 0.2 ml micro-tubes (Eppendorf). The High Fidelity Expand Polymerase PCR system (Roche) was used for the amplification of DNA to be used in plasmid or strain construction for its proof-reading capability ensures correct DNA sequence duplication. RedTaq Ready-Mix (Sigma) was used for routine analytical PCR. PCR reactions with Expand Polymerase were prepared as a final volume of 50 µl reactions, by adding primers, genomic DNA/plasmid, appropriate buffer, dNTPs and polymerase, according to the manufacturer's instructions (Table 2.8). RedTaq contains all the necessary components for PCR excluding primers and genomic DNA/plasmid template. PCR reactions using RedTaq were prepared by adding 10 µl of the RedTaq along with primers, genomic DNA/plasmid and sterile water to make a final volume of 20 µl. The first denaturing temperature was set to 98 ^{0}C to denature the template DNA. In the PCR cycle, the denaturing and annealing temperature for primers were set according to the primers melting temperature and the extension temperatures were calculated based on the expected

product size. A polymerisation step at 72 °C for 5 min was included after 30 cycles to ensure all amplification reactions had reached completion.

Table 2.8 : PCR mixture table for expand high fidelity enzyme

Component	Volume (20 µl reaction)	Volume (50 µl reaction)
Nucleotide mix	0.5 µl (200 µM each of dNTP)	1 µl (200 µM each of dNTP)
PCR primer mix	0.5 µl (300 nM each of primer)	1 µl (300 nM each of primer)
Template DNA	0.5 µl (0.1 - 250 ng)	1 µl (0.1 - 250 ng)
Expand High Fidelity buffer	0.25 µl	5 µl
Expand High Fidelity Enzyme mix	0.3 µl	0.75 µl
Sterile water	To make upto 25 µl	To make upto 50 µl

2.4.4. PCR product purification

PCR amplified DNA products were purified from the PCR reaction using phenol/chloroform DNA extraction and ethanol precipitation. To isolate the DNA from the protein within the PCR reaction mix, an equal volume of phenol:chloroform:iso-amyl alcohol-24:23:1 (Sigma) was added to the DNA solution and mixed thoroughly by vortexing. The two liquid phases were then separated by centrifuging for 5 min at 13000 rpm. The aqueous phase containing the PCR products was collected very carefully and transferred into a clean 2 ml micro-tube. 0.1 volume of 3 M NaAc and 2.5 volume of 100 % ethanol was added to the isolated DNA solution and mix well. This mixture was kept at -80 °C for 20 min and then centrifuged for 20 min at 14000 rpm. The supernatant was discarded and the DNA pellet was washed with 70 % ethanol. After air drying for 10 min, DNA was resuspended in 10 µl of sterile water.

2.4.5. Cloning : Restriction enzyme digestion and ligation of vector with DNA inserts

Purified DNA fragments and plasmids were digested with appropriate restriction enzymes (New England Biolabs) and ligated into the desired plasmids. Plasmid and DNA fragments which were to be ligated together were digested as separate reactions with the same restriction enzymes. Reactions were carried out as 20 µl final volume with 1 - 5 µl of plasmid (~ 1 µg) or PCR product (~0.2 µg), 2 µl of 10 x reaction buffer and 1-2 µl of restriction enzyme(s). Incubation periods, temperatures and buffer compatibility were adjusted according to the manufacturer's recommendations to maximise the restriction enzyme performance. The digested plasmids and DNA fragments were purified as explained in **2.4.4** and were resuspended in 10 µl of sterile water.

Ligation reactions were set up as a final volume of 10 µl with Quick ligase enzyme (New England Biolabs) or T4 DNA Ligase (New England Biolabs), 3 µl of the digested and purified DNA fragment, 1 µl of the digested and purified plasmid and buffer according to the manufactures directions (Table 2.9). The ligation reaction was kept at room temperature for 30 min and was transformed into competent cells as explained in 2.3.1.

Table 2.9 : Ligation mixture and concentration

Components	Volume (10 µl reaction)
digested and purified DNA fragment	3 µl (150 – 200 ng)
digested and purified plasmid	1 µl (50 ng)
10 x Quick ligase buffer	1 µl
Quick ligase enzyme	1 µl
Sterile water	To make upto 10 µl volume

Genetic complementation vectors for the *tetO7* strains were constructed using the blue-white screen technique with the TA Cloning® Kit (Invitrogen). Using High Fidelity Expand Polymerase PCR system, the desired gene was amplified from the genomic DNA. High

Fidelity Expand Polymerase PCR system has a nontemplate-dependent activity that adds a single deoxyadenosine (A) to the 3´ ends of PCR products. Linearized vector supplied in TA Cloning® Kit has single 3´ deoxythymidine (T) residues that allow PCR inserts to ligate efficiently with the vector. The ligated samples are transformed to the TOP10F´ competent cells and plated into a LB-agar plate with 100 mM Isopropyl β-D-1-thiogalactopyranoside (IPTG) and 40 mg/ml X-Gal. The plate was kept at 37°C overnight and the white colonies were picked and tested for the positive insert. From the TA vector, DNA fragments were re-digested and re-cloned into any other vector as required.

2.4.6. DNA sequencing

All the plasmids constructed were sequenced by Eurofins MWG Operon DNS sequencing service. 50-100 ng/µl of purified plasmid DNA was mixed with 2 pmol/µl of primers for an final volume of 15 µl for the sequencing. The sequences were analysed using the sequence alignment module of Clone manager Software (Sci-Ed Software).

2.5. Electrophoresis

2.5.1. Agarose gel electrophoresis

Agarose gels to separate and visualise DNA fragments were prepared by melting agarose (1 %) in TAE buffer (40 mM Tris-HCl, 0.11 % v/v glacial acetic acid, 1 mM EDTA, pH 8.0) with Ethidium bromide (0.2 µg/ml) or 0.1 % of SYBR safe DNA gel stain (Invitrogen). The gel was poured in the DNA gel casting tray with well-combs and was allowed to polymerise at room temperature. The DNA samples for electrophoresis were prepared by adding 1 µl of 5x concentrated DNA loading dye (30% (v/v) glycerol, 0.25% (w/v) bromophenol blue, 0.25% (w/v) xylene cyanol) into 5 µl of DNA solution. The DNA samples along with the GeneRuler™ 1 Kb DNA Ladder (250 – 10000 bp, Fermantas) were electrophoresed at 100 V in 1 x TAE buffer in a BioRad horizontal gel tank. After electrophoresis the DNA bands were visualised using a UV transilluminator (Biorad).

2.5.2. Denaturing polyacrylamide gel electrophoresis (SDS-PAGE)

Proteins were resolved by electrophoresis on pre-cast 4-20% SDS-polyacrylamide gels (NuSep Ltd) in HEPES buffer (100 mM Tris, 100 mM HEPES and 3 mM SDS) using a Biorad Electrophoresis system. Protein samples were mixed with 10 µl SDS-gel loading buffer (0.20 % w/v bromophenol blue, 4 % w/v SDS, 20 % v/v glycerol, 200 mM dithiothreitol (DTT), l00 mM Tris-HCl, pH 6.8, 0.1 % bromophenol blue), were heated for 5 min at 95 ^{0}C and electrophoresised. The protein samples were centrifuged at 13000 rpm for 10 sec before loading. Protein samples along with the PageRuler^{Tm} Plus (10 – 250 kDa; Fermantas) protein marker were electrophoresised at 100 V for 1-2 h until the protein marker was separated as desired. If required the protein gels were visualised using a UV transilluminator or were used for Western blotting.

2.6. Microscopy techniques

Visualisation of fluorescently tagged proteins (TCM and GFP) was performed on live cells grown in YNB media with all amino acids, glucose and adenine to avoid auto fluorescence. To visualise the distribution of TCM-tagged proteins coupled to the fluorescent dye FlAsH, 5 ml liquid cultures of individual yeast strains were grown overnight at 30 ^{0}C. The cells were diluted to an OD_{600} of 0.2 at 30 ^{0}C at 200 rpm and grown further to an OD_{600} of 0.6. 1 ml of this culture was harvested then resuspended in 100 µl of fresh media. Cells were incubated at 30 ^{0}C for 1-2 h in the dark with 2 µM – 4 µM of FlAsH and 10 µM EthileneDiThiol (EDT). FlasH is supplied as a 2 mM solution in DMSO and a working stock of 0.2 mM was made by dilution with 20 mM Tris-HCl pH 7.5. To remove and quench non-specifically bound FlAsH, the cells were resuspended in 1 ml of SC media with 25 µM EDT and incubated on a rotating wheel for 30 min in the dark. Cells were harvested and resuspended in 1 ml of SC media with 25 µM EDT and incubated for another 15 min. After another wash with 1 ml of SC media without EDT, the cells were resuspended in 10 µl of SC media. The cells were mounted onto slides coated with 0.5 % poly-L-lysine. Poly-L-lysine-coated slides were prepared by spreading 0.5 % poly-L-lysine on to the slides. The

slides were incubated in a humid chamber to prevent evaporation before gently removing the excess poly-L-lysine with running water and air drying.

For visualisation of GFP tagged proteins, 5 ml liquid cultures of individual yeast strains were grown overnight at 30 ^{0}C. The cells were diluted to an OD_{600} of 0.2 and grown further at 30 ^{0}C at 200 rpm to an OD_{600} of 0.6. 100 µl of the culture was resuspended in 1 ml of medium and 10 µl of the cells were mounted onto 0.5 % poly-L-lysine coated slides for visualisation. Clear nail varnish was used to seal the sides of the cover slips.

Rhodamine conjugated phalloidin staining of actin within cells expressing TCM tagged eEF1A was performed on fixed cells as described by Gross and Kinzy, 2005. Yeast cells growing in log phase (OD_{600} of 0.6) were collected and a final concentration of 4 % (v/v) formaldehyde (methanol free) and 0.5 % (v/v) Triton X-100 was added for the fixation of the cells. Cells were fixed by incubation for 30 min and then pelleted by centrifugation at 4000 rpm. Then the pellets were resuspended in Phosphate buffered saline (PBS) (137 mM NaCl, 2.7 mM KCl, 4.3 mM Na_2HPO_4 and 1.47 mM KH_2PO_4 adjusted to final pH 7.4) with 0.5 mM $MgCl_2$ and 4 % (v/v) formaldehyde for further fixation for 90 min at room temperature. The cells were washed once with PBS before addition of phalloidin conjugated to rhodamine (Invitrogen) to a final concentration of 0.6 µM in PBS and incubated for 1 h at room temperature in the dark. Yeast samples were subsequently washed three times with PBS. Cells were mounted on 0.5 % poly-L-lysine coated slides before visualisation.

The DNA in the nucleus of the yeast strains expressing TCM-tagged elongation and releasing factors was visualised with 4',6-diamidino-2-phenylindole (DAPI). The TCM-tagged strains were first treated with FlAsH as described above and after mounting on to the poly-L-lysine coated slides, 1 µl of 10 µg/ml DAPI was added to the cells and incubated for 1 h before visualisation.

All of the cells were visualised with a Zeiss LSM 510 confocal microscope with a 100x Plan-Apochromat oil objective (Numerical Aperture 1.4). An argon laser (540 nm) was

used for visualization and images were analyzed with Zeiss LSM software (Carl Zeiss MicroImaging, Inc.).

2.7. Growth analysis of yeast strains

Growth analyses of the yeast strains that contain TCM tags and ΔEFT2 strain were carried out in YPD medium. Overnight cultures were diluted into 20 ml to OD_{600} 0.1. Cells were grown at 30 ^{0}C at 200 rpm and the OD_{600} was determined every hour until the OD_{600} reach 1.0. The OD_{600} points for individual strains along with the wild-type cells were plotted against time. The slope of the curve was determined and compared with that of the wild-type cells. The wild-type growth curve slope served as a reference, and the percentage of the growth with respect to the wild-type strain growth was determined.

The strains containing a *tetO7* promoter were grown overnight in YNB media without methionine and with 2 % glucose. The culture was diluted to an OD_{600} 0.2 and grown for another 8 h. The cultures being incubated without doxycycline were diluted to OD_{600} 0.01, and those with doxycycline were diluted to an OD_{600} 0.02 and grown for 17 h. In the 17 h period the gene under *tetO7* promoter expression will be completely controlled by the concentration of the doxycycline in the medium. 17 h is identified to be the optimum time period for the complete doxycycline effect to occur. Different concentrations of doxycycline were used for different *tetO7* strains to compare growth. After growing for 17 h, cultures were diluted to specific OD's such that the strains reach about OD_{600} 0.4 after 4 h. This ensured that the strains were at the same growth stage when the experiments were performed. The differences in the slope of the growth curve indicate the effect that an addition of a specified concentration of doxycycline has on cell growth rate. The OD_{600} to which the strains have to be diluted was calculated based on the doubling time using the formulae:

$$N_0 = N_t / 2^G$$

Where N_0 is the OD which the cultures had to be diluted to N_t is the OD_{600} required after 4 h, in this study N_t is 0.4, and G is the number of generations the cultures go through.

G is calculated as

$$G = \log_2 (M_t / M_0)$$

where M_t is the final OD_{600} and M_0 is the initial OD_{600}. The doubling time of strains was calculated as T/G where T is the total time the culture grown for.

ODs were measured every hour for 4 h and after 4 h of growth the cultures were used to determine the level of protein. Growth rate was calculated by plotting the OD_{600} points against the time and the slope of the curve is determined. The slopes of individual *tetO7* strains were compared to the slope of the wild-type strains and the percentage of growth rate was calculated.

2.8. Cell counting

The number of yeast cells per 1 ml of culture in the logarithmic growth stage was determined using Cellometer auto M10 software (Cellometer, Peqlab). 20 µl of the cell culture was collected and placed on the slides provided by the manufacturers and analysed using the M10 software. The focus was corrected for clear visualisation and counting. Mean diameter, cell size and the distribution of the cell population with cell size were obtained.

2.9. Western Blotting

Cells were harvested by centrifugation from 10 ml culture grown to OD_{600} 0.4 (approximately $3x10^7$ cells/ml). The protocol for the extraction of protein from cells for Western blotting was adapted from von der Haar, 2007. Briefly, the cell pellet was resuspended in 200 µl of lysate buffer (0.1 M NaOH, 0.05 M EDTA, 2 % SDS, 2 % 2-mercaptoethanol) and was incubated at 90 ^{0}C for 10 min. 5 µl of 4 M acetic acid was added, vortexed for 30 sec and incubated at 90 ^{0}C for another 10 min. 50 µl of 4x loading buffer (0.25 M Tris-HCl pH 6.8, 50 % Glycerol and 0.05 % bromophenol blue) was added

to the mixture and proteins were separated using electrophoresis as explained in section 2.5.2. After electrophoresis, gels were washed in transfer buffer (5.8 g Tris Base, 0.37 g SDS, 2.9 Glycine, 200 ml methanol) for 30 min to remove the HEPES buffer. The protein was subsequently transferred to Hybond-C Extra Nitrocellulose membrane (Amersham Biosciences) in transfer buffer in a semi-dry transfer blot cell (Bio-Rad) at a constant current of 11 V and 400 mA for 60 min.

Table 2.10 : List of antibodies used in this study

Name	Antigen	Dilution	Source
A-eEF1A	yeast eEF1A	1:5000	Dr. Jenna Hutton
α-eEF1B	yeast eEF1B	1: 4000	Munshi et al, 2001
α-eEF2	yeast eEF2	1:10000	Ortiz et al, 2006
α-eEF3	yeast eEF3	1:10000	Ortiz et al, 2006
α-eRF1	yeast eRF1	1:5000	Von der Haar and Tuite, 2007
α-eRF3	yeast eRF3	1:5000	Von der Haar and Tuite, 2007
α-Hex	Yeast Hexokinase	1:2000	Sigma
α-FITC	Rabbit antibody	1:4000	Sigma

After transfer, the membrane was incubated with TBS buffer (6.06 g Tris with pH 6.8, 8.766 g NaCl) with 5 % milk powder (w/v) for 30 min at room temperature. The membrane was incubated overnight at 4 ^{0}C with TBS buffer, 5 % milk powder and the appropriate primary antibody (Table 2.10) with 10 % sodium azide. All the primary antibodies were raised in rabbit. After incubation with the primary antibody the membrane was subsequently washed 3 times with TBS buffer. The washed membrane was incubated with a second primary antibody (control, anti-Hexokinase) in TBS buffer, 5 % milk, Tween

(0.05 %) and 10 % Sodium Azide for 1 h at room temperature. The membrane was then washed three times with TBS buffer. Then the membrane was incubated with Fluorescein isothiocyanate (FITC) labelled anti-rabbit secondary antibody, α-FITC (Sigma, Table 2.10) in 5 % milk, TBS buffer and 10 % Sodium Azide, for 1 h at room temperature. The FITC-conjugated secondary antibody is light sensitive, so all subsequent procedures were performed in the dark. The secondary antibody was raised in goat. After incubating with the secondary antibody, the membrane was further washed 5 times with TBS buffer before drying. The dried membrane was scanned using the Molecular Dynamics Typhoon 8600 scanner and the fluorescence was quantified using ImageQuant software (GE Healthcare).

2.10. Polysomal gradient analysis

Polysomal gradient profiles were generated based on the protocol adapted and modified from Sagliocco et al., 1993.

2.10.1. Cell collection

20 ml of growth medium was inoculated with yeast, grown overnight at 30 ^{0}C (200 rpm) then diluted in 100 ml of medium to an OD_{600} of 0.2. The culture was further grown at 30 ^{0}C (200 rpm) and collected at OD_{600} of 0.5. A final concentration of 100 µg/ml of cycloheximide was added directly to the flask and mixed thoroughly to arrest the activity of ribosomes on the translating mRNA by inhibiting translation elongation. Subsequently, cells were harvested by centrifugation at 4000 rpm at 4 ^{0}C for 5 min. The cells were washed twice in sterile water and stored as pellets at -80 ^{0}C.

2.10.2. Cell lysis

The cell pellets were thawed and resuspended in 10 ml of cold cell lysis buffer (10 mM Tris-HCl pH 7.4, 100 mM NaCl, 30 mM $MgCl_2$) with 100 µg/ml of cycloheximide. Cells were harvested by centrifugation at 4000 rpm at 4 ^{0}C for 5 min. The cell pellet was resuspended in 600 µl of cell lysis buffer and transferred into a 2 ml micro-tube. An equal volume of glass-beads (Acid treated from Sigma) were added and cells were broken with 6 rounds of vortexing and cooling (30 sec each). Then the mixture was centrifuged at 12000

rpm at 4°C for 20 min and the supernatant was collected and transferred to clean 1.5 ml eppendorf tubes.

2.10.3. Preparing sucrose gradients

14%, 26%, 38% and 50% of sucrose solution was prepared in sucrose gradient buffer (50 mM Tris.HCl pH 7.4, 50 mM NH_4Cl, 12 mM $MgCl_2$) to make 14 - 50 % sucrose gradient for separating the ribosome subunits and polysomes. 1 mM Dithiothreitol (DTT) was added to each of the solutions. 2.75 ml aliquots of each sucrose solution were poured into Beckman SW40 ultracentrifuge tube placed in dry ice. The densest solution was poured first followed by other sucrose solutions, each aliquot being frozen before addition of the next.

2.10.4. Gradient centrifugation

Sucrose gradients were thawed at room temperature. 500 µl of the cell lysate was very carefully applied to the top of the gradient. The centrifuge tubes were balanced by adding extra cell lysis buffer if required. Samples were placed in pre-cooled SW 40Ti Beckman rotor. The gradients were centrifuged at 4 °C at 39000 rpm for 2.5 h in Beckman optima Le-80K centrifuge.

2.10.5. Polysome trace and fraction collection

Polysome traces were collected using the density gradient fractionator (ISCO Model 185). The sucrose gradients were displaced upwards by high density (55%) sucrose solution pumped through a syringe needle piercing the base of the tube, which push the gradient very slowly upwards, passing a UV detector and through to collection in 2 ml tubes. The UV detector measures the concentration of the gradient solution (A280) and the reading is traced on a chart. Subsequently the fraction is collected in the pre-arranged tubes. 2 ml micro-tubes were labelled and arranged on the fraction collector. For these measurements the UV/rotor was set with a sensitivity of 2.0 or 1.0, baseline adjusted to 4.0, lamp current

to 200 A, rise to 2.5 sec, chart speed of 15 cm/h, timer/counter 0.6 ml, and flow rate 0.375 ml/min.

2.11. In vivo protein synthesis

In vivo protein synthesis of exponentially growing yeast cells was measured using a method adapted from Sachs and Deardorff (1992). Yeast cells growing with an OD_{600} of ~ 0.4 were diluted to an OD_{600} 0.1 in pre-warmed YNB-Met medium with concentration of doxycycline ranging from 0 – 100 ng/ml. The culture was incubated at 30 ^{0}C for 15 min. Labelling mixture with [^{35}S]-methionine was prepared by adding 1.5 µl [^{35}S]-methionine (14.3 mCi/ml, Perkin Elmer) to 100 µl of the freshly prepared 2 times concentrated TEM (TCA 25%, 0.25 M EDTA and 166 mM methionine). Five fresh 2 ml micro-tubes were prepared containing 0.5 ml of TEM to collect the samples. After 15 min of growth in at 30 ^{0}C, 100 µl of the labelling mixture was added to the culture. 0.5 ml samples were taken at 0 min and every 2 minutes thereafter for a total of 10 minutes. The samples were transferred to the 2 ml micro-tube containing 500 µl TEM. These samples were vortexed for 3 sec and heated at 95 ^{0}C for 20 min before cooling on ice for 10 min. The samples were filtered through GF/C filters (Whatman) in a vacuum manifold (Millipore) and the filtered were washed first with 2 ml of the TEM and then with 2 ml of 95 % (w/v) ethanol. The filters were collected in fresh 2ml micro-tubes and transferred to clean scintillation vials. 1.5 ml of Optiphase HiSafe 3 scintillation solution (Perkin Elmer) was added to each vial and [^{35}S] incorporation was counted on a scintillation counter (Perkin Elmer) for 1 min.

2.12. Dual luciferase assay

Dual luciferase assays were performed with the dual luciferase reporter assay system (Promega). The protocol was adapted as described by McNabb et al., 2005. All the reagents were prepared as described by the manufactures. The *tetO7* promoter strains containing the pDLV-L2/L0 plasmid for the luciferase assay were grown overnight in YNB-Met-His media with 2 % glucose. The culture was diluted to an OD_{600} 0.2 and grown for 8 h. The strains without doxycycline were diluted to OD_{600} 0.01 and those with doxycycline were

diluted to an OD_{600} 0.02 for 17 h. Different concentrations of doxycycline were used to repress protein expression levels to 80% and 60% of the wild type. The OD_{600} was measured after 17 h and the growth rate was measured as described in the section 2.7. Based on the growth rate, the strains were diluted to an OD_{600} such that the OD_{600} reach 0.4 after 4 h of growth. 180 µl of the culture at exponential growth stage (OD_{600} ~ 0.4) was collected in four 1.5 ml eppendorf tubes for the assay.

45 µl of the 5 x passive lysis buffer (PLB) was added to the 180 µl of cells and votexed for 20 sec for cell lysis. After allowing cell lysis for another 10 sec, 5 µl of this cell lysate was added to 40 µl of the firefly luciferase reagent (LarII) in the luminometer tube. Samples were allowed to equilibrate for 10 sec and then, the firefly luciferase activity was measured using the luminometer (BERTHOLD Technologies Lumat LB 9507). After the measurement of the firefly luciferase activity, 45 µl of the *Renilla* luciferase reagent and firefly quenching (STOP & GLO) reagent (1 µl of Stop & Glo Substrate and 100 µl Stop & Glo Buffer) was added immediately. After allowing 10 sec of equilibration time, the Renilla luciferase activity was measure using the luminometer.

Chapter 3

Spatial Distribution of elongation and release factors

3.1. Introduction

3.1.1. Visualisation and distribution of translation factors

Comprehensive knowledge of the intra-cellular localization of proteins is crucial to understanding their functional roles and interactions. Translation factors are highly expressed in all stages of cellular growth and information about their distribution within the cell is relevant to translation control. Previously, the localisation of most yeast proteins, including translation factors, has been investigated using GFP or epitope-tagging methods (Huh et al., 2003, Kumar et al., 2002). In these global studies most of the translation factors are shown to be located in the cytoplasm. However, evident has been presented that the initiation factors eIF2 (α and γ subunits) and eIF2B (γ and ε subunits) have a specific localisation in the cytoplasm which results in translational regulation (Campbell et al., 2005). Moreover, the eIF2 components were found to shuttle between specific foci within the cytoplasm and a less restricted, diffuse cytoplamic pool for GDP to GTP exchange. However, other initiation factors, such as eIF4A1, eIF5, eIF4G1, eIF4E, and eIF3b were observed to be distributed in the cytoplasm without any apparent heterogeneity (Campbell et al., 2005).

In the high throughput global analysis of the distribution of yeast proteins fused GFP (Huh et al., 2003**,** http://yeastgfp.yeastgenome.org/), eEF1A has been shown to be homogenously

distributed in the cytoplasm, although nothing is known about the other elongation and release factors. Yeast genome wide epitope-tagging with GFP shows that all the elongation factors are located in the cytoplasm and eRF3 was predicted to be located in the nucleus (http://bioinfo.mbb.yale.edu/genome/localize/, Kumar et al., 2002). However, this study failed to determine the localisation properties of eIF2 (α and γ subunits) and eIF2B (γ and ε subunits). Therefore at present the distribution of elongation and release factors remains unclear.

3.1.2. Aim of this work

In this study, sub-cellular localisation of the translation, elongation and termination factors within yeast (*Saccharomyces Cerevisiae*) was examined using the tetra-cystiene motif (TCM) and GFP fluorescent tagging methods. For visualisation of protein distribution in live cells the tag of choice (TCM or GFP) was fused to the C-terminus of the genomic copy of the elongation and termination factor genes. Tags can be fused either to the N or to the C terminal of target genes, a choice that can be significant in obtaining accurate localization data. N-terminal reporter fusions may disrupt the promoter sequences, and can result in anomalous protein localizations. C-terminal tagging allows gene expression levels to remain under the control of the endogeneous promoter sequences, ensuring proteins are expressed at wild-type levels, but many still affect protein function and/or localization.

3.2. Results

3.2.1. Construction and phenotype analysis of Δ*EFT2* strains

In *S. cerevisiae*, the elongation factor eEF2 is encoded by two genes *EFT1* (chromosome XV) and *EFT2* (chromosome IV). Pairwise sequence alignment of these two genes using ClustalW2 (http://www.ebi.ac.uk/Tools/clustalw2/index.html) shows 99% sequence identity. Sequence alignment of the proteins coded by both of the genes shows 100% sequence identity, indicating that both of the genes encode the same protein. Therefore, one of these genes, *EFT2*, was deleted so that EF2 protein was encoded by only one gene which could be tagged using TCM to explore the cellular distribution. This strategy confirmed that all of the eEF2 expressed had a TCM tag.

The loxP-*KanMX*-loxP gene disruption method was used to construct the Δ*EFT2* strain (Figure 3.1). The gene disruption cassette (1.7Kb) with the *KanMX* gene was PCR amplified from the plasmid pUG5 using primers EFT2-Del-F and EFT2-Del-R (Table 2.4) and transformed into PTC41 yeast cells (Figure 3.2a). The *KanMX* cassette, with gene specific flanking regions, replaces the *EFT2* gene from the yeast chromosome IV. Subsequently, the *KanMX* gene from the Δ*EFT2* strain was removed using the single recombinase technique. The Δ*EFT2* strain was transformed with the *cre* expression plasmid pSH47 under the control of the inducible *GAL1* promoter. Expression of *cre* recombinase was induced by growing the transformed cells in YP galactose medium. The *cre* gene is expressed within 2 h of growth in galactose media thereby the recombinase on the *KanMX* gene cassette results in the excision of the *KanMX* gene from the yeast chromosome. Elimination of *KanMX* and *EFT2* genes were further confirmed by PCR using EFT2-Del-Check-F and EFT2-Del-Check-R primers (Figure 3.2b).

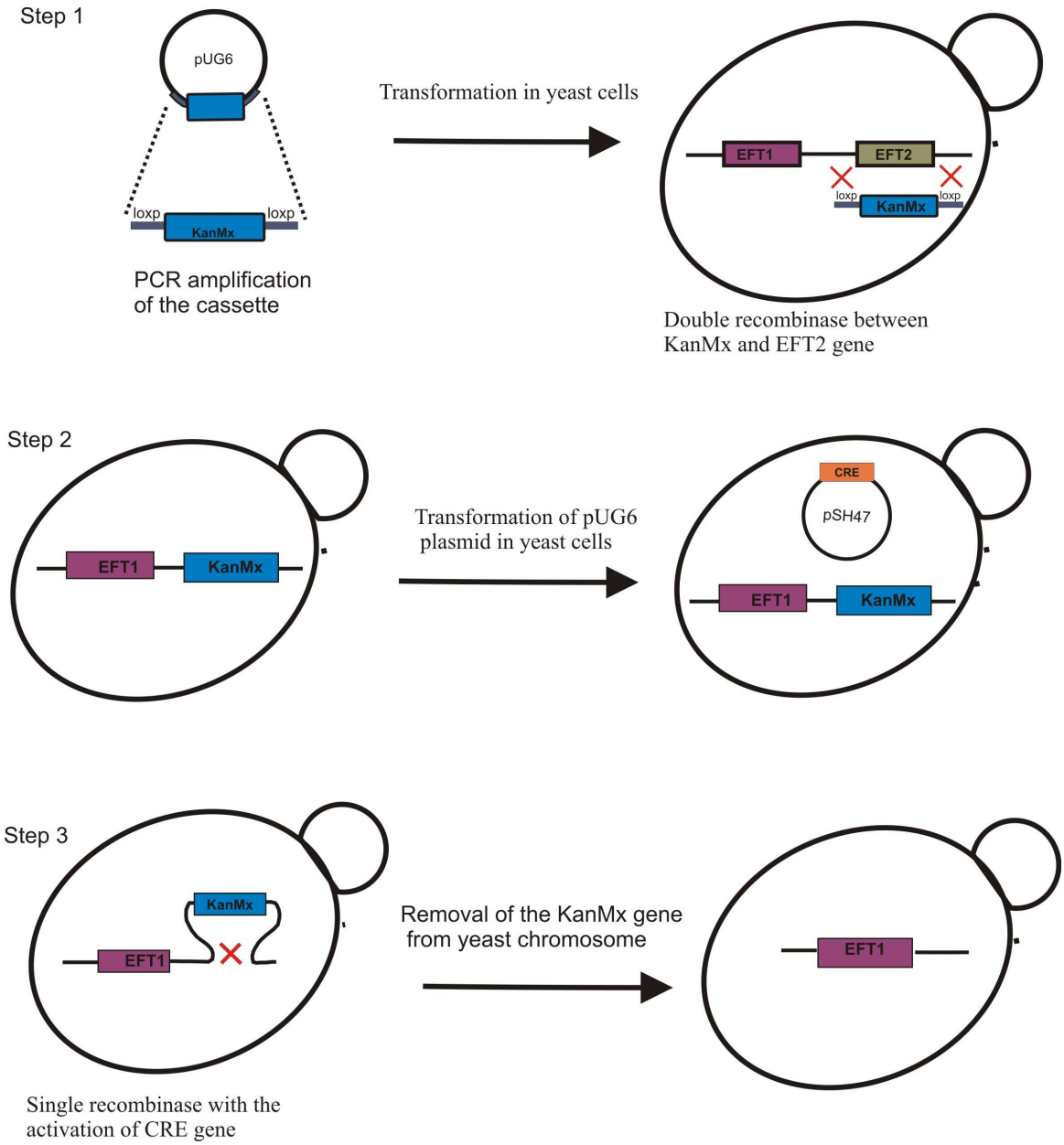

Figure 3.1: Schematic representation of the gene deletion method using loxP double recombinase. Step 1: *KanMX* and loxp cassette was PCR amplified from the pUG6 plasmid and transformed into the yeast cell. Due to the double recombinase activity, the *KanMX* cassette replaced the *EFT2* gene from the yeast chromosome. Step2: pSH47 plasmid with the *cre* gene was transformed into the Δ*EFT2* strain and grown in galactose media to activate the *cre* gene. Step 3: expression of the *cre* gene activates the single recombinase to remove the *KanMX* gene from the yeast chromosome.

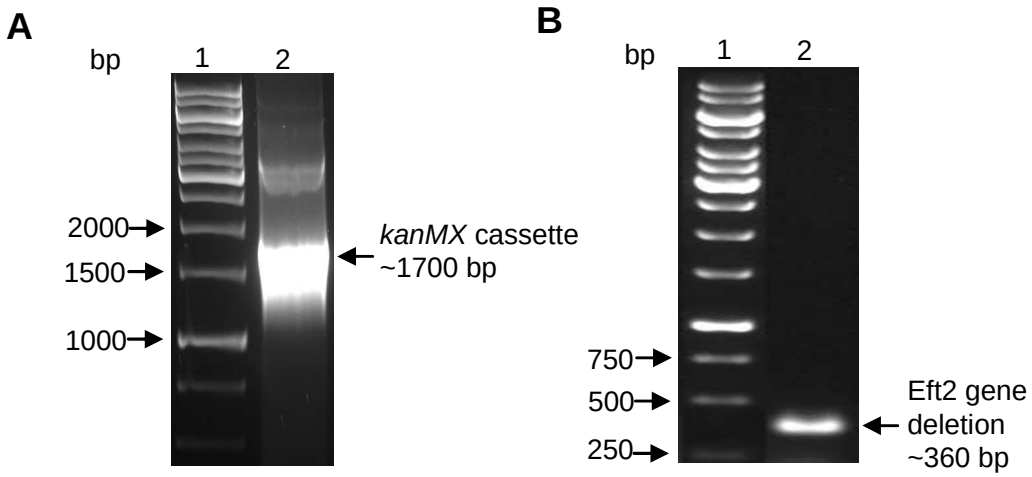

Figure 3.2: PCR confirmation of the Δ*EFT2* strain construction. A) Agarose gel showing the PCR amplification of loxP-*KanMX*-loxP gene cassette (1.7 Kb) from pUG6 plasmid. This cassette was transformed into the yeast cell to replace *EFT2* gene. The first lane is the DNA ladder (Generuler) and the second lane is the PCR product of the PUG6 plasmid using EFT2-Del-F and EFT2-Del-R primers B) PCR confirmation of *EFT2* gene deletion (~350b) (lane 2). The PCR was prepared using the genomic DNA of the Δ*EFT2* strain with EFT2-Del-Check-F and EFT2-Del-Check-r primers.

After construction of the Δ*EFT2* strain, the growth phenotype was analysed by comparing it with that of the wild type. The growth comparison shows that the Δ*EFT2* strain has 80% wild-type growth rate (Figure 3.3a). The expression level of the eEF2 protein in the Δ*EFT2* strain and wild-type cells were measured by Western blotting using a polyclonal antibody (Table 2.5) against the eEF2 protein. The expression levels of eEF2 in all strains were calculated relative to a loading control (Hexokinase) which is identified on these blots using a specific antibody. This study shows a 25% reduction in the eEF2 level compared to the wild-type (Figure 3.3b). The Δ*TEF2* strain (Constructed by Helena.Firczuk, University of Manchester) was used to generate a eEF1A-TCM strain to study the cellular localisation of eEF1A factor. Along with Δ*EFT2* strain, the growth phenotype of Δ*TEF2* strain was also analysed relative to that of the wild-type cells.

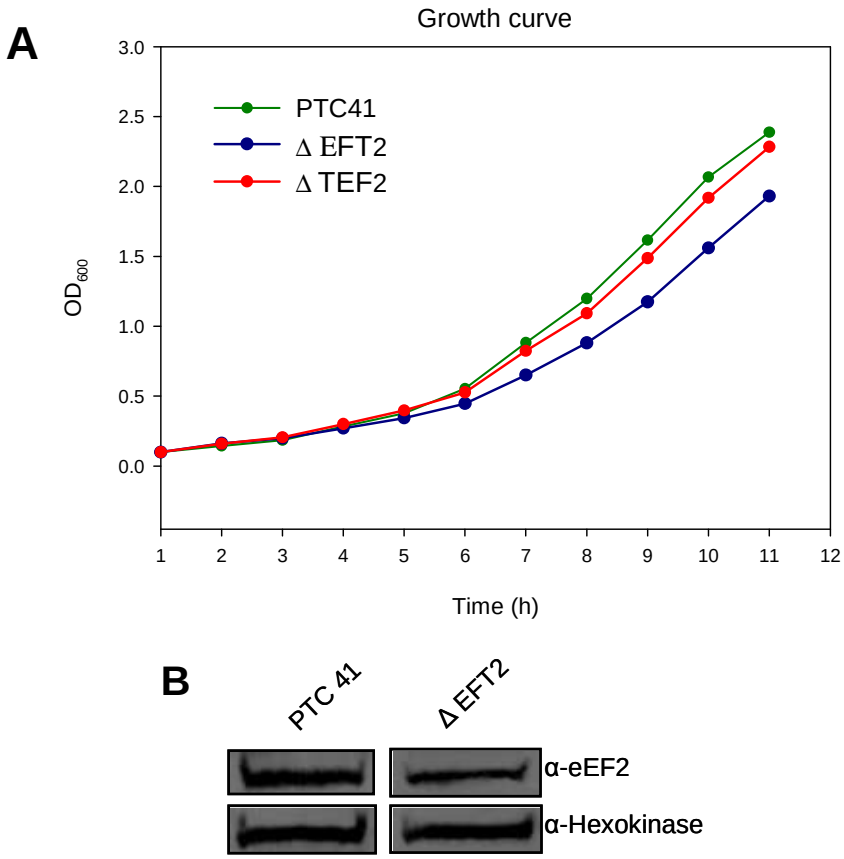

Figure 3.3: Growth rate analysis of Δ*EFT2* strains. A) The growth curve analysis of the Δ*EFT2* strain shows a 20% reduction in growth when compared to that of the wild type. All growth points were taken as the average of three independent experiments B) Level of eEF2 protein in wild-type and Δ*EFT2* strain. There was a 25% reduction in eEF2 protein level due to the deletion of *EFT2* gene that codes eEF2.

3.2.2. Construction of TCM-tagged elongation and release factors

Cellular localisation of the translation elongation and release factors was explored using the TCM tag. The TCM tag was amplified from the pNEWTC plasmid (Martin et al., 2005) using gene specific primers and the cassette was chromosomally integrated and fused to the C terminus of the elongation and release factors genes.

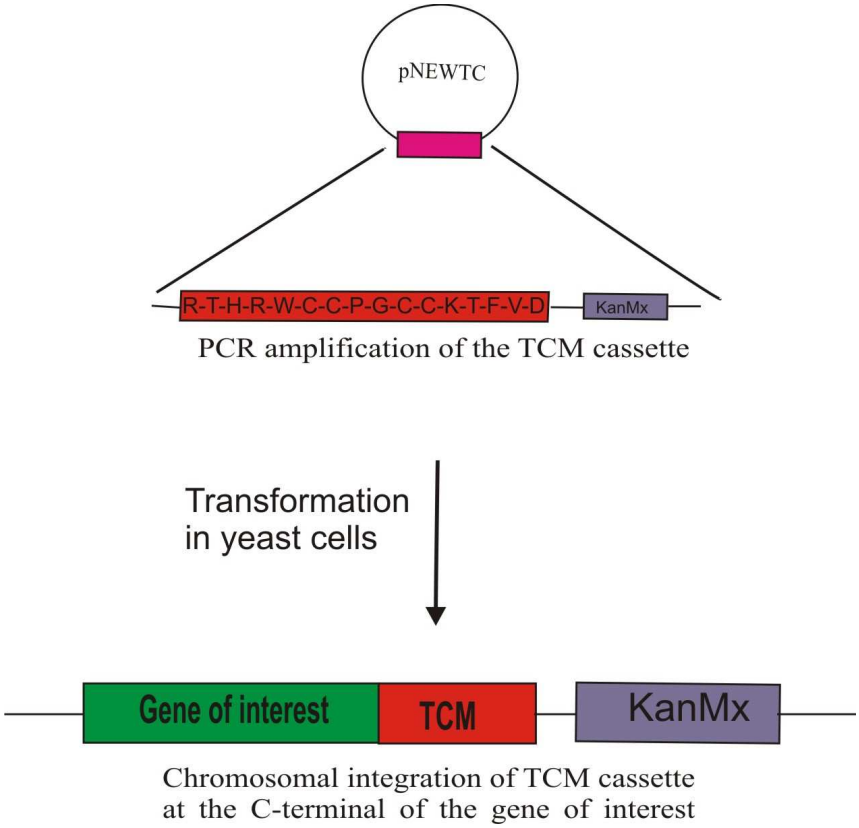

Figure 3.4: Schematic illustration of the chromosomal fusion of the TCM-tag to the C-terminus of the elongation and release factor gene. The TCM cassette including the *KanMX* gene and TCM tag was PCR amplified using gene specific primers and was transformed into the yeast cells. The TCM tag was inserted between the ORF and the stop codon of the yeast gene. The strains with TCM tags were selected by growing on YPD with G418.

All the translation elongation and release factor genes were C-terminally fused with TCM tags (Figure 3.4) using primers listed in Table 2.5. Primers were designed such that the TCM tag was integrated between the open reading frame and the stop codon. Integration of the TCM tag was confirmed by growing the strains on selective media of YPD with G418 (150 μg/ml). The integration of the TCM tag at the desired location was further confirmed by PCR amplification (Figure 3.5).

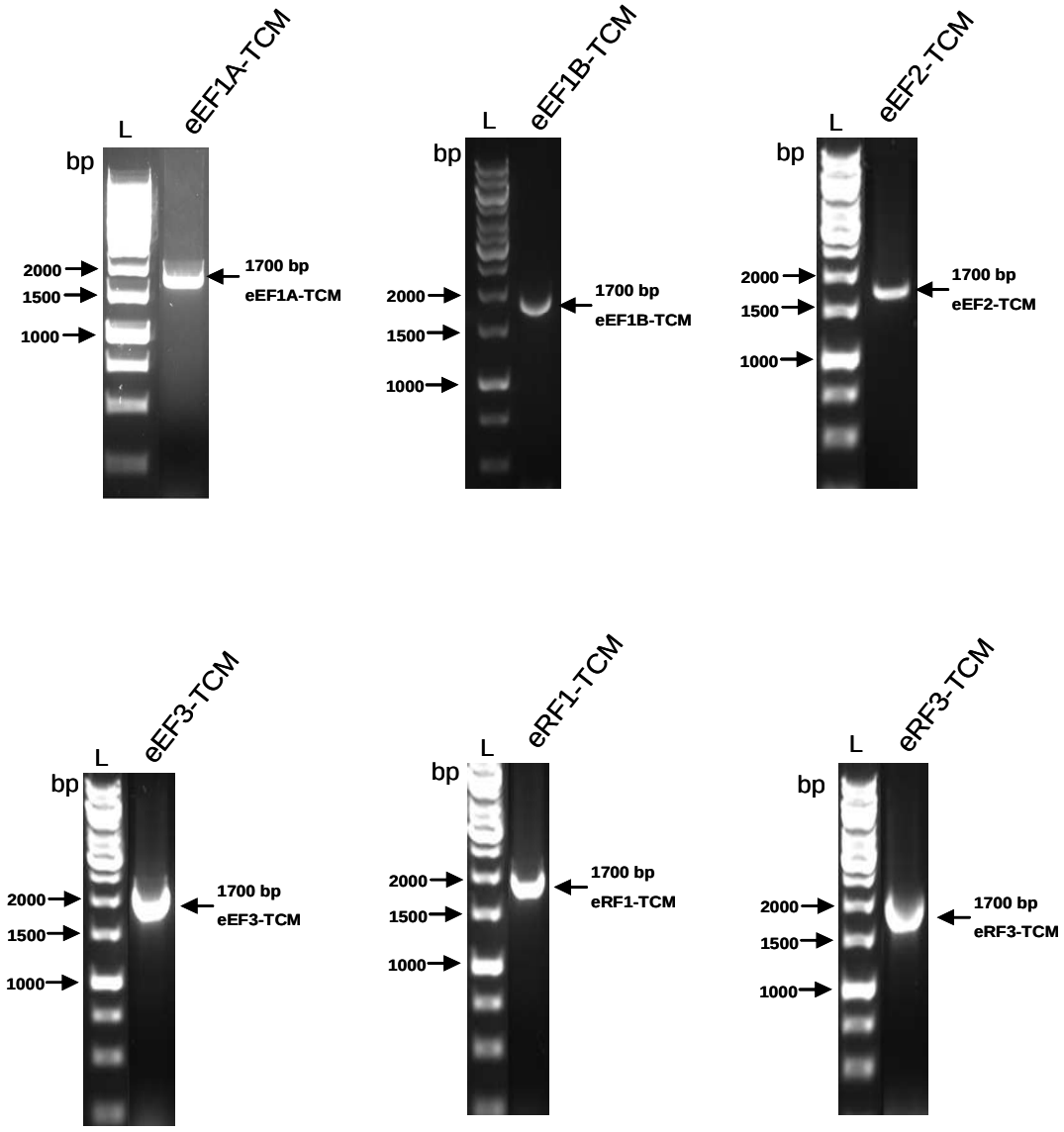

Figure 3.5: PCR confirmation of the TCM integration in translation elongation and release factors (1.7 Kb). Gene specific primers were used to confirm the TCM cassette with *KanMX* gene. Δ*TEF2* strain was used to construct the eEF1A-TCM strains and Δ*EFT2* strains were used to construct the eEF2-TCM strains. All the remaining TCM-tagged strains were constructed in a PTC41 wild-type background.

3.2.3. Phenotype analysis of TCM tagged elongation and release factor strains

The growth rates of all the strains containing a chromosomally TCM-tagged elongation or release factor were analysed to determine any possible growth deficiency. The growth

analyses revealed that the eEF1A-TCM strain grew at a similar rate to the wild-type strain, whereas eEF1B-TCM strains showed slightly slower growth (Figure 3.6a). The protein levels of both eEF1A and eEF1B in the TCM strains were compared with those found in the wild-type cells. There were no differences evident in the eEF1B protein level in the Western blot data (Figure 3.6b).

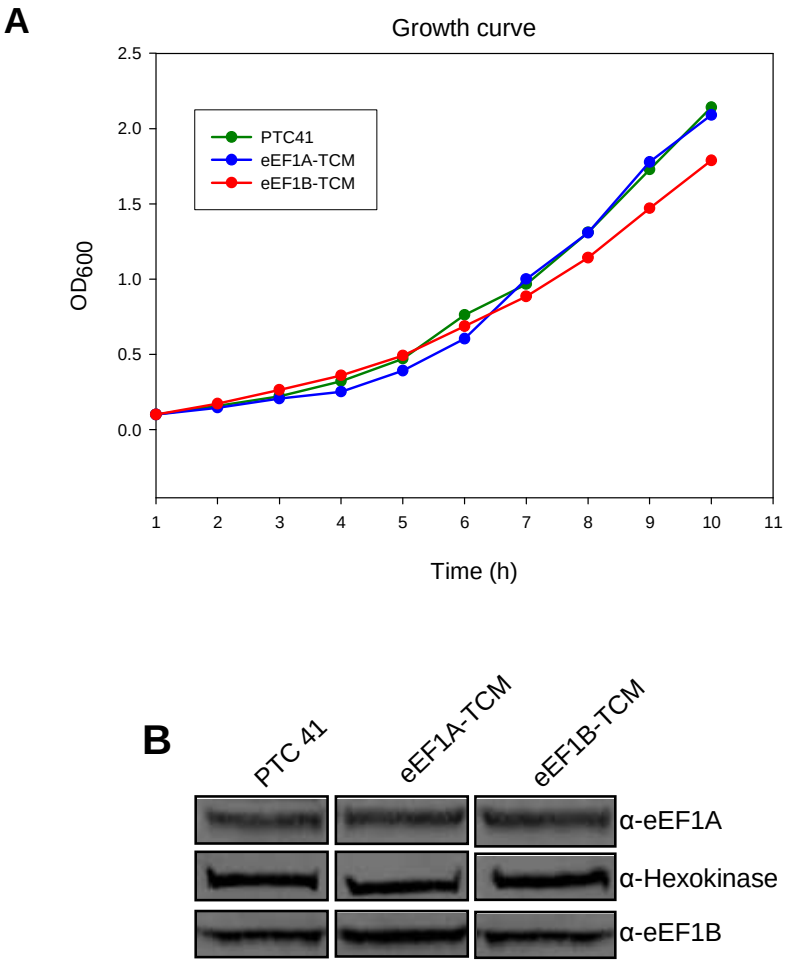

Figure 3.6: Phenotype analysis of eEF1A-TCM and eEF1B-TCM. A) The growth rates of eEF1A-TCM strains are comparable to that of the wild-type strain. This reveals that the eEF1B-TCM strain showed a slight decrease in growth B) Western blot analysis of the protein expression level of eEF1A and eEF1B in wild-type and TCM strains. There were no reductions in the level of eEF1A and eEF1B proteins in eEF1A-TCM and eEF1B-TCM strains due to TCM integration.

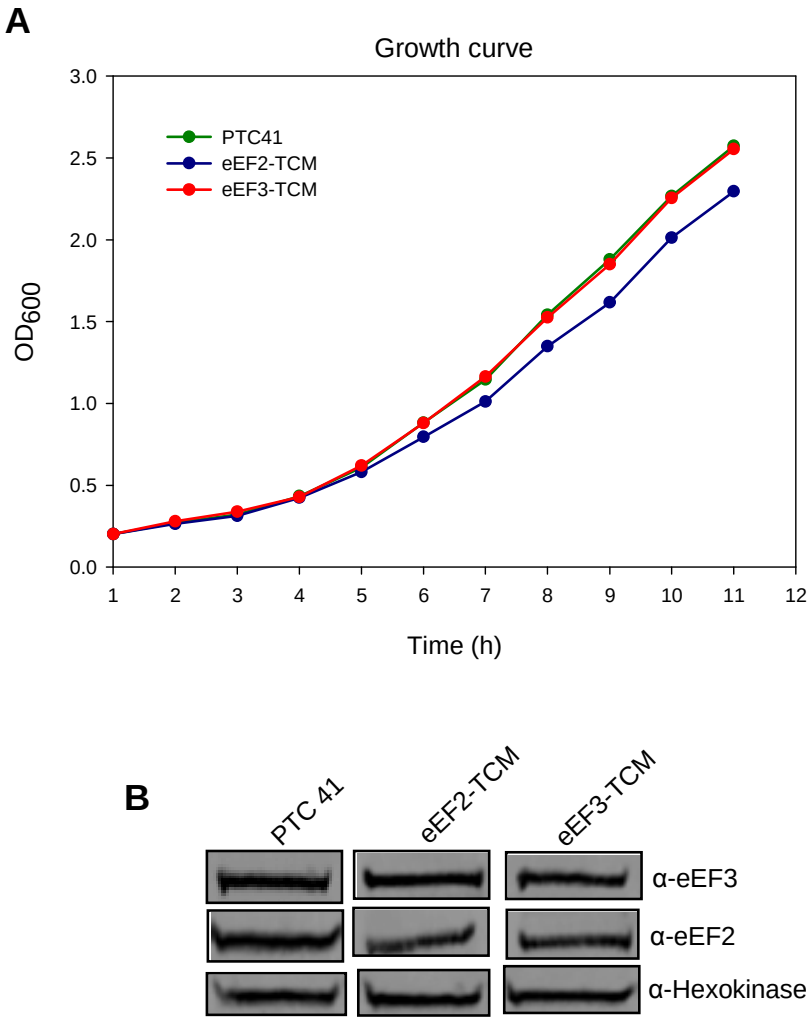

Figure 3.7: Phenotype analysis of eEF2 and eEF3 TCM strains. A) The growth curves of eEF2-TCM and eEF3-TCM were compared with that of the wild type. eEF2-TCM showed slower growth which is consistent with deletion of the *EFT2* gene however no growth difference was observed in the eEF3-TCM strain. B) Western blotting of cell extracts and probing with EFT2 and eFT3 antibodies. Hexokinase is a loading control. There was no significant difference in the cellular level of eEF3 factor in eEF3-TCM strain. Average of three independent experiments shows a slight decrease (8 %) in the level of eEF2 observed in the eEF2-TCM strain.

The growth curves of eEF2-TCM and eEF3-TCM strains were compared with that of wild-type cells (Figure 3.7a). There was no apparent difference in the growth rate of eEF3-TCM strains when compared to wild-type cells. However, the eEF2-TCM strains showed slightly slower growth which was also observed in the Δ*EFT2* strain. The eEF2-TCM strain showed

a consistent reduction in protein level. This degree of reduction in protein expression was similar to that observed upon deletion of *EFT2* (Δ*EFT2* strain) while the eEF3 level remained the same in both wild-type and the eEF3-TCM strain (Figure 3.7b). This indicates that the TCM tag is not interfering with any functional or structural properties of the factors.

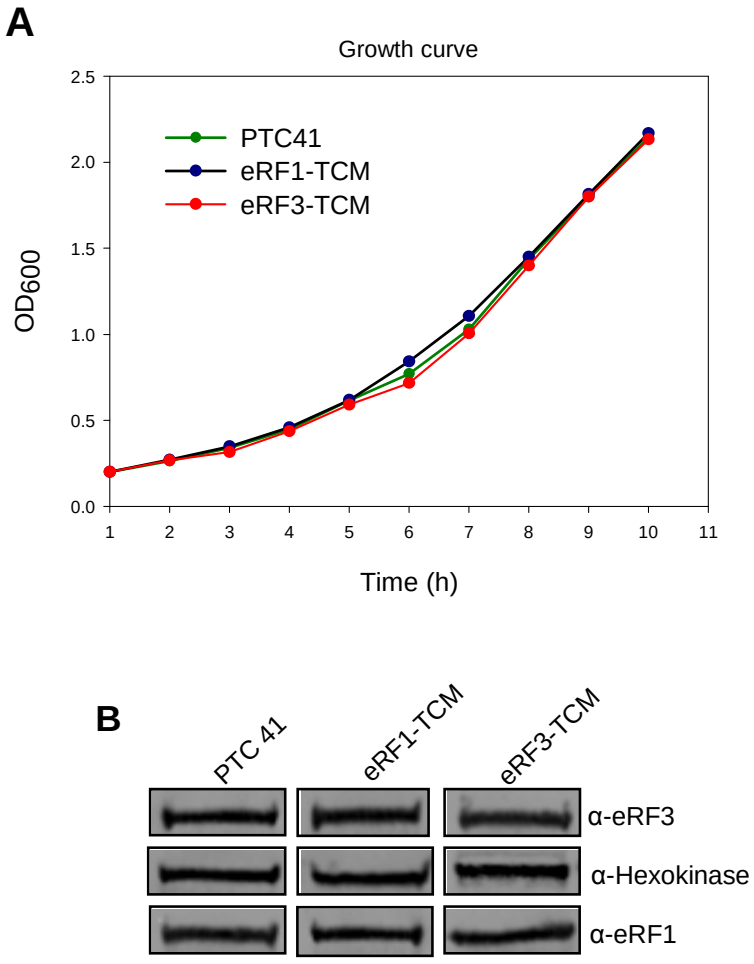

Figure 3.8: Phenotype analysis of eRF1 and eRF3 TCM strains. A) The growth curves of TCM-tagged release factors showed no apparent difference in growth rate compared to wild type. B) The Protein level of the release factors was determined and compared with that of the wild-type and Hexokinase was used as the control to determine the comparative level of the release factors. There were no decreases in the levels of either eRF1 or eRF3. This confirms that the integrated TCM tag is not affecting the expression level of release factors.

The release factors, eRF1 and eRF3 were also C-terminally tagged with TCM. The growth rates of the two strains were also compared with the wild-type strain. There were no differences in the growth rate or protein level of the strains containing eEF1-TCM or eRF3 compared to un-tagged wild-type strains (Figure 3.8a and 3.8c).

3.2.4. Cellular morphology and translational control

Previous studies have shown that changes in the protein expression levels of translation factors can have a significant influence on cell morphology (Munshi et al., 2000) and can influence translational regulation (Gross and Kinzy 2007). The cell morphology of each of the TCM tagged elongation and release factor strains was analysed to identify differences in the cell shape or size. Average cell diameter was measured using the Cellometer Auto M10 software (Cellometer, Peqlab) (Table 3.1). For all the TCM strains, the average cell diameter was smaller than the wildtype. For further verification, cells were further categorised into sub-populations on the basis of cell diameter. Cells were categorised as small: with cellular diameters less than 5µm, average: with cellular diameters between 5-10 µm and large: with cellular diameters larger than 10 µm. During logarithmic cell growth 95% of the cells are either small or average, indicating that the cells are actively budding, whereas in stationary growth phase 80% of the cell population is either average or large indicating that the cell division has decreased. This observation confirmed that there is no apparent difference in the cell morphology when compared to that of the wild-type (Figure 3.9).

Table 3.1: Average cell diameter of TCM tagged translation elongation and release factors compared to the wild-type cells in stationary and log phase.

Growth phase	PTC41	eEF1A-TCM	eEF1B-TCM	eEF2-TCM	eEF3-TCM	eRF1-TCM	eRF3-TCM
Log	7.3	6.1	6.4	6.6	6	5.9	5.8
Stationary	7.7	7	5.9	7.1	6.2	5.8	6.6

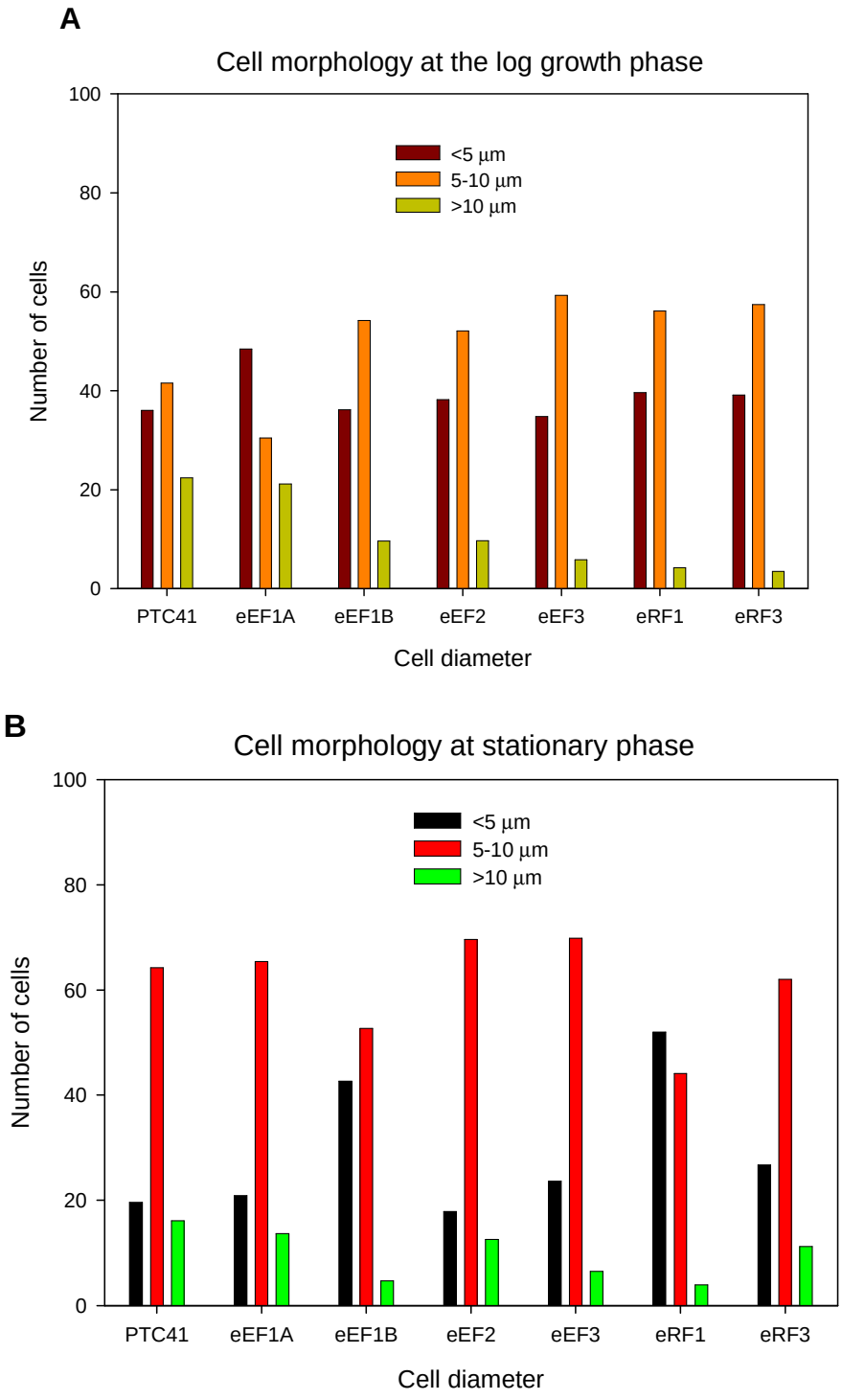

Figure 3.9 : Cell size distribution of strains containing TCM-tagged factors compared to that of the wild-type cells. A) during logarithmic growth more than 95% of all the TCM strains fall in the category of <5µm and 5-10 µm range indicating that the cells are actively dividing**,** B) whereas the stationary growth phase distribution of the cellular size indicate that more than 80% of the cells are in 5-10µm and >10µm category**.**

3.2.5. Interaction between eEF1A and actin

Previous studies have suggested that the binding of eIF1A to filamentous actin may regulate its organisation and thereby function in maintaining of the cell's shape. Also, over-expression of this factor in yeast has a very strong affect on cell morphology and the distribution of actin (Munshi et al., 2000). This putative interaction was investigated here to determine if the eEF1A-TCM strains exhibit any aberrant actin organisation. Calculation of the cellular diameter of the eEF1A-TCM-containing cells showed no difference in the cell size when compared with wild-type cells (Figure 3.9). The distribution of actin in the eEF1A-TCM strain was analysed using fluorescent rhodamine-conjugated phalloidin. Phalloidin selectively binds and stabilizes polymerized, filamentous actin without binding monomeric actin and its non-specific staining is negligible. Phalloidin is cell-impermeable, so cells to be stained have to be fixed and detergent-permeabilized. Cells to be stained should not be fixed with methanol because methanol fixation destroys the phalloidin-binding site on actin, thereby eliminating staining. Under normal conditions, budding yeast cells show a high concentration of actin at the tip of the bud (Munshi et al., 2000). Munshi and co-workers (2000) demonstrated that when eEF1A was over-expressed, actin filaments were disorganised and distributed along the length of the bud. Images presented in Figure 3.10 reveal that in eEF1A-TCM actin is concentrated at the bud tip with the same distribution as that observed in wild-type cells. This further shows that the TCM tag has no affect on cell morphology or the distribution of actin.

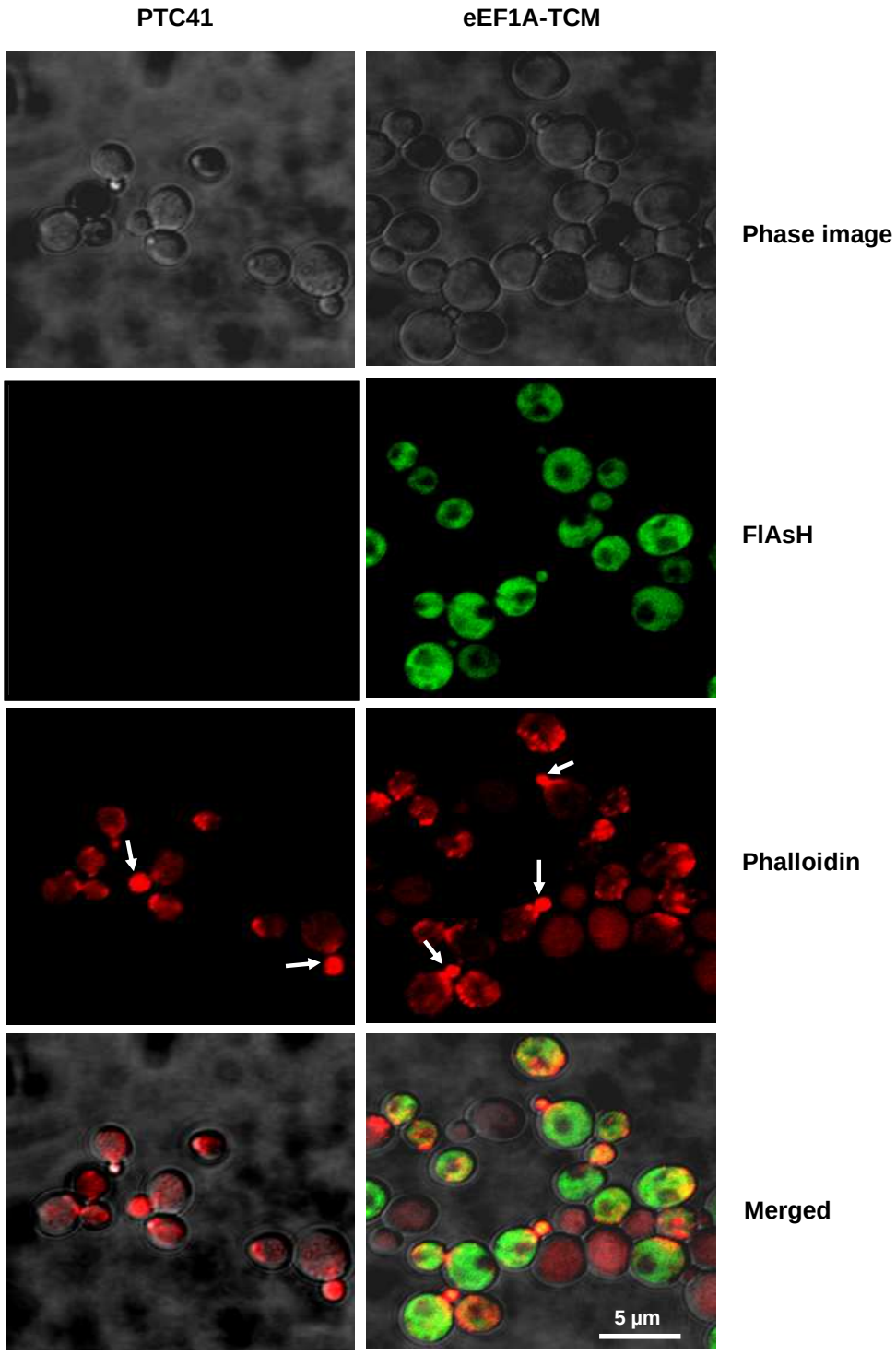

Figure 3.10: Rhodamine-phalloidin staining of actin in a yeast strain expressing eEF1A-TCM. Both wild-type and the eEF1A-TCM strains showed a concentrated distribution of the actin on the bud tip (shown using arrows). The actin filaments were not disorganised in the eEF1A-TCM strains confirming no effect on the actin distribution due to TCM tags.

3.2.6. Cytoplasmic distribution of elongation and release factors observed with TCM tag

TCM-tagged elongation and release factor strains were incubated with appropriate concentrations of FlAsH dye before microscopic analysis (Section 2.6). FlAsH is a cell-permeable dye that binds the four cysteine residues of the TCM-tag and upon binding fluoresces green. The concentration of FlAsH (2 uM-4 uM) was optimised for each strain to ensure maximal image quality and cell viability. Cells were treated carefully to avoid any stress conditions. In log phase, all the elongation factors and release factors were distributed homogeneously throughout the cytoplasm (Figure 3.11).

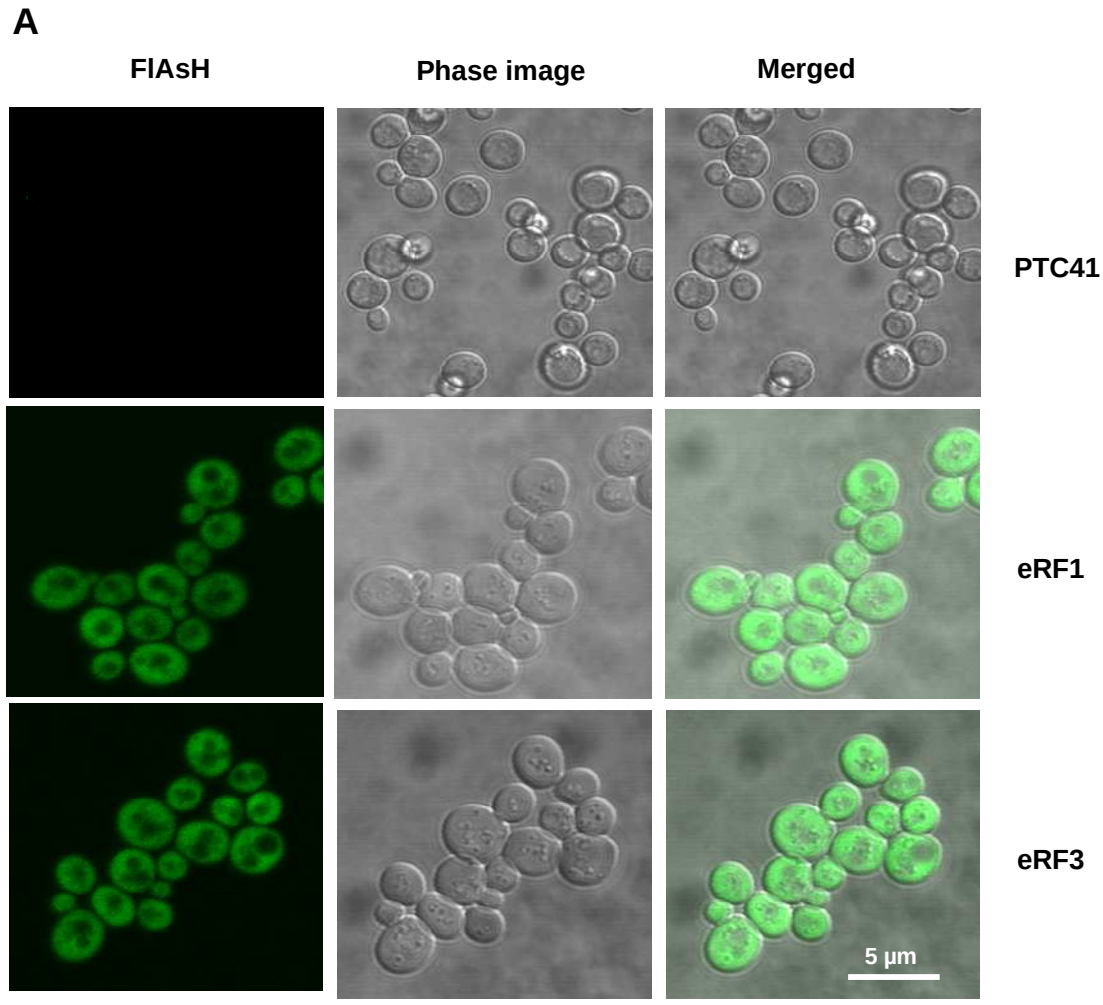

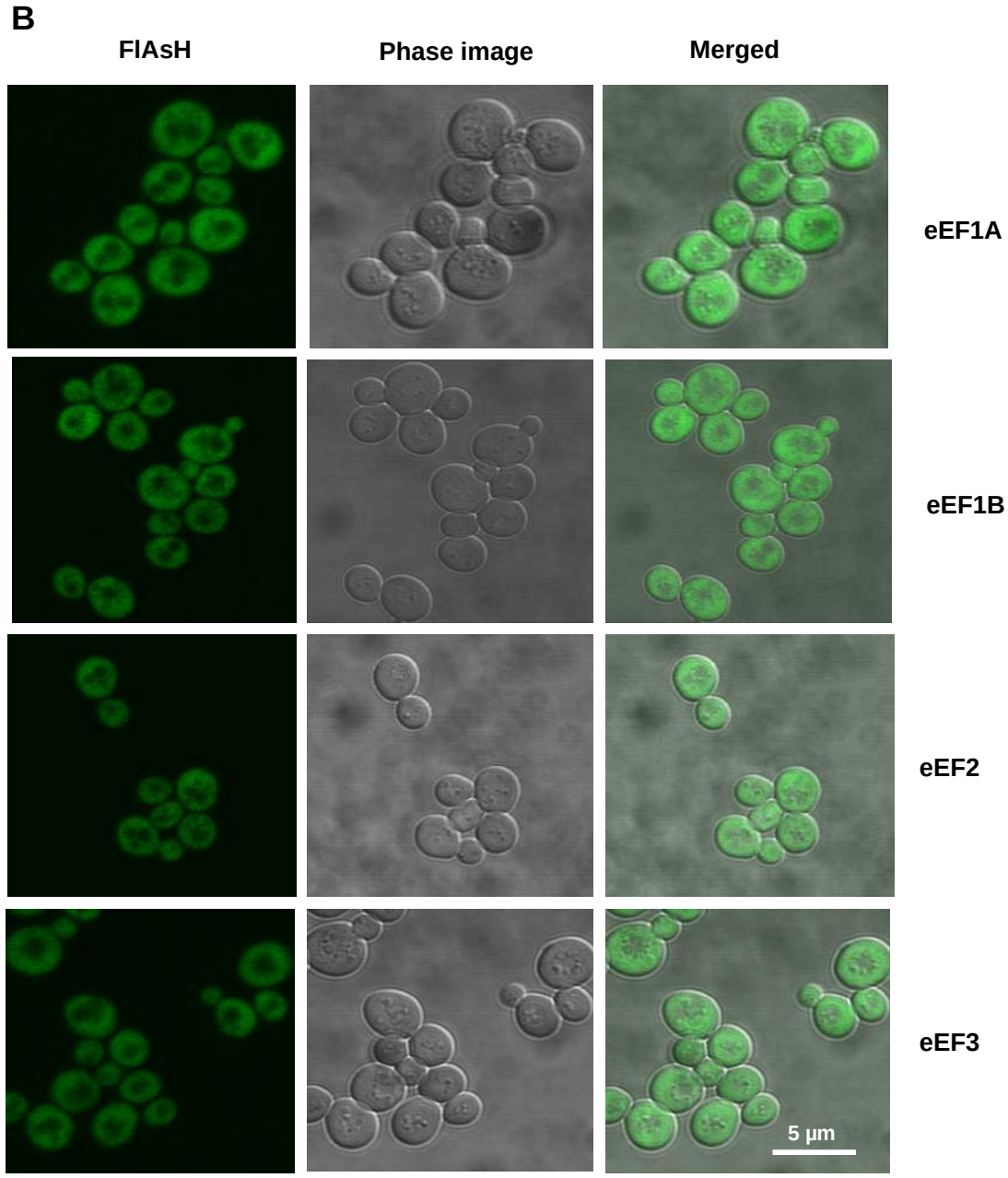

Figure 3.11: Distribution of TCM tagged translation factors in log phase. A) TCM tagged release factors B) TCM tagged elongation factors and wild type**.** All the factors were found to be homogenously distributed through out the cytoplasm.

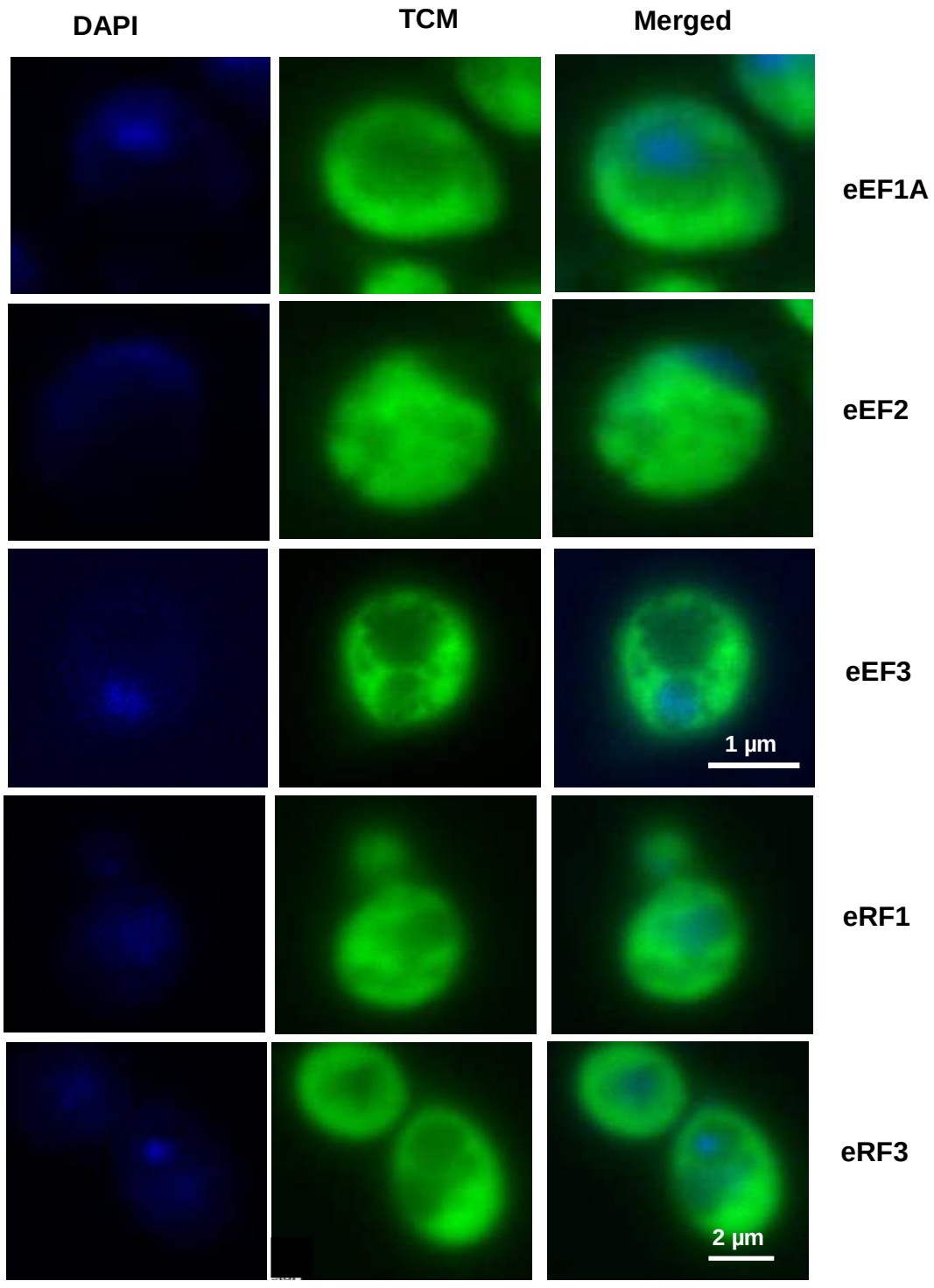

Figure 3.12 : DAPI staining of the TCM tagged elongation and release factors. There is no overlap between fluorescence, confirming that the translation factors are only distributed in the cytoplasm but not in the nucleus**.**

Yeast strains expressing TCM-tagged elongation and release factors were incubated with DAPI; a fluorescent dye that binds strongly to DNA and is therefore a good marker for the nucleus. The elongation and release factors were visualised with DAPI to determine any presence of the TCM-tagged factors within the nucleus. The images show no overlap between DAPI and TCM fluorescence indicating that the translation factors are not distributed within the nucleus (Figure 3.12).

3.2.7. Cytoplasmic distribution of elongation and release factors confirmed using GFP tag

The sub-cellular distribution of TCM-tagged elongation and release factors was compared with that of GFP-tagged elongation and release factors. The GFP tag was chromosomally fused to the c-terminus of the endogenous elongation and release factor gene. The growth phenotype of the GFP tagged elongation and release factors was compared with that of the wild-type strain (Figure 3.13). The strains expressing eEF1A-GFP and eEF2-GFP proteins contain both the genes coding these proteins. The GFP tags are fused with TEF1 and EFT1 genes respectively. There was no difference observed in the growth rate of these strains. These data confirm that the chromosomally GFP-tagged strains display a wild-type growth rate which indicates that the addition of a C-terminal GFP tag to these translation factors creates no adverse effects.

The intra-cellular distribution of the GFP-tagged elongation and release factors was examined in the log growth phase of the yeast strains. The images show that, as observed for the TCM-tags, elongation and release factors are homogenously distributed in the cytoplasm (Figure 3.14).

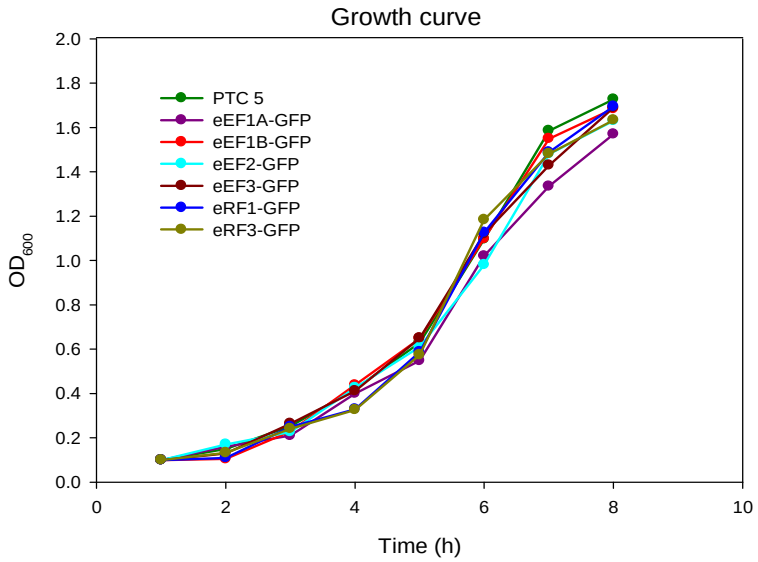

Figure 3.13 : The growth curve comparison of all the GFP-tagged elongation and release factors with wild-type cells. There was no significant growth phenotype observed in the GFP tagged strains.

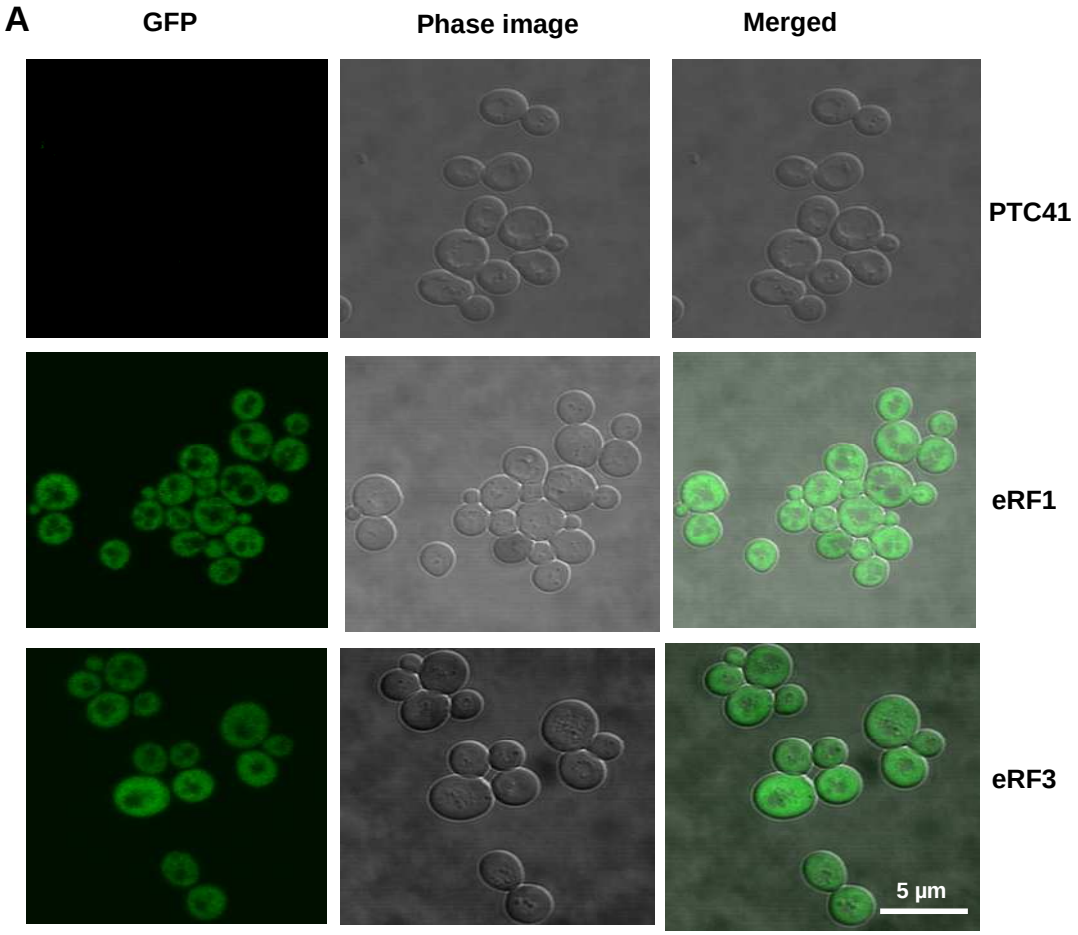

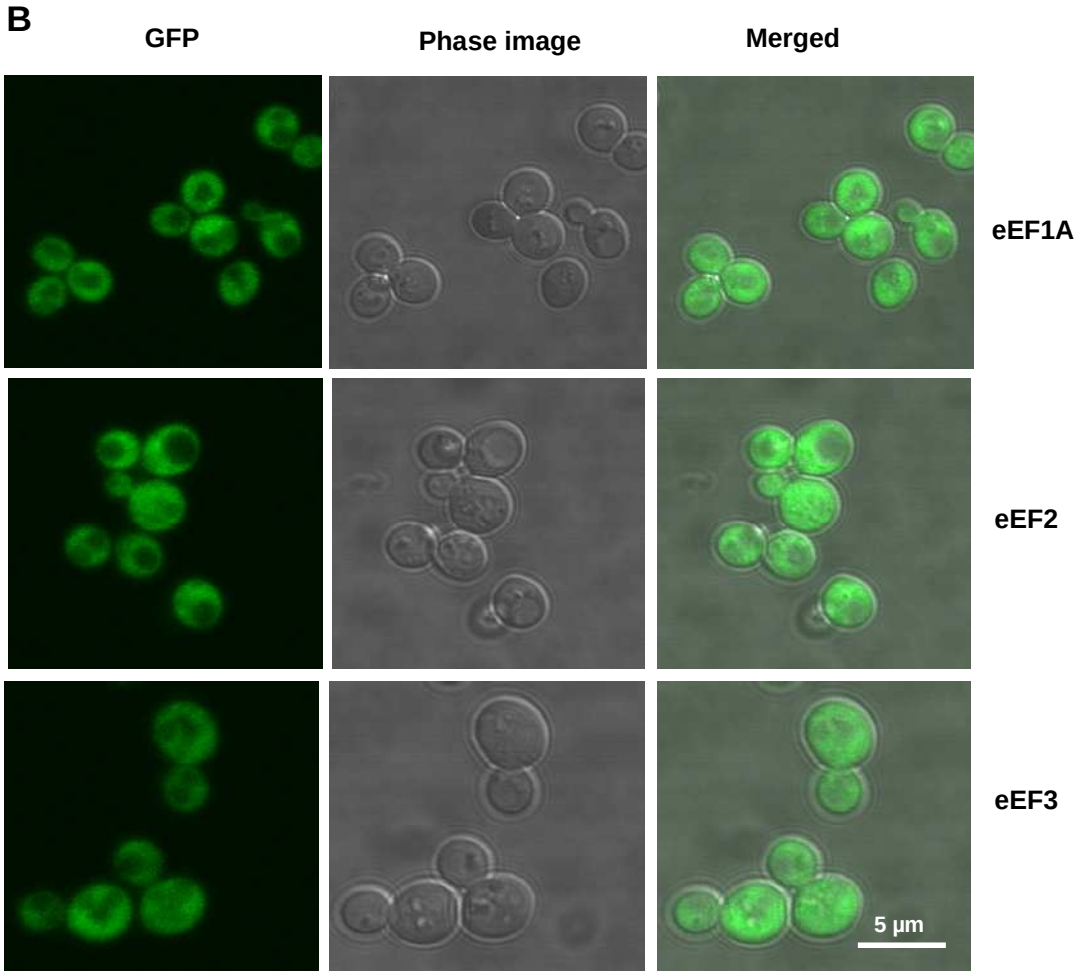

Figure 3.14: Distribution of GFP-tagged elongation and release factors in log phase. A) Distribution of release factors (b) elongation factors and wild type**.** All the factors were found to be distributed homogenously in the cytoplasm.

3.3. Discussion

3.3.1. Deletion of the *EFT2* gene causes growth defects and eEF2 factor reduction in *S. cerevisae*

In yeast, two genes code for the eEF2 translation factor, *EFT1* and *EFT2*. These genes produce peptides with 100% amino acid identity. The *EFT2* gene was deleted in this study and the *EFT1* gene was fused with the TCM tag for the localisation study. The growth curve analysis of the Δ*EFT2* strain shows a clear decrease in the growth efficiency. Moreover, a decrease in the eEF2 level was also observed in the Δ*EFT2* strain. Similar to the eEF2 factor, eEF1A is encoded by two genes, TEF1 and TEF2. However, defective growth was not observed in Δ*TEF2* strain. The growth defect observed in the Δ*EFT2* strain suggests that expression of eEF2 from a single copy gene is not sufficient for the endogenous protein expression level of eEF2 factor and normal growth of the yeast strain. This shows that both of the genes of eEF2 are required for normal growth of the yeast strains. Reduction in the protein expression level indicates that, even though both genes are expressing the same protein, the *EFT1* gene might be contributing about 75% and *EFT2* gene might be contributing about 25% of the total eEF2 protein in the yeast cell. The decrease in the growth rate exhibited by the Δ*EFT2* strain might be the result of decrease in the protein expression level of eEF2 factor. However, the reduction in the growth rate of these strains is unlikely to affect the distribution of the eEF1A and eEF2 factors within the cells. Δ*TEF2* and Δ*EFT2* strains were used to construct the TEF1-TCM and EFT2-TCM strains respectively.

3.3.2. TCM tags – a new fluorescent tag to investigate protein localisation in living cells

Visualising and tracking the proteins within the living cell to elucidate the distribution, interaction and dynamics of the proteins of interest has been of great importance. GFP has been used intensively to achieve these goals. But the relatively large size of GFP (23 kDa) is of concern as it could potentially affect the endogenous behaviour of the protein.

Specifically GFP can form dimers and trimers that may result in aberrant localisation of the fusion proteins, affect dynamics and protein-protein interaction. Work by the Tsien lab (Griffith et al., 1998) has generated the small (~10 a.a.) TCM-tag which would be expected to have a lower probability of causing the problems that might be associated with the larger GFP-tag. The TCM tag can be attached either at the C-terminal or N-terminal of the protein of interest. The tag binds to the membrane permeable dyes, FlAsH/ReAsH resulting in green/red fluorescence respectively upon binding.

For the first time, the yeast elongation and release factors were tagged with TCM to visualise their distribution. Phenotypic analysis of TCM-tagged yeast strains exhibited no effect on the cell growth, cell shape, tagged protein level or actin distribution. Only, TCM-tagged eEF1Bα exhibited slower growth when compared to wild-type cells. The cellular function of the eEF1Bα C-terminus domain is unknown. However, the slower growth observed with eEF1B-TCM strains might be due to an adverse effect of the C-terminal TCM tag on eEF1A-eEF1B complex formation (Figure 3.6a). This may cause slower translation, which results in slower growth. Another possibility is that the eEF1B is involved in another cellular process other than translation which is also affected by the C-terminal modification of the factor. None of the other factors showed any phenotypic changes due to inclusion of a TCM-tag indicating that the TCM-tag has no adverse effect on the strains and the tagged proteins are exhibiting normal behaviour.

3.3.3. Cytoplasmic distribution of elongation and release factors

Even though yeast translation initiation factors have been intensively studied for their distribution within the cell and the effect of their distribution over translation regulation, very little has been known about the distribution of elongation and release factors. In this study, for the first time, all yeast elongation and termination factors were C-terminally TCM-tagged to explore their distribution and contribution to translation regulation. The TCM-tag has a minimal effect on the endogenous behaviour of the protein. The intra-cellular distribution of the elongation and release factors were explored with live-cell imaging techniques. The growth phenotype and protein expression levels of each of the

elongation and release factors were measured to confirm that the factors are displaying wild-type protein behaviour.

Yeast elongation and release factors all were observed to be cytoplasmically distributed in the yeast cells. The nuclei of cells in strains expressing TCM-tagged elongation and release factors were visualised using DAPI to determine whether the elongation and release factors might also be evident in the nucleus. But the images revealed no evident of the presence of these factors in the nucleus.

3.3.4. Actin intra-cellular organisation is unaffected by TCM tagged eEF1A

The interaction of eEF1A and actin has been demonstrated in numerous organisms and the over-expression of eEF1A in yeast causes alterations in the intra-cellular distribution of actin (Munshi et al., 2000). To determine if the fusion of the TCM-tag to eEF1A causes actin re-organisation, TCM-tagged strains were visualised by confocal microscopy Figure 3.9 shows that there are no alterations in the actin distribution and the cell size or shape due to TCM-tagging of eEF1A. In yeast, actin has a role in bud formation and localises on the bud tip. It has been suggested that the regulation of eEF1A also causes enlargement of the yeast cells and the loss of the ability to form buds (Munshi et al., 2000). Actin localisation to the bud tip was observed in TCM-tagged eEF1A expressing yeast strain as observed in the wild-type cell (Figure 3.10**)**. This study confirms that the cell shape, size or bud formations are not altered by TCM tags.

3.3.5. GFP tags confirms the cytoplasmic distribution of elongation and release factors

The intra-cellular distribution of elongation and release factors in yeast was examined with GFP tags in order to provide an alternative means of determining their cytoplasmic distributions. In yeast, only the eEF1A distribution was investigated previously using the GFP tag. It was demonstrated that GFP-tagged eEF1A is diffusely distributed within the cytoplasm (Huh et al. 2003). The same cytoplasmic distribution of eEF1A was observed in

this study. All the other elongation and release factors were also found to be dispersed within the cytoplasm (Figure 3.14). The growth phenotypes of the yeast strains with GFP-tagged elongation and release factors were examined and showed no growth defect due to the tags. These data suggest that the yeast strains with GFP-tagged translation factors exhibit similar behaviour to that of the wild-type strains and strains with TCM-tagged proteins. Overall, the above data conclusively demonstrate that yeast elongation and release factors are cytoplasmically distributed. Furthermore these data confirm that since the elongation and release factors are cytoplasmically distributed throughout the cell, the spatial distribution of these factors might not be affecting the translational rate.

3.4. Conclusion

The intra-cellular distributions of the elongation and release factors were analysed *in vivo* in order to ascertain whether sub-cellular heterogeneity might play a role in the control of translation. The factors were tagged with both TCM and GFP tags to observe their cellular distribution. The results indicate that the translation elongation and release factors are homogenously distributed in the cytoplasm of the cell. This suggests that the spatial distribution of elongation and releasing factors are not affecting the translational control. Thus the sub-cellular distributions of the factor are not an aspect to be considered in the mathematical modelling of the translational control in yeast cells. The study also confirms that the elongation and release factors are not present in the nucleus of the yeast cells. The study also demonstrates the utility of the small tag, TCM, which can be chromosomally integrated in to the genome to enable visualisation of the proteins of interest *in vivo* with very little probability of functional defects.

Chapter 4

Rate control analysis of elongation and release factors

4.1. Introduction

mRNA translation is one of the most important and well controlled cellular processes requiring the combined function of a large number of molecular components. In *Saccharomyces cerevisiae*, 13,000 protein molecules per cell per second are produced by the translation machinery (von der Haar, 2008). Translation is the final step in the flow of the genetic information, and regulation at this level allows for an immediate and rapid response to changes in physiological conditions (McCarthy, 1998). However, the processes that facilitate the precise regulation of translation are not clearly defined. Regulation of a multistep pathway like translation involving more than 20 translation factors, can be exerted at different levels. However, most of the translational controls are believed to occur at the initiation stage of translation. Nevertheless, later stages of translation namely elongation and termination, are also actively involved in the translational control (Mathews et al. 2000). Previous studies of translation regulation suggest that the rate of translation depends on the rate of initiation, the rate of elongation/termination and the activation/repression of mRNA (Mathews et al. 2000).

Multiple or individual steps have been found capable of regulating translation. One of the very first steps of translation is the GDP to GTP exchange in eIF2, facilitated by eIF2B, which can control translation globally (Rowlands, 1988). Together with eIF2, the mRNA cap-binding protein eIF4E is thought to regulate the global translation rate. Loading of the

40S subunit onto mRNA together with other translation initiation factors is also one of the important steps in translation regulation (Sachs et al. 1997). In addition, translation rates are shown to be dramatically repressed when the amino acids levels are limited (Clemens, 1987). It has been suggested that the absolute quantities of ribosome and mRNA are not a rate-limiting factor in translation but this view is on limited validity in the context of system analysis (Henshaw et al. 1971). However, mRNA could be translation rate-limiting due to its secondary structure at the 5' cap region and upstream of AUG sequences (Mathews et al. 2000). When the translocation of the ribosome from the AUG codon is slower than the initiation rate, the elongation becomes extremely rate-limiting. The presence of mRNA encoding rare amino acids, the secondary structure in the mRNA and phosphorylation of elongation factors can cause a non-uniformity of the elongation rate (Wolin and Walter, 1988).

Recent studies of translation control have identified its role in many disease states and irregularities in growth (Silvera et al., 2010). However, a quantitative study of translational control at the systems level has not been available. In this study, for the first time, using a combination of molecular biology techniques, the response coefficients of the individual elongation and release factors have been determined. The response coefficient, the relationship between the intracellular abundance and control exerted by respective translation factors over the translation rates has been investigated. In addition the impact on translation and cellular growth rates due to the increase in the cellular levels of translation factors above endogenous levels were investigated.

4.2. Results

4.2.1. Construction and confirmation of *tetO7* promoter elongation and release factor strains

Intra-cellular levels of the elongation and release factors were repressed by substituting the endogenous promoter by the doxycycline regulatable *tetO7* promoter. The *tetO7* cassette comprises of the *kanMx4* gene as a selective marker, the tetracycline regulatable tTA gene and the *tetO7* promoter (Figure 4.1). Doxycycline binds to the tTA gene which suppresses the activation of *tetO7* promoter, consequently reducing the expression of the upstream gene (Bellı` et al 1998**)**.

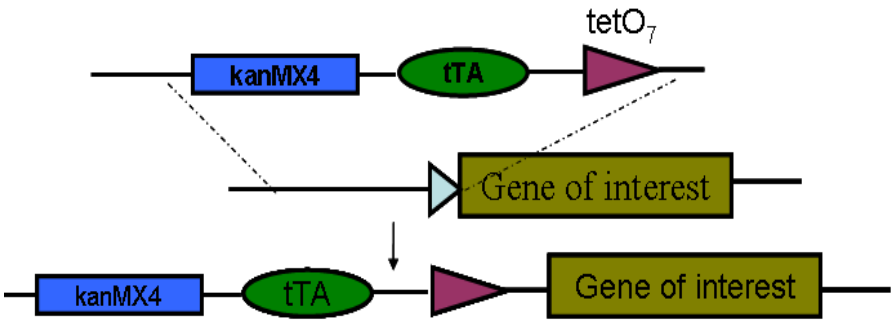

Figure 4.1: Schematic representation of *tetO7* cassette and the promoter substitution. The endogenous promoter of the elongation and release factors were substituted with the doxycycline regulatable *tetO7* promoter. The *tetO7* cassette was introduced into the yeast chromosome by homogenous recombinase. The level of gene expression is doxycycline dose-dependent.

The *tetO7* cassette was PCR amplified from the pCM225 plasmid (Table 2.3) using gene specific primers (Table 2.6). All the primers used in this study for the promoter substitution and for the confirmation of the promoter substitutions are listed in the Table 2.6. The gene specific *tetO7* cassette was transformed into yeast cells and positive colonies were confirmed by PCR. The *tetO7* cassette replaced the endogenous promoter of the gene of interest by targeted chromosomal homology substitution.

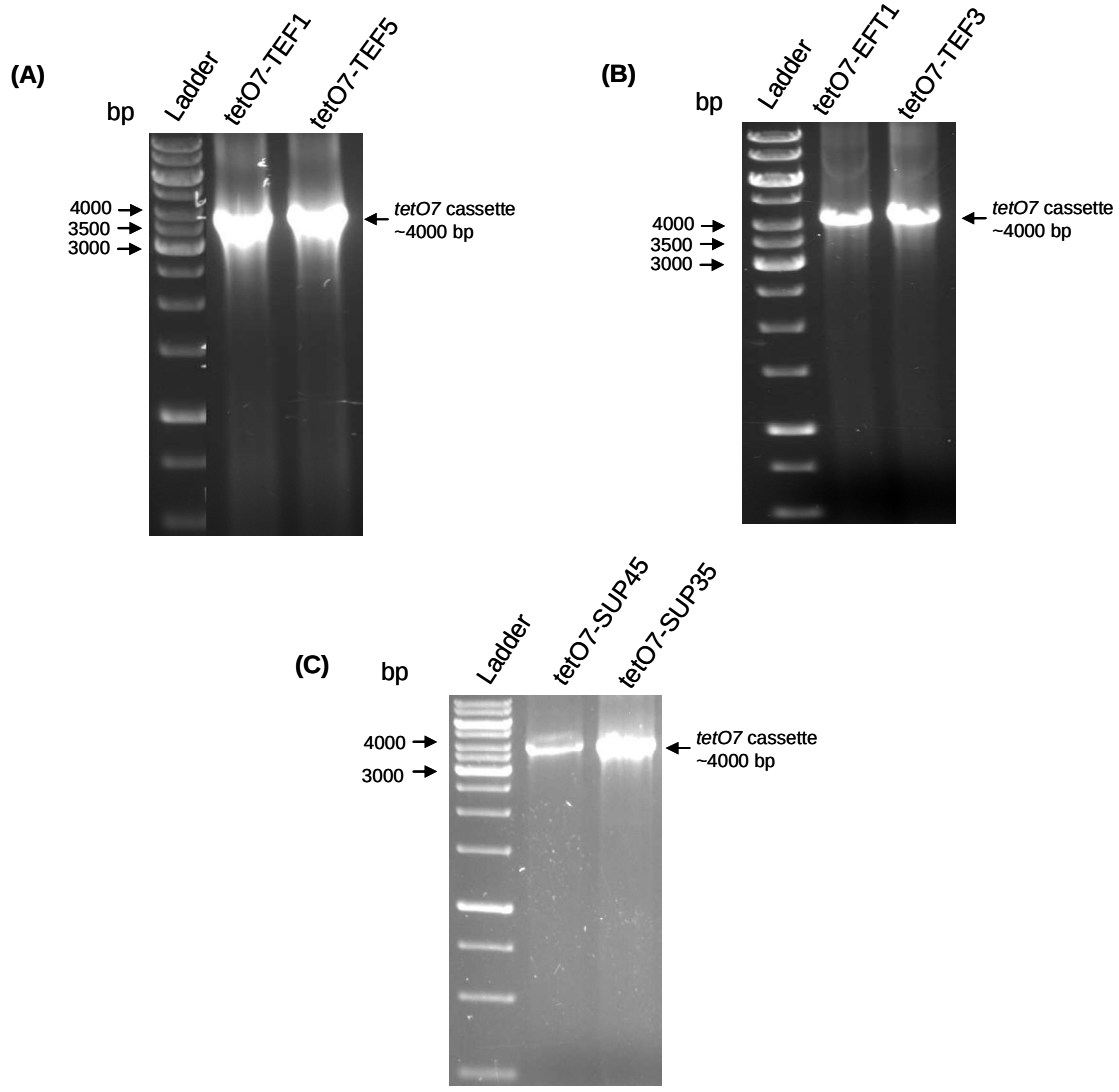

Figure 4.2 : PCR amplification of the *tetO7* cassette from genomic DNA to confirm the *tetO7* cassette integration with elongation and release factors. Generuler is the marker DNA ladder used in the agarose gel. The PCR product of the *tetO7* cassette of size ~4000 bp for the promoter substitution of A) eEF1A (*tetO7*-TEF1) and eEF1B (*tetO7*-TEF5) respectively B) eEF2 (*tetO7*-EFT1) and eEF3 (*tetO7*-TEF3) and C) eRF1 (*tetO7*-SUP45) and eRF3 (*tetO7*-SUP35) factors. Gene specific primers were employed to confirm the integration.

Strains with *tetO7* promoter substitution were confirmed by PCR amplifying the cassette from the genomic DNA of the *tetO7* strains. The *tetO7* promoter region was PCR amplified

using gene specific primers and the PCR product of size ~ 4000 bp confirms the substitution of the desired gene promoter (Figure 4.2).

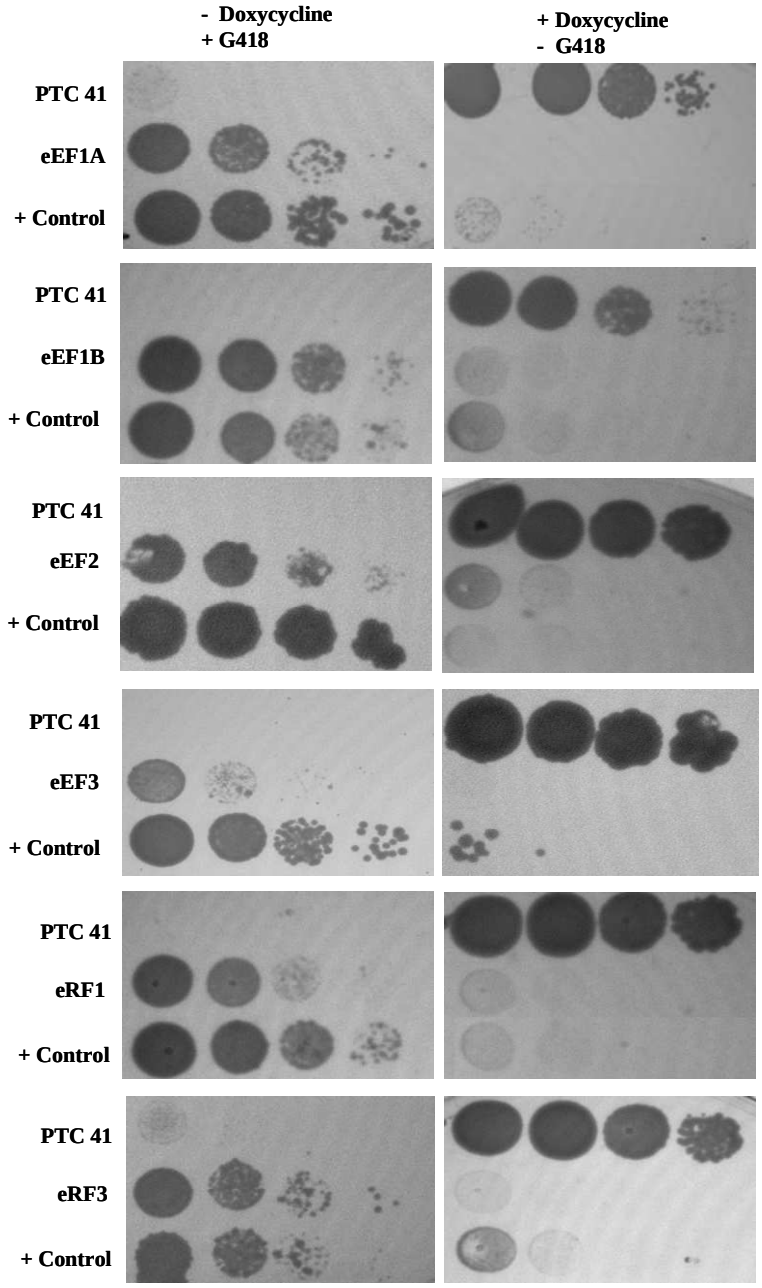

Figure 4.3: Serial dilution to determine the doxycycline sensitivity of elongation and release factors *tetO7* promoter strains. Ten-fold dilutions of all the strains are spotted on to the YPD plates with G418 (150 μM) and YPD plates with doxycycline (2 μM). Serial dilutions of the elongation and release factor *tetO7* strains. The *tetO7* strains are resistant to the G418 due to the kanMx selective gene and sensitive to doxycycline. However the wild-

type strains (PTC 41) are not sensitive to doxycycline but are non-resistant to G418. + Control (*tetO7-GCD11*) strain confirm the doxycycline sensitivity of the factors.

Strains with the *tetO7* promoter were further confirmed by examining their doxycycline sensitivity. Ten-fold serial dilutions of exponentially growing *tetO7* elongation and release factors strains were spotted on YPD with G418 (150 μM) and YPD with doxycycline (2 μM) plates (Figure 4.3). Strains with the *tetO7* promoter grew normally on YPD with G418 plates though exhibit repressed or no growth on YPD plates containing doxycycline. In contrast, the wild-type strains grow normally in the presence of doxycycline but growth is repressed in the presence of G418. An initiation factor, *tetO7-GCD11* (Dr. Helena Firczuk, University of Manchester) strain which is sensitive to the doxycycline was used as a control in the serial dilution to confirm the doxycycline sensitivity of the elongation and release factors.

4.2.2. Growth curves and intra-cellular protein level analysis of *tetO7* promoter elongation and release factor strains

Endogenous promoter substitution may cause variation in the protein expression levels which can have an effect on cellular growth rate. Any variations in the protein level and growth rate of the *tetO7* strains were examined. All the strains were grown in YNB media with all amino acids and cell density in liquid culture was determined by measuring the optical density (O.D.) at a wavelength of 600 nm (OD_{600}) at one hour time points. The protein expression level under the control of the *tetO7* promoter was determined by collecting samples in the exponential growth phase (OD_{600} = 0.6) and quantified using Western blotting (Figure 4.6).

tetO7-TEF1, *tetO7-TEF5* and *tetO7-EFT1* strains showed approximately 20-30% reduction in the protein level (Figure 4.6 A, B and C) whereas *tetO7-TEF3* showed approximately 70% reduction (Figure 4.6 D). Interestingly, *tetO7-SUP45* strains showed approximately 60% increase in the intra-cellular protein level (Figure 4.6 E**)**. Whereas the *tetO7-SUP35* intra-cellular level was approximately 50-60% reduced (Figure 4.6 E**)**.

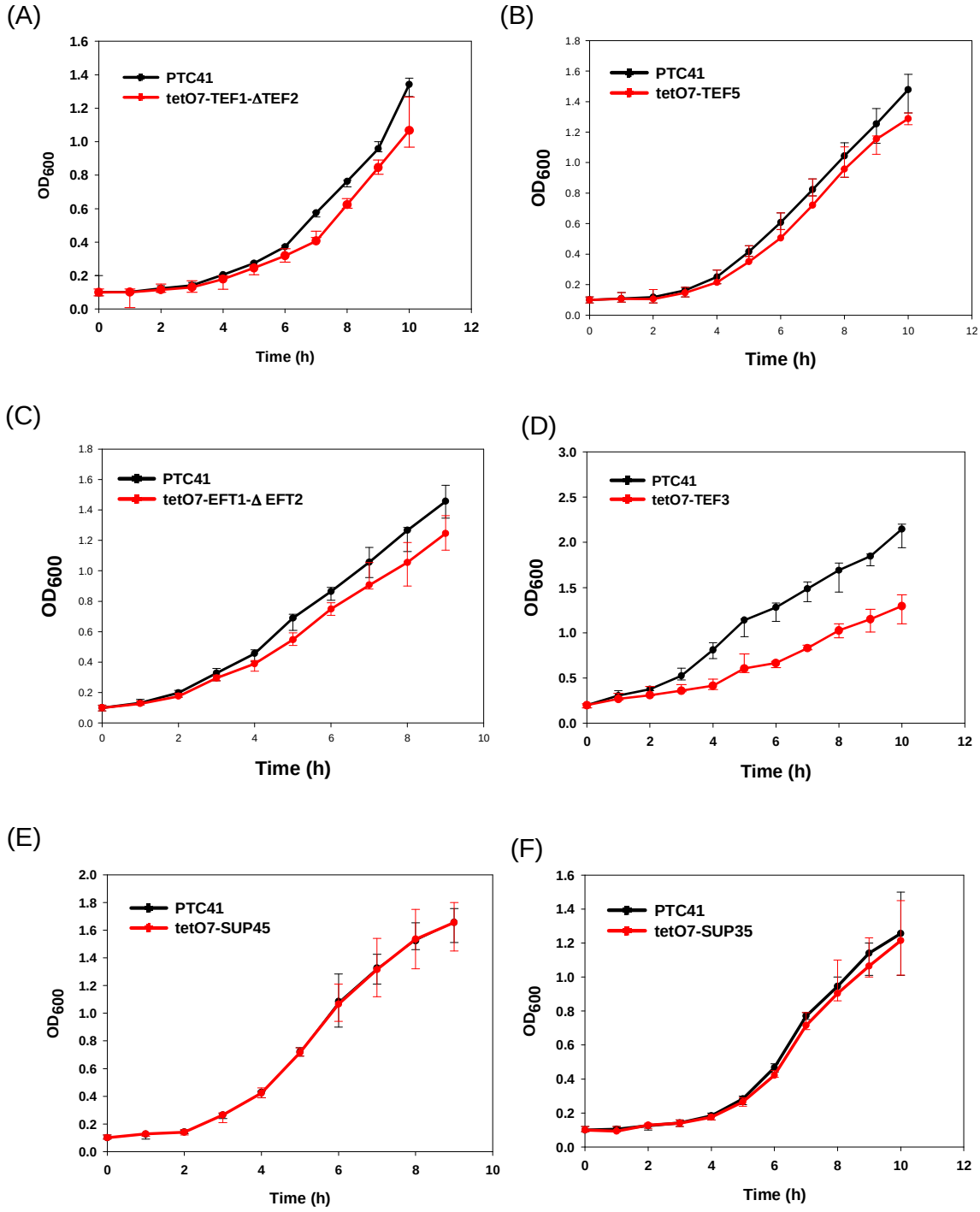

Figure 4.4: Growth curve comparison of the *tetO7* constructs of elongation and release factors strains with the wild-type cells (PTC-41). A) *tetO7-TEF1* and wild-type B) *tetO7-TEF5* and wild-type C) *tetO7-EFT1* and wild-type D) *tetO7-TEF3* and wild-type, E) *tetO7-SUP45* and wild-type and F) *tetO7-SUP35* and wild-type.

Growth curves of the *tetO7* strains were compared to that of the wild type to explore the effects of reductions in translation factor levels on growth. *tetO7-TEF1*, *tetO7-TEF5* and *tetO7-EFT1* (Figure 4.4 A, 4.4 B and 4.4 C) strains were growing approximately 10-20% slower growth when compared to that of the wild-type (PTC41) cells. The reduction in the growth rate correlates with the reduction in the protein level. Similarly, the growth rate of *tetO7-TEF3* (Figure 4.4 D) was reduced to 50-70% of that of the wild-type cells similar to the protein expression level. Interestingly, the increase in the protein level of release factor, eRF1 was not reflected in the growth curve. The growth curve of *tetO7-SUP45* was very similar to that of the wild-type (Figure 4.4 E) indicating no effect on the growth due to promoter substitution. On the contrary, the protein level of the eRF3 strain was about 50-60 % of the wild-type, however, the *tetO7-SUP35* (Figure 4.4 F) growth curve was approximately similar to wild-type cells with a growth difference of about 5%.

4.2.3. 'Top-up' to increase the protein expression level of elongation and release factors

The differences in protein expression levels observed due to promoter substitution were rescued by transformation of *tetO7* strains with specific 'top-up' plasmids. In order to return the protein levels in the *tetO7* strains to wild-type levels, individual elongation and release factor genes were cloned into a yeast expression vector. The elongation and release factor genes were PCR amplified (Figure 4.5A, 4.5C, 4.5E, 4.5F and 4.5I) from the genomic DNA of the wild-type and cloned into single copy plasmids pTefEx or pTrpEx. The plasmids expressing the individual translation factors were transformed into the *tetO7* strains. The pTefEx vector has the P_{TEF1} promoter which is stronger than the P_{TRP1} promoter in the pTrpEx vector. Both plasmids contain the *URA3* gene as a selective marker. The growth and doxycycline resistance of the transformed *tetO7* strains were examined. Ten-fold serial dilutions of the strains containing these 'complementation' plasmids were spotted on YNB media without uracil (URA) and with/without doxycycline (Figure 4.5B, 4.5 D, 4.5F, 4.5H and 4.5J).

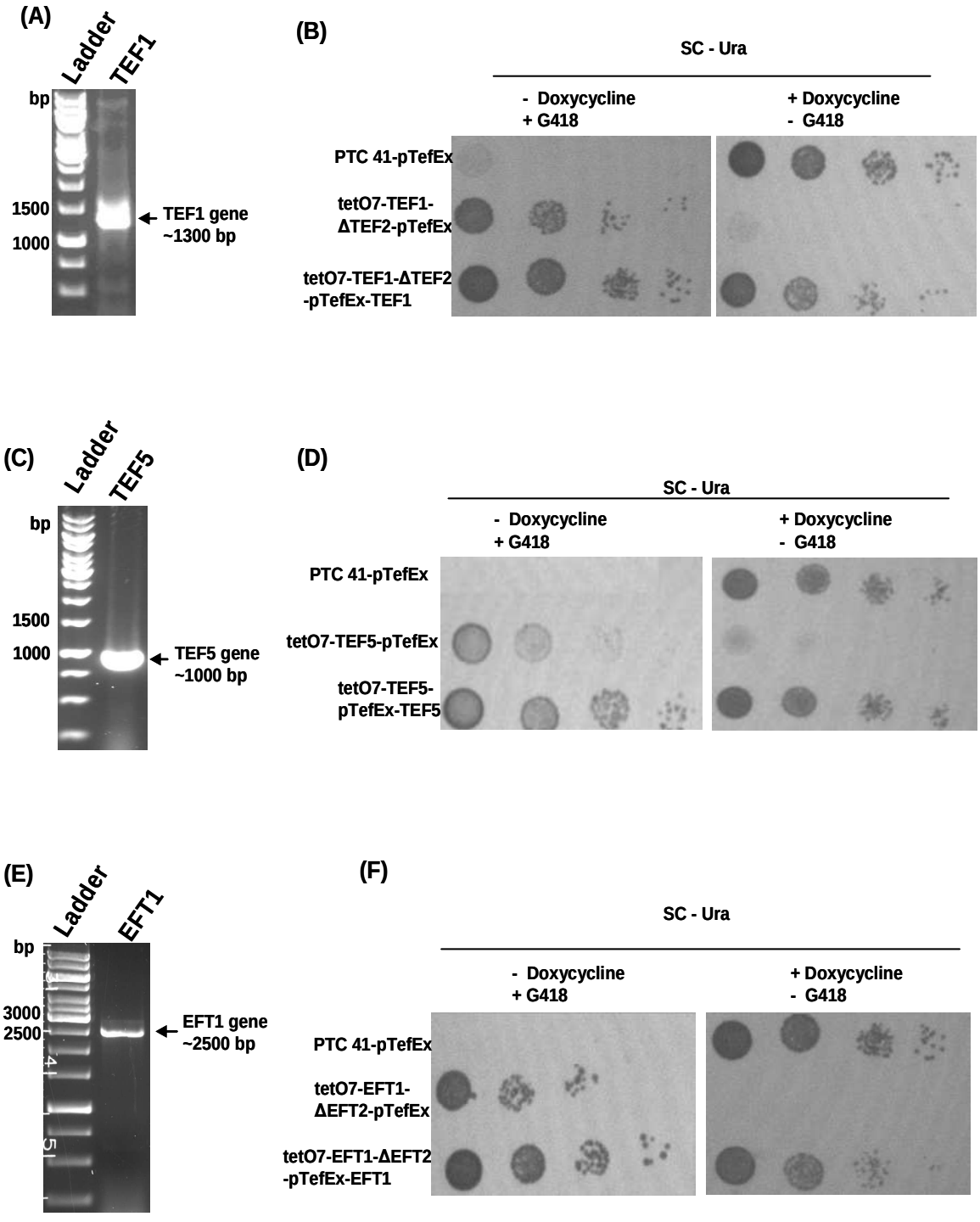
(A)
Ladder
TEF1
bp
1500
1000
TEF1 gene
~1300 bp
(B)
SC - Ura
- Doxycycline
+ G418
+ Doxycycline
- G418
PTC 41-pTefEx
tetO7-TEF1-
ΔTEF2-pTefEx
tetO7-TEF1-ΔTEF2
-pTefEx-TEF1
(C)
Ladder
TEF5
bp
1500
1000
TEF5 gene
~1000 bp
(D)
SC - Ura
- Doxycycline
+ G418
+ Doxycycline
- G418
PTC 41-pTefEx
tetO7-TEF5-pTefEx
tetO7-TEF5-
pTefEx-TEF5
(E)
Ladder
EFT1
bp
3000
2500
EFT1 gene
~2500 bp
(F)
SC - Ura
- Doxycycline
+ G418
+ Doxycycline
- G418
PTC 41-pTefEx
tetO7-EFT1-
ΔEFT2-pTefEx
tetO7-EFT1-ΔEFT2
-pTefEx-EFT1

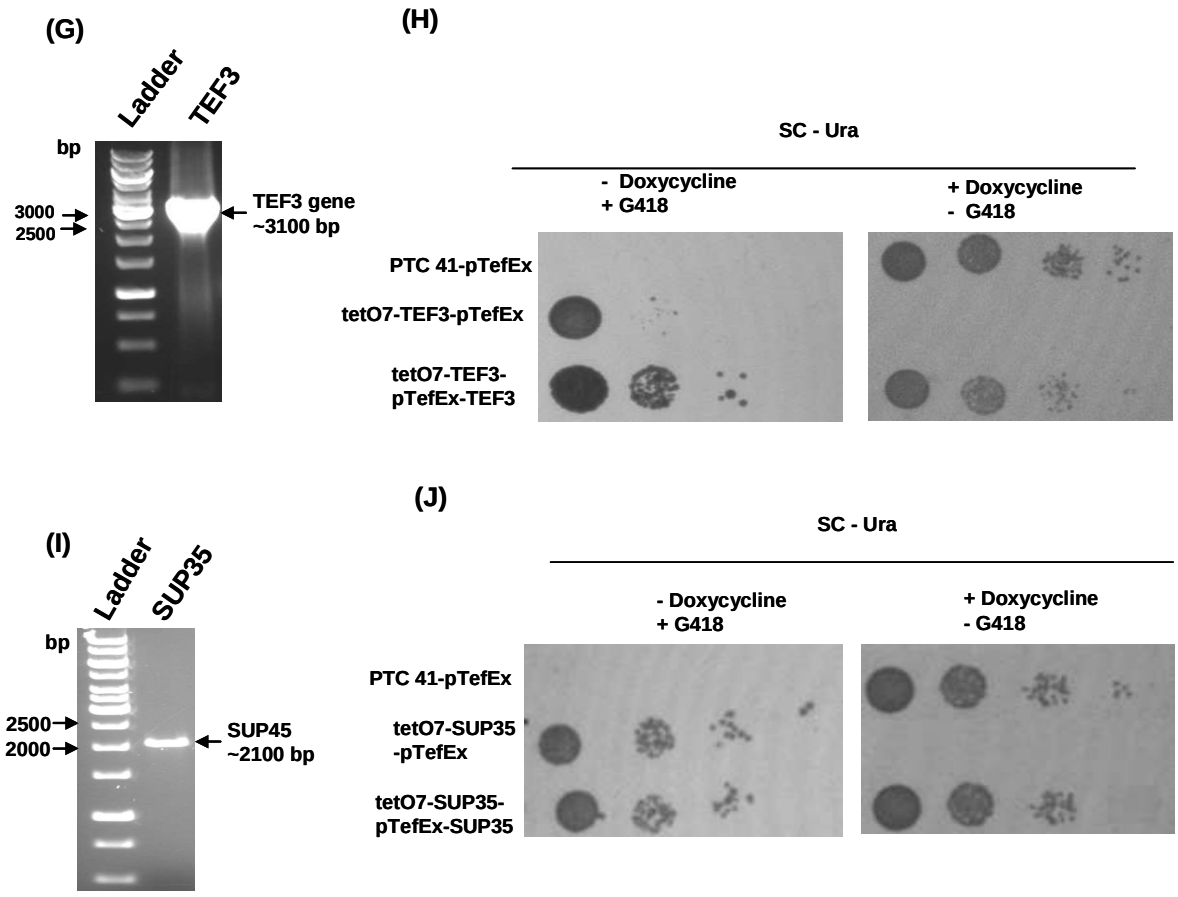

Figure 4.5: PCR amplification of the elongation and release factor genes and serial dilutions of the *tetO7* strains with genetic complementation. The elongation and release factor genes were PCR amplified from the genomic DNA of the wild-type cell (A, C, E, G and I). These genes were cloned to the pTefEX plasmid and transformed into the *tetO7* strains to rescue them from the decrease in the protein expression level. The increase in the protein expression level of the elongation and release factors resulted in reduction of growth defect. The serial dilution of the *tetO7* strains with the 'top-up' vectors exhibit growth improvement (B, D, F, H and J). The *tetO7* strains with the complementation vector are resistant to G418 and not sensitive to doxycycline. This indicates that the protein expression level of elongation and release factors are rescued through complementation vector.

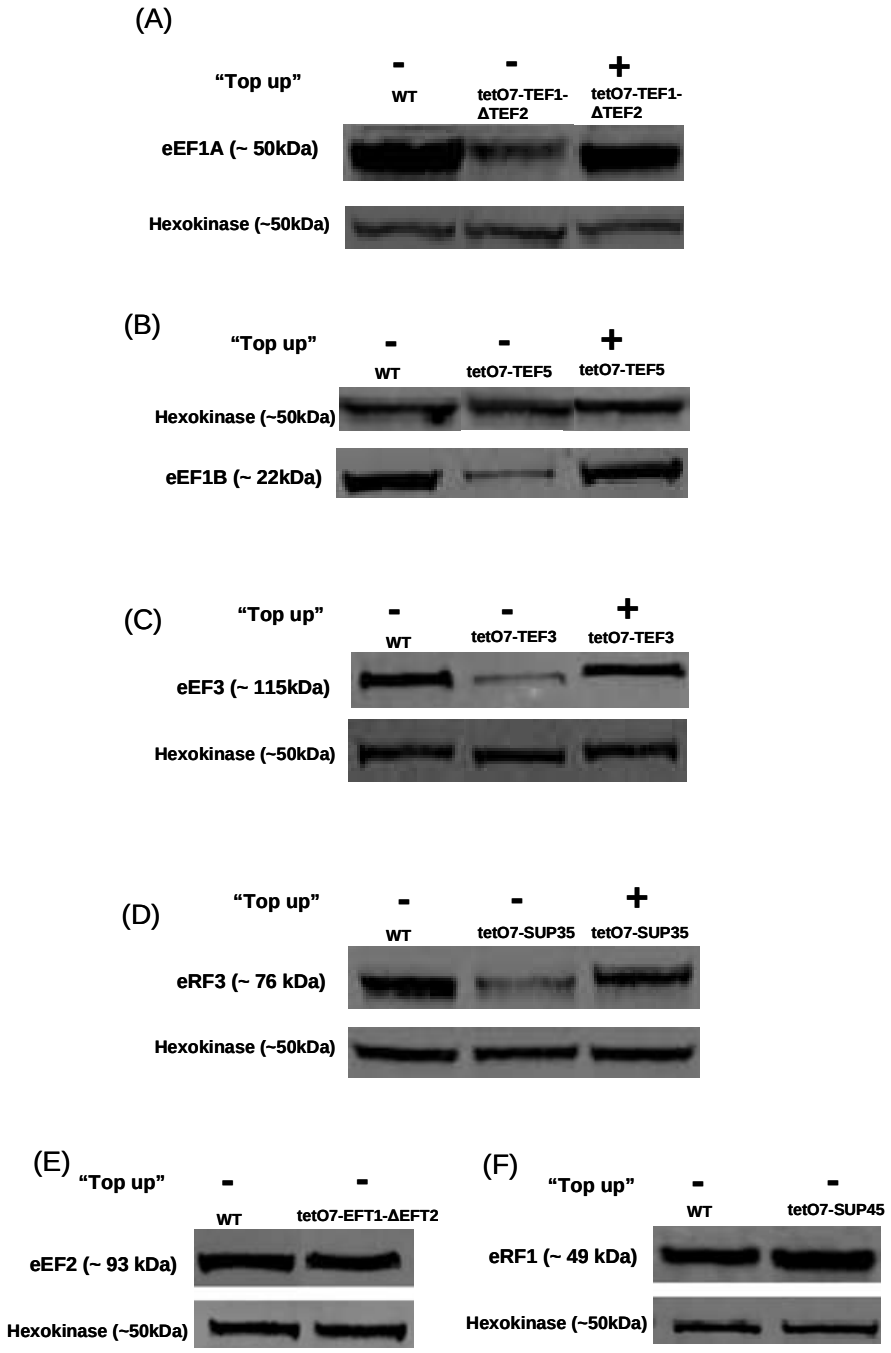

Figure 4.6: Western blot analysis of the protein levels of *tetO7* promoter elongation and release factors with or without 'top-up' plasmids. Reduction in the protein expression level of eEF1A in *tetO7-TEF1* strain (A), eEF1B in *tetO7-TEF5* strain (B), eEF3 in *tetO7-TEF3* strain (C), eRF3 in *tetO7-SUP35* strains were increased to the wild-type level using the 'top-up' vectors pTefEx. However, the protein expression level of *tetO7-EFT1* was not improved through complementation vectors. In contrast, the protein expression level of *tetO7-SUP45* strain was increased after promoter substitution.

The ‘top-up’ vectors restored the protein expression level and thus growth rate back to the wild-type level. The strains with ‘top-up’ vectors were expressing elongation and release factors from the P_{TEF1} promoter and thus the strains were partially resistant to doxycycline. Protein expression levels of eEF1A in the *tetO7-TEF1* strain were increased from 70% growth to 97% (Figure 4.6A). The increase in the protein expression level rescued the strain from the growth defect (Figure 4.7 A). The protein level of eEF1B was very low; it was approximately 50% of the wild type level and was increased to the wild-type level through the complementation vector (Figure 4.6 B**).** The reduction in the protein expression level of eEF1B had a limited effect on growth rate. Even though, the ‘top-up’ vector was employed to reduce difference in the growth rate of wild-type and *tetO7-TEF5* strains (Figure 4.7 B**).** eEF3 expression level in the *tetO7-TEF3* was only up to 30% of the wild-type level. However, the protein expression level was increased to 92 % through the ‘top-up’ complementation vector (Figure 4.6 C**).** This also improved the growth of the *tetO7-TEF3*strains to the wild-type level (Figure 4.7 C**).** The reduction in the protein expression level of *tetO7-EFT1* was not improved with by the ‘top-up’ complementation plasmid.

The protein level of the *tetO7-SUP45* strain was observed to be higher than that of the wild type (Figure 4.6 F). However, the strains were neither resistant to doxycycline nor showed any increase in growth. Since there is no reduction in the protein level or growth, no complementation vector was required for *tetO7-SUP45* strains (Figure 4.6 E). However, an appropriate concentration of doxycyline (3 ng/ml) was employed to bring the protein level to the endogenous level. As enormous difference in the protein expression level was observed in *tetO7-SUP35* strains compared to wild-type and this difference was decreased with the ‘top-up’ complementation vector (Figure 4.6 D). Even though, there was not much variation in the growth rate of the *tetO7-SUP35* strain with wild-type cells, growth of the *tetO7-SUP35* strain was improved through complementation vectors (Figure 4.7 D).

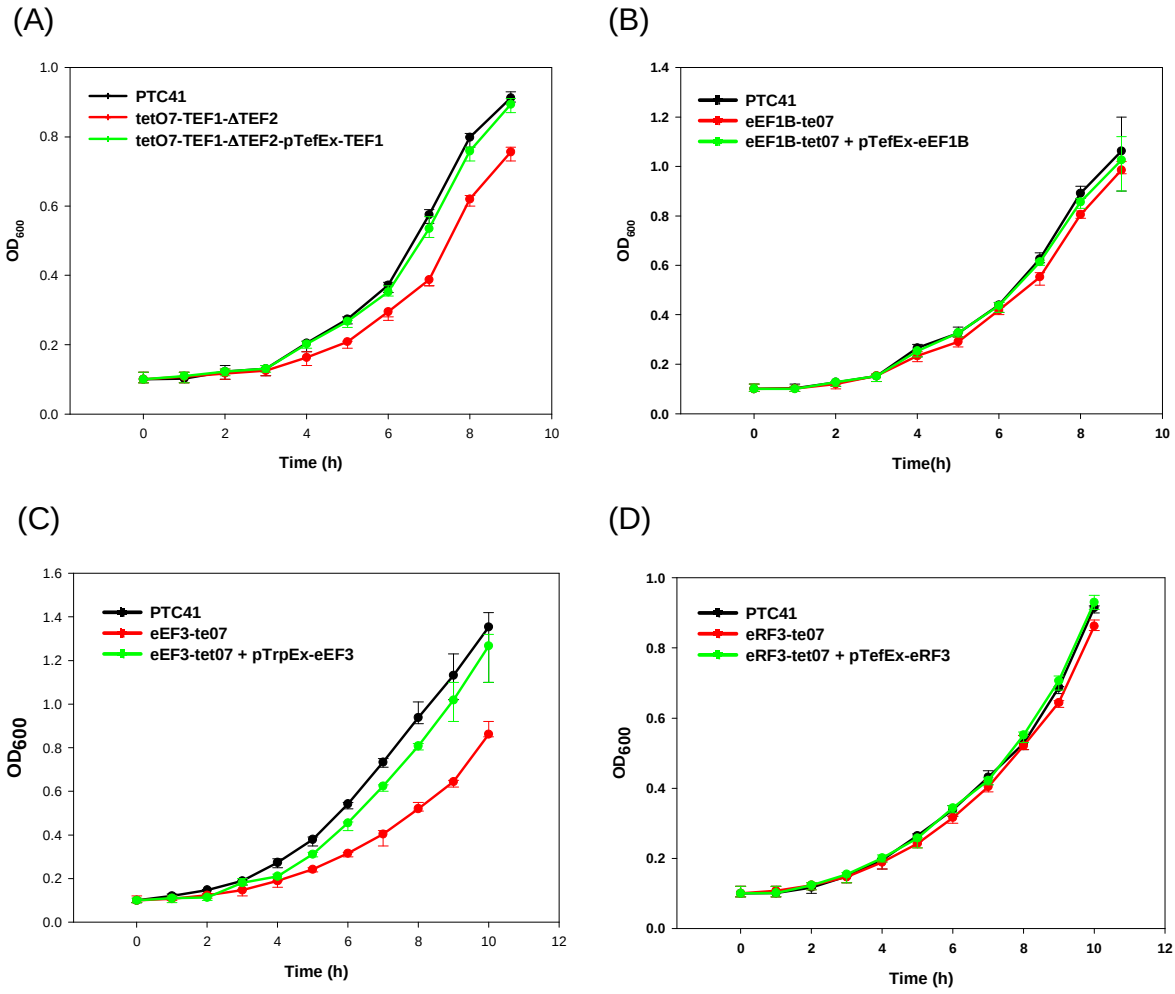

Figure 4.7: Growth curve comparison for the elongation and release factor strains with 'top-up' vectors. The genetic complementation technique was employed to rescue the growth defects and protein level reduction observed in the *tetO7* strains. The black line is the wild-type cell growth, red line represents the strains with no genetic complementation and the green line represents the strains with genetic complementation. A) *tetO7-TEF1* strain growth was improved by 'top-up' plasmids from 75% of the wild-type level to 98%. B) *tetO7-TEF5* exhibited small growth defect and the difference (5%) was recovered by 'top-up' plasmids. C) The *tetO7-TEF3* strain exhibited very high sensitivity to the promoter substitution; however, the growth defect was rescued by 'top-up' plasmids. D) Even though the growth of *tetO7-SUP35* strains was very similar to that of the wild-type, the small difference was complemented by the 'top-up' plasmids.

4.2.4. Growth rate and cellular protein level measurement of elongation and release factor strains at varying concentrations of doxycycline

The 'topped-up' *tetO7* strains were studied for their responses to varying concentrations of doxycycline (2 ng - 25 ng). Individual elongation and release factors were titrated over a range of doxycycline concentrations with and without the 'top-up' vectors (Figure 4.8). The reduction in the growth rate and cellular level of elongation and release factors was measured. The growth rates were measured as explained in section 2.7. Protein samples were collected and the intra-cellular concentration of each factor at the particular doxycycline concentration was quantified via Western blotting.

The growth rate of the *tetO7-TEF1* strains with different concentrations of doxycycline was plotted (Figure 4.10 A and B). The *tetO7-TEF1* strains showed a very sensitive reduction with increasing concentrations of doxycycline. Even though the growth rate of *tetO7-TEF5* (Figure 4.10 C and D) was reduced with higher concentrations of the doxycycline, the strains exhibited lower sensitivity. Until the level of eEF1B factor was decreased below 80% with doxycycline, the growth rate was not drastically affected. The *tetO7-EFT1* growth rates have been observed to reduce very rapidly at higher concentrations of doxycycline (Figure 4.10 E**).**

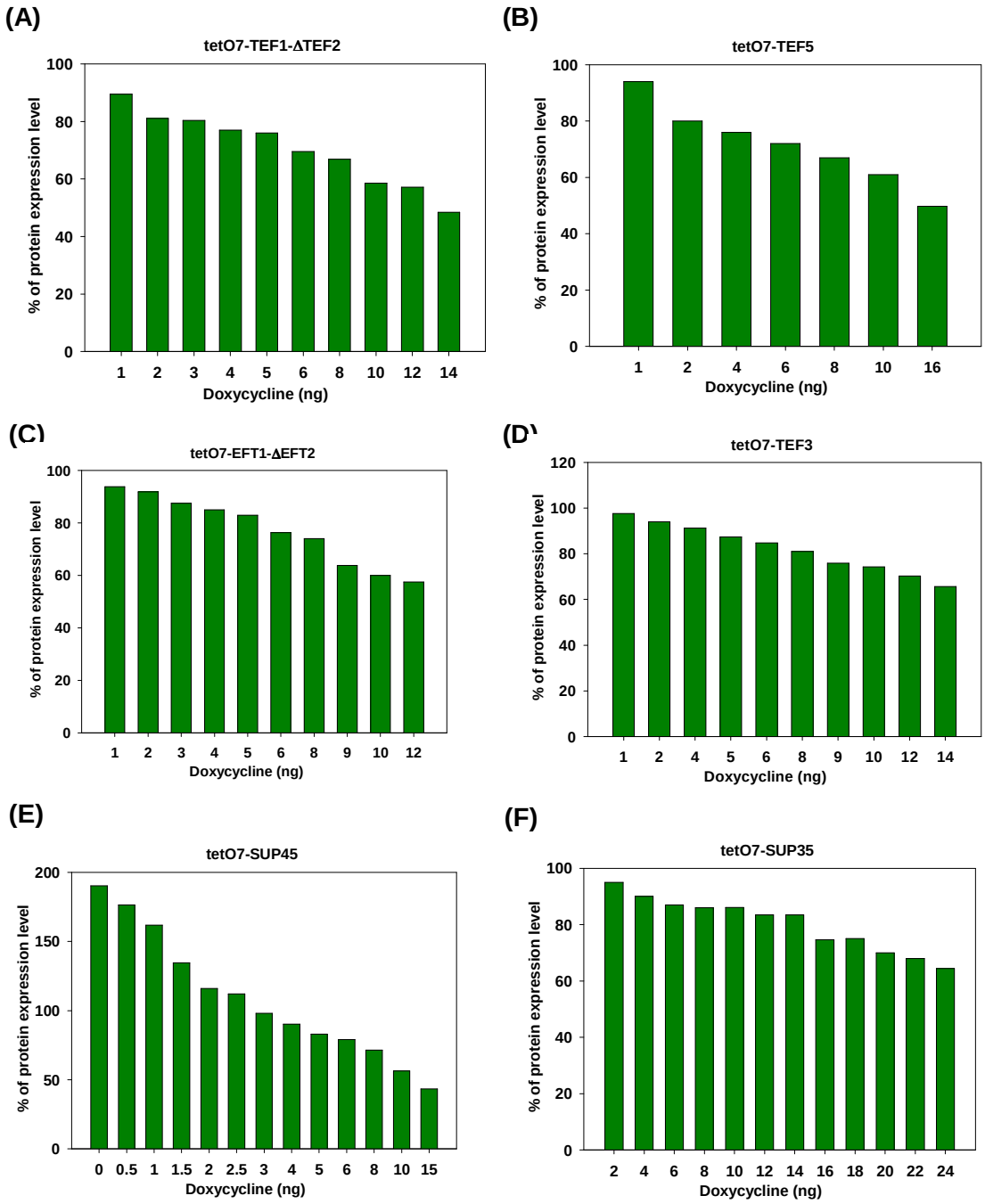

Figure 4.8 : Translation elongation and release factor expression level with varying levels of doxycycline. The expression level of the elongation and release factors were repressed with different concentrations of doxycycline (0-25 ng). Most of the elongation factors were repressed to 60 % of the endogenous level with approximately 10 ng doxycycline (A, B, C, D). However, eRF1 was observed to be more sensitive to doxycycline (E) whereas *tetO7-SUP35* requires higher doxycycline to repress the expression level of eRF3 factor.

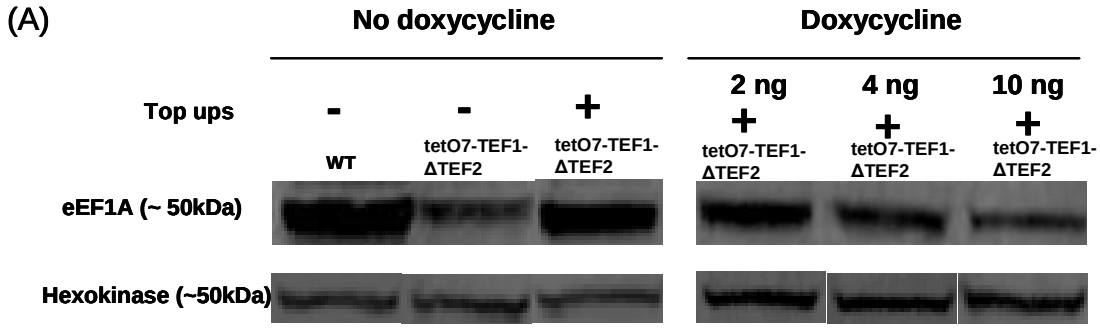
(A)
No doxycycline
Doxycycline
Top ups
-
-
+
2 ng
+
4 ng
+
10 ng
+
WT
tetO7-TEF1-ΔTEF2
tetO7-TEF1-ΔTEF2
tetO7-TEF1-ΔTEF2
tetO7-TEF1-ΔTEF2
tetO7-TEF1-ΔTEF2
eEF1A (~ 50kDa)
Hexokinase (~50kDa)

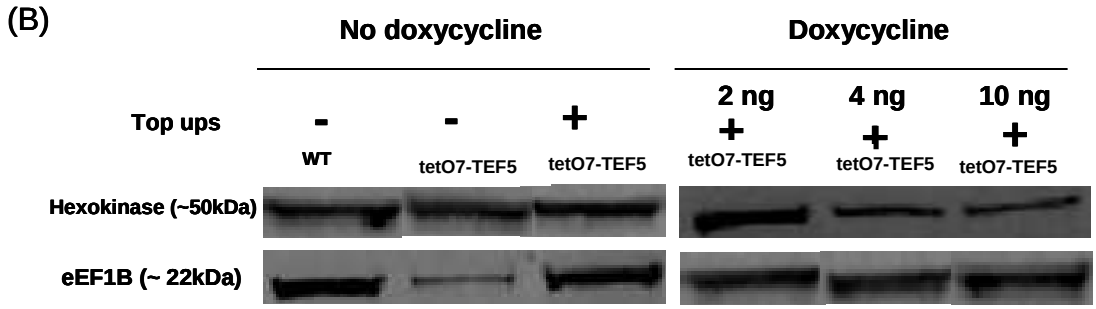
(B)
No doxycycline
Doxycycline
Top ups
-
-
+
2 ng
+
4 ng
+
10 ng
+
WT
tetO7-TEF5
tetO7-TEF5
tetO7-TEF5
tetO7-TEF5
tetO7-TEF5
Hexokinase (~50kDa)
eEF1B (~ 22kDa)

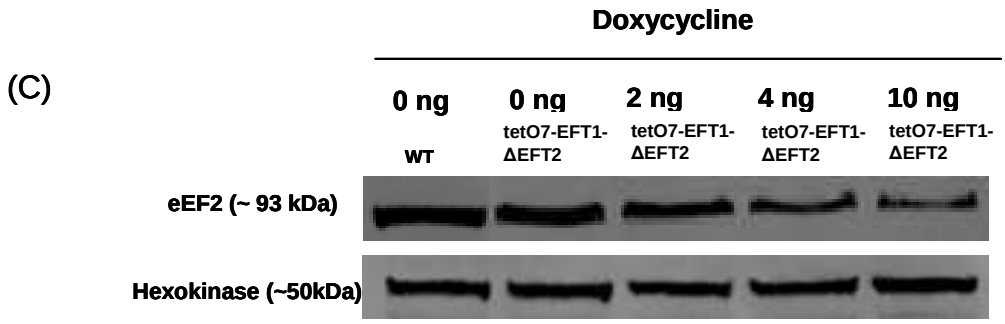
(C)
Doxycycline
0 ng
0 ng
2 ng
4 ng
10 ng
WT
tetO7-EFT1-ΔEFT2
tetO7-EFT1-ΔEFT2
tetO7-EFT1-ΔEFT2
tetO7-EFT1-ΔEFT2
eEF2 (~ 93 kDa)
Hexokinase (~50kDa)

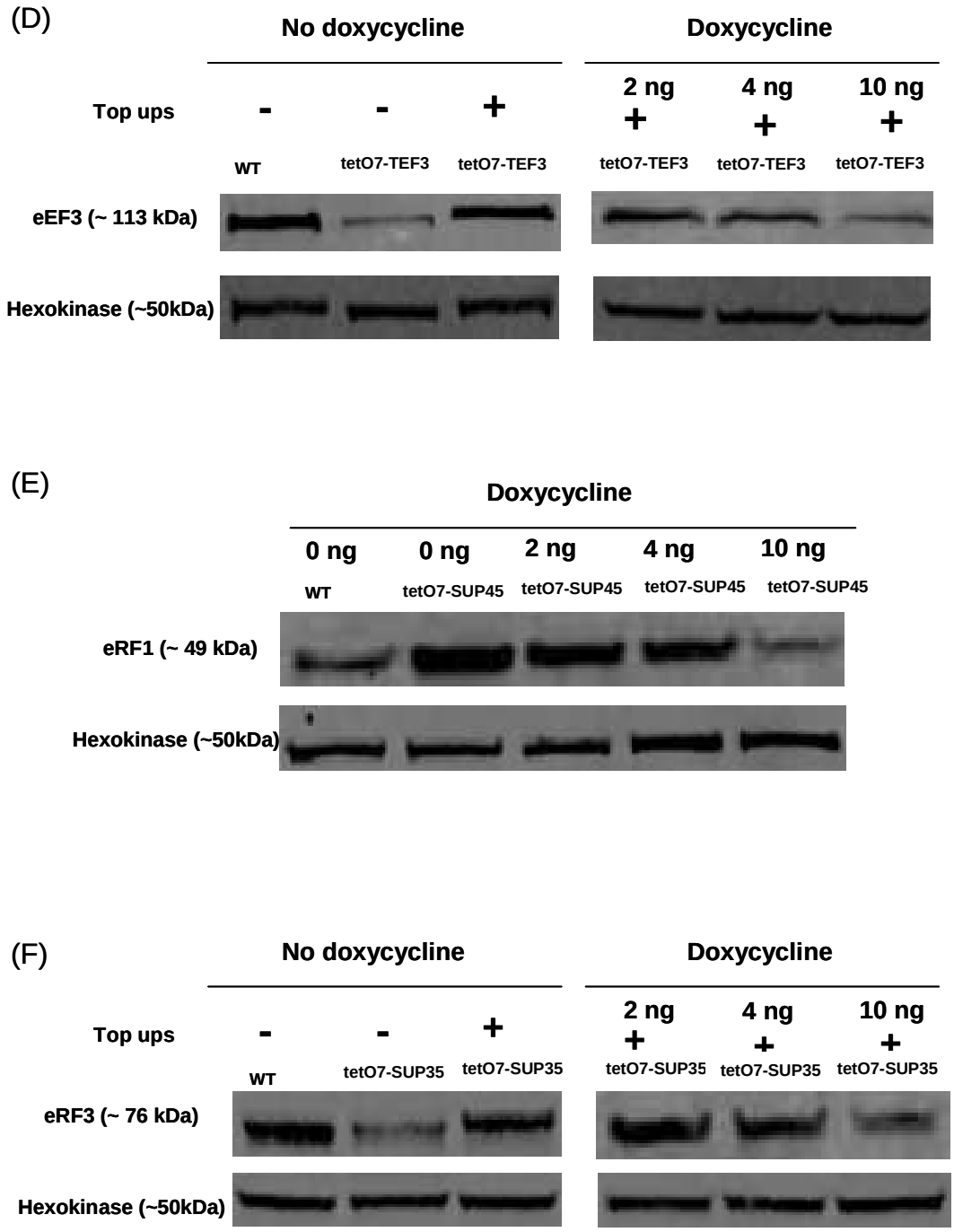

Figure 4.9: Western blots showing the protein levels of the elongation and release factors in the *tetO7* strains before and after complementation with 'top-up' vectors. Different concentrations of doxycycline was employed to systematically reduce the level of each of the factors. With the expression from the complementing plasmids, the reductions in protein expression were increased to the wild type level. Varying concentrations of doxycycline were employed to reduce the protein expression level of factors from 100 – 80%, 80 – 60%, and below 60 %.

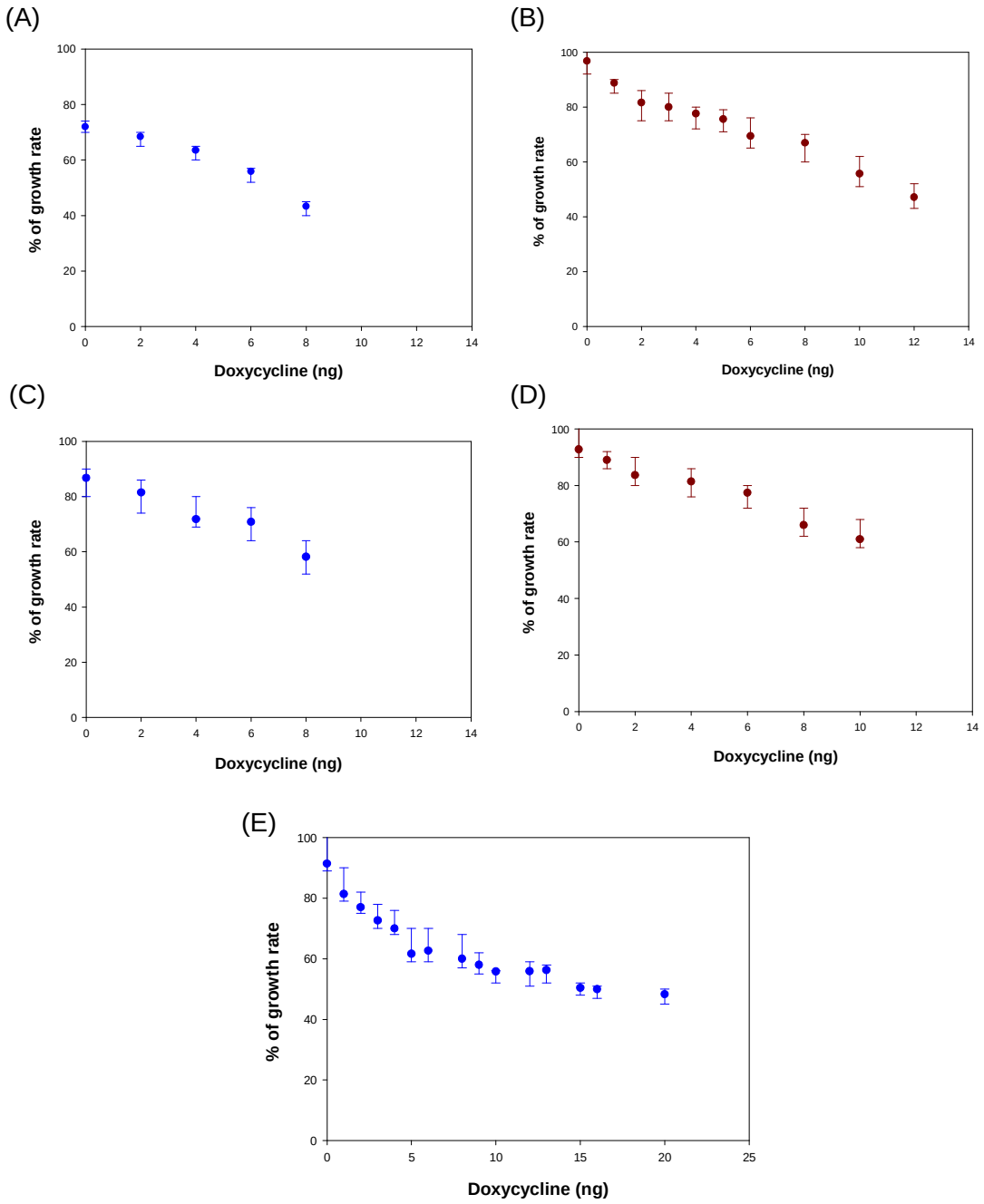

Figure 4.10: Growth rate measurement of *tetO7* elongation factor strains over varying concentrations of doxycycline with and without genetic complementation. The growth rate was measured as a percentage of the wild-type cell growth. Growth rate of *tetO7-TEF1* strains without (A) genetic complementation was about 75% of the wild-type level which was rescued by genetic complementation (B). Over a range of doxycycline concentration, the growth rate of the strain was progressively reduced from 100% to 40%. The growth rate of *tetO7-TEF5* strains without genetic complementation (C) was about 95% which have been rescued to be 95% with the external supply of the gene (D). Over a range of doxycycline, the *tetO7-EFT1* strain exhibits a systematic reduction in growth rate.

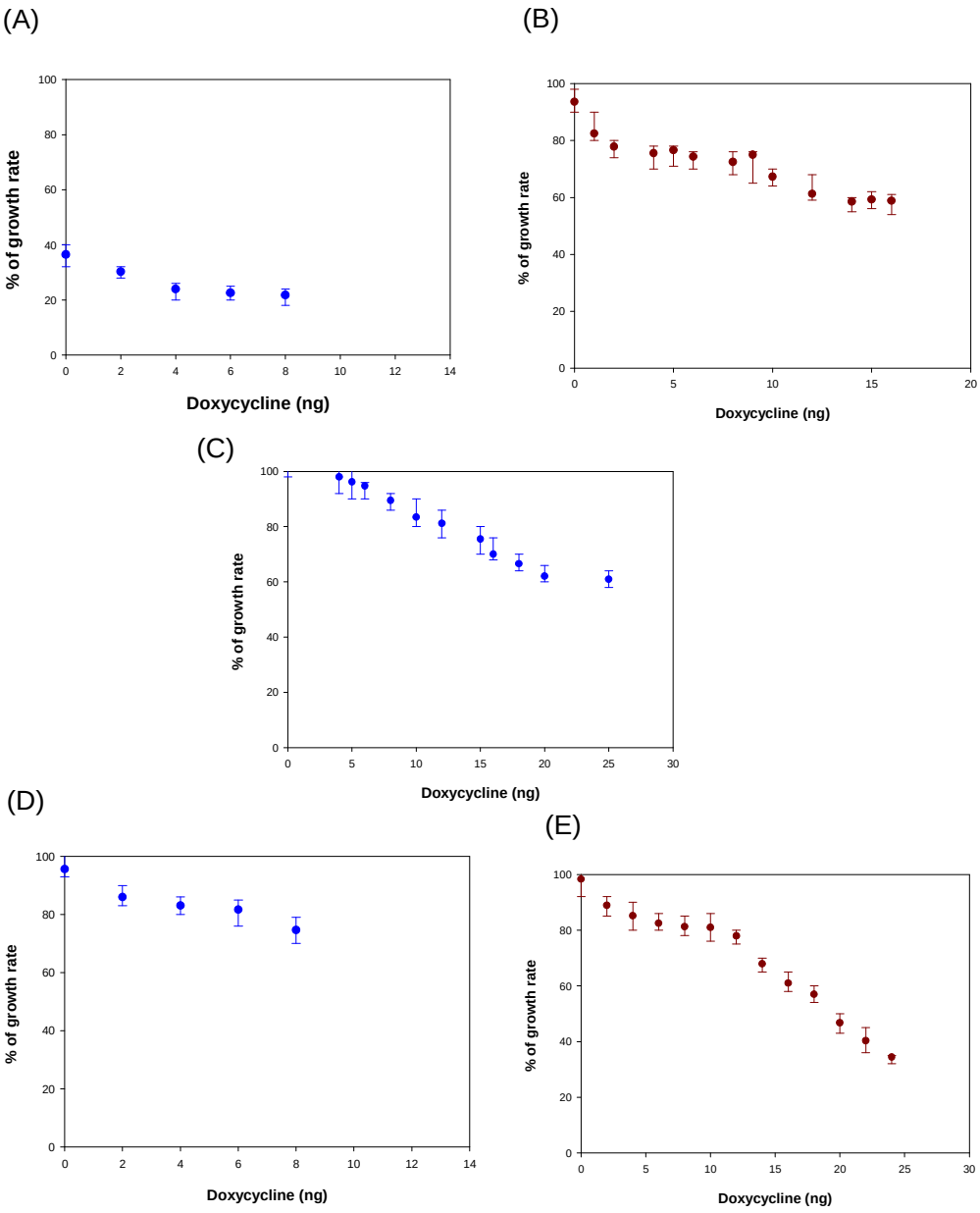

Figure 4.11: Growth rate comparison of the eEF3 and release factors over a range of doxycycline concentrations with and without 'top-up' plasmids. A) The *tetO7-TEF3* strain growth was about 30% of that of the wild type and showed very sensitive growth rate decreases with doxycycline level. B) The growth rate of the *tetO7-TEF3* strain was restored by 'top-up' plasmids and the strains exhibited a decrease in the growth rate. C) The growth rate of *tetO7-SUP45* was not reduced with promoter substitution, however a gradual reduction in the growth rate was observed in response to varying levels doxycycline. D) The *tetO7-SUP35* strain growth rate was not varied with the *tetO7* promoter. E) The *tetO7-SUP35* strain was observed to have much more stable growth with the addition of doxycycline. Higher levels of doxycycline have been used to reduce the growth rate to 40-60% of the wild-type level.

The *tetO7-TEF3* growth rate was markedly reduced because of the *tetO7* promoter substitution. Even at a limited level of doxycycline, the growth rate was strongly reduced (Figure 4.11 A**).** Through the 'top-up' plasmids, the growth rate of the *tetO7-TEF3* strain was restored to the wild-type range and the strain showed a very significant reduction in growth rate (Figure 4.11 B**).** When compared to the elongation factors, eRF1 growth rate changed by the promoter substitution. However, a very rapid change in the growth rate was observed with increasing concentration of doxycycline use indicating or implying that the factor is essential for the cell survival. *tetO7-SUP35* strains showed a very different growth rate pattern when compared to that of *tetO7-SUP45* strain. *tetO7-SUP35* strain growth rate was not much affected by the promoter substitution (Figure 4.11 C) and even with higher concentrations of doxycycline, the growth of the strain was not significantly reduced. The growth rate remained unchanged until the doxycycline concentration was increased to 12 ng/ml (Figure 4.11 D). This indicates that the eRF3 protein may not be that essential for the growth of the *tetO7* strains.

4.2.5. Protein synthesis rate measurement of *tetO7* promoter strains with varying concentrations of doxycycline

As with determination of the growth rate, protein synthesis of the *tetO7* strains was measured over a range of doxycycline concentrations. The protein synthesis rates of the *tetO7* strains were measured *in vivo* using a ^{35}S-methionine incorporation. The *tetO7* strains were grown and samples were collected as explained in section 2.11. Individual *tetO7* strains of the elongation and release factors were treated with varying concentrations (1 ng - 25 ng) of doxycycline. The protein synthesis rate at each level of the translation factors was measure along with the growth rate.

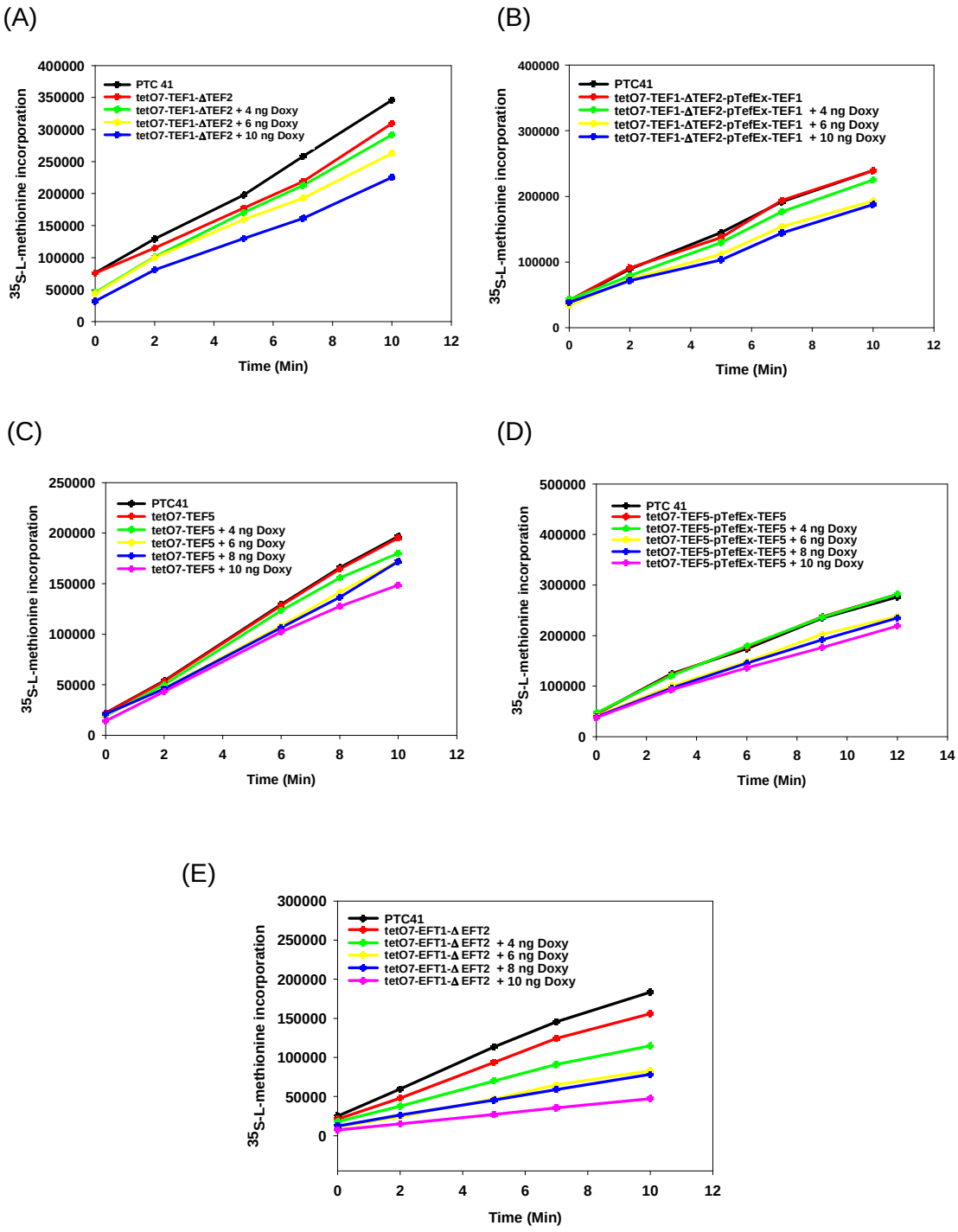

Figure 4.12 : Protein incorporation in the *tetO7* elongation factor strain with different concentrations of doxycycline. One of the protein incorporation experiments with *tetO7-TEF1* strains without (A) and with (B) complementation plasmids. Protein incorporation experiments with eEF2 (E), *tetO7-TEF3* strains without (C) and with (D) the complementation plasmid.

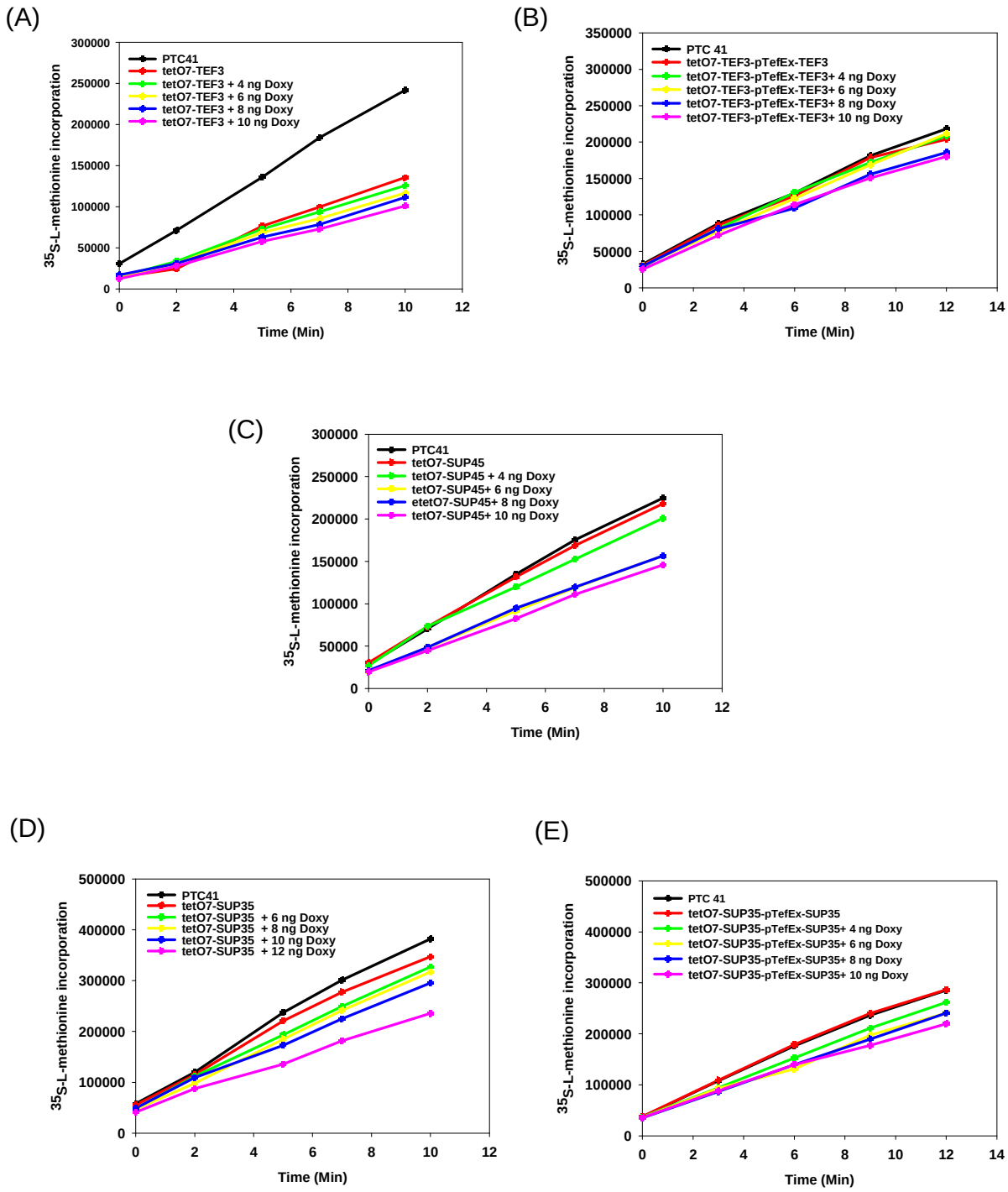

Figure 4.13 : Protein incorporation in the *tetO7* release factor strain with different concentrations of doxycycline. One of the protein incorporation experiments with *tetO7-TEF3* strains without A) and with B) complementation plasmid. Protein incorporation experiments of *tetO7-SUP45* strain (C) *tetO7-SUP35* strains without (D) and with (E) the complementation plasmid.

tetO7-TEF1 and *tetO7-EFT1* showed similar changes in the protein synthesis rate when treated with doxycycline (Figure 4.12 B and E). The protein synthesis rate for these two factors was reduced considerably with a low amount of doxycycline (Figure 4.12 B and E). The protein synthesis rate of *tetO7-TEF5* was not much altered when at high levels of doxycycline (Figure 4.12 D). Conversely, eEF3 was observed to manifest a strong dependence of protein synthesis on the concentration of doxycycline (Figure 4.13 B). The protein synthesis rate of the *tetO7-SUP45* strain was observed to decrease drastically in response to low doxycycline concentrations (Figure 4.13 C). In contrast, *tetO7-SUP35* protein synthesis was observed to be unchanged by high concentrations doxycycline (Figure 4.13 E).

4.2.6. Protein synthesis and growth rate at above the physiological levels of translation factors

An important question in relevance to rate control in the translation machinery is whether physiological levels of translation factors are in any way limiting to protein synthesis. In order to address this question, the intra-cellular protein concentrations of the elongation and translation factors were increased above the physiological level to identify any variation in growth or protein synthesis rate (Figure 4.18 and 4.19). The wild-type cells were transformed with the pTefEx plasmid with individual elongation and release factors. Each of the strains with increased protein expression levels of translation factors were analysed for any changes in the growth or protein synthesis rate. However, none of the *tetO7* elongation factor strains exhibited any variation in the protein synthesis or growth rate. In contrast, the eRF1 strain exhibited a small increase in the growth rate, but not in the protein synthesis rate.

4.2.7. Investigation of the possible involvement of elongation and release factors in scanning competence

The mRNA scanning by the 40S ribosomal sub-unit to identify the AUG start-codon in the initiation step is dependent solely on the initiation factors. The involvement of elongation and release factors in the scanning process is unknown. To investigate any possible role of the elongation and release factors in the scanning process, double luciferease assays (DLA) with firefly (*Photinus pyralis*) and sea pansy protein (*Renilla reniformis*) were employed. The DLA exploits the difference in the biochemical requirement for the luminescence of *Renilla* and *firefly luciferase* proteins (McNabb et al., 2005). Both the *firefly luciferase* and *Renilla* gene were cloned in the pDLV-L2/L0 plasmid with varying length of 5' UTRs. The firefly gene was cloned with the P_{TRP1} promoter and had a long 5' UTR (1240 nucleotides in length) whereas the *Renilla* gene was cloned with the P_{DCD1} promoter with a shorter 5' UTR (41 nucleotides in length) (Figure 4.14). The plasmid contains the *HIS3* gene as a selective marker. The plasmid was transformed into the *tetO7* elongation and termination strains and grown in selective medium with or without doxycycline.

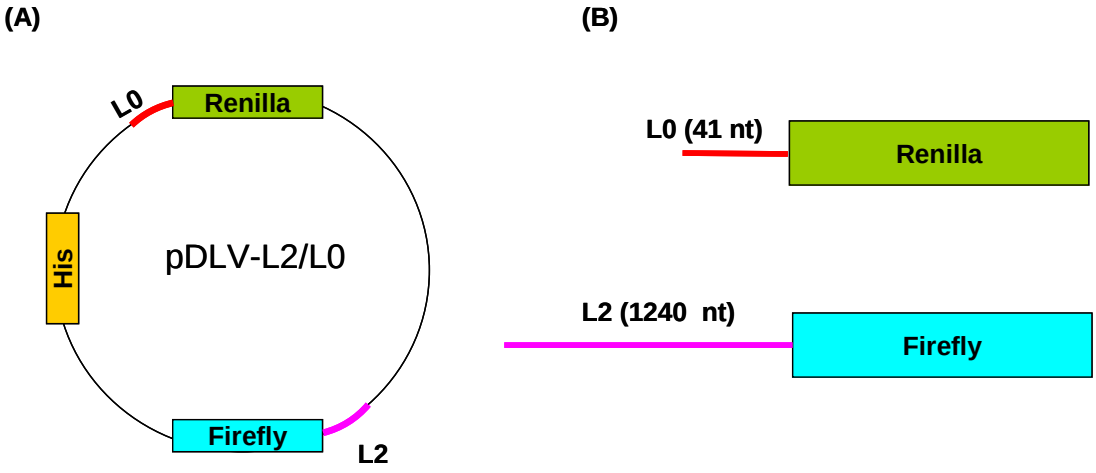

Figure 4.14 : Schematic representation of the pDLV-L2/L0 plasmid employed in DLA experiments. The plasmid contains two luciferase genes, the firefly gene with a long 5' UTR (L2) and the Renilla gene with a shorter 5' UTR (L0). The plasmid also contains a *HIS3* marker gene. The ratio between firefly and Renilla luminescence was measured to determine any possible scanning role of elongation and release factors.

Employing the DLA experiments, the ratio between the luminescence of the *firefly* (with a long UTR) and *renilla* (with a short UTR) gene were measured to analyse the ability of individual factors to promote scanning efficiency. The involvement of the elongation and release factors in the scanning process was examined by reducing the intra-cellular protein expression level of the factors to 80% of the wild-type level and examining the effect on the scanning efficiency. The ratio between the luminescence of the firefly and Renilla enzymes was compared with the wild-type cell luminescence ratio. Reductions in the protein expression levels of the elongation and release factors were not observed to have any significant effect on the scanning efficiency (Figure 4.15).

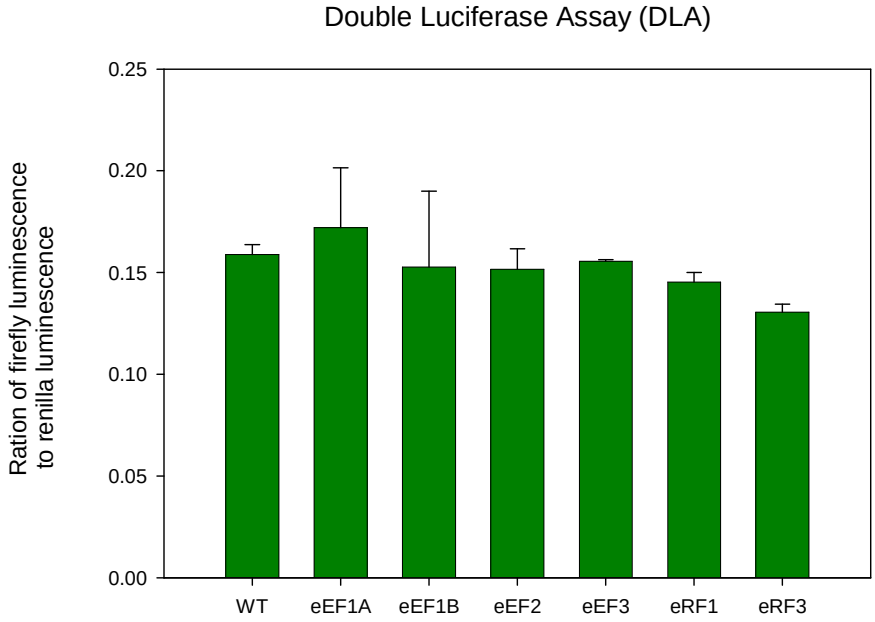

Figure 4.15 : The ratio between the luminescence of the firefly and Renilla luciferase of the elongation and release factors with the wild-type. The ratio between the luminescence encoded by the *firefly* (with a long UTR) and *Renilla* (with a short UTR) genes was measured to detect any potential involvement of the elongation and release factors in the scanning efficiency.

4.2.8. Polysome profiling of the *tetO7* strains

The polysome profiles of the *tetO7* strains expressing a 20% reduction in the level of initiation, elongation and release factors were examined to identify changes in the

monosome to polysome distribution. Polysome profiles were obtained from cells harvested during exponential growth (OD_{600} 0.5). Yeast strains were treated with cyclohexaminde (100 µg/ml) to inhibit translation elongation and thus retain ribosomes bound to mRNAs.

Priliminary data of the polysome traces of yeast strains in which the eIF2 level was decreased to 80% of the wild-type level reveal a very strong decrease in the polysosme peaks of the trace (Figure 4.16 B). Moreover, there was an increased accumulation of monosomes. However, when the level of eIF4B was decreased, the polysome-monosome ratio was not significantly changed (Figure 4.16 C). In contrast to the initiation factor profiles, the elongation factor profiles had larger polysome peaks when compared to that of the wild-type. Reduction in eEF1A (Figure 4.16 D) and eEF2 (Figure 4.17 A) yielded similar profiles in which the polysomal peaks were increased. Reduction in the factors eEF3 (Figure 4.17 B) and eRF1 (Figure 4.17 C) to 80% of the wild-type level caused rather smaller increase in the polysome-monosome ratio. However, the polysome profile was not much altered when the protein expression level of eRF3 was reduced to 80% of the wild-type level (Figure 4.17 D).

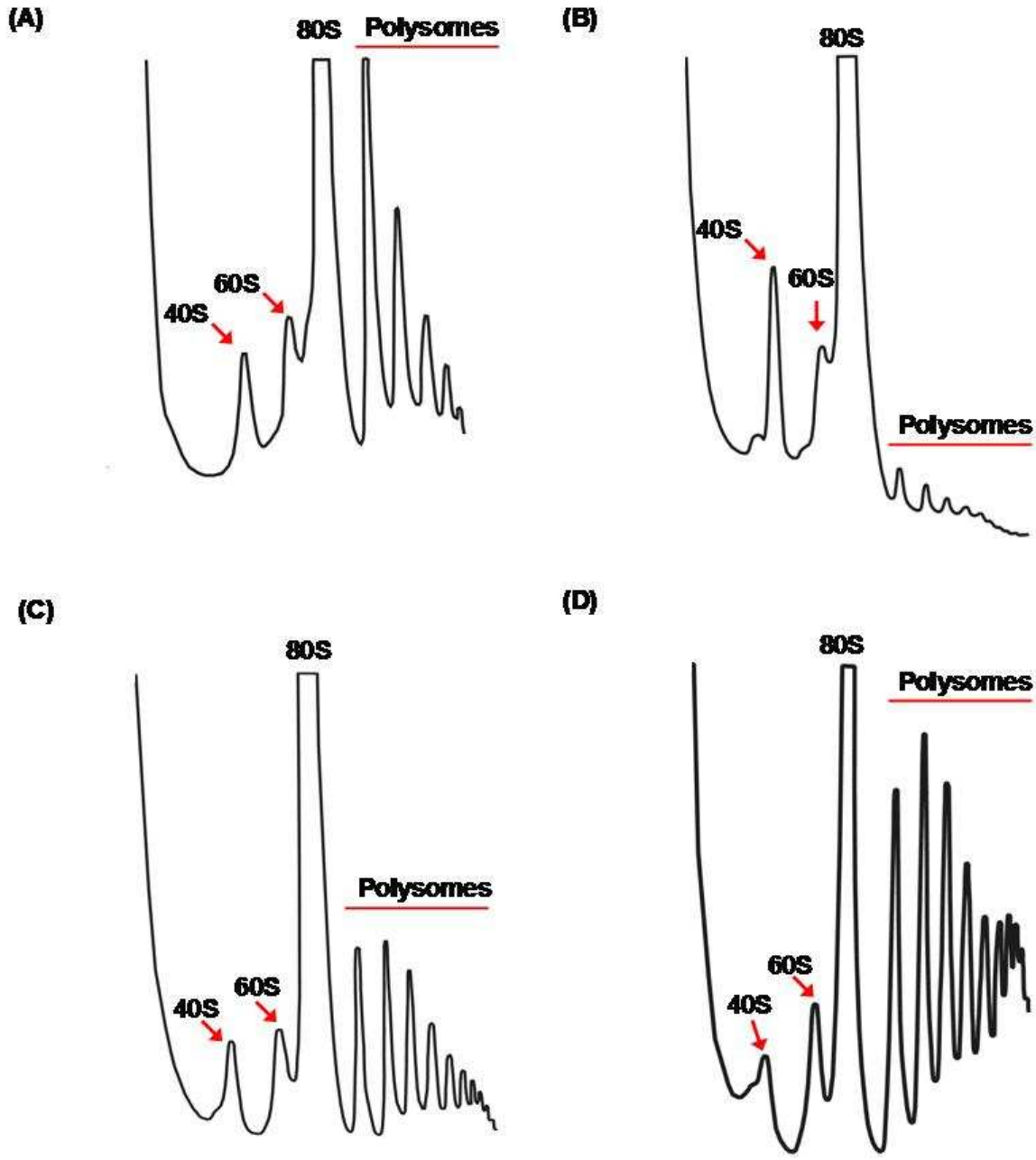

Figure 4.16 : Polysosme profiles of the initiation and elongation factor strains with wild-type. A) PTC 41 B) eIF2 c) eIF4B and D) eEF1A. The translation factors were reduced to 80% of the wild-type level. The polysome distributions of the *tetO7* strains were examined during exponential growth (OD_{600} 0.5). The polysomes of the initiation and elongation factors strains were compared with that of wild-type. Lower levels of eIF2 result in polysomal reduction and reductions in the elongation factor eIF1A have increased polysomal fractions.

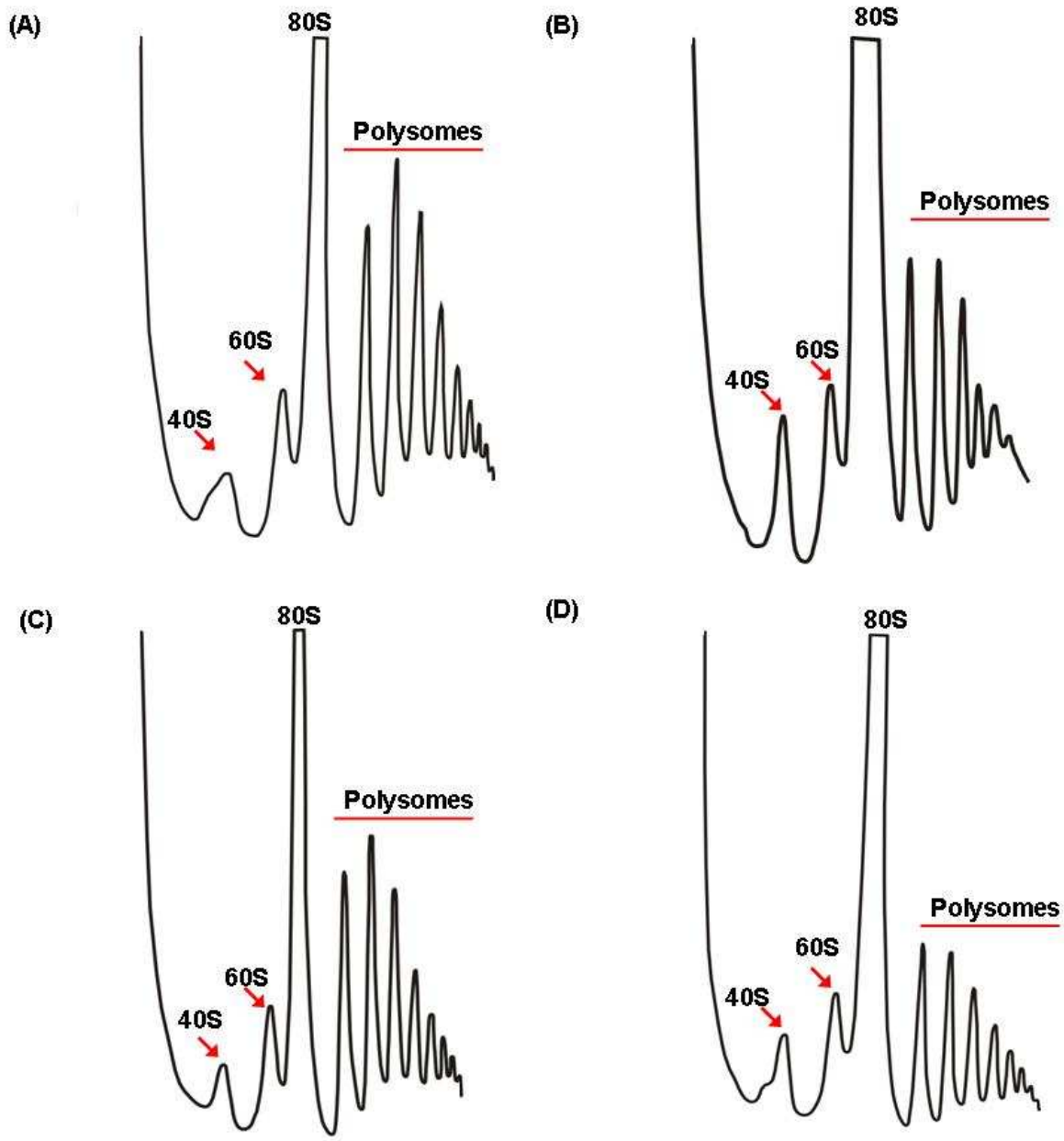

Figure 4.17: Polysome traces of the *tetO7* strains with reduced levels of elongation and release factors. A) eEF2 B)eEF3 c)eRF1 and D)eRF3. The protein expression level of the translation factors was reduced to 80% of the wild-type level. Polysome traces of eEF2, eEF3 and eRF1 showed increases in the polysome peaks. However polysome levels hardly changed in the eRF3 strain.

4.2.9. Response coefficients of the elongation and releasing factors

The protein synthesis rates at different levels of the elongation and release factors were measured using the *in vivo* ^{35}S-methionine incorporation method. The protein levels of individual elongation and release factors over the 100 – 80 % range relative to the wild-type level were plotted against the corresponding decrease in the protein synthesis rate. The response coefficient (R_1^J) is the gradient of the plot of protein level of translation factors in the 100% -80% ranges against the protein synthesis rate. Similarly R_2^J was measured from 80 % to 60 % of the physiological level. The response coefficient reveals the control extended each of the elongation and release factors. Response coefficient mostly falls between 0 to 1 and high response coefficient indicates stronger control over translation. However, the R^J values below 80 % may be influenced by a complex combination of factors related to larger reductions in gene expression, and therefore at this stage it is difficult to interpret with full confidence the higher values of R_2^J values.

Table 4.1 : The overall response coefficient and system specificity ratio of elongation and release factors

Translation factor name	$\mathbf{R}_{+1}^J$	$\mathbf{R}_1^J$	$\mathbf{R}_2^J$	$\mathbf{R^{Sp}}$
eEF1A	0.063	0.897	0.897	0.99
eEF1B	-0.007	-0.007	0.946	0.63
eEF2	-	0.937	0.937	1.02
eEF3	-0.012	-0.012	1.057	1.06
eRF1	0.162	0.748	0.748	1.10
eRF3	0.022	0.022	0.635	0.29

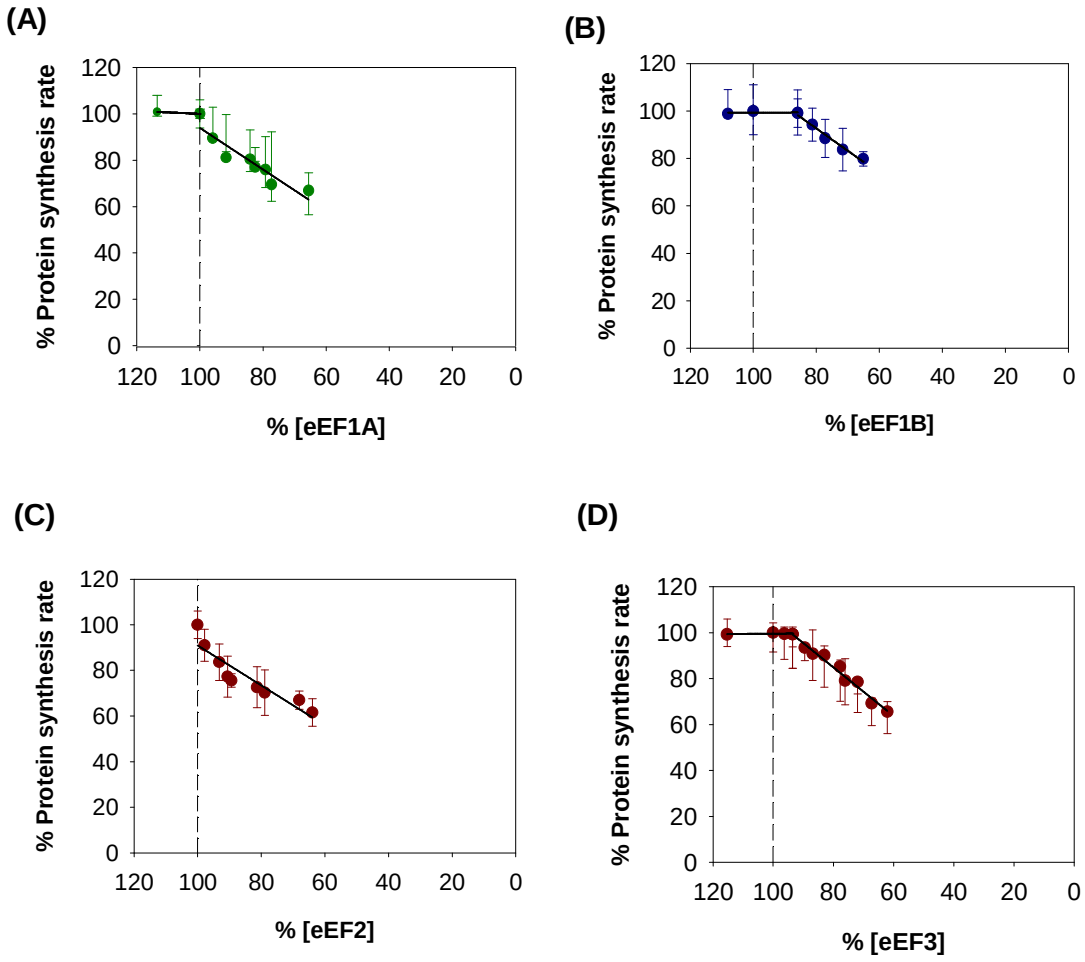

Figure 4.18: Measurement of response coefficient (R_1^J) of the elongation factors. The intra-cellular level of the elongation factors were systematically reduced about 100%-80% and respective protein synthesis rate were measured. Both the data were plotted together to obtain the R_1^J value. This indicates the dependence of the translation rate over the concentration of the elongation factors. *tetO7-TEF1* (A), *tetO7-EFT1* (C) and *tetO7-TEF3* (D) shows a very sudden decrease in the protein synthesis whereas *tetO7-TEF5* (B) shows a stable protein synthesis for a while and then reduces. The results indicate that eEF1A, eEF2 and eEF3 have better control over the translation than that of eEF1B.

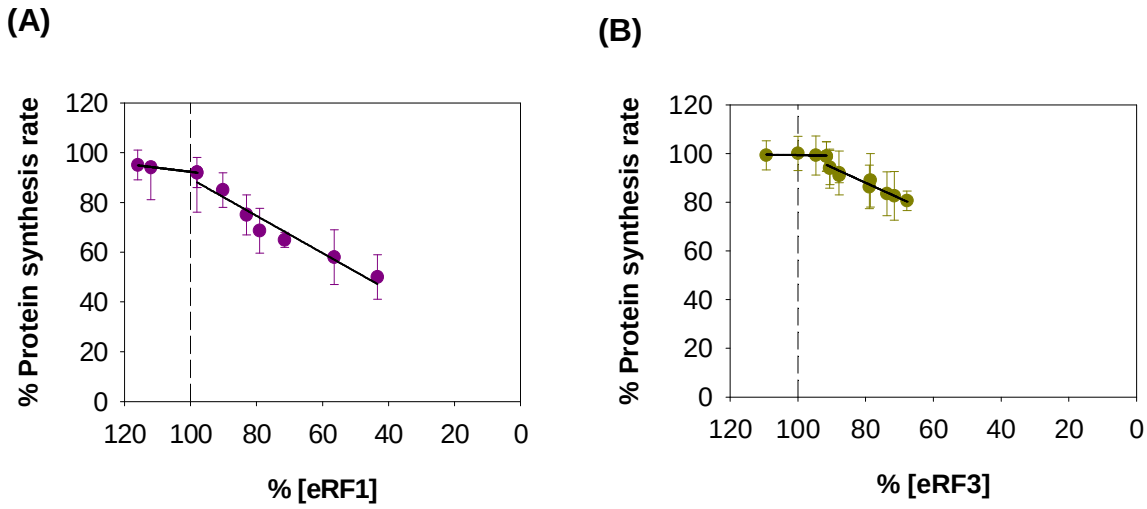

Figure 4.19: Measurement of response coefficients (R_1^J) of the release factors. The intra-cellular level of the release factors was systematically reduced from 100%-80% and beyond and the protein synthesis rates were measured. Both set of data were plotted together to obtain the R_1^J value. This indicates the dependence of the translation rate on the concentration of the release factors. The protein synthesis rate is very sensitive to the reduction in the level of eRF1, however, the protein synthesis rate was not reduced until the level of eRF3 was reduced to around 20% of the endogenous level.

4.2.10. System specificity ratio of the elongation and releasing factors

Most of the components of the translation machinery are likely to function solely in translation; however there are a number of factors which are though to be involved in other cellular functions. However, the degree of "dedication" of the components to the translation pathway has not previously been defined in an accurate, quantitatively meaningful manner. The system specificity ratio (R^{Sp}) is defined here as the relationship between the protein synthesis rates and the growth rate. To measure the system specificity ratio, the level of the individual translation factors are titrated down from 100 % – 40 % of the wild-type level and the corresponding growth rate and protein synthesis rates were measured and plotted against each other.

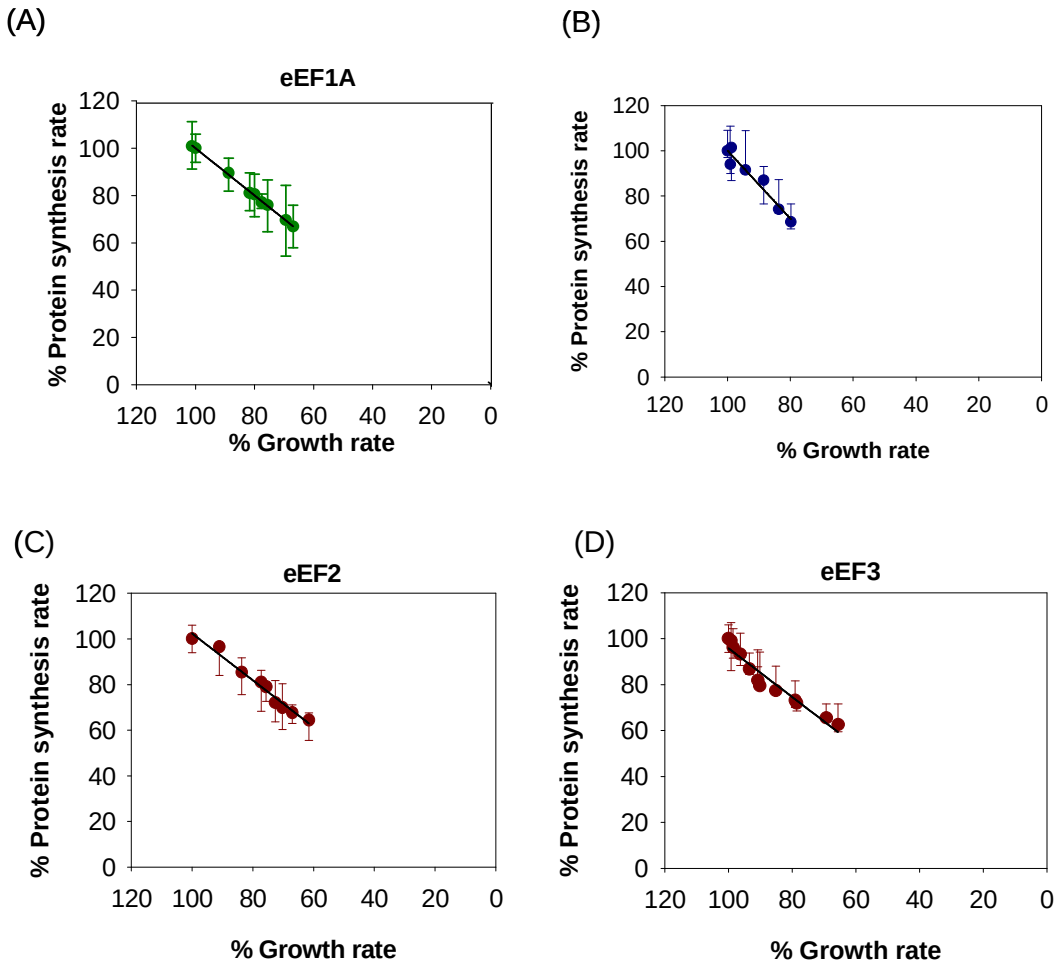

Figure 4.20: The system specificity ratios (R^{Sp}) for the elongation factors. The intracellular levels of the elongation factors were systematically reduced from 100%-80% and respective protein synthesis and growth rate were measured. Both the data sets were plotted together to obtain the R^{Sp} value of individual factors. The gradients for the elongation factors eEF1A, eEF2 and eEF3 were observed to have R^{Sp} values of around one indicating that they are dedicated factors of translation whereas the R^{Sp} of eEF1B was significantly lower than one indicating its involvement in another cellular function (Table 4.1).

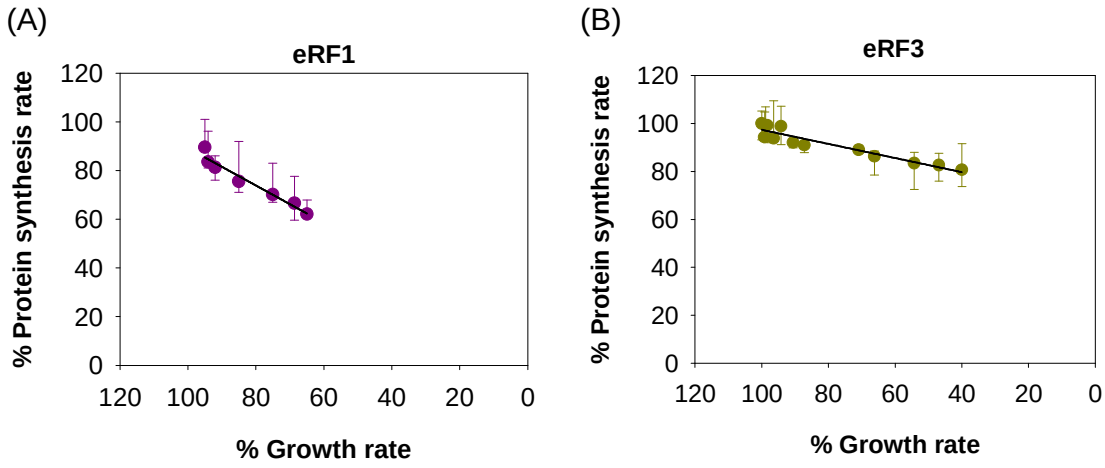

Figure 4.21: The specificity coefficients (R^{Sp}) of the release factors. The intra-cellular levels of the release factors were systematically reduced from 100%-80% and respective protein synthesis and growth rates were measured. Both the set of data were plotted to obtain the R^{Sp} value for each factors.

4.3. Discussions

4.3.1. Complementation with 'top-up' vectors rescued the phenotype of the *tetO7* strains

Most of the *tetO7* constructs were observed to support restricted production of elongation and release factors compared to wild-type cells even in the absence of doxycycline. As a consequence, decreases in growth rate were observed for the *tetO7* strains. This reduction in protein expression was rescued by the introduction of a plasmid containing the gene of interest expressed under the control of the TEF or TRP promoter in the *tetO7* strains. Two plasmids, pTefEx with P_{TEF1} promoter and pTrpEx plasmid with P_{TRP1} promoter were employed for the complementation. Even though most of the elongation and release factors exhibit reduction in the protein expression level, eRF1 was over-expressed with the *tetO7* promoter. The eRF1 protein level in the *tetO7* strain was 60% more than that of the endogenous promoter expression. However, no increased growth rate or protein synthesis rate was observed due to the over-expression of eRF1.

In the absence of the ‘top-up’ vector, the eEF1A protein expression level and growth rate of *tetO7-TEF1* strains were observed to be approximately 75 % of the wild-type. However, with genetic complementation, the protein expression level and growth were enhanced to about ~97% of the wild-type. Even though *tetO7-TEF3* strains were expressing eEF1B protein at about 50 % of the wild-type level, the growth rate remained similar to the wild-type. Reduction in the protein expression level of the strain was complemented by the pTefEx-eEf1B plasmid and the growth rate was improved to about 98% of the wild-type level. Similar to *tetO7-TEF1* strains, *tetO7-EFT1* strains were found to have about 85% of the protein expression and growth rate. However, the reductions in protein expression and growth rate were not rescued by ‘top-up’ vectors.

The *tetO7-TEF3* strains were identified to manifest severely reduced eEF3 production levels due to the promoter substitution. The growth rate and the eEF3 protein expression levels were reduced to about 30 % of the wild-type level. The drastic differences in growth rate and protein synthesis level were rescued by ‘top-up’ vectors. After complementation, the strains were observed to have about 97 % of the protein expression and growth when compared to that of the wild-type cells.

In contrast to the other strains considered here, eRF1-*tetO7* strain exhibited a higher expression level of eRF1. The strains synthesized about 60 % higher eRF1 than that of the wild-type cell. The *tetO7-SUP35* strains exhibited drastic reductions in the eRF3 expression level. However, growth was not detectably influenced by the reduction in the eRF3 expression level. The small difference in the growth rate and protein synthesis rate observed in the *tetO7-SUP35* strain was rescued with the ‘top-up’ complementation using pTefEx-eRF3 plasmid.

4.3.2. Response coefficients reflects the translational control exerted by elongation and release factors

The examination of R_1^J values for the elongation and release factors reveals two different kinds of response. Elongation factors such as eEF1A and eEF2 exhibited very high R_1^J values whereas eEF1B and eEF3 have relatively low R_1^J values (Figure 4.18). The elongation factor eEF1A was observed to have the same R_1^J and R_2^J values (0.897). The elongation factor eEF2, was observed to have a higher response coefficient of 0.9368. Similar to eEF1A, eEF2 also exhibited identical R_1^J and R_2^J values. This shows that the translation rates are highly sensitive to even minimal changes in the levels of eEF2 and eEF1A near the physiological levels. Moreover, the observed response coefficients clearly indicate that the absolute sub-cellular concentration of a factor and the level of control that it exerts on translation are not obviously correlated.

Protein synthesis was barely affected by the reductions in eEF1B and eEF3 down to 85 % of the wild-type level. In these two cases, below 85 % of factor abundance, there was high sensitivity of translation to changes in factor concentration. The eEF1B factor was measured to have an R_1^J of about - 0.007 and R_2^J of about 0.946. The eEF1B factor facilitates the exchange of GDP to GTP in eEF1A and is thus efficiently catalytic. The reduction of eEF1B level up to 85 % might not significantly influence facilitation of the recycling of eEF1A however; below 85 % of the wild-type level of eEF1B might have a considerable effect on eEF1A recycling and thus reduces the translational rate.

In the case of eEF3, the R_1^J value was observed to be -0.012 and R_2^J to be 1.057. This indicates that the translation rates are not altered by small reductions in the elongation factor eEF3 level. After reducing the eEF3 factor below 85 % the response coefficient was 1.057 which exhibits a high reduction in the translational rate. Overall, the above observations indicate that the factors eEF1A, eEF2 and eEF3 exert stronger control over translation than eEF1B.

The release factors were also observed to manifest two kinds of behaviour. The eRF1 factor has a higher R_1^J value than eRF3 (Figure 4.19). As pointed out for the elongation factors, these results indicate that eRF1 exerts more control over translation than eRF3. For eRF1, the R_1^J and R_2^J values were observed to be the same, 0.748. Translation is much more sensitive to variations in eRF1. eRF3 has R_1^J and R_2^J values of 0.022 and 0.635 respectively. These data indicate that translation is not particularly affected by a reduction in the eRF3 protein level. However, the R_2^J value of eRF3 was lower than those of eEF1B and eEF3, indicating that this factor might have less control over translation than all other translation elongation and release factors (Figure 4.22).

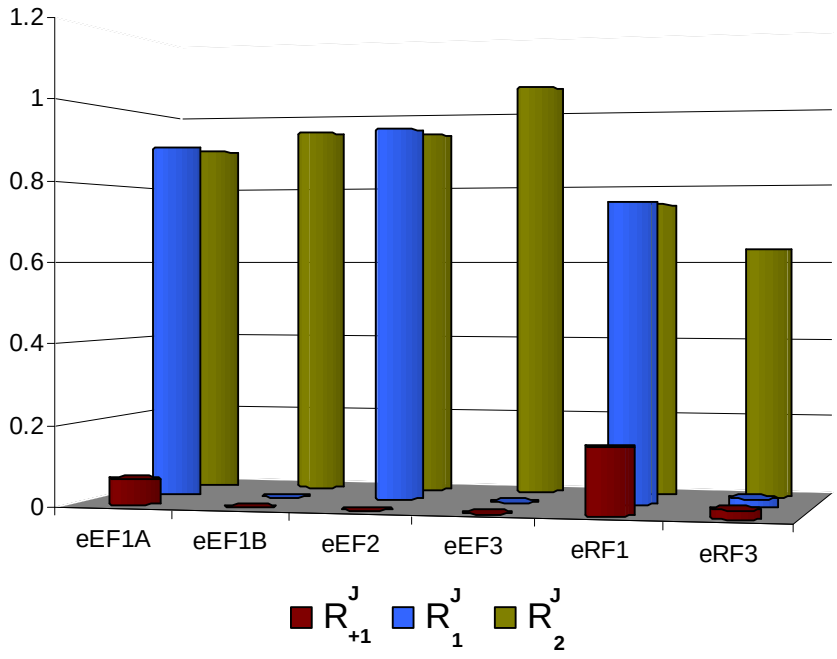

Figure 4.22 : Response coefficients of the elongation and release factors. The expression level of the elongation and release factors were altered from 120-100 % (R_{+1}^J), 100-80 % (R_1^J) and 80-60 % (R_2^J). The R_{+1}^J was calculated as the slope of the line connecting protein synthesis rate to the factor concentration over 100%, R_1^J was calculated as the slope of the line connecting protein synthesis rate to the factor concentration at 100 - 80% and R_2^J was calculated as the slope of the line connecting protein synthesis rate to the factor concentration over 80-60%.

4.3.3. System specificity ratio : the degree of "dedication" of translation factors

If the factors are dedicated only to translation, the slope of the linear curve between the protein synthesis and growth rate will be approximately equal to 1 whereas if the factor is involved in other cellular functions other than translation then the slope will be <1. Elongation factors eEF1A, eEF2, eEF3 and release factor eRF1 were observed to have a similar patterns of system specificity dependence (Figure 4.20 A, C, D and 4.21 A). The eEF1A R^{Sp} ratio was measured to be 0.99 (Table 4.1) indicating that the factor is a dedicated factor in translation. Similarly, R^{Sp} values of eEF2, eEF3 and eRF1 were observed to be 1.02, 1.06 and 1.1 respectively (Table 4.1). The data indicates that all of these factors are more involved in translation than in any other cellular functions. In contrast, the elongation factor eEF1B and the release factor eRF3 were identified to have lower R^{Sp} values (Figure 4.20 B and 4.21 B). The R^{Sp} values of eEF1B and eRF3 were observed to be 0.63 and 0.29, respectively. This observation indicates that these factors are involved in other cellular functions in addition to the translation. System specificity ratio analysis reveals that the elongation factors eEF1A, eEF2 and eEF3 and release factor eRF1 are mostly functionally involved in just translation whereas eRF3 and eEF1B are involved in other cellular functions in addition to translation (Figure 4.23).

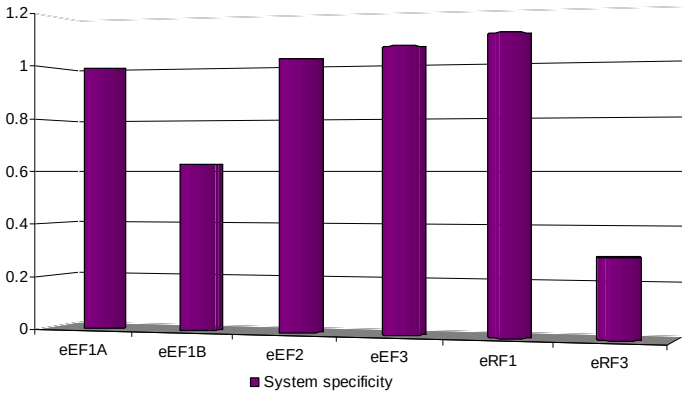

Figure 4.23: The system specificity ratio (R^{Sp}) of the elongation and release factors. The specificity ratio was measured as the slope of the curve between the protein synthesis rate and the growth rate of the *tetO7* strains with varying levels of elongation and releasing translation factors. The specificity ratio identifies the functionally dedicated translation factors. If the ratio is 1, it indicates that the factor is mostly involved in translation whereas <1 indicates involvement in other cellular functions.

4.3.4. Response coefficient and specificity ratios when elongation or release factors are expressed at levels higher than wild-type

The response coefficient (R^{J}_{+1}) and specificity ratio for elongation and release factors were also determined at above physiological levels to determine if this had any effect on protein synthesis or cell growth rates (Table 4.1). The intra-cellular levels of the elongation and release factors were increased to 120% of the endogenous level. Interestingly, none of the strains showed any significant increase in protein synthesis or growth rate (Figure 4.18 and 4.19). This raises an interesting question as to why no increases above physiological growth and protein synthesis rates are attainable. It might suggests that there may be further mechanism(s) to control the level of growth rate and protein synthesis rate even though the translation factors are increased to above the physiological level. This is also an indication that the translation and growth rate of yeast is maintained at an optimum level that is dictated by precisely controlled properties of the entire systems.

4.3.5. Scanning competency data show no participation of elongation and release factors in the 40S scanning

The 40S scanning process to identify the initiation codon is a poorly understood step in which the small ribosomal subunit, 40S, is reported to be capable of scanning more than 1000 nucleotides to identify the AUG codon (Kapp and Lorsch, 2004a). The DLA was employed to determine if reducing the protein concentration of elongation or release factors had any effect on the scanning and AUG recognition function of the 40S subunit. In the DLA assay, the luminescence activity of *Renilla* and *Firefly* genes are proportional to the efficiency of scanning of the 5' UTR by the 40S and other translation factors. Scanning competency of each of the translation factors was determined as the ratio of the luminescence of *Firefly* versus *Renilla*. Measurement of scanning competency reveals any influence on the efficiency of the scanning process. The data show that when the elongation and release factors were reduced to 80% of the endogenous level, no key variation in the scanning efficiency was observed. The experimental observations strongly suggest that the

elongation and release factors do not play a role in the mRNA scanning process of the 40S ribosomal subunit, and demonstrate that the initiation factors are exclusively responsible for controlling this step.

4.3.6. Reduction in the level of initiation, elongation and termination factors alters polysome distribution

Polysome distribution analysis is an efficient way to observe changes in the interaction between ribosomes and mRNA. Any alteration in the translation factors and ribosomal association with the mRNA has an impact on the polysome distribution which can be visualised by this technique. Polysome profiles of yeast strains were generated to determine the polysome distribution in response to changes in intra-cellular concentrations of the translation factors. The 40S and 60S peaks in the polysome profile represent the non-translating ribosomal subuits whereas the polysome peaks represent actively translating 80S ribosomes. The 80S peak itself corresponds to a combination of both non-translating 40S-60S 'couple' and translating 80S particles. The intra-cellular levels of the initiation, elongation and release factors were reduced to 80% of the endogenous level and the polysosme traces were compared with those generated from wild-type cell cultures.

When the endogenous level of eIF2 was reduced, an increase in the level of 40S ribosomal subunits along with a decrease in the polysome peaks was observed (Figure 4.16 B). eIF2 is involved in the delivery of Met-tRNA to the ribosome which is an essential event in the translation initiation step. Therefore it is likely that a reduction in the cellular concentration of this factor would have a very strong impact on the identification of the initiation codon and on the polypeptide synthesis. Reduction of eIF2 would affect the association of 40S and 60S, resulting in the accumulation of monosomes and a decrease in the number of actively translating polysomes. However, a drastic reduction in polysomes was not observed with a reduction in the eIF4B protein concentration. Even though there is a decrease in the polysomal peaks when compared to the wild-type trace, it is not as marked as the decrease observed with eIF2 protein level reduction. eIF4B indirectly binds to the mRNA cap with other initiation factor and the reduction of this factor may not affect the

active translation to a high extent. The results indicate that eIF2 has a very crucial role in the translation and a reduction in this factor can regulate translation.

When the eEF1A protein levels were decreased, there was an increase in the polysome peaks (Figure 4.16 D). eEF1A is involved in the delivery of aa-tRNA to the ribosome which is an essential event in elongation process. Consequently the reduction in the cellular concentration of this factor would have a very high impact on the elongation cycle, blocking the ribosome on the mRNA from continuing with elongation. This explains the observed increase in the polysome peaks when the protein cellular level of eEF1A was reduced. Similarly, when the eEF2 protein levels were decreased, the polysome level was increased (Figure 4.17 A). eEF2 factor is involved in the translocation of the ribosome on the mRNA. The reduction in the protein level of eEF2 could have attached the ribosome to the mRNA resulting in an increased level of polysomes. 60S monosome accumulation was not observed when the level of eEF2 or eEF3 was reduced. Reduction in the eEF3 level also caused an increase in the polysome peaks, but the increase was not as marked as that observed with eEF1A or eEF2.

Reductions in the release factors were observed to have an effect on the polysome distribution. Even though the increase in the polysome peaks was not as marked as those observed with the elongation factors, a reduction in the protein level of eRF1 caused an increase in the polysome peaks. eRF1 identifies all three of the stop codons in the eukaryotic translation pathway. The reduction in this factor can cause read-through mRNA or slow down termination thus potentially causing a queue towards the end of the mRNA. The reduction in eRF3 level was not observed to cause much effect on the polysome profile. The polysome trace was very similar to that of the wild-type equivalent indicating that eRF3 reduction was not affecting the polysome distribution. Both of these observations agree with the results obtained by the protein incorporation experiments.

4.4. Conclusion

In order to determine quantitatively the control exerted by elongation and release factors during translation, the expression of these factors was repressed and resulting variations in protein synthesis were measured. The elongation factors eEF1A and eEF2 and the release factor eRF1 were observed to exert the greatest control over translation. The protein synthesis rate was sharply reduced when these factors were expressed at 80% of wild-type level. However, eEF3 exerted the greatest effect over translation when it was repressed from 80 – 60 % of the wild-type level. eEF1B and eRF3 were observed to have the least control over translation compared to other elongation and release factors.

These observations were reinforced by the polysome profiles. The elongation and release factors were made limiting in the cell and the corresponding polysome distributions were analysed. The data indicates that when the eEF1A and eEF2 expression is repressed in the cell, the polysome levels were increased. This is likely to be the result of reductions in the elongation rate. Reduction in the eEF3 and eRF1 levels also resulted in increased polysosme levels; however; the increase was not as high as observed with eEF1A and eEF2 factor reduction. This indicates that the elongation rate is not strongly affected by the reduction in eEF3 and eRF1 over the 100 % - 80 % range.

The system specificity ratio of the elongation and release factors was measured to determine which factors function solely in the translation pathway and which factors may play a role in other cellular processes. The factors eEF1A, eEF2, eEF3 and eRF1 were observed to be solely involved in the translation pathway. A reduction in the cellular protein concentration of factors results in a proportional reduction of protein synthesis and growth. In contrast when the eEF1B and eRF3 factors were reduced, growth decreased faster than the protein synthesis rate suggesting that the reduction in these factors affects some other cellular function(s) in addition to translation. All of the above types of data are of relevance to the development of a comprehensive, quantitative model for the process of translation (chapter 5).

.

Chapter 5

A mathematical model of yeast translation

5.1. Introduction

Eukaryotic mRNA translation is a highly sophisticated and precisely controlled molecular process. Translation is one of the fundamental processes that are well conserved across all Kingdoms of life. Through translation, information is passed from mRNA to proteins. Translation comprises mainly of three stages: initiation, elongation and termination. The nature of fourth stage, recycling, is not understood in the eukaryotic system. In yeast, mRNA translation is controlled by more than 20 different proteins and vast amounts of RNA molecules. Each of the translation steps is facilitated by a number of translation factors. The translation factors are critically important components of the system. Apart from these components, mRNA, tRNA and ribosomal subunits constitute essential parts of the translation machinery. A vast amount of experimental work has been carried out to understand this complex process, most of it taking the form of studies of the roles of individual components. Depending on the environmental conditions and intrinsic capacity of the mRNA, the translational rates differ for individual proteins (Siwiak and Zielenkiewicz, 2010). There are numerous examples of translational control being exercised via the initiation step (Sonenberg and Hinnebusch, 2009, Mathews et al., 2000), yet the protein synthesis pathway can also be modulated at the elongation and termination steps (Wang et al., 2001) and the interplay between these steps is not understood. Mathematical modeling is a very powerful tool to incorporate all experimental data to understand how a complex process such as translation functions. Precise control of translation is difficult to understand without quantitative understanding based on an adequate mathematical model. A mathematical model can be used to develop a system-level view of the whole pathway rather than looking at the individual components of the

system. Several studies were been carried out previously to understand the complexity of the translation pathway using mathematical modelling. In the late 1960, translation was modelled as a set of kinetic reactions and ribosomal progression steps (McDonald et al., 1968). This was considered to be the first attempt to construct a mathematical model of translation. The model was later extended and modified to incorporate ribosomal crowding and its overall effect on translation (Heinrich and Rapoport, 1980).

This study states that initiation and elongation are rate-limiting whereas termination has no control over translation under the regular cellular conditions. Ribosomal crowding has been incorporated in a translation model for the bacterial system as well as considering elongation as a set of ribosomal states (Zourdis and Hetzimanikatis, 2007). This model takes into account possible variations in the elongation cycle due to differences in the amino acid codons in the mRNA. However, all of these models lack appropriate experimental data to verify the results they observed and therefore provide little insight into the true nature of translation control.

There are a number of software packages developed to model and simulate complex biological processes. COPASI (COmplex PAthway SImulator) has been employed to construct and simulate the translation model (Hoops et al., 2006). COPASI converts the biochemical reactions into mathematical formulations such as ordinary differential equations. Moreover, COPASI can accommodate different types of analyses such as steady state analysis, sensitivity analysis and metabolic control analysis.

In this work, a mathematical model for the eukaryotic mRNA translation has been developed. As well as considering every elementary step in the initiation, elongation and termination stages, ribosomal blocking at the AUG recognition stage of initiation and the translocation stage of elongation has been incorporated. This model examines rate-limiting steps in translation and variations in translation rate as a consequence of reduction in translation factors. The translation model has there been filled to the experimental data in order to allow us to simulate translational control under physiological conditions.

5.2. Results

5.2.1. Yeast translation machinery

The three main stages of mRNA translation are facilitated by specific factors. Initiation is a series of reactions in which the ribosomal small subunit associated with mRNA and identification of the initiation codon after which the large ribosomal subunit binds to the small subunit to synthesis polypeptide. Elongation is the cycle of reactions in which amino acids are added to the growing poly-peptide chain. Termination is the one step reaction that occurs after the identification of the stop codon by the release factors, after which the translation complex disassociates. According to the current consensus of translation, there are 13 translation initiation factors, 4 elongation factors and 2 termination factors involved in the process. Apart from the translation factors, the ribosomal subunits, mRNA, tRNAs and aa-tRNAs are also included in the model. The schema of the translation model is represented here using petri-net (Figure 5.1). 33 reactions have been formulated to represent the whole of translation process including the elongation cycle. The concentrations of the translation components in this model are listed in Table 2.11. The total amount of ribosome subunits are estimated in this model based on the ribosome concentration. In this model the ribosomes are regarded as large bodies moving in a step-wise manner. Prokaryotic ribosomes are reported to occupy 12 codons during elongation (Mathews et al. 2000) however, since the eukaryotic ribosomes are known to be larger than the prokaryotic ones, the ribosome is assumed to cover 15 codons of an mRNA during translation. The model constituents for the general mRNA translation and all mRNA species are assumed to have the same parameter values.

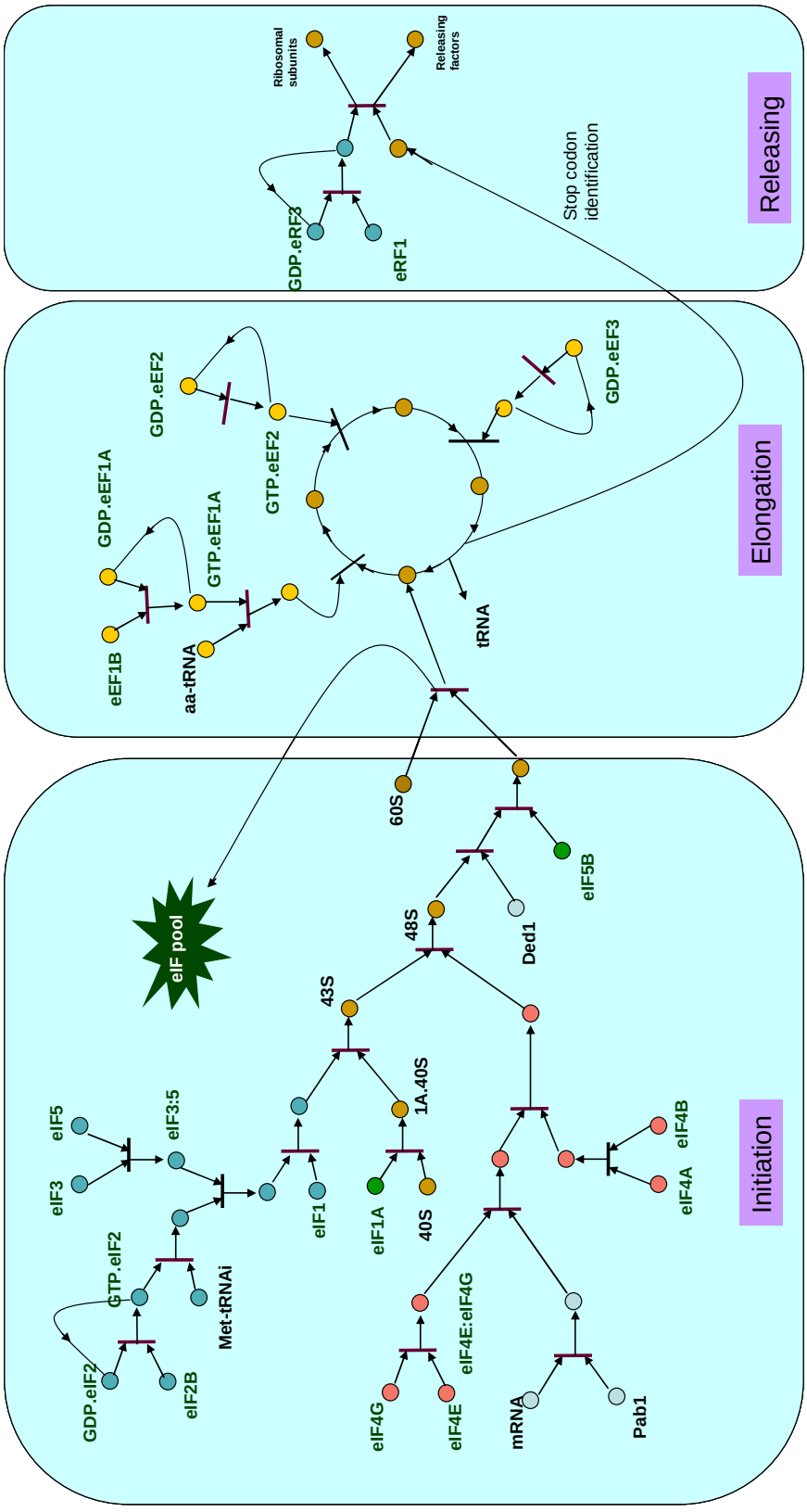

Figure 5.1 : Petri-net representation of the yeast translation pathway. Each stage of translation initiation, elongation and termination are represented as bi-molecular reactions. The factors are represented with circles and the reactions are represented as arrows. Each of the bi-molecular interactions is represented as a transition.

5.2.2. Model formulation

The mathematical model of the yeast mRNA translation pathway was developed as a deterministic system of ordinary differential equations. The model was developed in Complex Pathway Simulator (COPASI) (Development version 4.5.31) (Hoops et al., 2006) with the script developed in Perl (Dr. Juergen Pahle, University of Manchester). The three stages of translation: initiation, elongation and termination, were described using 33 key reactions with a subset of elongation reactions for each codon. The model was built with 19 translation factors, mRNA, tRNA, 40s, 60s and 80s of ribosome and the intermediate complexes. Mass action kinetics was applied for most of the initiation and releasing steps whereas blocking kinetics was introduced to describe the identification of the initiation codon and the translocation stage in elongation. All the set of differential equations are listed in appendix -1.

5.2.2.1. Parameter values

The concentration values for all the translation factors and reactions used in this model were taken from the published literature (Table 5.1). The kinetic values are taken as the default values from the model (appendix - 2). The rest of the parameters were optimized using experimental data with the parameter optimisation module of COPASI. The cell volume was selected as $42x10^{-15}$ L (Jorgensen et al., 2002). The model was fitted to the experimental data (protein synthesis rate) using the parameter estimation module of COPASI (appendix -3).

Table 5.1 : List of translation factors in the translation model along with their corresponding concentrations values

Name of Species	Gene name	Concentration (particle/cell)	Source
eIF1	SUI1	2.50E+05	von der Haar and McCarthy, 2002
eIF1A	TIF11	3.51E+04	Ghaemmaghami et al., 2003.

eIF2α	SUI2	1.71E+04	Ghaemmaghami et al., 2003 .
eIF2Bα	GCN3	8.97E+03	Ghaemmaghami et al., 2003.
eIF3a	RPG1(TIF32)	5.27E+04	Ghaemmaghami et al., 2003.
eIF4A	TIF1/TIF2	1.06E+05	Ghaemmaghami et al., 2003.
eIF4B	TIF3	2.40E+04	Ghaemmaghami et al., 2003.
eIF4E	CDC33	1.42E+04	Ghaemmaghami et al., 2003.
eIF4G1	TIF4631/ TIF4632	9.76E+03	Ghaemmaghami et al., 2003.
eIF5	TIF5	4.83E+04	Ghaemmaghami et al., 2003.
eIF5B	FUN12	1.34E+04	Ghaemmaghami et al., 2003.
Pab1	PAB1	1.98E+05	Ghaemmaghami et al., 2003.
Ded1	SPP81	5000	This study
eEF1A	TEF1/TEF2	3.77E+02	Ghaemmaghami et al., 2003.
eEF1B	TEF5	190549	von der Haar, 2008.
eEF2	EFT1/EFT2	8.27E+04	Ghaemmaghami et al., 2003.
eEF3	TEF3/YEF3	8.71E+05	Ghaemmaghami et al., 2003.
eRF1	SUP45	1.31E+04	Ghaemmaghami et al., 2003.
eRF3	SUP35	7.89E+04	Ghaemmaghami et al., 2003.
Met-tRNA		640000	This study
40S		222000	This study
60S		222000	This study
aa-tRNA		12800000	This study
mRNA		4900780	Chu and Maley, 1980
tRNA		6400000	This study

5.2.2.2. Model assumptions

Translation is a complex pathway and most of the parameters, including the concentration of factors and the rate of the reactions are not accurately determined. A number of assumptions were employed in the formulation of the translation mathematical model. The translation steps and factors which are not well studied were omitted in the model.

Assumption 1: Each ribosome physically covers 15 codon of the mRNA

The ribosomes were assumed to cover 15 codons during translation, thereby blocking the binding of another ribosome (and subsequent initiation of translation and translocation) on this stretch of mRNA. If the seventh and eighth codons are covered by the ribosome P and A site respectively, 7 codons upstream and downstream will be blocked by the ribosome in the initiation and translocation states.

Assumption 2: Concentration of the aa-tRNA and the elongation rate for individual codons was assumed to be the same

The concentration of the aa-tRNA in the cell was assumed to be the same for all amino acids. Similarly, the codon-anticodon base pairing for all the amino acids was assumed to be the same. This implies that the elongation rate is not limited by the concentration or rate of rare aa-tRNAs.

Assumption 3: mRNA length assumed to be 20 codons

The translation model developed is applies to the general mRNA translation in yeast. To implement the model, the mRNA translation length is assumed to be 20 codons. However, the model can be extended to study mRNA of any size longer than 15 codons. 15 codons is the minimum length required for the ribosome to bind to an mRNA.

5.2.2.3. Model construction

The model for translation is constructed based on the model first proposed by McDonald et al., 1968 and later extended by Heinrich and Rapoport, 1980. A number of assumptions were employed to simplify the complex model (section 2.13.3**)**. The model is a deterministic model generated using perl scripts as a set of differential equations and analysed in COPASI. Most of the initiation stages are considered to follow mass action kinetics. The elongation and termination stages, except translocation are also constructed as mass action kinetics. However, the subunit joining in the initiation stage and translocation in the elongation stage are constructed by considering ribosomal occupation of regions of mRNA. Ribosomes are assumed to block 15 codons on the mRNA during subunit joining and translocation. Blocking rate equations were formulated (Juergen Pahle, University of Manchester) to represent different stages of elongation and blocking properties of the ribosome.

If 'l' is the codons occupied by ribosome and if X_j is the probability that the j^{th} codon of the mRNA being translated is occupied by the front of the ribosome, then the probability that the initiation codon is free can be represented as

$$W_I^1 = \left(1 - \sum_{j=1}^{l} X_j\right)$$

Where, W_I^1 is the probability of the initiation site being free.

Then the rate of initiation blocking can be represented as

$$V_I^1 = S_1 S_2 k_I^1 M_{tot} W_I^1$$

Where V_I^1 is the rate of blocking, S_1 is the first substrate (40S), S_2 is the second substrate (60S), M_{tot} is the total concentration of mRNA in the translation and W_I^1 is the probability of initiation site being free.

Similarly, in the translocation stage, the fluxes for translocation can be formulated as

$$V_j = S_1 \, k_j \, X_j \, M_{tot} \, W_{j+1}$$

Where V_j is the flux through translocation, S_1 is the substrate (80S), k_j is the first order rate constant and W_{j+1} is the conditional probability that the j+1 position is free provided that the j^{th} position is occupied. It can be written as

$$V_j = S_1 \, k_j \, X_j \, M_{tot} \frac{\left(1 - \sum_{j=1}^{l} X_j\right)}{\left(1 - \sum_{j=1}^{l-1} X_j\right)}$$

5.2.3. Mass conservation

The model was constructed in COPASI. After model construction, the mass conservation of the model was determined. Mass conservation relations are algebraic sums of chemical species that are constant in any state of the model (Hoops et al., 2006**)**. If the model satisfies a mass conservation relation for a species, then that species could be represented as an expression of all the compounds that species involved with. In COPASI mass conservation is calculated using an algorithm described by Vallabhajosyula et al., 2006. Total concentration of each of the individual factor in the translation pathway remains constant in the model. Mass conservations are helpful in validating the mathematical conditions of the model. If one of the translation factors is not occurring in the mass conservation relation it means that the model is broken.

5.2.4. Time course simulations of the model

The model was simulated over a time period to analyse the behaviour of individual components of the model. In time course simulations the model behaviour is observed over a period of time with certain parameter values (Figure 5.2). COPASI calculates the time

courses for deterministic models using the LSODA integrator (Petzold. 1983). The translation model was simulated up to 10000 sec to observe the behaviour of the system. The model behaviour can be explored over duration of time specified for the time course simulations. The time series simulation of the model were plotted to analyse the result.

(A)

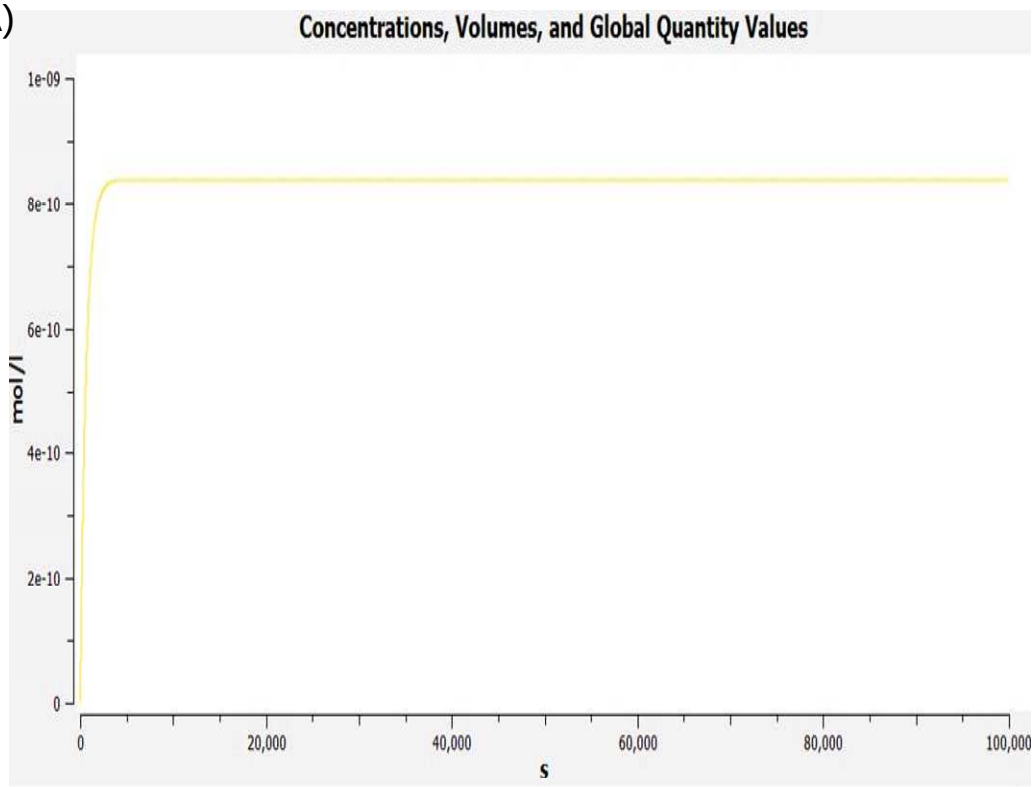

(B)

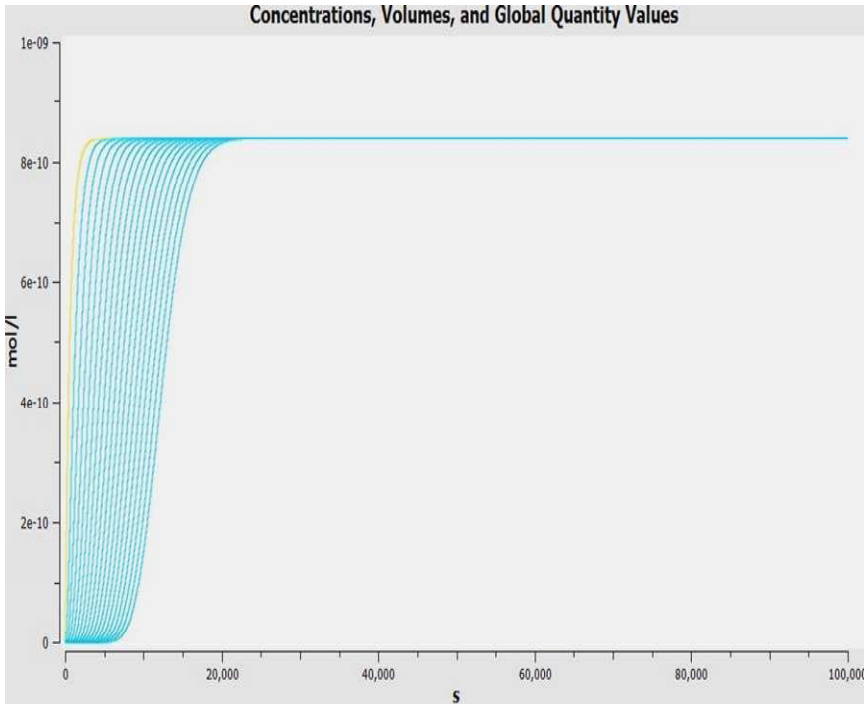

(C)

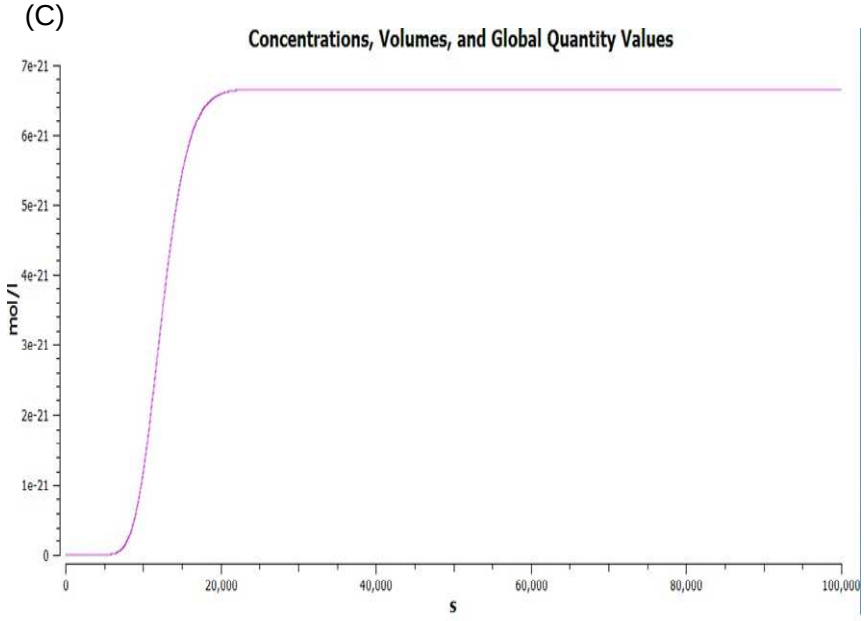

Figure 5.2 : Time course simulation of the translation model. Time course behaviour of the model before parameter fit. The model default values are used as the initial kinetic parameters (appendix -2). A) Formation of the 80S, the initiation stage of translation where the 40S associates with 60S B) 80S_aa-tRNA_eFF2_GTP formation for the whole elongation cycle and C) formation of 80S_eRF1_eRF3_GTP in the termination stage where translation is completed and all the factors dissociate.

5.2.5. Steady state calculation

After confirmation of mass conservation relation, the model was simulated to find a steady state. In steady state, the concentrations of the chemical species in the system do not change over time. Using COPASI steady states are determined using three different methods 1) the Newton–Raphson method 2) Forward integration of the ODEs and 3) Backward integration of the ODEs. Both the integrations are carried out using ODEs solver LSODA. COPASI can use either one of these methods or a combination of the three. Steady state calculation in COPASI is based on Schuster et al., 1999. The translation model was able to predict a steady state with the Newton–Raphson and forward integration method. The model found the resolution at 1e-09 without accepting any negative concentration in the model simulation. The resolution distinguishes the smallest values of the concentration change of species from zero. The model steady state fluxes are listed in Table 5.2.

Table 5.2 : List of all the reaction fluxes through the translational pathway.

Reactions	**Particle Flux (1/s)**
1. eIF2_GDP + eIF2B = eIF2_GDP_eIF2B	305.013
2. eIF2_GDP_eIF2B = eIF2_GTP + eIF2B	305.013
3. eIF2_GTP + Met-tRNA = eIF2_GTP_Met-tRNA	305.013
4. eIF3 + eIF5 = eIF3_eIF5	305.013
5. eIF2_GTP_Met-tRNA + eIF3_eIF5 = eIF3_eIF5_eIF2_GTP_Met-tRNA	305.013
6. eIF1 + eIF3_eIF5_eIF2_GTP_Met-tRNA = eIF1_eIF3_eIF5_eIF2_GTP_Met-tRNA	305.013
7. 40S + eIF1A = 40S_eIF1A	305.013
8. eIF1_eIF3_eIF5_eIF2_GTP_Met-tRNA + 40S_eIF1A -> 43S	305.013
9. eIF4E + eIF4G = eIF4E_eIF4G	305.013
10. mRNA_cap + Pab1 = mRNA_Pab1	305.013
11. eIF4E_eIF4G + mRNA_Pab1 = eIF4E_eIF4G_mRNA_Pab1	305.013

12. eIF4A + eIF4B = eIF4A_eIF4B	305.013
13. eIF4E_eIF4G_mRNA_Pab1 + eIF4A_eIF4B = eIF4E_eIF4G_mRNA_Pab1_eIF4A_eIF4B	305.013
14. 43S + eIF4E_eIF4G_mRNA_Pab1_eIF4A_eIF4B -> 48S	305.013
15. 48S + Ded1 -> 48S_Ded1	305.013
16. eIF5B_GDP = eIF5B_GTP	305.013
17. 48S_Ded1 + eIF5B_GTP -> 48S_Ded1_eIF5B_GTP	305.013
18. 60S + 48S_Ded1_eIF5B_GTP -> 80S_1 + eIF1 + eIF1A + eIF2_GDP + eIF3 + eIF4A + eIF4B + eIF4E + eIF4G + eIF5 + eIF5B_GDP + Pab1 + Ded1 + mRNA_cap	305.013
19. eEF1A_GDP + eEF1B = eEF1A_GDP_eEF1B	6100.25
20. eEF1A_GDP_eEF1B = eEF1A_GTP + eEF1B	6100.25
21. eEF1A_GTP + aa-tRNA = aa-tRNA_eEF1A_GTP	6100.25
22. eEF2_GDP = eEF2_GTP	6100.25
23. eEF3_GDP = eEF3_GTP	6100.25
24. aa-tRNA_eEF1A_GTP + 80S_1 = 80S_aa-tRNA_eEF1A_GTP_1	305.013
25. 80S_aa-tRNA_eEF1A_GTP_1 -> 80S_aa-tRNA_1 + eEF1A_GDP	305.013
26. eEF2_GTP + 80S_aa-tRNA_1 = 80S_aa-tRNA_eEF2_GTP_1	305.013
27. 80S_aa-tRNA_eEF2_GTP_1 -> 80S_tRNA_1 + eEF2_GDP	305.013
28. 80S_tRNA_1 + eEF3_GTP -> 80S_tRNA_eEF3_GTP_1	305.013
29. 80S_tRNA_eEF3_GTP_1 -> 80S_2 + eEF3_GDP + tRNA	305.013
30. eRF3_GDP = eRF3_GTP	305.013
31. eRF1 + eRF3_GTP = eRF1_eRF3_GTP	305.013
32. eRF1_eRF3_GTP +80S_tRNA_eEF3_GTP_20 -> 80S_tRNA_eEF3_GTP_eRF1_eRF3_GTP	305.013
33. 80S_tRNA_eEF3_GTP_eRF1_eRF3_GTP -> 40S + 60S + tRNA + eEF3_GDP + eRF1 + eRF3_GDP	305.011

5.2.6. Parameter Estimation

As described in previous chapters, the protein synthesis rates at varying levels of initiation, elongation and release factors have been measured using protein incorporation experiments. These experimental data were employed to set constrains on the translation model (appendix -3). The experimental data comprised a set of concentration values for individual translation factors and the corresponding protein synthesis rates. The total (maximal) protein synthesis rate was set at 13000 molecules/sec (von der Haar, 2008). The incorporation of this extensive set of new data into the model represents a major step-change in the development of a quantitatively meaningful understanding of translational control.

The experimental data were mapped onto the model to determine the unknown parameters in the model. The parameter estimation function in the COPASI software was employed to calculate the fit the model to the experimentally observed parameter values. Parameter estimation minimises the distance between the model simulation values and the experimental data and the distance is derived from a least-squares approach.

$$O(p) = \sum_i \sum_j \sum_k \omega_{k,i} \left(X_{k,i,j} - \mathrm{Y}_{k,i,j}(\boldsymbol{p}) \right)^2$$

where $X_{i,j,k}$ is the experimental value of variable i at measurement j within experiment k and the corresponding simulated data point is given by $\mathrm{Y}_{k,i,j}(\boldsymbol{p})$ where $\boldsymbol{p}$ is the vector of parameter values used for the simulation. It is important that the data for the different variables be of comparable magnitude so each group of values for each variable in each experiment is multiplied by a weight $\omega_{k,I}$ (Hoops et al., 2006**).**

5.3. Discussion

5.3.1. Integration of ribosomal blocking into the initiation and translocation stages of translation

A deterministic kinetic model of eukaryotic translation has been developed in order to understand the translational control exerted by individual translation factors. The model focuses on every elementary step in the translation pathway and considers the ribosomal blocking exerted during initiation and elongation. Yeast ribosomes are estimated to block 15 mRNA codons during translation. In the model, ribosomal blocking is introduced in two states, first, at the ribosomal subunit joining step during initiation and second during translocation step of elongation phase. The consideration of the blocking phenomena ensures that two ribosomes do not collide during translation. The termination stage of translation is mass action kinetics involving two translation release factors.

During initiation step the ribosomal subunit joining is only possible if the AUG codon and the seven codons downstream of the AUG codon are not occupied. Similarly, translocation of the ribosome from j^{th} codon to $j+1^{th}$ codon is only possible if the $j+8^{th}$ codon is unoccupied. Multiple initiation events can only take place if the previous ribosome has moved sufficiently far away (seven codons) from the initiation site so that the next ribosome can bind to the initiation codon. Ribosome translocation depends on the conditional probability that the codon adjacent to the codon occupied by the front of the ribosome is free, given that the previous codon is occupied by the front of the ribosome

5.3.2. Steady state determination and parameter estimation of the translation model

The translational model was analysed using the software COPASI with mass action kinetics for most of the translation steps. However, subunit joining in initiation and the translocation

state in elongation were represented using a ‘blocking’ rate constant for ribosomal possession of mRNA codons. After construction, the model was simulated to find the steady state. In a complex model like translation, most of the parameters are unknown. However, using the algorithms incorporated in COPASI, the steady state of the model was determined. The model with the steady state was further employed for the parameter estimation.

Most of the kinetic parameter of the translation is currently unknown. It is very crucial that the model is used to predict the unknown kinetic parameters for the reactions in translation. For predicting these parameters, the model was simulated with the experimental data. From previously explained experiments (Chapter 4), the concentration of each of the translation factors and their corresponding protein synthesis rate are known. 5 experimental data set were used for each of the translation factors. The parameter estimation simulation was able to find a set of values for each of the reaction kinetics based on the model fitting with each of the data set. These resulting data set for the reaction kinetics can be further analysed to estimate each of the reaction kinetics. The extra information about the mass action kinetics will enable the model to predict the translational control better.

5.4. Conclusions

Translation is one of the most challenging biological pathways to mathematically model and quantitatively understand due to the complexity and lack of enough experimental data. Construction of mathematical model is meaningful only with strong quantitative experimental data. Until now, most of the translation models were deficient of quantitative experimental data to construct and predict the underlying mechanism precisely.

In this work, a new type of detailed translation model has been developed that incorporate an extensive set of experimentally determined rate control data. This is the first ever example of a model that includes all three steps of the translation process and incorporate such precisely measured quantitative data. The model was constructed in perl script and analysed in COPASI which enables to easily incorporate any further information of the translation pathway. In the current study, the average mRNA length being translated was considered to be 20 codons, however, the length of the mRNA can be easily changed. The steady state of the model was determined using the differential equation solver in COPASI. Concentrations of individual translation factors with respective protein synthesis rate were incorporated into the model to estimate each of the kinetic parameters. Employing the parameter estimation algorithms in COPASI software, the model was fitted with the experimental data.

At this stage of the translation model construction, the model was able to converge to the steady state and was fitted with the experimental data for better estimation of the parameter values. The parameter estimation of the model produced a vast amount of data which require careful statistical analysis to estimate each of the unknown kinetic parameters of the model. Once the kinetic parameters are estimated precisely, the mathematical model of the translation is available as a valuable tool for understanding the nature of control in the eukaryotic translation system.

Chapter 6

General Discussion

6.1. mRNA translation and understanding the control mechanism

mRNA translation is a highly conserved cellular process in which the information encoded by the mRNA is deciphered by the ribosomes with the support of a number of proteins. In *Saccharomyces cerevisiae* there are more than 20 translation factor proteins directly participate in this complex cellular phenomenon. The control of translation is a critical step in the regulation of cell growth and adaptation to environmental conditions. Translational control is identified to be a crucial component of cancer development. Both global translational control and mRNA-specific translational control are reported to promote tumour cell survival, angiogenesis, transformation, invasion and metastasis (Silvera et al., 2010). Quantitative understanding of these controls is essential components in understanding the highly sophisticated and well conserved process of translation.

In this study, employing three different approaches, high resolution microscopy, molecular biology and mathematical modelling, comprehensive control of the yeast mRNA translation has been quantitatively assessed. This study precisely elucidates the mode of control exerted by individual translation factors at different stages of translation. The imaging approach explores the cellular distribution of translation factors to determine if these could be rate limiting in global translation. Employing molecular biology techniques, the translation factors have been made limiting in the cell to identify their controlling influence on translation. Finally, employing a mathematical modelling approach, the whole translation pathway is theoretically represented, to identify the system-level control of translation. These approaches seek to explain the adaptations in translation in response to different environmental conditions. Given the high degree of conservation of the translation

machinery, the principles of translation control elucidated using yeast as a model organism are relevant to all other higher eukaryotes.

Previous studies have shown that translation control is exerted at several different steps within the translation pathway. Specifically, more than thirteen protein factors participate in eukaryotic translation initiation and this step is believed to be one of the most regulated stages of translation. Cells under nutrient limiting conditions are known to regulate global translation by phosphorylating eIF2. This results in the inhibition of eIF2B mediated recycling of eIF2 to its active form and causes global translational regulation. Further initiation regulation occurs at the mRNA cap identification step. The initiation factor, eIF4E, an mRNA cap binding protein has been suggested to be a rate limiting factor in translation initiation (Koromilas et al., 1992). In addition translation termination has been identified as a key step in the translation regulatory mechanisms (Sonenberg and Hinnebusch, 2007). Translational control of specific mRNAs is a principal aspect in early embryonic development and differentiation (Sonenberg and Hinnebusch, 2007). Recent studies have reported that up-regulation of the protein expression levels and activity of the initiation factors is associated with different disease conditions such as cancer and heart diseases (Silvera et al., 2010). These studies have focussed on the control exerted by specific factors whereas this study looks at the translation pathway entirety to determine the relative control exerted by each factor across the whole process

6.2. Intra-cellular distributions of elongation and release factors do not suggest any form of spatial control on translation

The intra-cellular distribution of elongation and release factors was explored employing TCM and GFP tagging. Each gene encoding a translation factor was genetically modified to have a TCM or GFP tag at the C terminal end. Manipulating the genome of the yeast is an elegant yet easy method to modify selected proteins in a living cell. TCM tags are short fluorescent peptides of 10-12 amino acids, which can be fused with the protein of interest to visualise it *in vivo.* The elongation and release factors were observed to be cytoplasmically distributed in the exponential growth phase. The distribution patterns observed with the

elongation and release factors with TCM tags were identified to those obtained with the GFP tagged distribution analysis. This confirms that the cytoplasmic distribution of elongation and release factors observed in this study was not altered by TCM or GFP fluorescent tags. To determine any possible presence of elongation and release factors within the nucleus cells were also labelled with DAPI, a DNA stain. The data indicates that none of the elongation and release factors is present at significant levels in the nucleus of the yeast cells. The data demonstrating the homogenous distribution of the elongation and release factors suggests that the spatial distribution of the elongation and release factors are not a rate limiting aspect of global translation.

Characterisation of the intra-cellular distributions of the individual factors in the molecular process is essential in order to a better understanding of the process of translation. Translation factors are some of the most highly synthesised, utilised and functionally essential proteins in the cell. Thus, availability and accessibility of these factors is crucial to the translation process. Previous studies have shown that most of the translation initiation factors are cytoplasmically distributed in the cell (Huh et al., 2003, Kumar et al., 2002). However, initiation factors such as eIF2 (α and γ subunits) and eIF2B (γ and ε subunits) have reported to assume a specific localisation in the cytoplasm, which could in term play a role in translational regulation (Campbell et al., 2005). The sub-cellular distributions of the elongation and release factors have not been subjected to imaging analysis. In this study, the translational elongation and release factors are shown to be cytoplasmically distributed. This agrees with the distribution analysis carried out with the GFP-tagged eEF1A as part of the global yeast protein localisation study (Huh et al., 2003). In this the distribution of all the elongation and release factors were explored extensively using GFP and TCM fluorescent tags. This study suggests that the intra-cellular distribution of the elongation and release factors are not a translational rate limiting step because the factors are homogenously distributed in the cytoplasm and readily available for translation.

6.3. The response coefficient reflects the degree of translational regulation exerted by the elongation and release factors

Translational regulation is vital for the rapid response and adaptation to environmental changes and therefore precise understanding of translational control is crucial. In this study, the intra-cellular protein expression level of the elongation and the release factors were reduced and the corresponding protein synthesis rate was measured. The response coefficient (R_1^J), the gradient of the ratio between the intra-cellular level of individual translation factors and the corresponding protein synthesis rate, was determined. The response coefficient explains the control of translation rate exerted by each of the translation factors studied. The response coefficient is measured from 0 to 1 with a high response coefficient indicates higher control over translation. When the gradient between the protein concentration and the protein synthesis rate is higher, it suggests that the protein synthesis rate is more affected with even the smaller changes in the protein expression level of that factor.

The endogenous promoters of the individual elongation and release factors were substituted with the Doxycycline regulatable synthetic *tetO7* promoter. Expression levels of the translation were titrated down from 100 % to 60 % of the physiological level with a range of concentrations of doxycycline. The response coefficient was calculated by reducing the level of translation factors to 100 – 80 % of the physiological level. R_2^J was calculated as the response coefficient when the level of factors were reduced to 80 – 60 %.

As mentioned previously, regulation of translation is thought to be exerted at different stages of the initiation phase of translation (Sonenberg and Hinnebusch, 2009). However, recent studies have also reported that the elongation step exerts a strong influence on translational control (Wang et al., 2001). However, comprehensive knowledge about these controls is yet to be determined. As initiation play much an important role in translation regulation, extensive studies have been carried out over many decades to determine the specific control exerted by initiation factors. In a quantitative translational control study,

the response coefficients of translation initiation factors eIF1A, eIF4E, eIF4G1 and eIF5B were measured (Sangthong et al., 2007). Additionally, large differences in the intra-cellular concentration of the translation factors have been identified (von der Haar and McCarthy, 2002; von der Haar, 2008). However, the relationship between the intra-cellular abundance of individual translation factors and their control over translation has remained unclear. In this study, the response coefficients of the elongation and release factors were determined from which the relative translational control exerted by each of these factors can be identified.

The elongation factors eEF1A and eEF2 were observed to have a very high response coefficient. The high response coefficient (0.897) observed for eEF1A can be clearly understood by analysing the functions of these factors in the translation elongation cycle. eEF1A factors are responsible for delivering the aminoacyle tRNA to the ribosome. The elongation cycles are reported to be subject to limitation by the rare amino acids. Also, eEF1A availability to deliver the amino acids is crucial. Delay in the amino acid delivery due to the reduction in the factor eEF1A can have a great impact on the translational rate. The eEF2 factor is responsible for one of the most essential steps in the elongation cycle translocation and in this study the factor was observed to have a high response coefficient of 0.937. In translocation the ribosomes moves from one codon to the next available codon of mRNA. A limitation in eEF2 activity could prevent translocation and cause ribosome to stall on mRNA. This can cause a reduction in the rate of translation.

However, eEF1B and eEF3 exhibited lower R_1^J values. This could be explained by the functional roles these factors fulfil in translation. eEF1B recycles eEF1A factors by GDP to GTP conversion. However, other studies have suggested that eEF1A has a similar preference for GTP and GDP (Janssen et al., 1988). So even at a reduced eEF1B levels, eEF1A might be recycled to its active form. eEF3 is an unique factor in the fungi group and this factor functions to remove the tRNA from the E site of the ribosome. Unexceptionally, eEF3 exhibited a very low R_1^J value yet has a very high R_2^J value. This indicates that translation was not much affected when the level of eEF3 was reduced to approximately 85 % of the endogenous level. However, when the protein expression level was further

reduced, the translation rate was reduced significantly. The eEF3 protein has been shown to present at approximately 871000 molecules per cell which is significantly higher than the expression level of other elongation and release factors (Ghaemmaghami et al., 2003). The above studies suggest that there may be an excess of eEF3 in the cell with respect to translation so that the cell can afford to lose some of this pool without suffering significant reductions in translation rate.

The release factors were also observed to have two distinctive response coefficients. Yeast strains with reduced levels of eRF1 were observed to have a significantly reduced translational rate. eRF1 is responsible for the identification of the stop codon in the mRNA. Reductions in this factor can cause non-recognition of the stop codons, which results in the accumulation of proteins with extended c-terminus. Reductions in the eRF1 may also cause the ribosome to become stalled on the mRNA due to a reduction in the termination rate. This can cause reductions in the global translational rate. However, eRF3 was observed to have a lower R_1^J and R_2^J indicating that the reduction in the expression level of this factor has minimal affect on translation. eRF3 provides the energy required for the interaction between the stop codon and the eRF1. However, the lower response coefficient can be explained by suggesting that there must be some other factor facilitating the binding of eRF1 or that this could be possible without energy consumption.

The affect of reduced protein expression level of translation elongation and release factors on the global translation were observed by analysing the polysomal distribution. The factors were reduced to the 80% of the wild-type level and the polysomal profiles were compared and analysed with wild-type polysomal profiles. The polysome profile of cells expressing reduced levels of eEF1A and eEF2 observed to have increased level of polysosmes and 60S monosome. This could be the impact of the reduced elongation rate which causes the ribosomes to stall on mRNA. Polysome distribution of the cells expressing reduction level of other elongation and release factors were also observed to have a increased polysomal level, but not as major as observed for eEF1A and eEF2. These observations suggest that the reduction in the level of the factors eEF1A and eEF2 has a

high impact on the rate of the translation and these factors play a significant role in the regulation of global translation.

In this study effect on translation rate exerted by over-expression of elongation or release factors were explored. Interestingly, even when the elongation and release factors were increased to 120% of the wild-type level, the protein synthesis rate was not increased. Moreover, over expression of the factors not exhibited any protein synthesis inhibition. This indicates that the translation and growth rates of wild-type yeast are optimally set by the physiologically normal translational machinery.

6.4. System specificity of the elongation and release factors

A number of these factors are identified to be involved in other cellular functions distinct from the translation process. The relationship between translation and the growth rate were explored in this study. This study determined which factors functioned solely in translation and which played a role in translation and other cellular processes. The growth rate and protein synthesis rate exhibit a linear relationship and the gradient of the line (the system specificity ratio, R^{Sp}) was measured. From the system specificity ratio the translation factors which function solely in translation were identified. If the factors are solely involved in translation, the system specificity ratio will be approximately equal to 1 whereas if the factor is involved in other cellular functions apart from translation then the slope will be <1.

The elongation factors eEF1A, eEF2 and eEF3 were observed to have an R^{Sp} values of approximately 1. The growth rate to protein synthesis rate relationship of these factors was linear with a gradient of 1. eEF1A, eEF2 and eEF3 exhibited 0.99, 1.02 and 1.06 R^{Sp} values respectively. The elongation factor eEF1A has been reported to be involved in actin organisation in yeast cells (Munshi et al, 2001). However, the R^{Sp} values of the factors suggest that the reduction in eEF1A has no additional affect on the growth rate that is attributed to this role in actin organisation. The system specificity ratio reveals that the reduction in the growth rate observed with lower levels of eEF1A was due to the reduction

in protein synthesis rate. eEF2 and eEF3 have been thought to function only in the translation pathway and the R^{Sp} value agrees with this (Justice et al., 1998, Anand et al., 2003). The translation elongation factor eEF1B on the other hand, was observed to have an R^{Sp} value of 0.63. When the factor was reduced, the growth rate reduced faster than the translation rate. This strongly suggests that eEF1B has a role in atleast one cellular process other than translation. While, eEF1B is not known to be involved in any other cellular function apart from translation (Kinzy and Woolford, 1995, Jeppesen et al., 2003), this requires further investigation.

The release factors were observed to have two very distinct R^{Sp} values. eRF1 was observed to have a very high R^{Sp} value, 1.10. The reduction in eRF1 abundance correlates with a reduction in the growth rate and protein synthesis rate. This suggests that eRF1 is only involved in the translation pathway. In sharp contrast, eRF3 was observed to have a lower R^{Sp} value, 0.29. This reveals that when eRF3 is made limiting, the growth rate is reducing quicker than the protein synthesis rate. This data suggests there is another cellular function of eRF3 in addition to the translation process. eRF3 is known to protein aggregates, and to act as a prion in yeast (Derkatch et al., 2001). The lower system specificity ratio might therefore be the result of prion activity.

6.5. Building a mathematical model of the translation pathway

Decades of study have generated a vast amount of information about the steps, components and regulation of mRNA translation. These data need to be integrated in to a systems framework for a better understanding of the underlying properties of this process. Mathematical formulation of the translation could be a powerful tool to visualize translation in a systems level. However, there are very few quantitative experimental data to study translation mathematically.

In this study, a detailed comprehensive model of translation has been developed incorporating an extensive set of quantitative data. Eukaryotic translation has been represented as a set of differential equations using mass kinetics combining with a

representation of mRNA occupances to elucidate translational control. The respective concentrations of the translation factors were derived from previous studies (Ghaemmaghami et al., 2003). In addition to consideration of every detail of the translation stages, the subunit association and elongation cycle have been modelled considering the ribosomal occupation of mRNA codon. Eukaryotic ribosomes are assumed to occupy 15 codons of the mRNA during translation. This detailed information has been incorporated into the model and a separate kinetic law which considers this 'blocking' phenomenon has been incorporated. These blocking kinetics ensure that ribosomes do not collide with each other during translation. The model has been constructed using perl script and simulated using the software COPASI. The model was successfully determined steady state and was fitted with the rate control data to estimate the kinetic parameters. The parameter estimation of the model has produced a subset of data which has to be precisely analysed to estimate the unknown paramters of the model. After the estimation of all kinetic parameters, the model can be used to predict and analyse different behavioural scenarios for the translation pathway. The model can be used to analyse the control exerted by individual translation factors over the translation and the result can be compared with the experimental data. These comparisons between the model predictions and experimentally observed control responses can determine the quality of the model. The model can be further used to predict sensitivity of the pathway towards reduction in the expression of more than one translation factor and the resulting change in translational control.

Due to the complexity and lack of the quantitative data available for the translation pathway, most of the previous models address only one stage of translation. Prokaryotic translation is less complex and most of the parameter values are known. This encouraged formulation of mathematical models of prokaryotic translation covering all three stages of translation (Zouridis and Hatzimanikatis, 2007). However, most of the reaction parameters have not been determined experimentally in a eukaryotic system. In another study on bacterial translation, the initiation step has been modelled to help find ways to increase the translation efficiency and thus to boost protein yields (Zhang et al., 2010). The model incorporates the mRNA folding dynamics, ribosome binding dynamics and mRNA sequence information to represent the translation rate.

An earlier deterministic model of yeast translation initiation investigates the control of each initiation factor over translation using flux control coefficients (Dimelow and Wilkinson, 2009). However, this model lacks experimental data to fit the model and the kinetic parameters used in it are completely based on the assumed values. The aminoacylation and initiation of yeast translation have been modelled using ordinary differential equations (You et al., 2010). The model investigates the kinetic behaviour of translation initiation factors in response to amino acids limitation and examines the changes in the translation initiation rate at varying concentrations of initiation factors and external perturbations. Even though the nutrient limitation model was based on experimental data, the response of the translation rate with varying concentrations of the initiation factors was based on assumptions. In a recent work, a complete translation model for the yeast translation has been developed (Siwiak and Zielenkiewicz, 2010). This model concentrates on the differences in the translational rate of the individual 64 codons on the mRNA. However, this model does not explain the overall translation rate and the effect of individual translation factor on the translational rate. Moreover, the model lacks experimental support. Very few models attempt to incorporate all three stages; initiation, elongation and termination of translation with all the minute details and enough experimental data to support the model. And all of these models suffer from being under-parameterized. However, the eukaryotic translational mode constructed in this study incorporates all three stages of the eukaryotic translation pathway. Moreover, it is constructed based on an extensive set of quantitative experimental data which enables it to confidently determine other kinetic parameters in the model. Thus, this translational model is a useful tool to analyse and predict translation pathway behaviours.

6.6. Future directions

A systems biology study integrating experimentally determined parameters and mathematical modelling was performed to better understand translational control in yeast. Because of the importance and the complexity of the translation pathway, many studies have sought to determine the translation mechanisms, most focusing on individual factors.

This systems level study now provides a platform for developing a far deeper understanding of translational control in eukaryotes. In particular, quantitative studies of translation control exerted by the elongation and release factors in nutrient limiting conditions or at varying temperatures will be for more enlightening in the context of a high quality model. A further aspect of importance is that the level of parameterization will be continuously increased over time, thus improvising the predictive power of the model. For example more accurate determination of intracellular factor levels can be determined employing quantitative mass spectroscopy techniques such as QconCAT (Pratt et al., 2006). The absolute concentration of the translation factors can be employed to improve the current observations as well as included in the translational model. Also, any possible change in the distribution of elongation and release factors with varying growth conditions such as temperature or carbon and nitrogen nutrient sources can be explored. The change in the growth condition might cause translational regulation and cause subcellular redistribution of translation factors to regulate global translation.

The mathematical model of translation can be further refined to understand the changes in control in response to multi-site variation in component activity. Currently, most of the reaction kinetics in the eukaryotic translation pathway is missing. This additional information about the kinetics of each of the translational steps would improve the predictive power of the translation model. The additional data will include newly determined values for the on and off rates for all of the interactions between the translation machinery components.

The striking similarity between the yeast and human translational mechanisms means that the model is also relevant to human cells. Identification of the influence of translation factors and their control in many diseases could potentially lead to development of new gene/protein-targeted therapies for treatment of these diseases. New approaches from systems biology, combining molecular biology and mathematical modelling can be employed to decipher mRNA translation role in human diseases. Further, specific target components of the translation apparatus can be identified for the development of cancer therapeutics.

References

Acker, M. G., Shin, B. S., Dever, T. E., and Lorsch, J. R. (2006). Interaction between eukaryotic initiation factors 1A and 5B is required for efficient ribosomal subunit joining. J Biol Chem *281*, 8469-8475.

Alksne, L. E., Anthony, R. A., Liebman, S. W., and Warner, J. R. (1993). An accuracy center in the ribosome conserved over 2 billion years. Proc Natl Acad Sci U S A *90*, 9538-9541.

Altmann, M., Muller, P. P., Wittmer, B., Ruchti, F., Lanker, S., and Trachsel, H. (1993). A Saccharomyces cerevisiae homologue of mammalian translation initiation factor 4B contributes to RNA helicase activity. Embo J *12*, 3997-4003.

Altmann, M., Wittmer, B., Methot, N., Sonenberg, N., and Trachsel, H. (1995). The Saccharomyces cerevisiae translation initiation factor Tif3 and its mammalian homologue, eIF-4B, have RNA annealing activity. Embo J *14*, 3820-3827.

Anand, M., Balar, B., Ulloque, R., Gross, S. R., and Kinzy, T. G. (2006). Domain and nucleotide dependence of the interaction between Saccharomyces cerevisiae translation elongation factors 3 and 1A. J Biol Chem *281*, 32318-32326.

Anand, M., Chakraburtty, K., Marton, M. J., Hinnebusch, A. G., and Kinzy, T. G. (2003). Functional interactions between yeast translation eukaryotic elongation factor (eEF) 1A and eEF3. J Biol Chem *278*, 6985-6991.

Andersen, E. S., Rosenblad, M. A., Larsen, N., Westergaard, J. C., Burks, J., Wower, I. K., Wower, J., Gorodkin, J., Samuelsson, T., and Zwieb, C. (2006). The tmRDB and SRPDB resources. Nucleic Acids Res *34*, D163-168.

Anderson, P., and Kedersha, N. (2008). Stress granules: the Tao of RNA triage. Trends Biochem Sci *33*, 141-150.

Armengol, G., Rojo, F., Castellvi, J., Iglesias, C., Cuatrecasas, M., Pons, B., Baselga, J., and Ramon y Cajal, S. (2007). 4E-binding protein 1: a key molecular "funnel factor" in human cancer with clinical implications. Cancer Res *67*, 7551-7555.

Asano, K., Clayton, J., Shalev, A., and Hinnebusch, A. G. (2000). A multifactor complex of eukaryotic initiation factors, eIF1, eIF2, eIF3, eIF5, and initiator tRNA(Met) is an important translation initiation intermediate in vivo. Genes Dev *14*, 2534-2546.

Baer, B. W., and Kornberg, R. D. (1980). Repeating structure of cytoplasmic poly(A)-ribonucleoprotein. Proc Natl Acad Sci U S A *77*, 1890-1892.

Baer, B. W., and Kornberg, R. D. (1983). The protein responsible for the repeating structure of cytoplasmic poly(A)-ribonucleoprotein. J Cell Biol *96*, 717-721.

Bailleul, P. A., Newnam, G. P., Steenbergen, J. N., and Chernoff, Y. O. (1999). Genetic study of interactions between the cytoskeletal assembly protein sla1 and prion-forming domain of the release factor Sup35 (eRF3) in Saccharomyces cerevisiae. Genetics *153*, 81-94.

Baronas-Lowell, D. M., and Warner, J. R. (1990). Ribosomal protein L30 is dispensable in the yeast Saccharomyces cerevisiae. Mol Cell Biol *10*, 5235-5243.

Belli, G., Gari, E., Aldea, M., and Herrero, E. (1998). Functional analysis of yeast essential genes using a promoter-substitution cassette and the tetracycline-regulatable dual expression system. Yeast *14*, 1127-1138.

Bergmann, J. E., and Lodish, H. F. (1979). A kinetic model of protein synthesis. Application to hemoglobin synthesis and translational control. J Biol Chem *254*, 11927-11937.

Berthelot, K., Muldoon, M., Rajkowitsch, L., Hughes, J., and McCarthy, J. E. (2004). Dynamics and processivity of 40S ribosome scanning on mRNA in yeast. Mol Microbiol *51*, 987-1001.

Bonekamp, F., Dalboge, H., Christensen, T., and Jensen, K. F. (1989). Translation rates of individual codons are not correlated with tRNA abundances or with frequencies of utilization in Escherichia coli. J Bacteriol *171*, 5812-5816.

Bourne, H. R., Sanders, D. A., and McCormick, F. (1990). The GTPase superfamily: a conserved switch for diverse cell functions. Nature *348*, 125-132.

Campbell, S. G., Hoyle, N. P., and Ashe, M. P. (2005). Dynamic cycling of eIF2 through a large eIF2B-containing cytoplasmic body: implications for translation control. J Cell Biol *170*, 925-934.

Caruthers, J. M., Johnson, E. R., and McKay, D. B. (2000). Crystal structure of yeast initiation factor 4A, a DEAD-box RNA helicase. Proc Natl Acad Sci U S A *97*, 13080-13085.

Chu, F. K., and Maley, F. (1980). Growth phase dependence of invertase mRNA levels in yeast. J Biol Chem *255*, 6387-6391.

Clemens, M. (1987). Translational control. Developments in development. Nature *330*, 699-700.

Cui, Y., Dinman, J. D., Kinzy, T. G., and Peltz, S. W. (1998). The Mof2/Sui1 protein is a general monitor of translational accuracy. Mol Cell Biol *18*, 1506-1516.

Das, S., Ghosh, R., and Maitra, U. (2001). Eukaryotic translation initiation factor 5 functions as a GTPase-activating protein. J Biol Chem *276*, 6720-6726.

Dasmahapatra, B., and Chakraburtty, K. (1981). Protein synthesis in yeast. I. Purification and properties of elongation factor 3 from Saccharomyces cerevisiae. J Biol Chem *256*, 9999-10004.

Derkatch, I. L., Bradley, M. E., Hong, J. Y., and Liebman, S. W. (2001). Prions affect the appearance of other prions: the story of [PIN(+)]. Cell *106*, 171-182.

Dimelow, R. J., and Wilkinson, S. J. (2009). Control of translation initiation: a model-based analysis from limited experimental data. J R Soc Interface *6*, 51-61.

Donahue, T. F., Cigan, A. M., Pabich, E. K., and Valavicius, B. C. (1988). Mutations at a Zn(II) finger motif in the yeast eIF-2 beta gene alter ribosomal start-site selection during the scanning process. Cell *54*, 621-632.

El'skaya, A. V., Ovcharenko, G. V., Palchevskii, S. S., Petrushenko, Z. M., Triana-Alonso, F. J., and Nierhaus, K. H. (1997). Three tRNA binding sites in rabbit liver ribosomes and role of the intrinsic ATPase in 80S ribosomes from higher eukaryotes. Biochemistry *36*, 10492-10497.

Erickson, F. L., and Hannig, E. M. (1996). Ligand interactions with eukaryotic translation initiation factor 2: role of the gamma-subunit. Embo J *15*, 6311-6320.

Fortes, P., Inada, T., Preiss, T., Hentze, M. W., Mattaj, I. W., and Sachs, A. B. (2000). The yeast nuclear cap binding complex can interact with translation factor eIF4G and mediate translation initiation. Mol Cell *6*, 191-196.

Freistroffer, D. V., Pavlov, M. Y., MacDougall, J., Buckingham, R. H., and Ehrenberg, M. (1997). Release factor RF3 in E.coli accelerates the dissociation of release factors RF1 and RF2 from the ribosome in a GTP-dependent manner. Embo J *16*, 4126-4133.

Fringer, J. M., Acker, M. G., Fekete, C. A., Lorsch, J. R., and Dever, T. E. (2007). Coupled release of eukaryotic translation initiation factors 5B and 1A from 80S ribosomes following subunit joining. Mol Cell Biol *27*, 2384-2397.

Frolova, L. Y., Merkulova, T. I., and Kisselev, L. L. (2000). Translation termination in eukaryotes: polypeptide release factor eRF1 is composed of functionally and structurally distinct domains. Rna *6*, 381-390.

Gebauer, F., and Hentze, M. W. (2004). Molecular mechanisms of translational control. Nat Rev Mol Cell Biol *5*, 827-835.

Geoghegan, T., Cereghini, S., and Brawerman, G. (1979). Inactive mRNA-protein complexes from mouse sarcoma-180 ascites cells. Proc Natl Acad Sci U S A *76*, 5587-5591.

Ghaemmaghami, S., Huh, W. K., Bower, K., Howson, R. W., Belle, A., Dephoure, N., O'Shea, E. K., and Weissman, J. S. (2003). Global analysis of protein expression in yeast. Nature *425*, 737-741.

Gray, N. K., Coller, J. M., Dickson, K. S., and Wickens, M. (2000). Multiple portions of poly(A)-binding protein stimulate translation in vivo. Embo J *19*, 4723-4733.

Green, R., and Noller, H. F. (1997). Ribosomes and translation. Annu Rev Biochem *66*, 679-716.

Gregio, A. P., Cano, V. P., Avaca, J. S., Valentini, S. R., and Zanelli, C. F. (2009) eIF5A has a function in the elongation step of translation in yeast. Biochem Biophys Res Commun 380, 785-90.

Grentzmann, G., Brechemier-Baey, D., Heurgue, V., Mora, L., and Buckingham, R. H. (1994). Localization and characterization of the gene encoding release factor RF3 in Escherichia coli. Proc Natl Acad Sci U S A *91*, 5848-5852.

Griffin, B. A., Adams, S. R., and Tsien, R. Y. (1998). Specific covalent labeling of recombinant protein molecules inside live cells. Science *281*, 269-272.

Gross, S. R., and Kinzy, T. G. (2005). Translation elongation factor 1A is essential for regulation of the actin cytoskeleton and cell morphology. Nat Struct Mol Biol *12*, 772-778.

Guldener, U., Heck, S., Fielder, T., Beinhauer, J., and Hegemann, J. H. (1996). A new efficient gene disruption cassette for repeated use in budding yeast. Nucleic Acids Res *24*, 2519-2524.

Gunnery, S., and Mathews, M. B. (1995). Functional mRNA can be generated by RNA polymerase III. Mol Cell Biol *15*, 3597-3607.

Heinrich, R., and Rapoport, T. A. (1980). Mathematical modelling of translation of mRNA in eucaryotes; steady state, time-dependent processes and application to reticulocytes. J Theor Biol *86*, 279-313.

Henshaw, E. C., Hirsch, C. A., Morton, B. E., and Hiatt, H. H. (1971). Control of protein synthesis in mammalian tissues through changes in ribosome activity. J Biol Chem *246*, 436-446.

Hinnebusch, A. G., Asano, K., Olsen, D. S., Phan, L., Nielsen, K. H., and Valasek, L. (2004). Study of translational control of eukaryotic gene expression using yeast. Ann N Y Acad Sci *1038*, 60-74.

Hoops, S., Sahle, S., Gauges, R., Lee, C., Pahle, J., Simus, N., Singhal, M., Xu, L., Mendes, P., and Kummer, U. (2006). COPASI--a COmplex PAthway SImulator. Bioinformatics *22*, 3067-3074.

Hou, Y. M. (1997). Discriminating among the discriminator bases of tRNAs. Chem Biol *4*, 93-96.

Huang, H. K., Yoon, H., Hannig, E. M., and Donahue, T. F. (1997). GTP hydrolysis controls stringent selection of the AUG start codon during translation initiation in Saccharomyces cerevisiae. Genes Dev *11*, 2396-2413.

Huh, W. K., Falvo, J. V., Gerke, L. C., Carroll, A. S., Howson, R. W., Weissman, J. S., and O'Shea, E. K. (2003). Global analysis of protein localization in budding yeast. Nature *425*, 686-691.

Iost, I., Dreyfus, M., and Linder, P. (1999). Ded1p, a DEAD-box protein required for translation initiation in Saccharomyces cerevisiae, is an RNA helicase. J Biol Chem *274*, 17677-17683.

Janssen, G. M., Maessen, G. D., Amons, R., and Moller, W. (1988). Phosphorylation of elongation factor 1 beta by an endogenous kinase affects its catalytic nucleotide exchange activity. J Biol Chem *263*, 11063-11066.

Jeppesen, M. G., Ortiz, P., Shepard, W., Kinzy, T. G., Nyborg, J., and Andersen, G. R. (2003). The crystal structure of the glutathione S-transferase-like domain of elongation factor 1Bgamma from Saccharomyces cerevisiae. J Biol Chem *278*, 47190-47198.

Johnstone, O., and Lasko, P. (2001). Translational regulation and RNA localization in Drosophila oocytes and embryos. Annu Rev Genet *35*, 365-406.

Jorgensen, P., Nishikawa, J. L., Breitkreutz, B. J., and Tyers, M. (2002). Systematic identification of pathways that couple cell growth and division in yeast. Science *297*, 395-400.

Jorgensen, R., Merrill, A. R., and Andersen, G. R. (2006). The life and death of translation elongation factor 2. Biochem Soc Trans *34*, 1-6.

Jorgensen, R., Ortiz, P. A., Carr-Schmid, A., Nissen, P., Kinzy, T. G., and Andersen, G. R. (2003). Two crystal structures demonstrate large conformational changes in the eukaryotic ribosomal translocase. Nat Struct Biol *10*, 379-385.

Justice, M. C., Hsu, M. J., Tse, B., Ku, T., Balkovec, J., Schmatz, D., and Nielsen, J. (1998). Elongation factor 2 as a novel target for selective inhibition of fungal protein synthesis. J Biol Chem *273*, 3148-3151.

Kanaya, S., Yamada, Y., Kudo, Y., and Ikemura, T. (1999). Studies of codon usage and tRNA genes of 18 unicellular organisms and quantification of Bacillus subtilis tRNAs: gene expression level and species-specific diversity of codon usage based on multivariate analysis. Gene *238*, 143-155.

Kang, H. A., and Hershey, J. W. (1994). Effect of initiation factor eIF-5A depletion on protein synthesis and proliferation of Saccharomyces cerevisiae. J Biol Chem *269*, 3934-3940.

Kapp, L. D., and Lorsch, J. R. (2004a). GTP-dependent recognition of the methionine moiety on initiator tRNA by translation factor eIF2. J Mol Biol *335*, 923-936.

Kapp, L. D., and Lorsch, J. R. (2004b). The molecular mechanics of eukaryotic translation. Annu Rev Biochem *73*, 657-704.

Kessler, S. H., and Sachs, A. B. (1998). RNA recognition motif 2 of yeast Pab1p is required for its functional interaction with eukaryotic translation initiation factor 4G. Mol Cell Biol *18*, 51-57.

Kinzy, T. G., and Woolford, J. L., Jr. (1995). Increased expression of Saccharomyces cerevisiae translation elongation factor 1 alpha bypasses the lethality of a TEF5 null allele encoding elongation factor 1 beta. Genetics *141*, 481-489.

Kisselev, L. L., and Buckingham, R. H. (2000). Translational termination comes of age. Trends Biochem Sci *25*, 561-566.

Koromilas, A. E., Lazaris-Karatzas, A. and Sonenberg, N. (1992). mRNAs containing extensive secondary structure in their 50 noncoding region translate efficiently in cells overexpressing initiation factor eIF4E. EMBO J 11, 4153–4158.

Kozak, M. (1980). Role of ATP in binding and migration of 40S ribosomal subunits. Cell *22*, 459-467.

Kumar, A., Agarwal, S., Heyman, J. A., Matson, S., Heidtman, M., Piccirillo, S., Umansky, L., Drawid, A., Jansen, R., Liu, Y., *et al.* (2002). Subcellular localization of the yeast proteome. Genes Dev *16*, 707-719.

Kyrpides, N. C., and Woese, C. R. (1998). Archaeal translation initiation revisited: the initiation factor 2 and eukaryotic initiation factor 2B alpha-beta-delta subunit families. Proc Natl Acad Sci U S A *95*, 3726-3730.

Laurino, J. P., Thompson, G. M., Pacheco, E., and Castilho, B. A. (1999). The beta subunit of eukaryotic translation initiation factor 2 binds mRNA through the lysine repeats and a region comprising the C2-C2 motif. Mol Cell Biol *19*, 173-181.

Lee, J. H., Pestova, T. V., Shin, B. S., Cao, C., Choi, S. K., and Dever, T. E. (2002). Initiation factor eIF5B catalyzes second GTP-dependent step in eukaryotic translation initiation. Proc Natl Acad Sci U S A *99*, 16689-16694.

Linder, P. (1992). Molecular biology of translation in yeast. Antonie Van Leeuwenhoek *62*, 47-62.

Lodish, H. F., and Jacobsen, M. (1972). Regulation of hemoglobin synthesis. Equal rates of translation and termination of - and -globin chains. J Biol Chem *247*, 3622-3629.

Maag, D., Fekete, C. A., Gryczynski, Z., and Lorsch, J. R. (2005). A conformational change in the eukaryotic translation preinitiation complex and release of eIF1 signal recognition of the start codon. Mol Cell *17*, 265-275.

MacDonald, C. T., Gibbs, J. H., and Pipkin, A. C. (1968). Kinetics of biopolymerization on nucleic acid templates. Biopolymers *6*, 1-5.

Marcotrigiano, J., Gingras, A. C., Sonenberg, N., and Burley, S. K. (1997). Cocrystal structure of the messenger RNA 5' cap-binding protein (eIF4E) bound to 7-methyl-GDP. Cell *89*, 951-961.

Marintchev, A., Edmonds, K. A., Marintcheva, B., Hendrickson, E., Oberer, M., Suzuki, C., Herdy, B., Sonenberg, N., and Wagner, G. (2009). Topology and regulation of the human eIF4A/4G/4H helicase complex in translation initiation. Cell *136*, 447-460.

Martin, B. R., Giepmans, B. N., Adams, S. R., and Tsien, R. Y. (2005). Mammalian cell-based optimization of the biarsenical-binding tetracysteine motif for improved fluorescence and affinity. Nat Biotechnol *23*, 1308-1314.

Mathews, M. B., Sonenberg, N. & Hershey, J.W.B. (2000). Origins and Principles of Translational Control, In Translational Control of Gene Expression, N. Sonenberg, Hershey, J.W.B., Mathews, M.B. , ed. (Cold Spring Harbor Laboratory Press).

May, E. E., Vouk, M. A., Bitzer, D. L., and Rosnick, D. I. (2004). Coding theory based models for protein translation initiation in prokaryotic organisms. Biosystems *76*, 249-260.

McCarthy, J. E. (1998). Posttranscriptional control of gene expression in yeast. Microbiol Mol Biol Rev *62*, 1492-1553.

McNabb, D. S., Reed, R., and Marciniak, R. A. (2005). Dual luciferase assay system for rapid assessment of gene expression in Saccharomyces cerevisiae. Eukaryot Cell *4*, 1539-1549.

Merrick, C. W., Nyborg, J. (2000). The protein biosynthesis elongation cycle, In Translational Control of Gene Expression., N. Sonenberg, Hershey,J.W.B. and Mathews,M.B., ed. (NY: Cold Spring Harbor Laboratory Press), pp. 89–125.

Meyuhas, O., Thompson, E. A., Jr., and Perry, R. P. (1987). Glucocorticoids selectively inhibit translation of ribosomal protein mRNAs in P1798 lymphosarcoma cells. Mol Cell Biol *7*, 2691-2699.

Moore, P. B., and Steitz, T. A. (2003). After the ribosome structures: how does peptidyl transferase work? Rna *9*, 155-159.

Munshi, R., Kandl, K. A., Carr-Schmid, A., Whitacre, J. L., Adams, A. E., and Kinzy, T. G. (2001). Overexpression of translation elongation factor 1A affects the organization and function of the actin cytoskeleton in yeast. Genetics *157*, 1425-1436.

Nairn, A. C., and Palfrey, H. C. (1987). Identification of the major Mr 100,000 substrate for calmodulin-dependent protein kinase III in mammalian cells as elongation factor-2. J Biol Chem *262*, 17299-17303.

Naranda, T., Sirangelo, I., Fabbri, B. J., and Hershey, J. W. (1995). Mutations in the NKXD consensus element indicate that GTP binds to the gamma-subunit of translation initiation factor eIF2. FEBS Lett *372*, 249-252.

Neff, C. L., and Sachs, A. B. (1999). Eukaryotic translation initiation factors 4G and 4A from Saccharomyces cerevisiae interact physically and functionally. Mol Cell Biol *19*, 5557-5564.

Ortiz, P. A., Ulloque, R., Kihara, G. K., Zheng, H., and Kinzy, T. G. (2006). Translation elongation factor 2 anticodon mimicry domain mutants affect fidelity and diphtheria toxin resistance. J Biol Chem *281*, 32639-32648.

Palmer, T. D., Miller, A. D., Reeder, R. H., and McStay, B. (1993). Efficient expression of a protein coding gene under the control of an RNA polymerase I promoter. Nucleic Acids Res *21*, 3451-3457.

Parker, R., and Sheth, U. (2007). P bodies and the control of mRNA translation and degradation. Mol Cell *25*, 635-646.

Passmore, L. A., Schmeing, T. M., Maag, D., Applefield, D. J., Acker, M. G., Algire, M. A., Lorsch, J. R., and Ramakrishnan, V. (2007). The eukaryotic translation initiation factors eIF1 and eIF1A induce an open conformation of the 40S ribosome. Mol Cell *26*, 41-50.

Paushkin, S. V., Kushnirov, V. V., Smirnov, V. N., and Ter-Avanesyan, M. D. (1997). In vitro propagation of the prion-like state of yeast Sup35 protein. Science *277*, 381-383.

Pavitt, G. D., Ramaiah, K. V., Kimball, S. R., and Hinnebusch, A. G. (1998). eIF2 independently binds two distinct eIF2B subcomplexes that catalyze and regulate guanine-nucleotide exchange. Genes Dev *12*, 514-526.

Pestova, T. V., de Breyne, S., Pisarev, A. V., Abaeva, I. S., and Hellen, C. U. (2008). eIF2-dependent and eIF2-independent modes of initiation on the CSFV IRES: a common role of domain II. Embo J *27*, 1060-1072.

Petzold, L. (1983). Automatic selection of methods for solving stiff and nonstiff systems of ordinary differential equations. SIAM J Sci Stat Comput *4*, 136–148.

Phan, L., Schoenfeld, L. W., Valasek, L., Nielsen, K. H., and Hinnebusch, A. G. (2001). A subcomplex of three eIF3 subunits binds eIF1 and eIF5 and stimulates ribosome binding of mRNA and tRNA(i)Met. Embo J *20*, 2954-2965.

Phan, L., Zhang, X., Asano, K., Anderson, J., Vornlocher, H. P., Greenberg, J. R., Qin, J., and Hinnebusch, A. G. (1998). Identification of a translation initiation factor 3 (eIF3) core complex, conserved in yeast and mammals, that interacts with eIF5. Mol Cell Biol *18*, 4935-4946.

Pisarev, A. V., Hellen, C. U., and Pestova, T. V. (2007). Recycling of eukaryotic posttermination ribosomal complexes. Cell *131*, 286-299.

Proweller, A., and Butler, J. S. (1996). Ribosomal association of poly(A)-binding protein in poly(A)-deficient Saccharomyces cerevisiae. J Biol Chem *271*, 10859-10865.

Qin, S. L., Xie, A. G., Bonato, M. C., and McLaughlin, C. S. (1990). Sequence analysis of the translational elongation factor 3 from Saccharomyces cerevisiae. J Biol Chem *265*, 1903-1912.

Rodnina, M. V., Serebryanik, A. I., Ovcharenko, G. V., and El'Skaya, A. V. (1994). ATPase strongly bound to higher eukaryotic ribosomes. Eur J Biochem *225*, 305-310.

Rowlands, A. G., Panniers, R., and Henshaw, E. C. (1988). The catalytic mechanism of guanine nucleotide exchange factor action and competitive inhibition by phosphorylated eukaryotic initiation factor 2. J Biol Chem *263*, 5526-5533.

Sachs, A. B., and Davis, R. W. (1989). The poly(A) binding protein is required for poly(A) shortening and 60S ribosomal subunit-dependent translation initiation. Cell *58*, 857-867.

Sachs, A. B., and Deardorff, J. A. (1992). Translation initiation requires the PAB-dependent poly(A) ribonuclease in yeast. Cell *70*, 961-973.

Sachs, A. B., Sarnow, P., and Hentze, M. W. (1997). Starting at the beginning, middle, and end: translation initiation in eukaryotes. Cell *89*, 831-838.

Sagliocco, F. A., Vega Laso, M. R., Zhu, D., Tuite, M. F., McCarthy, J. E., and Brown, A. J. (1993). The influence of 5'-secondary structures upon ribosome binding to mRNA during translation in yeast. J Biol Chem *268*, 26522-26530.

Saha, S. K., and Chakraburtty, K. (1986). Protein synthesis in yeast. Isolation of variant forms of elongation factor 1 from the yeast Saccharomyces cerevisiae. J Biol Chem *261*, 12599-12603.

Salnikova, A. B., Kryndushkin, D. S., Smirnov, V. N., Kushnirov, V. V., and Ter-Avanesyan, M. D. (2005). Nonsense suppression in yeast cells overproducing Sup35 (eRF3) is caused by its non-heritable amyloids. J Biol Chem *280*, 8808-8812.

Sangthong, P., Hughes, J., and McCarthy, J. E. (2007). Distributed control for recruitment, scanning and subunit joining steps of translation initiation. Nucleic Acids Res *35*, 3573-3580.

Schirmaier, F., and Philippsen, P. (1984). Identification of two genes coding for the translation elongation factor EF-1 alpha of S. cerevisiae. Embo J *3*, 3311-3315.

Schmeing, T. M., and Ramakrishnan, V. (2009). What recent ribosome structures have revealed about the mechanism of translation. Nature *461*, 1234-1242.

Schuster, S., Dandekar, T., and Fell, D. A. (1999). Detection of elementary flux modes in biochemical networks: a promising tool for pathway analysis and metabolic engineering. Trends Biotechnol *17*, 53-60.

Scolnick, E., Tompkins, R., Caskey, T., and Nirenberg, M. (1968). Release factors differing in specificity for terminator codons. Proc Natl Acad Sci U S A *61*, 768-774.

Seit-Nebi, A., Frolova, L., Justesen, J., and Kisselev, L. (2001). Class-1 translation termination factors: invariant GGQ minidomain is essential for release activity and ribosome binding but not for stop codon recognition. Nucleic Acids Res *29*, 3982-3987.

Sherman, F. (2002). Getting started with yeast. Methods Enzymol *350*, 3-41.

Shimomura, O., Johnson, F. H., and Saiga, Y. (1962). Extraction, purification and properties of aequorin, a bioluminescent protein from the luminous hydromedusan, Aequorea. J Cell Comp Physiol *59*, 223-239.

Silvera, D., Formenti, S. C., and Schneider, R. J. (2010). Translational control in cancer. Nat Rev Cancer *10*, 254-266.

Siwiak, M., and Zielenkiewicz, P. (2010). A comprehensive, quantitative, and genome-wide model of translation. PLoS Comput Biol *6*, e1000865.

Sonenberg, N., and Hinnebusch, A. G. (2009). Regulation of translation initiation in eukaryotes: mechanisms and biological targets. Cell *136*, 731-745.

St Johnston, D. (1995). The intracellular localization of messenger RNAs. Cell *81*, 161-170.

Stansfield, I., Jones, K. M., Kushnirov, V. V., Dagkesamanskaya, A. R., Poznyakovski, A. I., Paushkin, S. V., Nierras, C. R., Cox, B. S., Ter-Avanesyan, M. D., and Tuite, M. F. (1995). The products of the SUP45 (eRF1) and SUP35 genes interact to mediate translation termination in Saccharomyces cerevisiae. Embo J *14*, 4365-4373.

Stotz, A., and Linder, P. (1990). The ADE2 gene from Saccharomyces cerevisiae: sequence and new vectors. Gene *95*, 91-98.

Terenin, I. M., Dmitriev, S. E., Andreev, D. E., and Shatsky, I. N. (2008). Eukaryotic translation initiation machinery can operate in a bacterial-like mode without eIF2. Nat Struct Mol Biol *15*, 836-841.

Triana-Alonso, F. J., Chakraburtty, K., and Nierhaus, K. H. (1995). The elongation factor 3 unique in higher fungi and essential for protein biosynthesis is an E site factor. J Biol Chem *270*, 20473-20478.

Valasek, L., Mathew, A. A., Shin, B. S., Nielsen, K. H., Szamecz, B., and Hinnebusch, A. G. (2003). The yeast eIF3 subunits TIF32/a, NIP1/c, and eIF5 make critical connections with the 40S ribosome in vivo. Genes Dev *17*, 786-799.

Valasek, L., Nielsen, K. H., and Hinnebusch, A. G. (2002). Direct eIF2-eIF3 contact in the multifactor complex is important for translation initiation in vivo. Embo J *21*, 5886-5898.

Vallabhajosyula, R. R., Chickarmane, V., and Sauro, H. M. (2006). Conservation analysis of large biochemical networks. Bioinformatics *22*, 346-353.

Varshney, U., Lee, C. P., and RajBhandary, U. L. (1993). From elongator tRNA to initiator tRNA. Proc Natl Acad Sci U S A *90*, 2305-2309.

Vasudevan, S., Tong, Y., and Steitz, J. A. (2007). Switching from repression to activation: microRNAs can up-regulate translation. Science *318*, 1931-1934.

Verschoor, A., Warner, J. R., Srivastava, S., Grassucci, R. A., and Frank, J. (1998). Three-dimensional structure of the yeast ribosome. Nucleic Acids Res *26*, 655-661.

von der Haar, T. (2007). Optimized protein extraction for quantitative proteomics of yeasts. PLoS One *2*, e1078.

von der Haar, T. (2008). A quantitative estimation of the global translational activity in logarithmically growing yeast cells. BMC Syst Biol *2*, 87.

von der Haar, T., and McCarthy, J. E. (2002). Intracellular translation initiation factor levels in Saccharomyces cerevisiae and their role in cap-complex function. Mol Microbiol *46*, 531-544.

von der Haar, T., and Tuite, M. F. (2007). Regulated translational bypass of stop codons in yeast. Trends Microbiol *15*, 78-86.

Wilker, E. W., van Vugt, M. A., Artim, S. A., Huang, P. H., Petersen, C. P., Reinhardt, H. C., Feng, Y., Sharp, P. A., Sonenberg, N., White, F. M., and Yaffe, M. B. (2007). 14-3-3sigma controls mitotic translation to facilitate cytokinesis. Nature *446*, 329-332.

Wolin, S. L., and Walter, P. (1988). Ribosome pausing and stacking during translation of a eukaryotic mRNA. Embo J *7*, 3559-3569.

You, T., Coghill, G. M., and Brown, A. J. (2010). A quantitative model for mRNA translation in Saccharomyces cerevisiae. Yeast.

Zhang, G., Fedyunin, I., Miekley, O., Valleriani, A., Moura, A., and Ignatova, Z. (2010). Global and local depletion of ternary complex limits translational elongation. Nucleic Acids Res.

Zhang, G., Hubalewska, M., and Ignatova, Z. (2009). Transient ribosomal attenuation coordinates protein synthesis and co-translational folding. Nat Struct Mol Biol *16*, 274-280.

Zhouravleva, G., Frolova, L., Le Goff, X., Le Guellec, R., Inge-Vechtomov, S., Kisselev, L., and Philippe, M. (1995). Termination of translation in eukaryotes is governed by two interacting polypeptide chain release factors, eRF1 and eRF3. Embo J *14*, 4065-4072.

Zouridis, H., and Hatzimanikatis, V. (2007). A model for protein translation: polysome self-organization leads to maximum protein synthesis rates. Biophys J *92*, 717-730.

$$
\begin{aligned}
\frac{d([40S] \cdot V_{compartment})}{dt} &= +V_{compartment} \cdot (2e+008 \cdot [80S_eRF1_eRF3_GTP]) \\
&\quad -V_{compartment} \cdot (5.28e+008 \cdot [40S] \cdot [eIF1A]) \\
\frac{d([40S_eIF1A] \cdot V_{compartment})}{dt} &= +V_{compartment} \cdot (5.28e+008 \cdot [40S] \cdot [eIF1A]) \\
&\quad -V_{compartment} \cdot (1.6e+008 \cdot [eIF1_eIF3_eIF5_eIF2_GTP_{Met}-tRNA] \cdot [40S_eIF1A]) \\
\frac{d([43S] \cdot V_{compartment})}{dt} &= -V_{compartment} \cdot (8.0e+009 \cdot [43S] \cdot [eIF4E_eIF4G_mRNApab1_eIF4A_eIF4B]) \\
&\quad +V_{compartment} \cdot (1.6e+008 \cdot [eIF1_eIF3_eIF5_eIF2_GTP_{Met}-tRNA] \cdot [40S_eIF1A]) \\
\frac{d([eIF4E_eIF4G] \cdot V_{compartment})}{dt} &= -V_{compartment} \cdot ((225000 \cdot [eIF4E_eIF4G] \cdot [mRNApab1] - 1000 \cdot [eIF4E_eIF4G_mRNApab1])) \\
&\quad +V_{compartment} \cdot ((3e+006 \cdot [eIF4E] \cdot [eIF4G] - 1000 \cdot [eIF4E_eIF4G]))
\end{aligned}
$$

$$\frac{d([eIF2B] \cdot V_{compartment})}{dt} = -V_{compartment} \cdot ((280000 \cdot [eIF2_GDP] \cdot [eIF2B] - 1000 \cdot [eIF2_GDP_eIF2B])) + V_{compartment} \cdot ((2e+008 \cdot [eIF2_GDP_eIF2B] - 1000 \cdot [eIF2_GTP] \cdot [eIF2B]))$$

$$\frac{d([eIF2_GDP_eIF2B] \cdot V_{compartment})}{dt} = +V_{compartment} \cdot ((280000 \cdot [eIF2_GDP] \cdot [eIF2B] - 1000 \cdot [eIF2_GDP_eIF2B])) - V_{compartment} \cdot ((2e+008 \cdot [eIF2_GDP_eIF2B] - 1000 \cdot [eIF2_GTP] \cdot [eIF2B]))$$

$$\frac{d([eIF2_GTP] \cdot V_{compartment})}{dt} = +V_{compartment} \cdot ((2e+008 \cdot [eIF2_GDP_eIF2B] - 1000 \cdot [eIF2_GTP] \cdot [eIF2B])) - V_{compartment} \cdot ((6.86e+008 \cdot [eIF2_GTP] \cdot [Met-tRNA] - 1000 \cdot [eIF2_GTP_Met-tRNA]))$$

$$\frac{d([mRNApab1] \cdot V_{compartment})}{dt} = -V_{compartment} \cdot ((225000 \cdot [eIF4E_eIF4G] \cdot [mRNApab1] - 1000 \cdot [eIF4E_eIF4G_mRNApab1])) + V_{compartment} \cdot ((2e+006 \cdot [mRNA_cap] \cdot [Pab1] - 1000 \cdot [mRNApab1]))$$

$$\frac{d([48S] \cdot V_{compartment})}{dt} = +V_{compartment} \cdot (8.9e+009 \cdot [43S] \cdot [eIF4E_eIF4G_mRNApab1_eIF4A_eIF4B]) - V_{compartment} \cdot ((2e+010 \cdot [48S] \cdot [Ded1] - 1000 \cdot [48S_Ded1]))$$

$$\frac{d([48S_Ded1] \cdot V_{compartment})}{dt} = +V_{compartment} \cdot ((2e+010 \cdot [48S] \cdot [Ded1] - 1000 \cdot [48S_Ded1])) - V_{compartment} \cdot ((6.52e+010 \cdot [48S_Ded1] \cdot [eIF5B_GTP] - 1000 \cdot [48S_Ded1_eIF5B_GTP]))$$

$$\frac{d([eIF5B_GTP] \cdot V_{compartment})}{dt} = +V_{compartment} \cdot ((2e+006 \cdot [eIF5B_GDP] - 1000 \cdot [eIF5B_GTP])) - V_{compartment} \cdot ((6.52e+010 \cdot [48S_Ded1] \cdot [eIF5B_GTP] - 1000 \cdot [48S_Ded1_eIF5B_GTP]))$$

$$
\begin{aligned}
\frac{\mathrm{d}([\mathrm{eEF1A_GDP}] \cdot V_{\mathrm{compartment}})}{\mathrm{dt}} = \quad & + V_{\mathrm{compartment}} \cdot (\mathrm{k23f} \cdot [80\mathrm{S_a a} - \mathrm{tRNA_e EF1A_G TP_14}]) \\
& + V_{\mathrm{compartment}} \cdot (\mathrm{k23f} \cdot [80\mathrm{S_a a} - \mathrm{tRNA_e EF1A_G TP_15}]) \\
& + V_{\mathrm{compartment}} \cdot (\mathrm{k23f} \cdot [80\mathrm{S_a a} - \mathrm{tRNA_e EF1A_G TP_16}]) \\
& + V_{\mathrm{compartment}} \cdot (\mathrm{k23f} \cdot [80\mathrm{S_a a} - \mathrm{tRNA_e EF1A_G TP_17}]) \\
& + V_{\mathrm{compartment}} \cdot (\mathrm{k23f} \cdot [80\mathrm{S_a a} - \mathrm{tRNA_e EF1A_G TP_18}]) \\
& + V_{\mathrm{compartment}} \cdot (\mathrm{k23f} \cdot [80\mathrm{S_a a} - \mathrm{tRNA_e EF1A_G TP_19}]) \\
& - V_{\mathrm{compartment}} \cdot (7.5\mathrm{e}+009 \cdot [\mathrm{eEF1A_GDP}] \cdot [\mathrm{eEF1B}]) \\
& - (1000 \cdot [\mathrm{eEF1A_GDP_e EF1B}]) \\
& + V_{\mathrm{compartment}} \cdot (\mathrm{k23f} \cdot [80\mathrm{S_a a} - \mathrm{tRNA_e EF1A_G TP_1}]) \\
& + V_{\mathrm{compartment}} \cdot (\mathrm{k23f} \cdot [80\mathrm{S_a a} - \mathrm{tRNA_e EF1A_G TP_2}]) \\
& + V_{\mathrm{compartment}} \cdot (\mathrm{k23f} \cdot [80\mathrm{S_a a} - \mathrm{tRNA_e EF1A_G TP_3}]) \\
& + V_{\mathrm{compartment}} \cdot (\mathrm{k23f} \cdot [80\mathrm{S_a a} - \mathrm{tRNA_e EF1A_G TP_4}]) \\
& + V_{\mathrm{compartment}} \cdot (\mathrm{k23f} \cdot [80\mathrm{S_a a} - \mathrm{tRNA_e EF1A_G TP_5}]) \\
& + V_{\mathrm{compartment}} \cdot (\mathrm{k23f} \cdot [80\mathrm{S_a a} - \mathrm{tRNA_e EF1A_G TP_6}]) \\
& + V_{\mathrm{compartment}} \cdot (\mathrm{k23f} \cdot [80\mathrm{S_a a} - \mathrm{tRNA_e EF1A_G TP_7}]) \\
& + V_{\mathrm{compartment}} \cdot (\mathrm{k23f} \cdot [80\mathrm{S_a a} - \mathrm{tRNA_e EF1A_G TP_8}]) \\
& + V_{\mathrm{compartment}} \cdot (\mathrm{k23f} \cdot [80\mathrm{S_a a} - \mathrm{tRNA_e EF1A_G TP_9}]) \\
& + V_{\mathrm{compartment}} \cdot (\mathrm{k23f} \cdot [80\mathrm{S_a a} - \mathrm{tRNA_e EF1A_G TP_10}]) \\
& + V_{\mathrm{compartment}} \cdot (\mathrm{k23f} \cdot [80\mathrm{S_a a} - \mathrm{tRNA_e EF1A_G TP_11}]) \\
& + V_{\mathrm{compartment}} \cdot (\mathrm{k23f} \cdot [80\mathrm{S_a a} - \mathrm{tRNA_e EF1A_G TP_12}]) \\
& + V_{\mathrm{compartment}} \cdot (\mathrm{k23f} \cdot [80\mathrm{S_a a} - \mathrm{tRNA_e EF1A_G TP_13}])
\end{aligned}
$$

$$
\begin{aligned}
\frac{\mathrm{d}([\mathrm{eEF1B}]\cdot V_{\mathrm{compartment}})}{\mathrm{d}t} &= -V_{\mathrm{compartment}}\cdot((7.5e+009\cdot[\mathrm{eEF1A_GDP}]\cdot[\mathrm{eEF1B}]-1000\cdot[\mathrm{eEF1A_GDP_eEF1B}])) \\
&\quad +V_{\mathrm{compartment}}\cdot((1e+008\cdot[\mathrm{eEF1A_GDP_eEF1B}]-1000\cdot[\mathrm{eEF1A_GTP}]\cdot[\mathrm{eEF1B}])) \\
\frac{\mathrm{d}([\mathrm{eEF1A_GDP_eEF1B}]\cdot V_{\mathrm{compartment}})}{\mathrm{d}t} &= +V_{\mathrm{compartment}}\cdot((7.5e+009\cdot[\mathrm{eEF1A_GDP}]\cdot[\mathrm{eEF1B}]-1000\cdot[\mathrm{eEF1A_GDP_eEF1B}])) \\
&\quad -V_{\mathrm{compartment}}\cdot((1e+008\cdot[\mathrm{eEF1A_GDP_eEF1B}]-1000\cdot[\mathrm{eEF1A_GTP}]\cdot[\mathrm{eEF1B}])) \\
\frac{\mathrm{d}([\mathrm{eEF1A_GTP}]\cdot V_{\mathrm{compartment}})}{\mathrm{d}t} &= +V_{\mathrm{compartment}}\cdot((1e+008\cdot[\mathrm{eEF1A_GDP_eEF1B}]-1000\cdot[\mathrm{eEF1A_GTP}]\cdot[\mathrm{eEF1B}])) \\
&\quad -V_{\mathrm{compartment}}\cdot((20000\cdot[\mathrm{eEF1A_GTP}]\cdot[\mathrm{aa-tRNA}]-1000\cdot[\mathrm{aa-tRNA_eEF1A_GTP}])) \\
\frac{\mathrm{d}([\mathrm{80S_a a-tRNA_eEF1A_GTP_1}]\cdot V_{\mathrm{compartment}})}{\mathrm{d}t} &= +V_{\mathrm{compartment}}\cdot((\mathrm{k22f}\cdot[\mathrm{aa-tRNA_eEF1A_GTP}]\cdot[\mathrm{80S_1}]-\mathrm{k22b}\cdot[\mathrm{80S_a a-tRNA_eEF1A_GTP_1}])) \\
&\quad -V_{\mathrm{compartment}}\cdot(\mathrm{k23f}\cdot[\mathrm{80S_a a-tRNA_eEF1A_GTP_1}]) \\
\frac{\mathrm{d}([\mathrm{80S_a a-tRNA_1}]\cdot V_{\mathrm{compartment}})}{\mathrm{d}t} &= +V_{\mathrm{compartment}}\cdot(\mathrm{k23f}\cdot[\mathrm{80S_a a-tRNA_eEF1A_GTP_1}]) \\
&\quad -V_{\mathrm{compartment}}\cdot((\mathrm{k25f}\cdot[\mathrm{eEF2_GTP}]\cdot[\mathrm{80S_a a-tRNA_1}]-\mathrm{k25b}\cdot[\mathrm{80S_a a-tRNA_eEF2_GTP_1}])) \\
\frac{\mathrm{d}([\mathrm{80S_2}]\cdot V_{\mathrm{compartment}})}{\mathrm{d}t} &= -V_{\mathrm{compartment}}\cdot((\mathrm{k22f}\cdot[\mathrm{aa-tRNA_eEF1A_GTP}]\cdot[\mathrm{80S_2}]-\mathrm{k22b}\cdot[\mathrm{80S_a a-tRNA_eEF1A_GTP_2}])) \\
&\quad +V_{\mathrm{compartment}}\cdot(\mathrm{k29f}\cdot[\mathrm{80S_t RNA_eEF3_GTP_2}]) \\
\frac{\mathrm{d}([\mathrm{80S_a a-tRNA_eEF1A_GTP_2}]\cdot V_{\mathrm{compartment}})}{\mathrm{d}t} &= +V_{\mathrm{compartment}}\cdot((\mathrm{k22f}\cdot[\mathrm{aa-tRNA_eEF1A_GTP}]\cdot[\mathrm{80S_2}]-\mathrm{k22b}\cdot[\mathrm{80S_a a-tRNA_eEF1A_GTP_2}])) \\
&\quad -V_{\mathrm{compartment}}\cdot(\mathrm{k23f}\cdot[\mathrm{80S_a a-tRNA_eEF1A_GTP_2}]) \\
\frac{\mathrm{d}([\mathrm{80S_a a-tRNA_2}]\cdot V_{\mathrm{compartment}})}{\mathrm{d}t} &= +V_{\mathrm{compartment}}\cdot(\mathrm{k23f}\cdot[\mathrm{80S_a a-tRNA_eEF1A_GTP_2}]) \\
&\quad -V_{\mathrm{compartment}}\cdot((\mathrm{k25f}\cdot[\mathrm{eEF2_GTP}]\cdot[\mathrm{80S_a a-tRNA_2}]-\mathrm{k25b}\cdot[\mathrm{80S_a a-tRNA_eEF2_GTP_2}])) \\
\frac{\mathrm{d}([\mathrm{80S_t RNA_eEF3_GTP_2}]\cdot V_{\mathrm{compartment}})}{\mathrm{d}t} &= +V_{\mathrm{compartment}}\cdot(\mathrm{k28f}\cdot[\mathrm{80S_t RNA_2}]\cdot[\mathrm{eEF3_GTP}]) \\
&\quad -V_{\mathrm{compartment}}\cdot(\mathrm{k29f}\cdot[\mathrm{80S_t RNA_eEF3_GTP_2}]) \\
\frac{\mathrm{d}([\mathrm{80S_3}]\cdot V_{\mathrm{compartment}})}{\mathrm{d}t} &= -V_{\mathrm{compartment}}\cdot((\mathrm{k22f}\cdot[\mathrm{aa-tRNA_eEF1A_GTP}]\cdot[\mathrm{80S_3}]-\mathrm{k22b}\cdot[\mathrm{80S_a a-tRNA_eEF1A_GTP_3}])) \\
&\quad +V_{\mathrm{compartment}}\cdot(\mathrm{k29f}\cdot[\mathrm{80S_t RNA_eEF3_GTP_3}])
\end{aligned}
$$

$$\frac{\mathrm{d}([\mathrm{eEF1B}] \cdot V_{\mathrm{compartment}})}{\mathrm{d}t} = -V_{\mathrm{compartment}} \cdot ((7.5e+009 \cdot [\mathrm{eEF1A_GDP}] \cdot [\mathrm{eEF1B}] - 1000 \cdot [\mathrm{eEF1A_GDP_eEF1B}]))$$
$$+V_{\mathrm{compartment}} \cdot ((1e+008 \cdot [\mathrm{eEF1A_GDP_eEF1B}] - 1000 \cdot [\mathrm{eEF1A_GTP}] \cdot [\mathrm{eEF1B}]))$$

$$\frac{\mathrm{d}([\mathrm{eEF1A_GDP_eEF1B}] \cdot V_{\mathrm{compartment}})}{\mathrm{d}t} = +V_{\mathrm{compartment}} \cdot ((7.5e+009 \cdot [\mathrm{eEF1A_GDP}] \cdot [\mathrm{eEF1B}] - 1000 \cdot [\mathrm{eEF1A_GDP_eEF1B}]))$$
$$-V_{\mathrm{compartment}} \cdot ((1e+008 \cdot [\mathrm{eEF1A_GDP_eEF1B}] - 1000 \cdot [\mathrm{eEF1A_GTP}] \cdot [\mathrm{eEF1B}]))$$

$$\frac{\mathrm{d}([\mathrm{eEF1A_GTP}] \cdot V_{\mathrm{compartment}})}{\mathrm{d}t} = +V_{\mathrm{compartment}} \cdot ((1e+008 \cdot [\mathrm{eEF1A_GDP_eEF1B}] - 1000 \cdot [\mathrm{eEF1A_GTP}] \cdot [\mathrm{eEF1B}]))$$
$$-V_{\mathrm{compartment}} \cdot ((20000 \cdot [\mathrm{eEF1A_GTP}] \cdot [\mathrm{aa-tRNA}] - 1000 \cdot [\mathrm{aa-tRNA_eEF1A_GTP}]))$$

$$\frac{\mathrm{d}([80\mathrm{S_a}\text{a}-\mathrm{tRNA_eEF1A_GTP_1}] \cdot V_{\mathrm{compartment}})}{\mathrm{d}t} = +V_{\mathrm{compartment}} \cdot ((\mathrm{k22f} \cdot [\mathrm{aa-tRNA_eEF1A_GTP}] \cdot [80\mathrm{S_1}] - \mathrm{k22b} \cdot [80\mathrm{S_a}\text{a}-\mathrm{tRNA_eEF1A_GTP_1}]))$$
$$-V_{\mathrm{compartment}} \cdot (\mathrm{k23f} \cdot [80\mathrm{S_a}\text{a}-\mathrm{tRNA_eEF1A_GTP_1}])$$

$$\frac{\mathrm{d}([80\mathrm{S_a}\text{a}-\mathrm{tRNA_1}] \cdot V_{\mathrm{compartment}})}{\mathrm{d}t} = +V_{\mathrm{compartment}} \cdot (\mathrm{k23f} \cdot [80\mathrm{S_a}\text{a}-\mathrm{tRNA_eEF1A_GTP_1}])$$
$$-V_{\mathrm{compartment}} \cdot ((\mathrm{k25f} \cdot [\mathrm{eEF2_GTP}] \cdot [80\mathrm{S_a}\text{a}-\mathrm{tRNA_1}] - \mathrm{k25b} \cdot [80\mathrm{S_a}\text{a}-\mathrm{tRNA_eEF2_GTP_1}]))$$

$$\frac{\mathrm{d}([80\mathrm{S_2}] \cdot V_{\mathrm{compartment}})}{\mathrm{d}t} = -V_{\mathrm{compartment}} \cdot ((\mathrm{k22f} \cdot [\mathrm{aa-tRNA_eEF1A_GTP}] \cdot [80\mathrm{S_2}] - \mathrm{k22b} \cdot [80\mathrm{S_a}\text{a}-\mathrm{tRNA_eEF1A_GTP_2}]))$$
$$+V_{\mathrm{compartment}} \cdot (\mathrm{k29f} \cdot [80\mathrm{S_t}\mathrm{RNA_eEF3_GTP_2}])$$

$$\frac{\mathrm{d}([80\mathrm{S_a}\text{a}-\mathrm{tRNA_eEF1A_GTP_2}] \cdot V_{\mathrm{compartment}})}{\mathrm{d}t} = +V_{\mathrm{compartment}} \cdot ((\mathrm{k22f} \cdot [\mathrm{aa-tRNA_eEF1A_GTP}] \cdot [80\mathrm{S_2}] - \mathrm{k22b} \cdot [80\mathrm{S_a}\text{a}-\mathrm{tRNA_eEF1A_GTP_2}]))$$
$$-V_{\mathrm{compartment}} \cdot (\mathrm{k23f} \cdot [80\mathrm{S_a}\text{a}-\mathrm{tRNA_eEF1A_GTP_2}])$$

$$\frac{\mathrm{d}([80\mathrm{S_a}\text{a}-\mathrm{tRNA_2}] \cdot V_{\mathrm{compartment}})}{\mathrm{d}t} = +V_{\mathrm{compartment}} \cdot (\mathrm{k23f} \cdot [80\mathrm{S_a}\text{a}-\mathrm{tRNA_eEF1A_GTP_2}])$$
$$-V_{\mathrm{compartment}} \cdot ((\mathrm{k25f} \cdot [\mathrm{eEF2_GTP}] \cdot [80\mathrm{S_a}\text{a}-\mathrm{tRNA_2}] - \mathrm{k25b} \cdot [80\mathrm{S_a}\text{a}-\mathrm{tRNA_eEF2_GTP_2}]))$$

$$\frac{\mathrm{d}([80\mathrm{S_t}\mathrm{RNA_eEF3_GTP_2}] \cdot V_{\mathrm{compartment}})}{\mathrm{d}t} = +V_{\mathrm{compartment}} \cdot (\mathrm{k28f} \cdot [80\mathrm{S_t}\mathrm{RNA_2}] \cdot [\mathrm{eEF3_GTP}])$$
$$-V_{\mathrm{compartment}} \cdot (\mathrm{k29f} \cdot [80\mathrm{S_t}\mathrm{RNA_eEF3_GTP_2}])$$

$$\frac{\mathrm{d}([80\mathrm{S_3}] \cdot V_{\mathrm{compartment}})}{\mathrm{d}t} = -V_{\mathrm{compartment}} \cdot ((\mathrm{k22f} \cdot [\mathrm{aa-tRNA_eEF1A_GTP}] \cdot [80\mathrm{S_3}] - \mathrm{k22b} \cdot [80\mathrm{S_a}\text{a}-\mathrm{tRNA_eEF1A_GTP_3}]))$$
$$+V_{\mathrm{compartment}} \cdot (\mathrm{k29f} \cdot [80\mathrm{S_t}\mathrm{RNA_eEF3_GTP_3}])$$

$$
\begin{aligned}
\frac{\mathrm{d}([80S_a a{-}tRNA_5]\cdot V_{compartment})}{\mathrm{dt}} &= +V_{compartment}\cdot(k23f\cdot[80S_a a-tRNA_e EF1A_G TP_5]) \\
&\quad -V_{compartment}\cdot((k25f\cdot[eEF2_G TP]\cdot[80S_a a-tRNA_5]-k25b\cdot[80S_a a-tRNA_e EF2_G TP_5])) \\
\frac{\mathrm{d}([80S_t RNA_e EF3_G TP_5]\cdot V_{compartment})}{\mathrm{dt}} &= +V_{compartment}\cdot(k28f\cdot[80S_t RNA_5]\cdot[eEF3_G TP]) \\
&\quad -V_{compartment}\cdot(k29f\cdot[80S_t RNA_e EF3_G TP_5]) \\
\frac{\mathrm{d}([80S_6]\cdot V_{compartment})}{\mathrm{dt}} &= -V_{compartment}\cdot((k22f\cdot[aa-tRNA_e EF1A_G TP]\cdot[80S_6]-k22b\cdot[80S_a a-tRNA_e EF1A_G TP_6])) \\
&\quad +V_{compartment}\cdot(k29f\cdot[80S_t RNA_e EF3_G TP_6]) \\
\frac{\mathrm{d}([80S_a a{-}tRNA_e EF1A_G TP_6]\cdot V_{compartment})}{\mathrm{dt}} &= +V_{compartment}\cdot((k22f\cdot[aa-tRNA_e EF1A_G TP]\cdot[80S_6]-k22b\cdot[80S_a a-tRNA_e EF1A_G TP_6])) \\
&\quad -V_{compartment}\cdot(k23f\cdot[80S_a a-tRNA_e EF1A_G TP_6]) \\
\frac{\mathrm{d}([80S_a a{-}tRNA_6]\cdot V_{compartment})}{\mathrm{dt}} &= +V_{compartment}\cdot(k23f\cdot[80S_a a-tRNA_e EF1A_G TP_6]) \\
&\quad -V_{compartment}\cdot((k25f\cdot[eEF2_G TP]\cdot[80S_a a-tRNA_6]-k25b\cdot[80S_a a-tRNA_e EF2_G TP_6])) \\
\frac{\mathrm{d}([80S_a a{-}tRNA_e EF2_G TP_6]\cdot V_{compartment})}{\mathrm{dt}} &= +V_{compartment}\cdot((k25f\cdot[eEF2_G TP]\cdot[80S_a a-tRNA_6]-k25b\cdot[80S_a a-tRNA_e EF2_G TP_6])) \\
&\quad -V_{compartment}\cdot(k26f\cdot[80S_a a-tRNA_e EF2_G TP_6]\cdot mRNA_s ot) \\
\frac{\mathrm{d}([80S_t RNA_e EF3_G TP_6]\cdot V_{compartment})}{\mathrm{dt}} &= +V_{compartment}\cdot(k28f\cdot[80S_t RNA_6]\cdot[eEF3_G TP]) \\
&\quad -V_{compartment}\cdot(k29f\cdot[80S_t RNA_e EF3_G TP_6]) \\
\frac{\mathrm{d}([80S_7]\cdot V_{compartment})}{\mathrm{dt}} &= -V_{compartment}\cdot((k22f\cdot[aa-tRNA_e EF1A_G TP]\cdot[80S_7]-k22b\cdot[80S_a a-tRNA_e EF1A_G TP_7])) \\
&\quad +V_{compartment}\cdot(k29f\cdot[80S_t RNA_e EF3_G TP_7]) \\
\frac{\mathrm{d}([80S_a a{-}tRNA_e EF1A_G TP_7]\cdot V_{compartment})}{\mathrm{dt}} &= +V_{compartment}\cdot((k22f\cdot[aa-tRNA_e EF1A_G TP]\cdot[80S_7]-k22b\cdot[80S_a a-tRNA_e EF1A_G TP_7])) \\
&\quad -V_{compartment}\cdot(k23f\cdot[80S_a a-tRNA_e EF1A_G TP_7])
\end{aligned}
$$

$$
\begin{aligned}
\frac{\mathrm{d}([80S_a a-tRNA_5]\cdot V_{compartment})}{\mathrm{d}t} &= +V_{compartment}\cdot(k23f\cdot[80S_a a-tRNA_e EF1A_G TP_5])\\
&\quad -V_{compartment}\cdot((k25f\cdot[eEF2_G TP]\cdot[80S_a a-tRNA_5]-k25b\cdot[80S_a a-tRNA_e EF2_G TP_5]))\\
\frac{\mathrm{d}([80S_t RNA_e EF3_G TP_5]\cdot V_{compartment})}{\mathrm{d}t} &= +V_{compartment}\cdot(k28f\cdot[80S_t RNA_5]\cdot[eEF3_G TP])\\
&\quad -V_{compartment}\cdot(k29f\cdot[80S_t RNA_e EF3_G TP_5])\\
\frac{\mathrm{d}([80S_6]\cdot V_{compartment})}{\mathrm{d}t} &= -V_{compartment}\cdot((k22f\cdot[aa-tRNA_e EF1A_G TP]\cdot[80S_6]-k22b\cdot[80S_a a-tRNA_e EF1A_G TP_6]))\\
&\quad +V_{compartment}\cdot(k29f\cdot[80S_t RNA_e EF3_G TP_6])\\
\frac{\mathrm{d}([80S_a a-tRNA_e EF1A_G TP_6]\cdot V_{compartment})}{\mathrm{d}t} &= +V_{compartment}\cdot((k22f\cdot[aa-tRNA_e EF1A_G TP]\cdot[80S_6]-k22b\cdot[80S_a a-tRNA_e EF1A_G TP_6]))\\
&\quad -V_{compartment}\cdot(k23f\cdot[80S_a a-tRNA_e EF1A_G TP_6])\\
\frac{\mathrm{d}([80S_a a-tRNA_6]\cdot V_{compartment})}{\mathrm{d}t} &= +V_{compartment}\cdot(k23f\cdot[80S_a a-tRNA_e EF1A_G TP_6])\\
&\quad -V_{compartment}\cdot((k25f\cdot[eEF2_G TP]\cdot[80S_a a-tRNA_6]-k25b\cdot[80S_a a-tRNA_e EF2_G TP_6]))\\
\frac{\mathrm{d}([80S_a a-tRNA_e EF2_G TP_6]\cdot V_{compartment})}{\mathrm{d}t} &= +V_{compartment}\cdot((k25f\cdot[eEF2_G TP]\cdot[80S_a a-tRNA_6]-k25b\cdot[80S_a a-tRNA_e EF2_G TP_6]))\\
&\quad -V_{compartment}\cdot(k26f\cdot[80S_a a-tRNA_e EF2_G TP_6]\cdot mRNA_t ot)\\
\frac{\mathrm{d}([80S_t RNA_e EF3_G TP_6]\cdot V_{compartment})}{\mathrm{d}t} &= +V_{compartment}\cdot(k28f\cdot[80S_t RNA_6]\cdot[eEF3_G TP])\\
&\quad -V_{compartment}\cdot(k29f\cdot[80S_t RNA_e EF3_G TP_6])\\
\frac{\mathrm{d}([80S_7]\cdot V_{compartment})}{\mathrm{d}t} &= -V_{compartment}\cdot((k22f\cdot[aa-tRNA_e EF1A_G TP]\cdot[80S_7]-k22b\cdot[80S_a a-tRNA_e EF1A_G TP_7]))\\
&\quad +V_{compartment}\cdot(k29f\cdot[80S_t RNA_e EF3_G TP_7])\\
\frac{\mathrm{d}([80S_a a-tRNA_e EF1A_G TP_7]\cdot V_{compartment})}{\mathrm{d}t} &= +V_{compartment}\cdot((k22f\cdot[aa-tRNA_e EF1A_G TP]\cdot[80S_7]-k22b\cdot[80S_a a-tRNA_e EF1A_G TP_7]))\\
&\quad -V_{compartment}\cdot(k23f^2\cdot[80S_a a-tRNA_e EF1A_G TP_7])
\end{aligned}
$$

$$
\begin{aligned}
\frac{\mathrm{d}([80S_t RNA_8] \cdot V_{compartment})}{dt} &= +V_{compartment} \cdot (k26f \cdot [80S_a a - tRNA_e EF2_G TP_7] \cdot mRNA_t ot) \\
&\quad -V_{compartment} \cdot (k28f \cdot [80S_t RNA_8] \cdot [eEF3_G TP]) \\
\frac{\mathrm{d}([80S_t RNA_e EF3_G TP_8] \cdot V_{compartment})}{dt} &= +V_{compartment} \cdot (k28f \cdot [80S_t RNA_8] \cdot [eEF3_G TP]) \\
&\quad -V_{compartment} \cdot (k29f \cdot [80S_t RNA_e EF3_G TP_8]) \\
\frac{\mathrm{d}([80S_9] \cdot V_{compartment})}{dt} &= -V_{compartment} \cdot ((k22f \cdot [aa - tRNA_e EF1A_G TP] \cdot [80S_9] - k22b \cdot [80S_a a - tRNA_e EF1A_G TP_9])) \\
&\quad +V_{compartment} \cdot (k29f \cdot [80S_t RNA_e EF3_G TP_9]) \\
\frac{\mathrm{d}([80S_a a - tRNA_e EF1A_G TP_9] \cdot V_{compartment})}{dt} &= +V_{compartment} \cdot ((k22f \cdot [aa - tRNA_e EF1A_G TP] \cdot [80S_9] - k22b \cdot [80S_a a - tRNA_e EF1A_G TP_9])) \\
&\quad -V_{compartment} \cdot (k23f \cdot [80S_a a - tRNA_e EF1A_G TP_9]) \\
\frac{\mathrm{d}([80S_a a - tRNA_9] \cdot V_{compartment})}{dt} &= +V_{compartment} \cdot (k23f \cdot [80S_a a - tRNA_e EF1A_G TP_9]) \\
&\quad -V_{compartment} \cdot ((k25f \cdot [eEF2_G TP] \cdot [80S_a a - tRNA_9] - k25b \cdot [80S_a a - tRNA_e EF2_G TP_9])) \\
\frac{\mathrm{d}([80S_a a - tRNA_e EF2_G TP_9] \cdot V_{compartment})}{dt} &= +V_{compartment} \cdot ((k25f \cdot [eEF2_G TP] \cdot [80S_a a - tRNA_9] - k25b \cdot [80S_a a - tRNA_e EF2_G TP_9])) \\
&\quad -V_{compartment} \cdot (k26f \cdot [80S_a a - tRNA_e EF2_G TP_9] \cdot mRNA_t ot) \\
\frac{\mathrm{d}([80S_t RNA_9] \cdot V_{compartment})}{dt} &= +V_{compartment} \cdot (k26f \cdot [80S_a a - tRNA_e EF2_G TP_8] \cdot mRNA_t ot) \\
&\quad -V_{compartment} \cdot (k28f \cdot [80S_t RNA_9] \cdot [eEF3_G TP]) \\
\frac{\mathrm{d}([80S_t RNA_e EF3_G TP_9] \cdot V_{compartment})}{dt} &= +V_{compartment} \cdot (k28f \cdot [80S_t RNA_9] \cdot [eEF3_G TP]) \\
&\quad -V_{compartment} \cdot (k29f \cdot [80S_t RNA_e EF3_G TP_9])
\end{aligned}
$$

$$
\begin{aligned}
\frac{\mathrm{d}([80S_i0]\cdot V_{\mathrm{compartment}})}{\mathrm{d}t} &= -V_{\mathrm{compartment}}\cdot((\mathrm{k22f}\cdot[\mathrm{aa-tRNA_eEF1A_GTP}]\cdot[80S_i0]-\mathrm{k22b}\cdot[80S_a\mathrm{a-tRNA_eEF1A_GTP_10}])) \\
&\quad +V_{\mathrm{compartment}}\cdot(\mathrm{k29f}\cdot[80S_i\mathrm{RNA_eEF3_GTP_10}]) \\
\frac{\mathrm{d}([80S_a\mathrm{a-tRNA_eEF1A_GTP_10}]\cdot V_{\mathrm{compartment}})}{\mathrm{d}t} &= +V_{\mathrm{compartment}}\cdot((\mathrm{k22f}\cdot[\mathrm{aa-tRNA_eEF1A_GTP}]\cdot[80S_i0]-\mathrm{k22b}\cdot[80S_a\mathrm{a-tRNA_eEF1A_GTP_10}])) \\
&\quad -V_{\mathrm{compartment}}\cdot(\mathrm{k23f}\cdot[80S_a\mathrm{a-tRNA_eEF1A_GTP_10}]) \\
\frac{\mathrm{d}([80S_a\mathrm{a-tRNA_1}0]\cdot V_{\mathrm{compartment}})}{\mathrm{d}t} &= +V_{\mathrm{compartment}}\cdot(\mathrm{k23f}\cdot[80S_a\mathrm{a-tRNA_eEF1A_GTP_10}]) \\
&\quad -V_{\mathrm{compartment}}\cdot((\mathrm{k25f}\cdot[\mathrm{eEF2_GTP}]\cdot[80S_a\mathrm{a-tRNA_1}0]-\mathrm{k25b}\cdot[80S_a\mathrm{a-tRNA_eEF2_GTP_10}])) \\
\frac{\mathrm{d}([80S_a\mathrm{a-tRNA_eEF2_GTP_10}]\cdot V_{\mathrm{compartment}})}{\mathrm{d}t} &= +V_{\mathrm{compartment}}\cdot((\mathrm{k25f}\cdot[\mathrm{eEF2_GTP}]\cdot[80S_a\mathrm{a-tRNA_1}0]-\mathrm{k25b}\cdot[80S_a\mathrm{a-tRNA_eEF2_GTP_10}])) \\
&\quad -V_{\mathrm{compartment}}\cdot(\mathrm{k26f}\cdot[80S_a\mathrm{a-tRNA_eEF2_GTP_10}]\cdot\mathrm{mRNA_tot}) \\
\frac{\mathrm{d}([80S_i\mathrm{RNA_1}0]\cdot V_{\mathrm{compartment}})}{\mathrm{d}t} &= +V_{\mathrm{compartment}}\cdot(\mathrm{k26f}\cdot[80S_a\mathrm{a-tRNA_eEF2_GTP_9}]\cdot\mathrm{mRNA_tot}) \\
&\quad -V_{\mathrm{compartment}}\cdot(\mathrm{k28f}\cdot[80S_i\mathrm{RNA_1}0]\cdot[\mathrm{eEF3_GTP}]) \\
\frac{\mathrm{d}([80S_i\mathrm{RNA_eEF3_GTP_10}]\cdot V_{\mathrm{compartment}})}{\mathrm{d}t} &= +V_{\mathrm{compartment}}\cdot(\mathrm{k28f}\cdot[80S_i\mathrm{RNA_1}0]\cdot[\mathrm{eEF3_GTP}]) \\
&\quad -V_{\mathrm{compartment}}\cdot(\mathrm{k29f}\cdot[80S_i\mathrm{RNA_eEF3_GTP_10}]) \\
\frac{\mathrm{d}([80S_i1]\cdot V_{\mathrm{compartment}})}{\mathrm{d}t} &= -V_{\mathrm{compartment}}\cdot((\mathrm{k22f}\cdot[\mathrm{aa-tRNA_eEF1A_GTP}]\cdot[80S_i1]-\mathrm{k22b}\cdot[80S_a\mathrm{a-tRNA_eEF1A_GTP_11}])) \\
&\quad +V_{\mathrm{compartment}}\cdot(\mathrm{k29f}\cdot[80S_i\mathrm{RNA_eEF3_GTP_11}]) \\
\frac{\mathrm{d}([80S_a\mathrm{a-tRNA_eEF1A_GTP_11}]\cdot V_{\mathrm{compartment}})}{\mathrm{d}t} &= +V_{\mathrm{compartment}}\cdot((\mathrm{k22f}\cdot[\mathrm{aa-tRNA_eEF1A_GTP}]\cdot[80S_i1]-\mathrm{k22b}\cdot[80S_a\mathrm{a-tRNA_eEF1A_GTP_11}])) \\
&\quad -V_{\mathrm{compartment}}\cdot(\mathrm{k23f}\cdot[80S_a\mathrm{a-tRNA_eEF1A_GTP_11}]) \\
\frac{\mathrm{d}([80S_a\mathrm{a-tRNA_1}1]\cdot V_{\mathrm{compartment}})}{\mathrm{d}t} &= +V_{\mathrm{compartment}}\cdot(\mathrm{k23f}\cdot[80S_a\mathrm{a-tRNA_eEF1A_GTP_11}]) \\
&\quad -V_{\mathrm{compartment}}\cdot((\mathrm{k25f}\cdot[\mathrm{eEF2_GTP}]\cdot[80S_a\mathrm{a-tRNA_1}1]-\mathrm{k25b}\cdot[80S_a\mathrm{a-tRNA_eEF2_GTP_11}]))
\end{aligned}
$$

$$
\begin{aligned}
\frac{\mathrm{d}([80S_1 0] \cdot V_{\mathrm{compartment}})}{\mathrm{d}t} &= -V_{\mathrm{compartment}} \cdot ((\mathrm{k22f} \cdot [\mathrm{aa-tRNA_eEF1A_GTP}] \cdot [80S_1 0] - \mathrm{k22b} \cdot [80S_a\mathrm{a-tRNA_eEF1A_GTP_1 0}])) \\
&\quad + V_{\mathrm{compartment}} \cdot (\mathrm{k29f} \cdot [80S_t\mathrm{RNA_eEF3_GTP_1 0}]) \\
\frac{\mathrm{d}([80S_a\mathrm{a-tRNA_eEF1A_GTP_1 0}] \cdot V_{\mathrm{compartment}})}{\mathrm{d}t} &= +V_{\mathrm{compartment}} \cdot ((\mathrm{k22f} \cdot [\mathrm{aa-tRNA_eEF1A_GTP}] \cdot [80S_1 0] - \mathrm{k22b} \cdot [80S_a\mathrm{a-tRNA_eEF1A_GTP_1 0}])) \\
&\quad - V_{\mathrm{compartment}} \cdot (\mathrm{k23f} \cdot [80S_a\mathrm{a-tRNA_eEF1A_GTP_1 0}]) \\
\frac{\mathrm{d}([80S_a\mathrm{a-tRNA}_1 0] \cdot V_{\mathrm{compartment}})}{\mathrm{d}t} &= +V_{\mathrm{compartment}} \cdot (\mathrm{k23f} \cdot [80S_a\mathrm{a-tRNA_eEF1A_GTP_1 0}]) \\
&\quad - V_{\mathrm{compartment}} \cdot ((\mathrm{k25f} \cdot [\mathrm{eEF2_GTP}] \cdot [80S_a\mathrm{a-tRNA}_1 0] - \mathrm{k25b} \cdot [80S_a\mathrm{a-tRNA_eEF2_GTP_1 0}])) \\
\frac{\mathrm{d}([80S_a\mathrm{a-tRNA_eEF2_GTP_1 0}] \cdot V_{\mathrm{compartment}})}{\mathrm{d}t} &= +V_{\mathrm{compartment}} \cdot ((\mathrm{k25f} \cdot [\mathrm{eEF2_GTP}] \cdot [80S_a\mathrm{a-tRNA}_1 0] - \mathrm{k25b} \cdot [80S_a\mathrm{a-tRNA_eEF2_GTP_1 0}])) \\
&\quad - V_{\mathrm{compartment}} \cdot (\mathrm{k26f} \cdot [80S_a\mathrm{a-tRNA_eEF2_GTP_1 0}] \cdot \mathrm{mRNA_tot}) \\
\frac{\mathrm{d}([80S_t\mathrm{RNA}_1 0] \cdot V_{\mathrm{compartment}})}{\mathrm{d}t} &= +V_{\mathrm{compartment}} \cdot (\mathrm{k26f} \cdot [80S_a\mathrm{a-tRNA_eEF2_GTP_9}] \cdot \mathrm{mRNA_tot}) \\
&\quad - V_{\mathrm{compartment}} \cdot (\mathrm{k28f} \cdot [80S_t\mathrm{RNA}_1 0] \cdot [\mathrm{eEF3_GTP}]) \\
\frac{\mathrm{d}([80S_t\mathrm{RNA_eEF3_GTP_1 0}] \cdot V_{\mathrm{compartment}})}{\mathrm{d}t} &= +V_{\mathrm{compartment}} \cdot (\mathrm{k28f} \cdot [80S_t\mathrm{RNA}_1 0] \cdot [\mathrm{eEF3_GTP}]) \\
&\quad - V_{\mathrm{compartment}} \cdot (\mathrm{k29f} \cdot [80S_t\mathrm{RNA_eEF3_GTP_1 0}]) \\
\frac{\mathrm{d}([80S_1 1] \cdot V_{\mathrm{compartment}})}{\mathrm{d}t} &= -V_{\mathrm{compartment}} \cdot ((\mathrm{k22f} \cdot [\mathrm{aa-tRNA_eEF1A_GTP}] \cdot [80S_1 1] - \mathrm{k22b} \cdot [80S_a\mathrm{a-tRNA_eEF1A_GTP_1 1}])) \\
&\quad + V_{\mathrm{compartment}} \cdot (\mathrm{k29f} \cdot [80S_t\mathrm{RNA_eEF3_GTP_1 1}]) \\
\frac{\mathrm{d}([80S_a\mathrm{a-tRNA_eEF1A_GTP_1 1}] \cdot V_{\mathrm{compartment}})}{\mathrm{d}t} &= +V_{\mathrm{compartment}} \cdot ((\mathrm{k22f} \cdot [\mathrm{aa-tRNA_eEF1A_GTP}] \cdot [80S_1 1] - \mathrm{k22b} \cdot [80S_a\mathrm{a-tRNA_eEF1A_GTP_1 1}])) \\
&\quad - V_{\mathrm{compartment}} \cdot (\mathrm{k23f} \cdot [80S_a\mathrm{a-tRNA_eEF1A_GTP_1 1}]) \\
\frac{\mathrm{d}([80S_a\mathrm{a-tRNA}_1 1] \cdot V_{\mathrm{compartment}})}{\mathrm{d}t} &= +V_{\mathrm{compartment}} \cdot (\mathrm{k23f} \cdot [80S_a\mathrm{a-tRNA_eEF1A_GTP_1 1}]) \\
&\quad - V_{\mathrm{compartment}} \cdot ((\mathrm{k25f} \cdot [\mathrm{eEF2_GTP}] \cdot [80S_a\mathrm{a-tRNA}_1 1] - \mathrm{k25b} \cdot [80S_a\mathrm{a-tRNA_eEF2_GTP_1 1}]))
\end{aligned}
$$

$$\frac{d([80S_13] \cdot V_{compartment})}{dt} = -V_{compartment} \cdot ((k22f \cdot [aa-tRNA_eEF1A_GTP] \cdot [80S_13] - k22b \cdot [80S_aa-tRNA_eEF1A_GTP_13]))$$
$$+V_{compartment} \cdot (k29f \cdot [80S_tRNA_eEF3_GTP_13])$$

$$\frac{d([80S_aa-tRNA_eEF1A_GTP_13] \cdot V_{compartment})}{dt} = +V_{compartment} \cdot ((k22f \cdot [aa-tRNA_eEF1A_GTP] \cdot [80S_13] - k22b \cdot [80S_aa-tRNA_eEF1A_GTP_13]))$$
$$-V_{compartment} \cdot (k23f \cdot [80S_aa-tRNA_eEF1A_GTP_13])$$

$$\frac{d([80S_aa-tRNA_13] \cdot V_{compartment})}{dt} = +V_{compartment} \cdot (k23f \cdot [80S_aa-tRNA_eEF1A_GTP_13])$$
$$-V_{compartment} \cdot ((k25f \cdot [eEF2_GTP] \cdot [80S_aa-tRNA_13] - k25b \cdot [80S_aa-tRNA_eEF2_GTP_13]))$$

$$\frac{d([80S_aa-tRNA_eEF2_GTP_13] \cdot V_{compartment})}{dt} = +V_{compartment} \cdot ((k25f \cdot [eEF2_GTP] \cdot [80S_aa-tRNA_13] - k25b \cdot [80S_aa-tRNA_eEF2_GTP_13]))$$
$$-V_{compartment} \cdot (k26f \cdot [80S_aa-tRNA_eEF2_GTP_13] \cdot mRNA_tot)$$

$$\frac{d([80S_tRNA_13] \cdot V_{compartment})}{dt} = +V_{compartment} \cdot (k26f \cdot [80S_aa-tRNA_eEF2_GTP_12] \cdot mRNA_tot)$$
$$-V_{compartment} \cdot (k28f \cdot [80S_tRNA_13] \cdot [eEF3_GTP])$$

$$\frac{d([80S_tRNA_eEF3_GTP_13] \cdot V_{compartment})}{dt} = +V_{compartment} \cdot (k28f \cdot [80S_tRNA_13] \cdot [eEF3_GTP])$$
$$-V_{compartment} \cdot (k29f \cdot [80S_tRNA_eEF3_GTP_13])$$

$$\frac{d([80S_14] \cdot V_{compartment})}{dt} = +V_{compartment} \cdot (k29f \cdot [80S_tRNA_eEF3_GTP_14])$$
$$-V_{compartment} \cdot ((k22f \cdot [aa-tRNA_eEF1A_GTP] \cdot [80S_14] - k22b \cdot [80S_aa-tRNA_eEF1A_GTP_14]))$$

$$\frac{d([80S_aa-tRNA_eEF1A_GTP_14] \cdot V_{compartment})}{dt} = -V_{compartment} \cdot (k23f \cdot [80S_aa-tRNA_eEF1A_GTP_14])$$
$$+V_{compartment} \cdot ((k22f \cdot [aa-tRNA_eEF1A_GTP] \cdot [80S_14] - k22b \cdot [80S_aa-tRNA_eEF1A_GTP_14]))$$

$$\frac{d([80S_aa-tRNA_14] \cdot V_{compartment})}{dt} = +V_{compartment} \cdot (k23f \cdot [80S_aa-tRNA_eEF1A_GTP_14])$$
$$-V_{compartment} \cdot ((k25f \cdot [eEF2_GTP] \cdot [80S_aa-tRNA_14] - k25b \cdot [80S_aa-tRNA_eEF2_GTP_14]))$$

$$
\begin{aligned}
\frac{\mathrm{d}([80S_{1}3]\cdot V_{\mathrm{compartment}})}{\mathrm{d}t} &= -V_{\mathrm{compartment}}\cdot((\mathrm{k22f}\cdot[\mathrm{aa-tRNA_{e}EF1A_{G}TP}]\cdot[80S_{1}3]-\mathrm{k22b}\cdot[80S_{a}a-\mathrm{tRNA_{e}EF1A_{G}TP}_{1}3])) \\
&\quad +V_{\mathrm{compartment}}\cdot(\mathrm{k29f}\cdot[80S_{t}\mathrm{RNA_{e}EF3_{G}TP}_{1}3]) \\
\frac{\mathrm{d}([80S_{a}a-\mathrm{tRNA_{e}EF1A_{G}TP}_{1}3]\cdot V_{\mathrm{compartment}})}{\mathrm{d}t} &= +V_{\mathrm{compartment}}\cdot((\mathrm{k22f}\cdot[\mathrm{aa-tRNA_{e}EF1A_{G}TP}]\cdot[80S_{1}3]-\mathrm{k22b}\cdot[80S_{a}a-\mathrm{tRNA_{e}EF1A_{G}TP}_{1}3])) \\
&\quad -V_{\mathrm{compartment}}\cdot(\mathrm{k23f}\cdot[80S_{a}a-\mathrm{tRNA_{e}EF1A_{G}TP}_{1}3]) \\
\frac{\mathrm{d}([80S_{a}a-\mathrm{tRNA}_{1}3]\cdot V_{\mathrm{compartment}})}{\mathrm{d}t} &= +V_{\mathrm{compartment}}\cdot(\mathrm{k23f}\cdot[80S_{a}a-\mathrm{tRNA_{e}EF1A_{G}TP}_{1}3]) \\
&\quad -V_{\mathrm{compartment}}\cdot((\mathrm{k25f}\cdot[\mathrm{eEF2_{G}TP}]\cdot[80S_{a}a-\mathrm{tRNA}_{1}3]-\mathrm{k25b}\cdot[80S_{a}a-\mathrm{tRNA_{e}EF2_{G}TP}_{1}3])) \\
\frac{\mathrm{d}([80S_{a}a-\mathrm{tRNA_{e}EF2_{G}TP}_{1}3]\cdot V_{\mathrm{compartment}})}{\mathrm{d}t} &= +V_{\mathrm{compartment}}\cdot((\mathrm{k25f}\cdot[\mathrm{eEF2_{G}TP}]\cdot[80S_{a}a-\mathrm{tRNA}_{1}3]-\mathrm{k25b}\cdot[80S_{a}a-\mathrm{tRNA_{e}EF2_{G}TP}_{1}3])) \\
&\quad -V_{\mathrm{compartment}}\cdot(\mathrm{k26f}\cdot[80S_{a}a-\mathrm{tRNA_{e}EF2_{G}TP}_{1}3]\cdot\mathrm{mRNA_{t}ot}) \\
\frac{\mathrm{d}([80S_{t}\mathrm{RNA}_{1}3]\cdot V_{\mathrm{compartment}})}{\mathrm{d}t} &= +V_{\mathrm{compartment}}\cdot(\mathrm{k26f}\cdot[80S_{a}a-\mathrm{tRNA_{e}EF2_{G}TP}_{1}2]\cdot\mathrm{mRNA_{t}ot}) \\
&\quad -V_{\mathrm{compartment}}\cdot(\mathrm{k28f}\cdot[80S_{t}\mathrm{RNA}_{1}3]\cdot[\mathrm{eEF3_{G}TP}]) \\
\frac{\mathrm{d}([80S_{t}\mathrm{RNA_{e}EF3_{G}TP}_{1}3]\cdot V_{\mathrm{compartment}})}{\mathrm{d}t} &= +V_{\mathrm{compartment}}\cdot(\mathrm{k28f}\cdot[80S_{t}\mathrm{RNA}_{1}3]\cdot[\mathrm{eEF3_{G}TP}]) \\
&\quad -V_{\mathrm{compartment}}\cdot(\mathrm{k29f}\cdot[80S_{t}\mathrm{RNA_{e}EF3_{G}TP}_{1}3]) \\
\frac{\mathrm{d}([80S_{1}4]\cdot V_{\mathrm{compartment}})}{\mathrm{d}t} &= +V_{\mathrm{compartment}}\cdot(\mathrm{k29f}\cdot[80S_{t}\mathrm{RNA_{e}EF3_{G}TP}_{1}4]) \\
&\quad -V_{\mathrm{compartment}}\cdot((\mathrm{k22f}\cdot[\mathrm{aa-tRNA_{e}EF1A_{G}TP}]\cdot[80S_{1}4]-\mathrm{k22b}\cdot[80S_{a}a-\mathrm{tRNA_{e}EF1A_{G}TP}_{1}4])) \\
\frac{\mathrm{d}([80S_{a}a-\mathrm{tRNA_{e}EF1A_{G}TP}_{1}4]\cdot V_{\mathrm{compartment}})}{\mathrm{d}t} &= -V_{\mathrm{compartment}}\cdot(\mathrm{k23f}\cdot[80S_{a}a-\mathrm{tRNA_{e}EF1A_{G}TP}_{1}4]) \\
&\quad +V_{\mathrm{compartment}}\cdot((\mathrm{k22f}\cdot[\mathrm{aa-tRNA_{e}EF1A_{G}TP}]\cdot[80S_{1}4]-\mathrm{k22b}\cdot[80S_{a}a-\mathrm{tRNA_{e}EF1A_{G}TP}_{1}4])) \\
\frac{\mathrm{d}([80S_{a}a-\mathrm{tRNA}_{1}4]\cdot V_{\mathrm{compartment}})}{\mathrm{d}t} &= +V_{\mathrm{compartment}}\cdot(\mathrm{k23f}\cdot[80S_{a}a-\mathrm{tRNA_{e}EF1A_{G}TP}_{1}4]) \\
&\quad -V_{\mathrm{compartment}}\cdot((\mathrm{k25f}\cdot[\mathrm{eEF2_{G}TP}]\cdot[80S_{a}a-\mathrm{tRNA}_{1}4]-\mathrm{k25b}\cdot[80S_{a}a-\mathrm{tRNA_{e}EF2_{G}TP}_{1}4]))
\end{aligned}
$$

$$\frac{\mathrm{d}([80S_tRNA_eEF3_GTP_15]\cdot V_{compartment})}{\mathrm{d}t} = +V_{compartment}\cdot(k28f\cdot[80S_tRNA_15]\cdot[eEF3_GTP])$$
$$-V_{compartment}\cdot(k29f\cdot[80S_tRNA_eEF3_GTP_15])$$

$$\frac{\mathrm{d}([80S_16]\cdot V_{compartment})}{\mathrm{d}t} = -V_{compartment}\cdot((k22f\cdot[aa-tRNA_eEF1A_GTP]\cdot[80S_16]-k22b\cdot[80S_aa-tRNA_eEF1A_GTP_16]))$$
$$+V_{compartment}\cdot(k29f\cdot[80S_tRNA_eEF3_GTP_16])$$

$$\frac{\mathrm{d}([80S_aa-tRNA_eEF1A_GTP_16]\cdot V_{compartment})}{\mathrm{d}t} = +V_{compartment}\cdot((k22f\cdot[aa-tRNA_eEF1A_GTP]\cdot[80S_16]-k22b\cdot[80S_aa-tRNA_eEF1A_GTP_16]))$$
$$-V_{compartment}\cdot(k23f\cdot[80S_aa-tRNA_eEF1A_GTP_16])$$

$$\frac{\mathrm{d}([80S_aa-tRNA_16]\cdot V_{compartment})}{\mathrm{d}t} = +V_{compartment}\cdot(k23f\cdot[80S_aa-tRNA_eEF1A_GTP_16])$$
$$-V_{compartment}\cdot((k25f\cdot[eEF2_GTP]\cdot[80S_aa-tRNA_16]-k25b\cdot[80S_aa-tRNA_eEF2_GTP_16]))$$

$$\frac{\mathrm{d}([80S_aa-tRNA_eEF2_GTP_16]\cdot V_{compartment})}{\mathrm{d}t} = +V_{compartment}\cdot((k25f\cdot[eEF2_GTP]\cdot[80S_aa-tRNA_16]-k25b\cdot[80S_aa-tRNA_eEF2_GTP_16]))$$
$$-V_{compartment}\cdot(k26f\cdot[80S_aa-tRNA_eEF2_GTP_16]\cdot mRNA_tot)$$

$$\frac{\mathrm{d}([80S_tRNA_16]\cdot V_{compartment})}{\mathrm{d}t} = +V_{compartment}\cdot(k26f\cdot[80S_aa-tRNA_eEF2_GTP_15]\cdot mRNA_tot)$$
$$-V_{compartment}\cdot(k28f\cdot[80S_tRNA_16]\cdot[eEF3_GTP])$$

$$\frac{\mathrm{d}([80S_tRNA_eEF3_GTP_16]\cdot V_{compartment})}{\mathrm{d}t} = +V_{compartment}\cdot(k28f\cdot[80S_tRNA_16]\cdot[eEF3_GTP])$$
$$-V_{compartment}\cdot(k29f\cdot[80S_tRNA_eEF3_GTP_16])$$

$$\frac{\mathrm{d}([80S_17]\cdot V_{compartment})}{\mathrm{d}t} = -V_{compartment}\cdot((k22f\cdot[aa-tRNA_eEF1A_GTP]\cdot[80S_17]-k22b\cdot[80S_aa-tRNA_eEF1A_GTP_17]))$$
$$+V_{compartment}\cdot(k29f\cdot[80S_tRNA_eEF3_GTP_17])$$

$$\frac{\mathrm{d}([80S_aa-tRNA_eEF1A_GTP_17]\cdot V_{compartment})}{\mathrm{d}t} = +V_{compartment}\cdot((k22f\cdot[aa-tRNA_eEF1A_GTP]\cdot[80S_17]-k22b\cdot[80S_aa-tRNA_eEF1A_GTP_17]))$$
$$-V_{compartment}\cdot(k23f\cdot[80S_aa-tRNA_eEF1A_GTP_17])$$

$$
\begin{aligned}
\frac{\mathrm{d}([80S_a a{-}tRNA_1 7]\cdot V_{\mathrm{compartment}})}{\mathrm{d}t} &= +V_{\mathrm{compartment}}\cdot(\mathrm{k23f}\cdot[80S_a a-tRNA_e EF1A_G TP_1 7])\\
&\quad -V_{\mathrm{compartment}}\cdot((\mathrm{k25f}\cdot[eEF2_G TP]\cdot[80S_a a-tRNA_1 7]-\mathrm{k25b}\cdot[80S_a a-tRNA_e EF2_G TP_1 7]))\\
\frac{\mathrm{d}([80S_a a{-}tRNA_e EF2_G TP_1 7]\cdot V_{\mathrm{compartment}})}{\mathrm{d}t} &= +V_{\mathrm{compartment}}\cdot((\mathrm{k25f}\cdot[eEF2_G TP]\cdot[80S_a a-tRNA_1 7]-\mathrm{k25b}\cdot[80S_a a-tRNA_e EF2_G TP_1 7]))\\
&\quad -V_{\mathrm{compartment}}\cdot(\mathrm{k26f}\cdot[80S_a a-tRNA_e EF2_G TP_1 7]\cdot mRNA_t ot)\\
\frac{\mathrm{d}([80S_t RNA_1 7]\cdot V_{\mathrm{compartment}})}{\mathrm{d}t} &= +V_{\mathrm{compartment}}\cdot(\mathrm{k26f}\cdot[80S_a a-tRNA_e EF2_G TP_1 6]\cdot mRNA_t ot)\\
&\quad -V_{\mathrm{compartment}}\cdot(\mathrm{k28f}\cdot[80S_t RNA_1 7]\cdot[eEF3_G TP])\\
\frac{\mathrm{d}([80S_t RNA_e EF3_G TP_1 7]\cdot V_{\mathrm{compartment}})}{\mathrm{d}t} &= +V_{\mathrm{compartment}}\cdot(\mathrm{k28f}\cdot[80S_t RNA_1 7]\cdot[eEF3_G TP])\\
&\quad -V_{\mathrm{compartment}}\cdot(\mathrm{k29f}\cdot[80S_t RNA_e EF3_G TP_1 7])\\
\frac{\mathrm{d}([80S_1 8]\cdot V_{\mathrm{compartment}})}{\mathrm{d}t} &= -V_{\mathrm{compartment}}\cdot((\mathrm{k22f}\cdot[aa-tRNA_e EF1A_G TP]\cdot[80S_1 8]-\mathrm{k22b}\cdot[80S_a a-tRNA_e EF1A_G TP_1 8]))\\
&\quad +V_{\mathrm{compartment}}\cdot(\mathrm{k29f}\cdot[80S_t RNA_e EF3_G TP_1 8])\\
\frac{\mathrm{d}([80S_a a{-}tRNA_e EF1A_G TP_1 8]\cdot V_{\mathrm{compartment}})}{\mathrm{d}t} &= +V_{\mathrm{compartment}}\cdot((\mathrm{k22f}\cdot[aa-tRNA_e EF1A_G TP]\cdot[80S_1 8]-\mathrm{k22b}\cdot[80S_a a-tRNA_e EF1A_G TP_1 8]))\\
&\quad -V_{\mathrm{compartment}}\cdot(\mathrm{k23f}\cdot[80S_a a-tRNA_e EF1A_G TP_1 8])\\
\frac{\mathrm{d}([80S_a a{-}tRNA_1 8]\cdot V_{\mathrm{compartment}})}{\mathrm{d}t} &= +V_{\mathrm{compartment}}\cdot(\mathrm{k23f}\cdot[80S_a a-tRNA_e EF1A_G TP_1 8])\\
&\quad -V_{\mathrm{compartment}}\cdot((\mathrm{k25f}\cdot[eEF2_G TP]\cdot[80S_a a-tRNA_1 8]-\mathrm{k25b}\cdot[80S_a a-tRNA_e EF2_G TP_1 8]))\\
\frac{\mathrm{d}([80S_a a{-}tRNA_e EF2_G TP_1 8]\cdot V_{\mathrm{compartment}})}{\mathrm{d}t} &= +V_{\mathrm{compartment}}\cdot((\mathrm{k25f}\cdot[eEF2_G TP]\cdot[80S_a a-tRNA_1 8]-\mathrm{k25b}\cdot[80S_a a-tRNA_e EF2_G TP_1 8]))\\
&\quad -V_{\mathrm{compartment}}\cdot(\mathrm{k26f}\cdot[80S_a a-tRNA_e EF2_G TP_1 8]\cdot mRNA_t ot)\\
\frac{\mathrm{d}([80S_t RNA_1 8]\cdot V_{\mathrm{compartment}})}{\mathrm{d}t} &= +V_{\mathrm{compartment}}\cdot(\mathrm{k26f}\cdot[80S_a a-tRNA_e EF2_G TP_1 7]\cdot mRNA_t ot)\\
&\quad -V_{\mathrm{compartment}}\cdot(\mathrm{k28f}\cdot[80S_t RNA_1 8]\cdot[eEF3_G TP])\\
\frac{\mathrm{d}([80S_t RNA_e EF3_G TP_1 8]\cdot V_{\mathrm{compartment}})}{\mathrm{d}t} &= +V_{\mathrm{compartment}}\cdot(\mathrm{k28f}\cdot[80S_t RNA_1 8]\cdot[eEF3_G TP])\\
&\quad -V_{\mathrm{compartment}}\cdot(\mathrm{k29f}\cdot[80S_t RNA_e EF3_G TP_1 8])
\end{aligned}
$$

$$\frac{d([80S_19] \cdot V_{compartment})}{dt} = -V_{compartment} \cdot ((k22f \cdot [aa - tRNA_eEF1A_GTP] \cdot [80S_19] - k22b \cdot [80S_aa - tRNA_eEF1A_GTP_19]))$$
$$+V_{compartment} \cdot (k29f \cdot [80S_tRNA_eEF3_GTP_19])$$

$$\frac{d([80S_aa-tRNA_eEF1A_GTP_19] \cdot V_{compartment})}{dt} = +V_{compartment} \cdot ((k22f \cdot [aa - tRNA_eEF1A_GTP] \cdot [80S_19] - k22b \cdot [80S_aa - tRNA_eEF1A_GTP_19]))$$
$$-V_{compartment} \cdot (k23f \cdot [80S_aa - tRNA_eEF1A_GTP_19])$$

$$\frac{d([80S_aa-tRNA_19] \cdot V_{compartment})}{dt} = +V_{compartment} \cdot (k23f \cdot [80S_aa - tRNA_eEF1A_GTP_19])$$
$$-V_{compartment} \cdot ((k25f \cdot [eEF2_GTP] \cdot [80S_aa - tRNA_19] - k25b \cdot [80S_aa - tRNA_eEF2_GTP_19]))$$

$$\frac{d([80S_aa-tRNA_eEF2_GTP_19] \cdot V_{compartment})}{dt} = +V_{compartment} \cdot ((k25f \cdot [eEF2_GTP] \cdot [80S_aa - tRNA_19] - k25b \cdot [80S_aa - tRNA_eEF2_GTP_19]))$$
$$-V_{compartment} \cdot (k26f \cdot [80S_aa - tRNA_eEF2_GTP_19] \cdot mRNA_tot)$$

$$\frac{d([80S_tRNA_19] \cdot V_{compartment})}{dt} = +V_{compartment} \cdot (k26f \cdot [80S_aa - tRNA_eEF2_GTP_18] \cdot mRNA_tot)$$
$$-V_{compartment} \cdot (k28f \cdot [80S_tRNA_19] \cdot [eEF3_GTP])$$

$$\frac{d([80S_tRNA_eEF3_GTP_19] \cdot V_{compartment})}{dt} = +V_{compartment} \cdot (k28f \cdot [80S_tRNA_19] \cdot [eEF3_GTP])$$
$$-V_{compartment} \cdot (k29f \cdot [80S_tRNA_eEF3_GTP_19])$$

$$\frac{d([80S_20] \cdot V_{compartment})}{dt} = +V_{compartment} \cdot (k29f \cdot [80S_tRNA_eEF3_GTP_20])$$
$$-V_{compartment} \cdot (2e+006 \cdot [eRF1_eRF3_GTP] \cdot [80S_20])$$

$$\frac{d([80S_tRNA_20] \cdot V_{compartment})}{dt} = +V_{compartment} \cdot (k26f \cdot [80S_aa - tRNA_eEF2_GTP_19] \cdot mRNA_tot)$$
$$-V_{compartment} \cdot (k28f \cdot [80S_tRNA_20] \cdot [eEF3_GTP])$$

$$\frac{d([80S_tRNA_eEF3_GTP_20] \cdot V_{compartment})}{dt} = +V_{compartment} \cdot (k28f \cdot [80S_tRNA_20] \cdot [eEF3_GTP])$$
$$-V_{compartment} \cdot (k29f \cdot [80S_tRNA_eEF3_GTP_20])$$

$$\frac{d([eRF3_GDP] \cdot V_{compartment})}{dt} = -V_{compartment} \cdot ((2e+008 \cdot [eRF3_GDP] - 1000 \cdot [eRF3_GTP]))$$
$$+V_{compartment} \cdot (2e+008 \cdot [80S_eRF1_eRF3_GTP])$$

$$
\begin{aligned}
\frac{\mathrm{d}([\mathrm{eRF3_G TP}] \cdot V_{\mathrm{compartment}})}{\mathrm{d}t} &= +V_{\mathrm{compartment}} \cdot ((2e+008 \cdot [\mathrm{eRF3_G DP}] - 1000 \cdot [\mathrm{eRF3_G TP}])) \\
&\quad -V_{\mathrm{compartment}} \cdot ((3.5e+010 \cdot [\mathrm{eRF1}] \cdot [\mathrm{eRF3_G TP}] - 1000 \cdot [\mathrm{eRF1_e RF3_G TP}])) \\
\frac{\mathrm{d}([\mathrm{eRF1}] \cdot V_{\mathrm{compartment}})}{\mathrm{d}t} &= -V_{\mathrm{compartment}} \cdot ((3.5e+010 \cdot [\mathrm{eRF1}] \cdot [\mathrm{eRF3_G TP}] - 1000 \cdot [\mathrm{eRF1_e RF3_G TP}])) \\
&\quad +V_{\mathrm{compartment}} \cdot (2e+008 \cdot [\mathrm{80S_e RF1_e RF3_G TP}]) \\
\frac{\mathrm{d}([\mathrm{eRF1_e RF3_G TP}] \cdot V_{\mathrm{compartment}})}{\mathrm{d}t} &= +V_{\mathrm{compartment}} \cdot ((3.5e+010 \cdot [\mathrm{eRF1}] \cdot [\mathrm{eRF3_G TP}] - 1000 \cdot [\mathrm{eRF1_e RF3_G TP}])) \\
&\quad -V_{\mathrm{compartment}} \cdot (2e+006 \cdot [\mathrm{eRF1_e RF3_G TP}] \cdot [\mathrm{80S_2 0}]) \\
\frac{\mathrm{d}([\mathrm{80S_e RF1_e RF3_G TP}] \cdot V_{\mathrm{compartment}})}{\mathrm{d}t} &= +V_{\mathrm{compartment}} \cdot (2e+006 \cdot [\mathrm{eRF1_e RF3_G TP}] \cdot [\mathrm{80S_2 0}]) \\
&\quad -V_{\mathrm{compartment}} \cdot (2e+008 \cdot [\mathrm{80S_e RF1_e RF3_G TP}])
\end{aligned}
$$

$$
\begin{aligned}
\frac{\mathrm{d}([\mathrm{aa{-}tRNA_eEF1A_GTP}]\cdot V_{\mathrm{compartment}})}{\mathrm{d}t} = \;& -V_{\mathrm{compartment}}\cdot((\mathrm{k22f}\cdot[\mathrm{aa-tRNA_eEF1A_GTP}]\cdot[80S_15]-\mathrm{k22b}\cdot[80S_a\mathrm{a-tRNA_eEF1A_GTP}_15])) \\
& -V_{\mathrm{compartment}}\cdot((\mathrm{k22f}\cdot[\mathrm{aa-tRNA_eEF1A_GTP}]\cdot[80S_16]-\mathrm{k22b}\cdot[80S_a\mathrm{a-tRNA_eEF1A_GTP}_16])) \\
& -V_{\mathrm{compartment}}\cdot((\mathrm{k22f}\cdot[\mathrm{aa-tRNA_eEF1A_GTP}]\cdot[80S_17]-\mathrm{k22b}\cdot[80S_a\mathrm{a-tRNA_eEF1A_GTP}_17])) \\
& -V_{\mathrm{compartment}}\cdot((\mathrm{k22f}\cdot[\mathrm{aa-tRNA_eEF1A_GTP}]\cdot[80S_18]-\mathrm{k22b}\cdot[80S_a\mathrm{a-tRNA_eEF1A_GTP}_18])) \\
& -V_{\mathrm{compartment}}\cdot((\mathrm{k22f}\cdot[\mathrm{aa-tRNA_eEF1A_GTP}]\cdot[80S_19]-\mathrm{k22b}\cdot[80S_a\mathrm{a-tRNA_eEF1A_GTP}_19])) \\
& +V_{\mathrm{compartment}}\cdot((20000\cdot[\mathrm{eEF1A_GTP}]\cdot[\mathrm{aa-tRNA}]-1000\cdot[\mathrm{aa-tRNA_eEF1A_GTP}])) \\
& -V_{\mathrm{compartment}}\cdot((\mathrm{k22f}\cdot[\mathrm{aa-tRNA_eEF1A_GTP}]\cdot[80S_1]-\mathrm{k22b}\cdot[80S_a\mathrm{a-tRNA_eEF1A_GTP}_1])) \\
& -V_{\mathrm{compartment}}\cdot((\mathrm{k22f}\cdot[\mathrm{aa-tRNA_eEF1A_GTP}]\cdot[80S_2]-\mathrm{k22b}\cdot[80S_a\mathrm{a-tRNA_eEF1A_GTP}_2])) \\
& -V_{\mathrm{compartment}}\cdot((\mathrm{k22f}\cdot[\mathrm{aa-tRNA_eEF1A_GTP}]\cdot[80S_3]-\mathrm{k22b}\cdot[80S_a\mathrm{a-tRNA_eEF1A_GTP}_3])) \\
& -V_{\mathrm{compartment}}\cdot((\mathrm{k22f}\cdot[\mathrm{aa-tRNA_eEF1A_GTP}]\cdot[80S_4]-\mathrm{k22b}\cdot[80S_a\mathrm{a-tRNA_eEF1A_GTP}_4])) \\
& -V_{\mathrm{compartment}}\cdot((\mathrm{k22f}\cdot[\mathrm{aa-tRNA_eEF1A_GTP}]\cdot[80S_5]-\mathrm{k22b}\cdot[80S_a\mathrm{a-tRNA_eEF1A_GTP}_5])) \\
& -V_{\mathrm{compartment}}\cdot((\mathrm{k22f}\cdot[\mathrm{aa-tRNA_eEF1A_GTP}]\cdot[80S_6]-\mathrm{k22b}\cdot[80S_a\mathrm{a-tRNA_eEF1A_GTP}_6])) \\
& -V_{\mathrm{compartment}}\cdot((\mathrm{k22f}\cdot[\mathrm{aa-tRNA_eEF1A_GTP}]\cdot[80S_7]-\mathrm{k22b}\cdot[80S_a\mathrm{a-tRNA_eEF1A_GTP}_7])) \\
& -V_{\mathrm{compartment}}\cdot((\mathrm{k22f}\cdot[\mathrm{aa-tRNA_eEF1A_GTP}]\cdot[80S_8]-\mathrm{k22b}\cdot[80S_a\mathrm{a-tRNA_eEF1A_GTP}_8])) \\
& -V_{\mathrm{compartment}}\cdot((\mathrm{k22f}\cdot[\mathrm{aa-tRNA_eEF1A_GTP}]\cdot[80S_9]-\mathrm{k22b}\cdot[80S_a\mathrm{a-tRNA_eEF1A_GTP}_9])) \\
& -V_{\mathrm{compartment}}\cdot((\mathrm{k22f}\cdot[\mathrm{aa-tRNA_eEF1A_GTP}]\cdot[80S_10]-\mathrm{k22b}\cdot[80S_a\mathrm{a-tRNA_eEF1A_GTP}_10])) \\
& -V_{\mathrm{compartment}}\cdot((\mathrm{k22f}\cdot[\mathrm{aa-tRNA_eEF1A_GTP}]\cdot[80S_11]-\mathrm{k22b}\cdot[80S_a\mathrm{a-tRNA_eEF1A_GTP}_11])) \\
& -V_{\mathrm{compartment}}\cdot((\mathrm{k22f}\cdot[\mathrm{aa-tRNA_eEF1A_GTP}]\cdot[80S_12]-\mathrm{k22b}\cdot[80S_a\mathrm{a-tRNA_eEF1A_GTP}_12])) \\
& -V_{\mathrm{compartment}}\cdot((\mathrm{k22f}\cdot[\mathrm{aa-tRNA_eEF1A_GTP}]\cdot[80S_13]-\mathrm{k22b}\cdot[80S_a\mathrm{a-tRNA_eEF1A_GTP}_13])) \\
& -V_{\mathrm{compartment}}\cdot((\mathrm{k22f}\cdot[\mathrm{aa-tRNA_eEF1A_GTP}]\cdot[80S_14]-\mathrm{k22b}\cdot[80S_a\mathrm{a-tRNA_eEF1A_GTP}_14]))
\end{aligned}
$$

$$
\begin{aligned}
\frac{\mathrm{d}([\mathrm{eEF3_G DP}] \cdot V_{\mathrm{compartment}})}{\mathrm{d}t} = \; & + V_{\mathrm{compartment}} \cdot (\mathrm{k29f} \cdot [80\mathrm{S_t RNA_e EF3_G TP_1 4}]) \\
& + V_{\mathrm{compartment}} \cdot (\mathrm{k29f} \cdot [80\mathrm{S_t RNA_e EF3_G TP_1 5}]) \\
& + V_{\mathrm{compartment}} \cdot (\mathrm{k29f} \cdot [80\mathrm{S_t RNA_e EF3_G TP_1 6}]) \\
& + V_{\mathrm{compartment}} \cdot (\mathrm{k29f} \cdot [80\mathrm{S_t RNA_e EF3_G TP_1 7}]) \\
& + V_{\mathrm{compartment}} \cdot (\mathrm{k29f} \cdot [80\mathrm{S_t RNA_e EF3_G TP_1 8}]) \\
& + V_{\mathrm{compartment}} \cdot (\mathrm{k29f} \cdot [80\mathrm{S_t RNA_e EF3_G TP_1 9}]) \\
& + V_{\mathrm{compartment}} \cdot (\mathrm{k29f} \cdot [80\mathrm{S_t RNA_e EF3_G TP_2 0}]) \\
& - V_{\mathrm{compartment}} \cdot ((2000 \cdot [\mathrm{eEF3_G DP}] - 100 \cdot [\mathrm{eEF3_G TP}])) \\
& + V_{\mathrm{compartment}} \cdot (\mathrm{k29f} \cdot [80\mathrm{S_t RNA_e EF3_G TP_2}]) \\
& + V_{\mathrm{compartment}} \cdot (\mathrm{k29f} \cdot [80\mathrm{S_t RNA_e EF3_G TP_3}]) \\
& + V_{\mathrm{compartment}} \cdot (\mathrm{k29f} \cdot [80\mathrm{S_t RNA_e EF3_G TP_4}]) \\
& + V_{\mathrm{compartment}} \cdot (\mathrm{k29f} \cdot [80\mathrm{S_t RNA_e EF3_G TP_5}]) \\
& + V_{\mathrm{compartment}} \cdot (\mathrm{k29f} \cdot [80\mathrm{S_t RNA_e EF3_G TP_6}]) \\
& + V_{\mathrm{compartment}} \cdot (\mathrm{k29f} \cdot [80\mathrm{S_t RNA_e EF3_G TP_7}]) \\
& + V_{\mathrm{compartment}} \cdot (\mathrm{k29f} \cdot [80\mathrm{S_t RNA_e EF3_G TP_8}]) \\
& + V_{\mathrm{compartment}} \cdot (\mathrm{k29f} \cdot [80\mathrm{S_t RNA_e EF3_G TP_9}]) \\
& + V_{\mathrm{compartment}} \cdot (\mathrm{k29f} \cdot [80\mathrm{S_t RNA_e EF3_G TP_1 0}]) \\
& + V_{\mathrm{compartment}} \cdot (\mathrm{k29f} \cdot [80\mathrm{S_t RNA_e EF3_G TP_1 1}]) \\
& + V_{\mathrm{compartment}} \cdot (\mathrm{k29f} \cdot [80\mathrm{S_t RNA_e EF3_G TP_1 2}]) \\
& + V_{\mathrm{compartment}} \cdot (\mathrm{k29f} \cdot [80\mathrm{S_t RNA_e EF3_G TP_1 3}])
\end{aligned}
$$

$$
\begin{aligned}
\frac{\mathrm{d}([\mathrm{eEF3_G TP}] \cdot V_{\mathrm{compartment}})}{\mathrm{d}t} = \; & -V_{\mathrm{compartment}} \cdot (\mathrm{k28f} \cdot [80\mathrm{S_t RNA_1}4] \cdot [\mathrm{eEF3_G TP}]) \\
& -V_{\mathrm{compartment}} \cdot (\mathrm{k28f} \cdot [80\mathrm{S_t RNA_1}5] \cdot [\mathrm{eEF3_G TP}]) \\
& -V_{\mathrm{compartment}} \cdot (\mathrm{k28f} \cdot [80\mathrm{S_t RNA_1}6] \cdot [\mathrm{eEF3_G TP}]) \\
& -V_{\mathrm{compartment}} \cdot (\mathrm{k28f} \cdot [80\mathrm{S_t RNA_1}7] \cdot [\mathrm{eEF3_G TP}]) \\
& -V_{\mathrm{compartment}} \cdot (\mathrm{k28f} \cdot [80\mathrm{S_t RNA_1}8] \cdot [\mathrm{eEF3_G TP}]) \\
& -V_{\mathrm{compartment}} \cdot (\mathrm{k28f} \cdot [80\mathrm{S_t RNA_1}9] \cdot [\mathrm{eEF3_G TP}]) \\
& -V_{\mathrm{compartment}} \cdot (\mathrm{k28f} \cdot [80\mathrm{S_t RNA_2}0] \cdot [\mathrm{eEF3_G TP}]) \\
& +V_{\mathrm{compartment}} \cdot ((2000 \cdot [\mathrm{eEF3_G DP}] - 100 \cdot [\mathrm{eEF3_G TP}])) \\
& -V_{\mathrm{compartment}} \cdot (\mathrm{k28f} \cdot [80\mathrm{S_t RNA_2}] \cdot [\mathrm{eEF3_G TP}]) \\
& -V_{\mathrm{compartment}} \cdot (\mathrm{k28f} \cdot [80\mathrm{S_t RNA_3}] \cdot [\mathrm{eEF3_G TP}]) \\
& -V_{\mathrm{compartment}} \cdot (\mathrm{k28f} \cdot [80\mathrm{S_t RNA_4}] \cdot [\mathrm{eEF3_G TP}]) \\
& -V_{\mathrm{compartment}} \cdot (\mathrm{k28f} \cdot [80\mathrm{S_t RNA_5}] \cdot [\mathrm{eEF3_G TP}]) \\
& -V_{\mathrm{compartment}} \cdot (\mathrm{k28f} \cdot [80\mathrm{S_t RNA_6}] \cdot [\mathrm{eEF3_G TP}]) \\
& -V_{\mathrm{compartment}} \cdot (\mathrm{k28f} \cdot [80\mathrm{S_t RNA_7}] \cdot [\mathrm{eEF3_G TP}]) \\
& -V_{\mathrm{compartment}} \cdot (\mathrm{k28f} \cdot [80\mathrm{S_t RNA_8}] \cdot [\mathrm{eEF3_G TP}]) \\
& -V_{\mathrm{compartment}} \cdot (\mathrm{k28f} \cdot [80\mathrm{S_t RNA_9}] \cdot [\mathrm{eEF3_G TP}]) \\
& -V_{\mathrm{compartment}} \cdot (\mathrm{k28f} \cdot [80\mathrm{S_t RNA_1}0] \cdot [\mathrm{eEF3_G TP}]) \\
& -V_{\mathrm{compartment}} \cdot (\mathrm{k28f} \cdot [80\mathrm{S_t RNA_1}1] \cdot [\mathrm{eEF3_G TP}]) \\
& -V_{\mathrm{compartment}} \cdot (\mathrm{k28f} \cdot [80\mathrm{S_t RNA_1}2] \cdot [\mathrm{eEF3_G TP}]) \\
& -V_{\mathrm{compartment}} \cdot (\mathrm{k28f} \cdot [80\mathrm{S_t RNA_1}3] \cdot [\mathrm{eEF3_G TP}])
\end{aligned}
$$

Appedix -2

NO:	Reaction	Kinetic values	Source
1	eIF2_GDP + eIF2B = eIF2_GDP_eIF2B	k1: 280 l/(mol*s) k2: 10 1/s	This study
2	eIF2_GDP_eIF2B = eIF2_GTP + eIF2B	k1: 20000 1/s k2: 0.5 l/(mol*s)	This study
3	eIF2_GTP + Met-tRNA = eIF2_GTP_Met-tRNA	k1:20000 l/(mol*s) k2: 0.1 1/s	This study
4	eIF3 + eIF5 = eIF3_eIF5	k1:20000 l/(mol*s) k2:0.1 1/s	This study
5	eIF2_GTP_Met-tRNA + eIF3_eIF5 = eIF3_eIF5_eIF2_GTP_Met-tRNA	k1:20000 l/(mol*s) k2:0.1 1/s	This study
6	eIF1 + eIF3_eIF5_eIF2_GTP_Met-tRNA = eIF1_eIF3_eIF5_eIF2_GTP_Met-tRNA	k1:20000 l/(mol*s) k2:0.1 1/s	This study
7	40S + eIF1A -> 40S_eIF1A	k1:20000 l/(mol*s)	This study
8	eIF1_eIF3_eIF5_eIF2_GTP_Met-tRNA + 40S_eIF1A -> 43S	k1:20000 l/(mol*s)	This study
9	eIF4E + eIF4G = eIF4E_eIF4G	k1: 3e+006 l/(mol*s) k2: 0.01 1/s	This study
10	mRNA_cap + Pab1 = mRNA_Pab1	k1:20000 l/(mol*s) k2:0.1 1/s	This study
11	eIF4E_eIF4G + mRNA_Pab1 = eIF4E_eIF4G_mRNA_Pab1	k1:20000 l/(mol*s) k2:0.1 1/s	This study
12	eIF4A + eIF4B = eIF4A_eIF4B	k1:20000 l/(mol*s) k2:0.1 1/s	This study
13	eIF4E_eIF4G_mRNA_Pab1 + eIF4A_eIF4B = eIF4E_eIF4G_mRNA_Pab1_eIF4A_eIF4B	k1:20000 l/(mol*s) k2:0.1 1/s	This study
14	43S + eIF4E_eIF4G_mRNA_Pab1_eIF4A_eIF4B -> 48S	k1:20000 l/(mol*s)	This study
15	48S + Ded1 = 48S_Ded1	k1:20000 l/(mol*s) k2:0.1 1/s	This study
16	eIF5B_GDP = eIF5B_GTP	k1:20000 1/s	This

		k2:12 1/s	study
17	48S_Ded1 + eIF5B_GTP = 48S_Ded1_eIF5B_GTP	k1:20000 l/(mol*s) k2:0.1 1/s	This study
18	60S + 48S_Ded1_eIF5B_GTP -> 80S_1 + eIF1 + eIF1A + eIF2_GDP + eIF3 + eIF4A + eIF4B + eIF4E + eIF4G + eIF5 + eIF5B_GDP + Pab1 + mRNA_cap	K:20000 l^2/(mol^2*s)	This study
19	eEF1A_GDP + eEF1B = eEF1A_GDP_eEF1B	k1: 7.5e+007 l/(mol*s) k2: 117 1/s	This study
20	eEF1A_GDP_eEF1B = eEF1A_GTP + eEF1B	k1: 1e+006 1/s k2: 25 l/(mol*s)	This study
21	eEF1A_GTP + aa-tRNA = aa-tRNA_eEF1A_GTP	k1:20000 l/(mol*s) k2: 0.1 1/s	This study
22	aa-tRNA_eEF1A_GTP + 80S_1 = 80S_aa-tRNA_eEF1A_GTP_1	k1: 1.948e+06 l/(mol*s) k2: 1000 (1/s)	This study
23	80S_aa-tRNA_eEF1A_GTP_1 -> 80S_aa-tRNA_1 + eEF1A_GDP	k1 :100000 (1/s)	This study
24	eEF2_GDP = eEF2_GTP	k1 : 20000 1/s k2 : 0.1 1/s	This study
25	eEF2_GTP + 80S_aa-tRNA_1 = 80S_aa-tRNA_eEF2_GTP_1	k1:10000 (l/(mol*s)) k2: 1000 (1/s)	This study
26	80S_aa-tRNA_eEF2_GTP_1 -> 80S_tRNA_1 + eEF2_GDP	k1: 250000 (1/s)	This study
27	eEF3_GDP = eEF3_GTP	k1: 20000 1/s k2 0.1 1/s	This study
28	80S_tRNA_1 + eEF3_GTP -> 80S_tRNA_eEF3_GTP_1	k1 : 1.5e+06 (l/(mol*s))	This study
29	80S_tRNA_eEF3_GTP_1 -> 80S_2 + eEF3_GDP + tRNA	K: 20000 (1/s) mRNA_tot : 4.9e+06 mol/l)	This study
30	eRF3_GDP = eRF3_GTP	k1: 20000 1/s k2: 0.1 1/s	This study

31	eRF1 + eRF3_GTP = eRF1_eRF3_GTP	k1: 3.5e-006 l/(mol*s) k2: 13 1/s	This study
32	eRF1_eRF3_GTP + 80S_tRNA_eEF3_GTP_20 -> 80S_tRNA_eEF3_GTP_eRF1_eRF3_GTP	k1: 20000 l/(mol*s)	This study
33	80S_tRNA_eEF3_GTP_eRF1_eRF3_GTP -> 40S + 60S + tRNA + eEF3_GDP + eRF1 + eRF3_GDP	k1 : 2000 1/s	This study

Appendix – 3: Protein synthesis rate with respective factor concentration used model fitting

[eIF1A]	Translation rate
497	95
115	95
71	94
54	90
50	85
42	80
37	78
30	72

[eIF4G1]	Translation rate
213	85
118	85
92	95
90	97
77	90

eIF2a	Translation rate
100.00	94.71
94.54	86.10
95.31	85.37
83.25	82.59
87.89	81.64

[Dbp5]	trans;
114	105
94	106
79	97
65.5	97.5
64	89
56	80
40	75
28	57.5

[eIF5B]	Translation rate
100	100
30	99
24	99
22	94
18	90
15	84
12	78
9	76
5	70
4	66

eIF4A	Translation rate
67	66
78	74
83	85
89	90
86	94

eIF2B	Translation rate
100	62
93	56
94	51
93	46
86	45

eIF3	Translation rate
99	65
79	66
92	69
105	69
98	71

eIF1	Translation rate
97.35	99.38
99.25	95.20
96.96	92.98
97.61	86.08
95.53	76.96

Pab1	Translation rate
103	66
92	59
83	53
77	50
48	32

eEF1A	Translation rate
73	87
70	78
67	70
62	70
61	67

eEF1B	Translation rate
94.00	94.00
80.73	93.18
76.40	88.59
72.59	83.17
67.28	78.68

eRF3	translation rate
95.00	88.05
90.00	87.37
87.00	87.00
86.00	83.00
86.09	82.63

eEF3	Translation rate
97.61	94.58
94.00	94.12
91.30	93.89
87.41	88.35
84.81	85.87

translation rate	[Hyp2]
100	100
103	62
101	52
98	54
98	48
94	27
88	17
81	20
79	13

eRF1	Translation rate
98.00	92.00
90.19	85.00
83.00	75.00
79.00	68.63
71.43	64.90

eEF2	Translation rate
93	91
91	83
87	76
85	70
83	69